VOLUME 102 | SUPPLEMENT 1 | MARCH 2022

LI

LABORATORY INVESTIGATION

THE BASIC AND TRANSLATIONAL PATHOLOGY RESEARCH JOURNAL

ABSTRACTS (372–507)

GASTROINTESTINAL PATHOLOGY

2022

USCAP 111TH ANNUAL MEETING

REAL INTELLIGENCE

MARCH 19–24, 2022 LOS ANGELES, CALIFORNIA

Published by
SPRINGER NATURE
www.ModernPathology.org

USCAP
Creating a Better Pathologist
AN OFFICIAL JOURNAL OF THE UNITED STATES AND CANADIAN ACADEMY OF PATHOLOGY

EDUCATION COMMITTEE

Rhonda K. Yantiss
Chair

Kristin C. Jensen
Chair, CME Subcommittee

Laura C. Collins
Chair, Interactive Microscopy Subcommittee

Yuri Fedoriw
Short Course Coordinator

Ilan Weinreb
Chair, Subcommittee for Unique Live Course Offerings

Carla L. Ellis
Chair, DEI Subcommittee

Adebowale J. Adeniran
Kimberly H. Allison
Sarah M. Dry
William C. Faquin
Karen J. Fritchie
Jennifer B. Gordetsky
Levon Katsakhyan, Pathologist-in-Training
Melinda J. Lerwill
M. Beatriz S. Lopes
Julia R. Naso, Pathologist-in-Training
Liron Pantanowitz
Carlos Parra-Herran
Rajiv M. Patel
Charles "Matt" Quick
David F. Schaeffer
Lynette M. Sholl
Olga K. Weinberg
Maria Westerhoff

ABSTRACT REVIEW BOARD

Benjamin Adam
Oyedele Adeyi
Mariam Priya Alexander
Daniela Allende
Catalina Amador
Vijayalakshmi Ananthanarayanan
Tatjana Antic
Manju Aron
Roberto Barrios
Gregory R. Bean
Govind Bhagat
Luis Zabala Blanco
Michael Bonert
Alain C. Borczuk
Tamar C. Brandler
Eric Jason Burks
Kelly J. Butnor
Sarah M. Calkins
Weibiao Cao
Wenqing (Wendy) Cao
Barbara Ann Centeno
Joanna SY Chan
Kung-Chao Chang
Hao Chen
Wei Chen
Yunn-Yi Chen
Sarah Chiang
Soo-Jin Cho
Shefali Chopra
Nicole A. Cipriani
Cecilia Clement
Claudiu Cotta
Jennifer A. Cotter
Sonika M. Dahiya
Elizabeth G. Demicco
Katie Dennis
Jasreman Dhillon
Anand S. Dighe
Bojana Djordjevic
Michelle R. Downes
Charles G. Eberhart
Andrew G. Evans
Fang Fan
Julie C. Fanburg-Smith
Gelareh Farshid
Michael Feely
Susan A. Fineberg
Dennis J. Firchau
Gregory A. Fishbein
Agnes B. Fogo
Andrew L. Folpe
Danielle Fortuna
Billie Fyfe-Kirschner
Zeina Ghorab
Giovanna A. Giannico
Anthony J. Gill
Tamar A. Giorgadze
Alessio Giubellino
Carolyn Glass
Carmen R. Gomez-Fernandez
Shunyou Gong
Purva Gopal
Abha Goyal
Christopher C. Griffith
Ian S. Hagemann
Gillian Leigh Hale
Suntrea TG Hammer
Malini Harigopal
Kammi J. Henriksen
Jonas J. Heymann
Carlo Vincent Hojilla
Aaron R. Huber
Jabed Iqbal
Shilpa Jain
Vickie Y. Jo
Ivy John
Dan Jones
Ridas Juskevicius
Meghan E. Kapp
Nora Katabi
Francesca Khani
Joseph D. Khoury
Benjamin Kipp
Veronica E. Klepeis
Christian A. Kunder
Stefano La Rosa
Stephen M. Lagana
Keith K. Lai
Goo Lee
Michael Lee
Vasiliki Leventaki
Madelyn Lew
Faqian Li
Ying Li
Chieh-Yu Lin
Mikhail Lisovsky
Lesley C. Lomo
Fang-I Lu
aDeqin Ma
Varsha Manucha
Rachel Angelica Mariani
Brock Aaron Martin
David S. McClintock
Anne M. Mills
Richard N. Mitchell
Hiroshi Miyamoto
Kristen E. Muller
Priya Nagarajan
Navneet Narula
Michiya Nishino
Maura O'Neil
Scott Roland Owens
Burcin Pehlivanoglu
Deniz Peker Barclift
Avani Anil Pendse
Andre Pinto
Susan Prendeville
Carlos N. Prieto Granada
Peter Pytel
Stephen S. Raab
Emilian V. Racila
Stanley J. Radio
Santiago Ramon Y Cajal
Kaaren K Reichard
Jordan P. Reynolds
Lisa M. Rooper
Andrew Eric Rosenberg
Ozlen Saglam
Ankur R. Sangoi
Kurt B. Schaberg
Qiuying (Judy) Shi
Wonwoo Shon
Pratibha S. Shukla
Gabriel Sica
Alexa Siddon
Anthony Sisk
Kalliopi P. Siziopikou
Stephanie Lynn Skala
Maxwell L. Smith
Isaac H. Solomon
Wei Song
Simona Stolnicu
Adrian Suarez
Paul E. Swanson
Benjamin Jack Swanson
Sara Szabo
Gary H. Tozbikian
Gulisa Turashvili
Andrew T. Turk
Efsevia Vakiani
Paul VanderLaan
Hanlin L. Wang
Stephen C. Ward
Kevin M. Waters
Jaclyn C. Watkins
Shi Wei
Hannah Y. Wen
Kwun Wah Wen
Kristy Wolniak
Deyin Xing
Ya Xu
Shaofeng N. Yan
Zhaohai Yang
Yunshin Albert Yeh
Huina Zhang
Xuchen Zhang
Bihong Zhao
Lei Zhao

To cite abstracts in this publication, please use the following format: **Author A, Author B, Author C, et al. Abstract title (abs#). In "File Title."** ***Laboratory Investigation*** **2022; 102 (suppl 1): page#**

372 Medullary Colon Cancer: Stage is the Most Important Prognostic Factor

Evi Abada[1], Hyejeong Jang[2], Seongho Kim[2], Othuke Abada[3], Rafic Beydoun[1]
[1]Wayne State University, Detroit, MI, [2]Karmanos Cancer Institute, Detroit, MI, [3]Ascension St. John Hospital, Detroit, MI

Disclosures: Evi Abada: None; Hyejeong Jang: None; Seongho Kim: None; Othuke Abada: None; Rafic Beydoun: None

Background: Medullary colon cancer (MCC) is a rare and distinct phenotype of colorectal cancers characterized histologically by poorly differentiated and undifferentiated carcinomas. We aimed to study the clinicopathologic characteristics, treatment received, and overall survival (OS) of this rare tumor in our patient population.

Design: We reviewed MCC cases from January 1996 to July 2020 at our institution and a total of 32 cases were identified. Five cases were excluded due to incomplete records. Histology slides were reviewed for characteristic tumor morphology. Additional clinical information including microsatellite instability (MSI) statuses was obtained from the electronic medical records. The univariable firth Cox regression analysis was performed for OS.

Results: Of the 27 patients included in the analysis, the median age at diagnosis was 76 years (range: 40-91). Sixteen (59%) were Caucasians, 5 (19%) were African Americans and 6 (22%) belonged to other ethnicities. MCC was more common in women (67%) than men (33%) and 96% of cases occurred in the right colon. The median CEA level at diagnosis was 2 ng/ml (range: 0.2-392.4). Pure medullary phenotype occurred in 52% of cases, medullary with mucinous differentiation was present in 37% of cases and medullary and other histologic patterns occurred in 11% of cases. Most tumors (93%) were poorly differentiated and 7% of tumors were undifferentiated. Lymphovascular invasion was present in 63%, perineural invasion occurred in 15% and, lymph node metastasis was present in 37% of cases respectively. Stage II and IV tumors were more common and occurred in 37% of cases respectively. In addition to surgery, 52% of patients received chemotherapy and only one patient (4%) received radiotherapy. Eleven patients (41%) had a metastatic disease which occurred more in the liver. Stage IV disease was associated with worse OS and this finding was statistically significant (HR:12.05, 95%CI:1.21-1624.38, P=0.031). Treatment received, mucinous differentiation, lymphovascular invasion, lymph node metastasis, perineural invasion and MSI status, all had no impact on overall survival. During a median follow up of 1.25 years (range: 1-5.25) the OS was not reached for all patients. The Cox proportional hazard regression analysis of OS is summarized in Table 1.

Univariable firth Cox proportional hazard regression analysis of overall survival (OS)

	Event/n	HR (95% CI)	P-value
Race			
White	1/16	Ref.	
African American	2/5	6.40 (0.82-71.86)	0.074
Other	1/6	3.29 (0.27-40.65)	0.317
Gender			
Female	4/18	Ref.	
Male	0/9	0.15 (0.00-1.46)	0.116
Portion of colon			
Right colon	4/26	Ref.	
Left colon	0/1	2.90 (0.02-30.25)	0.537
Histologic components			
Pure medullary	2/14	Ref.	
Medullary + mucinous	2/10	2.10 (0.32-13.97)	0.419
Medullary + others	0/3	0.90 (0.01-11.30)	0.946
Tumor grade			
Poor	4/25	Ref.	
Undifferentiated	0/2	0.78 (0.01-7.79)	0.868
Lymphovascular invasion			
Present	4/17	Ref.	
Absent	0/10	0.20 (0.00-1.85)	0.181
Lymph node metastasis			
Present	3/10	Ref.	
Absent	1/17	0.27 (0.03-1.63)	0.154
Perineural invasion			
Present	2/4	Ref.	
Absent	2/23	0.19 (0.03-1.27)	0.083
Margins			
Positive	1/4	Ref.	
Negative	3/23	0.33 (0.05-3.47)	0.305
AJCC Stage			
II	0/10	Ref.	

III	0/7	1.52 (0.01-280.26)	0.835
IV	4/10	12.05 (1.21-1624.38)	***0.031***
Chemotherapy			
Yes	2/14	Ref.	
No	2/13	1.10 (0.17-7.15)	0.913
Radiotherapy			
Yes	1/1	Ref.	
No	3/26	0.14 (0.02-1.54)	0.096
MSI high			
Yes	1/7	Ref.	
No	0/4	0.55 (0.00-10.55)	
Unknown	3/16	1.17 (0.19-12.22)	0.868

Event/n: The number of events and patients; HR: Hazard ratio; CI: Confidence interval; AJCC: Amere Event/n: The number of events and patients; HR: Hazard Ratio; CI: Confidence Interval; AJCC: American Joint Committee on Cancer; MSI: Microsatellite Instability

Figure 1 - 372

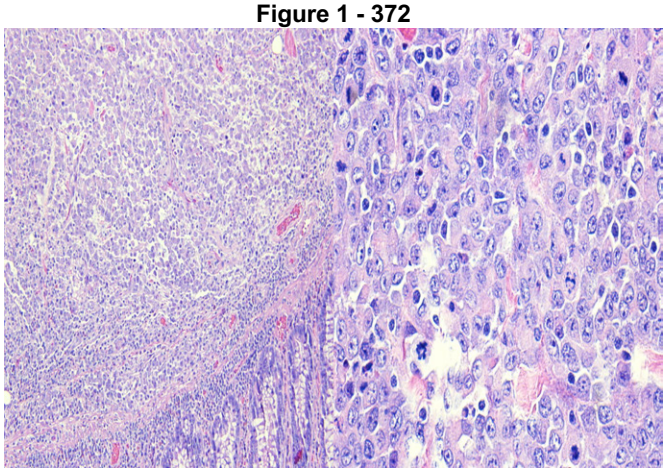

Figure 2 - 372

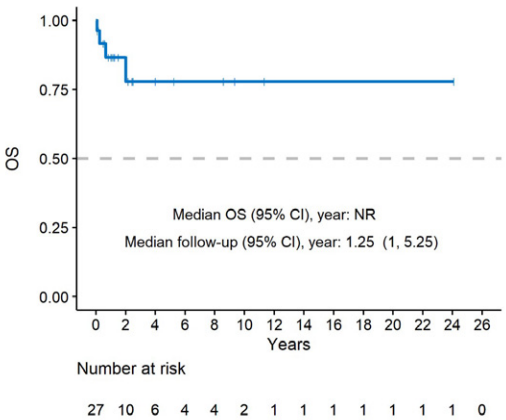

Conclusions: Based on our results, stage IV disease is associated with worse OS in MCC. Factors such as MSI status, mucinous differentiation, lymphovascular and perineural invasion have no impact on OS in MCC.

373 Grading Gastroenteropancreatic Neuroendocrine Tumors (GEP-NETs) Using Clinically Validated Ki-67 Digital Image Analysis Identifies Systematically Higher Proliferation Indices in Distant Metastases and the Superiority of Hotspot Over Whole Slide-Based Quantification

Ibrahim Abukhiran[1], Allen Choi[1], Andrew Bellizzi[1]
[1]University of Iowa Hospitals & Clinics, Iowa City, IA

Disclosures: Ibrahim Abukhiran: None; Allen Choi: None; Andrew Bellizzi: None

Background: There is ongoing controversy about best practice-grading of gastroenteropancreatic neuroendocrine tumors (GEP-NETs) using the Ki-67 proliferation index (PI). Guidance is lacking about the disease site (primary vs regional vs distant metastatic disease) and number of blocks to test. Manual counting of a hotspot field containing 500-2000 tumor nuclei is generally recommended, though digital image analysis could facilitate PI determination in whole tumor sections (the significance of which is not well-characterized). We sought to compare PIs in matched primary/regional/distant disease in both hotspots and whole tumor sections in our large institutional cohort of surgically resected GEP-NETs.

Design: Ki-67 immunohistochemistry (MIB 1; 1:200; HpH antigen retrieval) was performed on 371 whole tumor sections (167 primary tumors, 109 regional disease, and 95 distant metastasis) from 127 patients (43 pancreatic, 84 jejunoileal). Slides were digitally scanned at 20x magnification with a 3DHISTECH P1000 scanner (Budapest, Hungary). For each slide, two areas were annotated for subsequent digital image analysis: entire tumor area and one hotspot. Hotspots were identified by manual visualization of the entire tumor area at 10x magnification, selecting the most positive focus for digital annotation with an area of 0.46 mm2 (equal to a 40x field). The 3DHISTECH QuantCenter digital image analysis module was used to count and threshold

immunoreactive tumor cells using a clinically validated protocol in use in our laboratory since Spring 2020. Mann Whitney tests, one-way ANOVA, and simple linear regression were used with $p<0.05$ considered significant.

Results: The average number of nuclei counted in the hotspot annotations was 1400 (range 128-2737). In 69% (249/361) of sections, hotspot analysis revealed a higher PI compared to whole slide analysis. The mean Ki-67 PI for all sections was 3.6% using hotspot analysis vs 1.8% using whole slide analysis ($p<0.0001$). Hotspot analysis upgraded 16% of the sections from G1 to G2 (14%; 49/361) or G2 to G3 (2%; 7/361) compared to whole slide analysis. No cases were upgraded by whole slide analysis. The mean Ki-67 PI was higher in distant disease (mean PI 6.5%) compared to regional disease (mean PI 3.3%) or primary tumors (mean PI 3.7%) ($p= 0.01$). There was no statistically significant difference in the mean PI between regional and primary tumors. Primary tumor grade failed to predict the grade in regional and distant metastatic sites by simple linear regression. Detailed data are presented in the Table and Figures.

Tukey's Multiple Comparisons Test	Mean PI 1	Mean PI 2	P Value
Primary (1) vs Regional (2)	3.762	3.389	0.9276
Primary (1) vs Distant (2)	3.762	6.527	0.0356
Regional (1) vs Distant (2)	3.389	6.527	0.0143
	Grade (rows sum to 100%)		
Disease Site	G1	G2	G3
Primary tumor	84.1%	15.0%	0.9%
Regional disease	73.1%	26.9%	0.0%
Distant disease	62.6%	34.2%	3.2%
Case Level	75.41%	23.38%	1.22%
Grade Concordance in Matched Primary/Regional/Distant disease	**n**	**%**	
Concordant	41	56%	
Discordant	32	44%	
Type of Grade Discordance (n=32)	n	%	
Distant highest	17	53%	
Regional higher, no distant to compare	5	16%	
Primary highest	5	16%	
Regional highest	5	16%	
Analysis Protocol Comparison (one sample t test)	**Hotspot Analysis**	**Whole Slide Analysis**	
Actual mean (n=362)	3.606	1.861	<0.0001
Ki-67 proliferation index	n	%	
Higher PI by hotspot analysis	249	69%	
Higher PI by whole slide analysis	112	31%	
Grade Concordance Between Hotspot vs Whole Slide Analysis	n	%	
Concordant grades	305	84%	
Higher grade by hotspot analysis	56	16%	
Higher grade by whole slide analysis	0	0%	

Figure 1 - 373

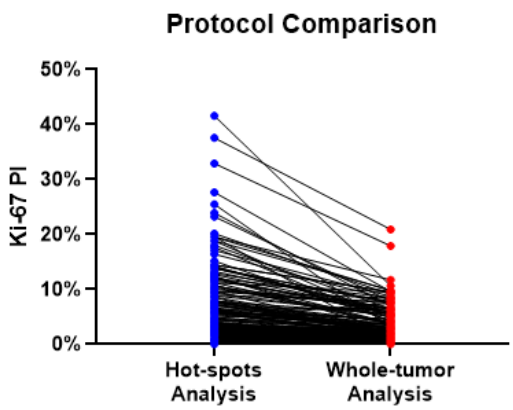

Figure 2 – 373

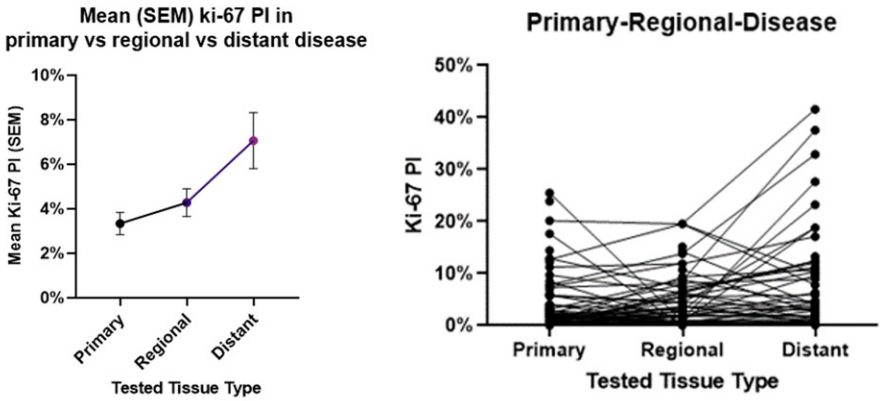

Conclusions:

- The Ki-67 PI demonstrates substantial intratumoral heterogeneity, both within sections and between disease sites. Hotspot analysis at the slide level identifies this heterogeneity, resulting in the identification of more higher grade cases.
- The Ki-67 PI is systematically higher in distant metastases compared to primary and regional disease. Thus, analysis of a single section of primary tumor is insufficient to identify higher grade tumor.
- In our practice we routinely perform Ki-67 PI digital image analysis in matched primary/regional/distant disease.

374 Tumour Budding is a Prognostic Biomarker in Biopsy and Resection Specimens of Post-Neoadjuvant Chemoradiotherapy–Treated Rectal Adenocarcinoma

Susan Aherne[1], Eanna Ryan[1], David Gibbons[1], Robert Geraghty[1], Aoife McCarthy[2], Matthew Davey[1], Iris Nagtegaal[3], Des Winter[1], Kieran Sheahan[1]
[1]St. Vincent's University Hospital, Dublin, Ireland, [2]Bon Secours Hospital Cork, Cork, Ireland, [3]Radboud University Medical Center, Nijmegen, Netherlands

Disclosures: Susan Aherne: None; Eanna Ryan: None; David Gibbons: None; Robert Geraghty: None; Aoife McCarthy: None; Matthew Davey: None; Iris Nagtegaal: None; Des Winter: None; Kieran Sheahan: *Grant or Research Support*, Roche

Background: Tumour budding (TB) in rectal cancer (RC) is a marker of tumour aggressiveness and predicts worse oncological outcomes. We aimed to investigate the feasibility and utility of TB assessment in diagnostic biopsy tissue for predicting outcomes and tailoring therapeutic decision-making in RC treated with neoadjuvant chemoradiotherapy (nCRT).

Design: A single centre, retrospective cohort study was conducted. TB was assessed using the “hotspot” and the “revised ITBCC” methodology (Zlobec at al. Virchows Archiv, 2021). Haematoxylin & Eosin (H&E) and AE1/AE3 Cytokeratin (CK) stains for the assessment of PTB and ITB in biopsy and subsequent resection specimens were compared. Logistic regression assessed peritumoral (PTB) and intratumoral budding (ITB) as predictors of lymph node metastasis (LNM). Cox regression and Kaplan-Meier analyses investigated their utility as a predictor of disease-free (DFS) and overall (OS) survival.

Results: One-hundred and forty-six patients were included of whom 91 were male (62.3%). In total, 37 cases (25.3%) had ITB on H&E and 79 (54.1%) had ITB on CK on biopsy tissue. On univariable analysis, H&E ITB (OR: 2.709, 95% CI: 1.261-5.822, p=0.011) and CK ITB (OR: 2.165; 95% CI: 1.076-4.357, p=0.030) predicted LNM. However, H&E ITB (OR: 2.749; 95% CI: 1.258-6.528, p=0.022) was the sole independent predictor of LNM. In Kaplan-Meier analysis, any ITB identified on biopsy was associated with worse OS (H&E: p=0.003, CK: p=0.009) and DFS (H&E: p=0.012; CK: p=0.045). Similarly, CK PTB was associated with worse OS (p=0.047) and both CK PTB and ITB with worse DFS (PTB: p=0.014; ITB: p=0.019). On multivariable analysis H&E ITB independently predicted OS (HR: 2.930; 95% CI: 1.261-6.809) and DFS (HR: 2.072; 95% CI: 1.031-4.164). CK PTB grading on resections independently predicted OS (HR: 3.417, 95% CI 1.45-8.053, p=0.005).

Conclusions: Assessment of TB using H&E and CK staining is feasible in RC biopsy and post-nCRT treated resection specimens, and is associated with LNM and worse survival outcomes. The revised ITBCC method may outperform the original in clinical practice. Future management strategies for RC could be tailored to incorporate these findings, in conjunction with an immunoscore.

375 What is My N-Terminus MSH6 Antibody Missing?

Beena Ahsan[1], Melissa Tjota[2], Peng Wang[2], Lindsay Alpert[1], Lindsay Yassan[1], Christopher Weber[1], Ardaman Shergill[1], Girish Venkataraman[2], Jeremy Segal[1], John Hart[1], Namrata Setia[1]
[1]University of Chicago, Chicago, IL, [2]University of Chicago Medical Center, Chicago, IL

Disclosures: Beena Ahsan: None; Melissa Tjota: None; Peng Wang: None; Lindsay Alpert: None; Lindsay Yassan: None; Christopher Weber: None; Ardaman Shergill: None; Girish Venkataraman: None; Jeremy Segal: None; John Hart: None; Namrata Setia: None

Background: Universal MMR immunohistochemical testing is an acceptable screen for identifying patients with Lynch syndrome-related cancers and potential immunotherapy candidates. The propensity of MSH6 immunohistochemistry (IHC) to show variable staining patterns has been reported. In this study, we explored if molecular or antibody parameters affected the MSH6 immunohistochemical staining pattern and reviewed the clinical impact of the variability in staining.

Design: Oncoplus data was queried to identify tumors with only pathogenic alteration(s) in the MSH6 gene. Tumor NGS and antibody parameters, including the location of the mutation, the number of MSH6 alteration/tumor, tumor MSI status, variant allele fractions, tumor-site specific driver mutation, and epitope for MSH6 antibody were reviewed. Information regarding the history of prior radiation treatment, germline testing for Lynch syndrome, and MLH1 promoter hypermethylation were obtained from chart review.

Results: Thirty-one pathogenic genomic alterations were found in the MSH6 gene from 24 solid tumor samples (Table 1). Length-altering mutations in the polycytosine repeat (C8) on exon 5 at/near amino acid 1088 were the most common alteration (19/31, Figure 1). MSH6 IHC was performed in 19 samples, of which 16 showed retained expression. Retained expression was seen despite more than one genomic alteration in the MSH6 gene in 5/16 cases and MSI-H status in 11/16 cases. Tumor-site-specific driver mutations were present in all cases. Of the 16 samples, MSH6 mutations were determined to be secondary to MSH6-Lynch syndrome in 5 samples, prior irradiation in 1 sample, and somatic hypermutation due to germline/sporadic DNA repair-deficient tumors in 10 samples. The MSH6 IHC antibody epitope for all tested cases was present within amino acids 1-50 in exon 1.

Etiology of MSH6 mutation	Age	Gender	Tumor site/Type	MSH6 alteration (pnomenclature, NM_000179.2)	MSH6 alteration#1	MSH6 alteration#2	IHC performed (Yes/No)	Antibody epitope	MSH6 IHC	MSI status	MSH6 VAF (TUMOR %)	Type-specific driver mutations (Present, pathogenic variants only)
Radiation-related MSH6 mutation	52	M	Pancreas/mucinous adenocarcinoma	F1088Sfs*2	del1 poly(C) repeat sequence of exon 5		Yes	aa 1-50 in exon 1	Loss	MSI	12% (30%)	Present (KRAS, GNAS, PALB2, MSH3 mut)
MSH6-mutation Lynch syndrome	67	F	Breast metastasis/parotid acinic cell carcinoma	A1320Sfs*5	dup19 in exon 9		Yes	aa 1-50	Loss	MSI	61% (90%)	Present (TP53, PTEN mut)
MSH6-mutation Lynch syndrome	68	F	Lung metastasis/ parotid acinic cell carcinoma	A1320Sfs*5	dup19 in exon 9		Yes	aa 1-50	Loss	MSI	40% (40%)	Present (TP53, PTEN mut)
Secondary hypermutation related MSH6 mutation	66	M	Colon/MLH1 promoter hypermethylation	F1088Lfs*5 , Y1159*	dup1 poly(C) repeat sequence of exon 5	dup1 in exon 6	Yes	aa 1-50	Retained	MSI	18%, 16% (25%)	Present (APC, KRAS mut)
Radiation-related MSH6 mutation	50	M	Colon/adenocarcinoma	F1088Sfs*2, MSH6 rearrangement	dup2 poly(C) repeat sequence of exon 5	rearrangement exon 5	Yes	aa 1-50	Retained	MSI	15% (50%)	Present (APC, ATM, TP53 mut)

MSH6-mutation Lynch syndrome	61	M	Chest wall/malignant mesothelioma	F1088Lfs*5	dup1 poly(C) repeat sequence of exon 5		Yes	aa 1-50	Retained	MSS	16% (85%)	Present (PTEN mut)
MSH6-mutation Lynch syndrome	61	M	Bone metastasis/malignant mesothelioma	F1088Lfs*5	dup1 poly(C) repeat sequence of exon 5		Yes	aa 1-50	Retained	MSS	22% (80%)	Present (PTEN mut)
MSH6-mutation Lynch syndrome	63	F	Ovarian adenocarcinoma and endometrial adenocarcinoma	R1334Q	intron/exon boundary of exon 9		Yes	aa 1-50	Retained	MSS	15% (70%)	Present (TP53/CDKN2A loss)
MSH6-mutation Lynch syndrome	79	M	Gastric/tubular type adenocarcinoma	F1104Lfs*11, F1088Lfs*5	dup1 poly(C) repeat sequence of exon 5	del1 poly(T) repeat sequence of exon 5	Yes	aa 1-50	Retained	MSI	12%, 6% (40%)	Present (TP53 mut)
MSH6-mutation Lynch syndrome	81	F	Soft tissue/low-intermediate grade sarcoma	F1088Lfs*5	del1 poly(C) repeat sequence of exon 5		Yes	aa 1-50	Retained	MSS	12%, 6% (40%)	Present (MDM2 amplification, CDKN2A loss)
Secondary hypermutation related MSH6 mutation	73	F	Colon/PMS2 mutated Lynch CRC	F1088Sfs*2	del1 poly(C) repeat sequence of exon 5		Yes	aa 1-50	Retained	MSI	19% (60%)	Present (APC mut)
Secondary hypermutation related MSH6 mutation	83	F	Colon/MLH1 promoter hypermethylated CRC	F1088Lfs*5	dup1 poly(C) repeat sequence of exon 5		Yes	aa 1-50	Retained	MSI	17% (70%)	Present (BRAF mut)
Secondary hypermutation related MSH6 mutation	66	F	Periaortic metastasis/uterine endometrioid adenocarcinoma	F1088Sfs*2	del1 poly(C) repeat sequence of exon 5		Yes	aa 1-50	Retained	MSI	48% (70%)	Present (ARID1A, CTNNB1, PTEN mut)
Secondary hypermutation related MSH6 mutation	71	M	Colon/sporadic MLH1 mutated CRC	F1088Sfs*2, F1088Lfs*5	del1 poly(C) repeat sequence of exon 5	dup1 poly(C) repeat sequence of exon 5	Yes	aa 1-50	Retained	MSI	14% (50%), 9% (50%)	Present (APC mut)
Secondary hypermutation related MSH6 mutation	67	M	Mesenteric metastasis/sporadic MLH1 mutated CRC	C1088Lfs*5	del1 poly(C) repeat sequence of exon 5		Yes	aa 1-50	Retained	MSI	14% (40%)	Present (ARID1A, ATM, FBXW7 mut)
Secondary hypermutation related MSH6 mutation	88	F	Colon/MLH1 promoter hypermethylated CRC	C1088Lfs*5	dup1 poly(C) repeat sequence of exon 5		Yes	aa 1-50	Retained	MSI	16% (40%)	Present (BRAF mut)
Secondary hypermutation related MSH6 mutation	38	M	Colon/POLE mut adenocarcinoma CRC	E1322*, E1234*	point mutation in exon 9	point mutation in exon 8	Yes	aa 1-50	Retained	MSS	32% (40%), 32% (40%)	Present (APC mut)
Secondary hypermutation related MSH6 mutation	49	F	Uterus/Endometrial MLH1 promoter hypermethylated adenocarcinoma	F1088Sfs*2, R174Sfs*7	del1 poly(C) repeat sequence of exon 5	del2 in exon 3	Yes	aa 1-50	Retained	MSI	16%, 5% (30%)	Present (ARID1A, AKT1, BRCA1 mut)
Secondary hypermutation related MSH6 mutation	53	F	Ileal metastasis/rectal MLH1 mutated Lynch CRC	F1088Sfs*2	del1 poly(C) repeat sequence of exon 5		Yes	aa 1-50	Retained NA	MSI	34 (70%)	Present (MLH1, MSH3, ARID1A, PIK3CA mut)
Radiation-related MSH6 mutation	78	M	Esophagus/adenocarcinoma	F1088Sfs*2	dup1 poly(C) repeat sequence of exon 5		No	NA	NA	MSI	16% (30%)	Present (CDH1, TP53 mut)

MSH6-mutation Lynch syndrome	63	F	Liver metastasis/uveal melanoma	R379*	del5 in exon 4		No	NA	NA	MSS	46% (60%)	Present (CHEK2 mut)
MSH6-mutation Lynch syndrome	60	M	Liver/well-differentiated hepatocellular carcinoma	D1112Efs*2	dup4 in exon 5		No	NA	NA	MSS	46% (70%)	Present (TERT promoter mut)
Secondary hypermutation related MSH6 mutation	71	M	Lymph node metastasis/lung SCC	F1088Lfs*5, R1005*	dup1 poly(C) repeat sequence of exon 5	point mutation in exon 4	No	NA	NA	MSI	52%, 29% (60%)	Present (TP53, PIK3CA mut)
Secondary hypermutation related MSH6 mutation	31	M	Retroperitoneum/PMS2 mutated Lynch sarcoma	F1088Lfs*5	dup1 poly(C) repeat sequence of exon 5		No	NA	NA	MSI	32% (80%)	Present (ATRX mut, RB1 loss)

Figure 1 - 375

Conclusions: MSH6 mutations are frequently present in the C(8) repeat at amino acid 1088 (near C-terminus), which may result in a disrupted or absent protein product. A disrupted but not absent protein product may result in false-positive staining with an N-terminus MSH6 antibody. The N-terminus antibody appropriately reduces the detection of secondary MSH6 mutations in the setting of somatic hypermutation; however, it may also give misleading retained MSH6 and/or MSS status MSH6-related Lynch syndrome patients and radiation-related tumors. Pathologists should be aware of this pitfall and alert the oncologists and gastroenterologists of this possibility.

376 Clinicopathologic Characteristics and Significance of Cecal/Periappendiceal Patch of Inflammation in Patients with Left-Sided Ulcerative Colitis

Nazire Albayrak[1], Bella Liu[1], Swati Bhardwaj[1], Hansen Lam[2], John Paulsen Jr.[1], Qingqing Liu[1], Noam Harpaz[3], Alexandros Polydorides[1]

[1]Icahn School of Medicine at Mount Sinai, New York, NY, [2]Mount Sinai Hospital, New York, NY, [3]Mount Sinai Medical Center, New York, NY

Disclosures: Nazire Albayrak: None; Bella Liu: None; Swati Bhardwaj: None; Hansen Lam: None; John Paulsen Jr.: None; Qingqing Liu: None; Noam Harpaz: None; Alexandros Polydorides: None

Background: Ulcerative colitis (UC) is characterized by continuous mucosal inflammation of the rectum extending uninterrupted to a variable portion of colon proximally; the Montreal Classification subdivides UC into proctitis, left-sided colitis and pancolitis. However, in some patients with distal colitis, a distinct pattern of skip inflammation involves the cecum and/or appendiceal orifice (cecal/periappendiceal “patch”), but data on this entity have been contradictory and its significance and prognosis are debated.

Design: We identified 102 cases of left-sided UC with a cecal/periappendiceal patch (2007-2021) and compared them to 105 controls (left-sided UC without patch) along demographics, severity/extent of colitis, and pharmacotherapy level (increasingly: salicylates, immunomodulators, biologics). Disease outcomes (colitis-related dysplasia, pouchitis, Crohn disease [CD] diagnosis) were compared among all cases and long-term progression (proximal disease extension, subsequent colectomy, pharmacotherapy escalation) was evaluated among biopsies.

Results: In multivariate analysis, patients with a patch were younger (median age 31 years [IQR: 25-45] vs. 40 years [IQR: 31-53]; p=0.014, OR: 1.02 per year [CI: 1.01-1.04]) and more likely to have proctosigmoiditis only (55.9% vs. 33.3%; p=0.002, OR: 2.54 [CI: 1.43-4.53]), compared to patients without a patch. There were no significant differences between the 2 groups in terms of sex, type of specimen, inflammation severity, and the presence of ileitis, appendicitis, *C. difficile* infection, or inflammatory polyps. During follow-up, patients with a patch were more likely to eventually be diagnosed with CD (6.9% vs. 1.0%, p=0.033), but had no differences in the rate of dysplasia, pouchitis, and highest pharmacotherapy level compared to patients with only left-sided colitis. Among biopsies, cases with a patch were more likely to show proximal extension of histologic inflammation (30.2% vs. 15.2%,

p=0.022), but showed similar rates of subsequent colectomy and pharmacotherapy escalation (above salicylates) to cases without a patch.

Conclusions: Cecal/periappendiceal skip inflammation in left-sided UC occurs more often in younger patients and those with proctosigmoiditis and is associated with proximal disease extension and, in a minority of cases, change of diagnosis to CD. However, it does not portend an increased risk of dysplasia, colectomy, or therapy escalation compared to patients with only left-sided UC.

377 Endometriosis Involving the Gastrointestinal Tract -Additional Observations on its Quasi-Neoplastic Nature

Khaled Algashaamy[1], Abhilasha Ghildyal[2], Satyapal Chahar[3], Monica Garcia-Buitrago[4], Elizabeth Montgomery[5]
[1]University of Miami/Jackson Memorial Hospital, Miami, FL, [2]Jackson Memorial Hospital, Miami, FL, [3]Memorial Sloan Kettering Cancer Center, New York, NY, [4]University of Miami Miller School of Medicine/Jackson Health System, Miami, FL, [5]University of Miami Miller School of Medicine, Miami, FL

Disclosures: Khaled Algashaamy: None; Abhilasha Ghildyal: None; Satyapal Chahar: None; Monica Garcia-Buitrago: None; Elizabeth Montgomery: None

Background: Endometriosis, while benign, displays neoplastic characteristics, including reported mutations in carcinoma-associated genes including *ARID1A*, *PIK3CA*, *KRAS*, or *PPP2R1A* in a subset of cases, invasive growth, and multicentricity. While endometriosis typically manifests in the ovaries; gastrointestinal tract involvement has been reported in 3% to 37% of women with endometriosis. We noted an index case in which endometriosis colonized colonic mucosa, replacing the epithelium overlying the pre-existing basement membrane in a manner identical to that of metastatic carcinomas. We studied the frequency of this phenomenon in cases reviewed in our institution.

Design: We conducted a retrospective search of our laboratory information system (LIS), retrieving all gastrointestinal specimens that had a diagnosis of endometriosis between 2016 and 2021. Our search included biopsies and resection specimens received by our laboratory for a variety of clinical indications. Identified cases were reviewed by the authors to assess for mucosal colonization.

Results: Our search identified 24 cases from women ranging in age from 29 to 83 years (mean and median, 48 years). Endometriosis most frequently involved the rectum (9, 37.5%), followed by the rectosigmoid and sigmoid colon (8, 33.3%), appendix (4, 16.7%), colon, not otherwise specified (2, 8.3%), and small intestine (1, 4.2%). Although most examples lacked extension into the mucosa, involving the muscularis propria, sub-serosal and serosal tissues (18; 75%), in 6 patients, endometriosis involved the mucosa (25%) of the rectum or sigmoid colon. Mucosal extension by the endometrial glands was seen with or without stroma. Epithelial colonization was seen in 4 of the 6 cases, and highlighted by immunohistochemical stains (estrogen receptor [ER] and paired box gene [PAX-8]).

Figure 1 - 377

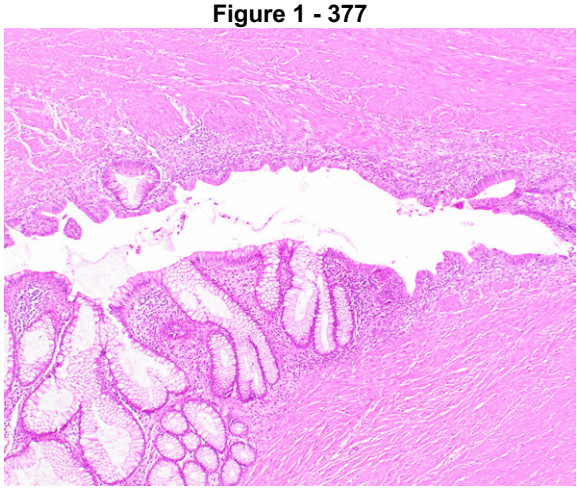

Figure 2 - 377

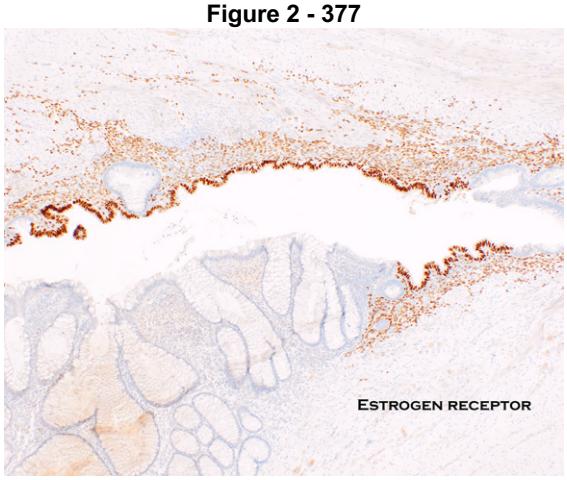

Conclusions: Epithelial colonization by endometriotic glands mirrors the phenomenon of colonization of pre-existing mucosa of the gastrointestinal tract by metastatic carcinomas, a further observation on the quasi-neoplastic qualities of endometriosis. Additionally, it presents a diagnostic pitfall. Attention to patient demographics, careful histologic examination and immunohistochemistry can assist in arriving at an accurate diagnosis in this situation.

378 Clinical Nodal Stage and Distance of Tumor Bed to Proximal Margin Predict Recurrence in Esophageal Cancer Patients with Pathologic Complete Response After Neoadjuvant Chemoradiation and Surgery

Khaled Alkhateeb[1], Jason Hornick[1], James Cleary[2], Jon Wee[1], Lei Zhao[1]
[1]Brigham and Women's Hospital, Harvard Medical School, Boston, MA, [2]Dana-Farber Cancer Institute, Brigham and Women's Hospital, Harvard Medical School, Boston, MA

Disclosures: Khaled Alkhateeb: None; Jason Hornick: *Consultant*, Aadi Biosciences, TRACON Pharmaceuticals; James Cleary: *Grant or Research Support*, Merck, AstraZeneca, Esperas Pharma, Bayer, Tesaro; *Advisory Board Member*, Syros Pharmaceuticals; Jon Wee: None; Lei Zhao: None

Background: Pathologic complete response (pCR) following neoadjuvant chemoradiotherapy and surgery (trimodality therapy) for esophageal adenocarcinoma (EAC) and squamous cell carcinoma (ESCC) is associated with significantly improved outcomes. However, approximately 20-30% of these patients develop recurrence. Strategies to risk stratify patients who achieve a pCR are greatly needed. The aim of this study was to identify features associated with recurrence in esophageal cancer patients who achieved pCR following trimodality therapy.

Design: Data from 238 esophageal cancer patients with pCR following trimodality therapy was retrospectively retrieved from a single-institution database. Clinical factors (including tumor location, clinical T (cT) and clinical N (cN) stage) and pathologic factors (including tumor type, total lymph nodes harvested, and presence of signet-ring-cell morphology on pretreatment biopsies) were evaluated in all patients (Table). Additional pathologic factors including tumor bed distance to resection margins and presence of treatment effect in lymph nodes were evaluated in 52 patients (Table).

Results: Among the 238 patients with pCR, 174 had EAC (73.1%), and 64 had ESCC (26.9%). Fifty-five patients (23.1%) developed recurrences (23.6% EAC, 21.9% ESCC). Patients with EAC developed recurrences significantly earlier than those with ESCC (mean = 10.7 months vs. 19.6 months; *P*=0.048). Locoregional recurrence was more frequent in patients with ESCC than those with EAC (*P*=0.09). Both overall and distant recurrences were associated with cN stage (*P*=0.001 and 0.003, respectively). Distance of tumor bed from the proximal resection margin within 5 cm was significantly associated with local recurrence (*P*=0.016) for both EAC and ESCC. The presence of a signet-ring-cell component in pre-treatment biopsies was a risk factor for local recurrence of EAC by COX regression analysis (hazard ratio: 9.1; *P*=0.007). For ESCC, only total lymph node harvest of <10 lymph nodes was associated with risk of distant recurrence (hazard ratio: 8.2; *P*=0.01).

Variable	Overall	EAC	ESCC	*P* value
n	238 (100%)	174 (73.1%)	64 (26.9%)	
Age (y) (n=238)	64.5 (±9.7)	65.0 (±9.8)	63.4 (±9.5)	0.26
Gender (n=238)				
M	180 (75.6%)	144 (82.8%)	36 (56.3%)	<0.001
F	58 (24.4%)	30 (17.2%)	28 (43.8%)	
Clinical T stage (n=201)				
cT1	9 (4.5%)	6 (4.0%)	3 (5.8%)	0.76
cT2	54 (26.9%)	39 (26.2%)	15 (28.8%)	
cT3	136 (67.7%)	103 (69.1%)	33 (63.5%)	
cT4	2 (1.0%)	1 (0.7%)	1 (1.9%)	
Clinical N stage (n=212)				0.61
cN0	70 (33.0%)	51 (32.9%)	19 (33.3%)	
cN1	111 (52.4%)	80 (51.6%)	31 (54.4%)	
cN2	24 (11.3%)	17 (11.0%)	7 (12.3%)	
cN3	4 (1.9%)	4 (2.6%)	0 (0%)	
cNX	3 (1.4%)	3 (1.9%)	0 (0%)	
Histologic grade (n=226)				0.04
G1	4 (1.8%)	2 (1.2%)	2 (3.4%)	

G2	58 (25.7%)	40 (24.0%)	18 (30.5%)	
G3	79 (35.0%)	67 (40.1%)	12 (20.3%)	
GX	85 (37.6%)	58 (34.7%)	27 (45.8%)	
Tumor location (n=238)				
Upper third	6 (2.5%)	0 (0%)	9 (9.4%)	<0.001
Middle third	45 (18.9%)	12 (6.9%)	33 (51.6%)	
Lower third/GEJ	187 (78.6%)	162 (93.1%)	25 (39.1%)	
Barrett's esophagus (n=238)	49 (20.6%)	44 (25.3%)	5 (7.8%)	0.003
Signet-ring-cell component on pretreatment biopsy (n=238)	15 (6.3%)	15 (8.6%)	0 (0%)	0.01
Tumor bed size (n=145)	3.2 (±1.8)	3.4 (±1.8)	2.6 (±1.5)	0.02
Distance to proximal margin (n=51)	6.9 (±3.3)	7.1 (±3.2)	6.0 (±3.8)	0.36
Distance to distal margin (n=52)	6.8 (±4.9)	5.8 (±3.0)	11.5 (±8.6)	<0.001
Distance to radial (n=46)	0.43 (±0.32)	0.45 (±0.33)	0.29 (±0.28)	0.23
Tumor bed entirely submitted (n=52)	50 (96.2%)	41 (95.3%)	19 (100%)	1.0
# of blocks with tumor bed (n=52)	11.3 (±7.5)	11.5 (±7.1)	10.7 (±9.7)	0.78
Acellular mucin (n=52)	7 (13.5%)	7 (16.3%)	0 (0%)	0.33
Lymph node count (n=238)	19.2 (±9.2)	19.4 (±9.7)	18.6 (±7.9)	0.52
Lymph nodes with treatment effect (n=51)	19 (37.3%)	16 (38.1%)	3 (33.3%)	1.0
Number of lymph nodes with treatment effect (n=19)	3.0 (±2.0)	3.2 (±2.1)	2.0 (±1.0)	0.36
Follow-up (y)(n=238)	3.4 (±3.1)	3.3 (±3.1)	3.7 (±3.1)	0.47
Overall survival (mo) (n=238)	41.5 (±37.1)	40.8 (±37.4)	43.4 (±36.6)	0.63
Disease-free survival (mo)(n=238)	38.4 (±37.6)	37.4 (±37.7)	41.1 (±37.3)	0.50
Recurrence (n=238)				
Overall	55 (23.1%)	41 (23.6%)	14 (21.9%)	0.86
Locoregional	12 (5.0%)	6 (3.4%)	6 (9.4%)	0.09
Distant	36 (15.1%)	30 (17.2%)	6 (9.4%)	0.16
Locoregional and distant	7 (2.9%)	5 (2.9%)	2 (3.1%)	1.0
Time to recurrence	13.0 (±14.66)	10.7 (±12.7)	19.6 (±18.1)	0.05

Figure 1 - 378

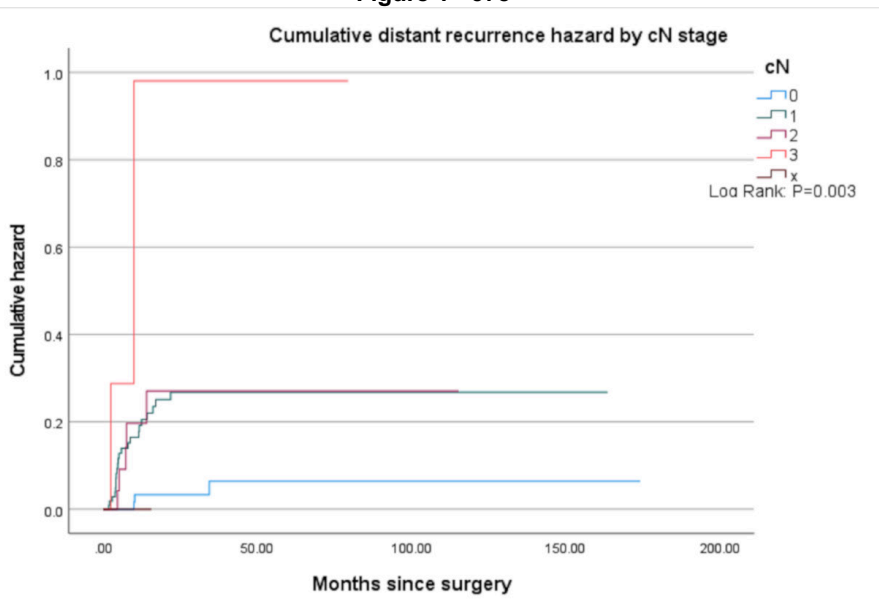

Figure 2 – 378

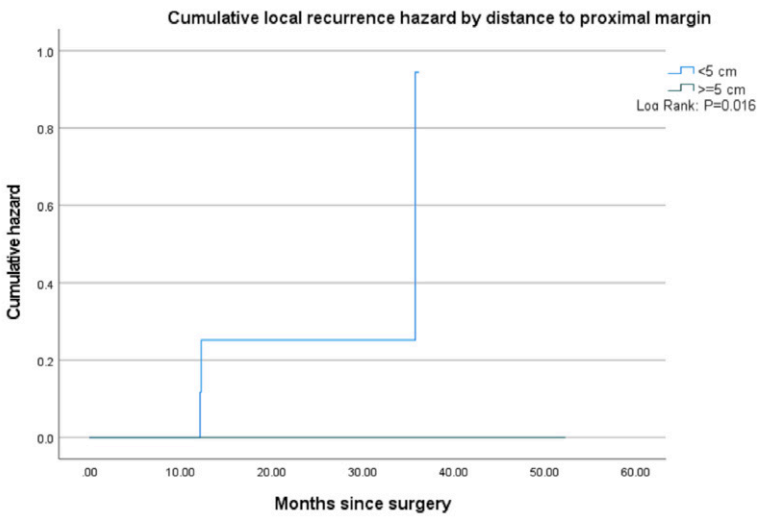

Conclusions: Our study shows that advanced cN stage, distance from the proximal margin, presence of a signet-ring-cell component and low total lymph node harvest were associated with recurrence following pCR. Considering the recent approval of immune checkpoint inhibitor adjuvant therapy for patients with residual EAC following neoadjuvant therapy, these findings have potential implications for the development of future treatment strategies for subsets of patients with pCR.

379 Study of Inflammatory Bowel Disease in Ethnic Groups and the Impact of the COVID-19 Pandemic

Krisha Amin[1], Pallavi Patil[2], Carlos Galliani[3]
[1]University of South Alabama College of Medicine, Mobile, AL, [2]Baylor University Medical Center Dallas, Dallas, TX, [3]USA, Children's and Women's Hospital, Mobile, AL

Disclosures: Krisha Amin: None; Pallavi Patil: None; Carlos Galliani: None

Background: Impact of the COVID-19 pandemic on disease management and progression of inflammatory bowel disease (IBD) in various ethnic groups is not known. We aimed to study the prevalence of IBD in various ethnic groups and the impact of the COVID-19 pandemic. The objectives of the study were to determine severity of IBD and compliance in various ethnic groups, to compare status at follow-up before the pandemic and recent follow-up during the pandemic.

Design: Our records were queried from 2017 to 2021 for diagnostic terms related to inflammatory bowel disease. Retrospective chart review was performed of the cases found in the search results to determine diagnosis of inflammatory bowel disease. Relevant clinicopathological parameters were recorded including status at follow-up before the pandemic and most recent follow-up during the pandemic.

Results: Total of 350 patients with inflammatory bowel disease included 232 White and 118 Black patients with a mean age of 43 years and 36 years respectively. Crohn's disease (CD) was found to be more common than ulcerative colitis (UC), only 5 cases of indeterminate colitis were noted, Table. In both UC and CD, more Black patients presented with anemia and emergency department (ED) visits. Overall Black patients had lower compliance to medication and follow-up appointments, Table. Loss of insurance was most frequently mentioned as the reason for loss of compliance. In CD, Black patients presented with greater severity of disease in the form of more ED visits, hospital admissions, duration of hospital stays, IBD related surgeries, Table. During the pandemic compliance for follow-up appointments significantly decreased for all patients (from 83% to 58% in White patients and from 69% to 48% in Black patients respectively), ($p<0.001$). No SARS-CoV-2 infection related exacerbation of IBD was reported.

Table: Comparison of clinicopathological features of inflammatory bowel disease in ethnic groups and impact of the COVID-19 pandemic							
		UC n=123		p-value	CD n=222		p-value
		White n=90	Black n=33		White n=138	Black n=84	
Mean age, years		46	40	0.083	42	35	**0.003**
Anemia n (%)		27 (30%)	21 (63.6%)	**0.001**	45 (32.6%)	54 (64.3%)	**0.00001**
Site of initial visit n (%)	**ED**	14 (15.6%)	10 (30.3%)	0.068	25 (18.1%)	54 (64.3%)	**<0.0005**
	Clinic	76 (84.4%)	23 (69.7%)		113 (81.9%)	30 (35.7%)	
Number of biopsies n (%)	1	23 (25.6%)	6 (18.2%)	0.389	38 (27.5%)	15 (17.9%)	0.103
	2-5	40 (44.4%)	16 (48.5%)	0.689	68 (49.3%)	39 (46.4%)	0.674
	6-10	25 (27.8%)	8 (24.2%)	0.689	24 (17.4%)	26 (30.1%)	**0.027**
	10+	2 (2.2%)	3 (9.1%)	0.472	8 (5.8%)	4 (4.8%)	0.749
Mean ED visits, n		0.5	1.563	**0.036**	1.14	3.4	**0.0003**
Mean hospital admissions, n		0.582	1.625	0.062	1.225	2.940	**0.004**
Mean hospital stay, days		0.316	0.843	0.112	0.629	1.565	**0.004**
Mean unscheduled follow-up, n		1.526	3.469	0.159	2.801	8.825	**0.0004**
Extraintestinal manifestations, n		14 (15.6%)	7 (21.2%)	0.465	51 (37%)	41 (48.8%)	0.083
Comorbidities, n		20 (22.2%)	7 (21.2%)	0.904	32 (23.2%)	22 (26.2%)	0.610
IBD related surgeries, n		33 (36.7%)	8 (24.2%)	0.194	74 (53.6%)	57 (67.9%)	**0.036**
Follow-up compliance before pandemic, n		63 (n=73) (86.3%)	24 (n=32) (75%)	0.159	92 (n=112) (82.1%)	51 (n=76) (67.1%)	**0.018**
Follow-up compliance during pandemic, n		48 (n=83) (57.8%)	17 (n=32) (53.1%)	0.645	75 (n=129) (58.1%)	38 (n=81) (46.9%)	0.126
Medication compliance		83 (92.2%)	24 (72.7%)	**0.004**	115 (83.3%)	56 (66.7%)	**0.004**

Conclusions: Socioeconomical factors and the COVID-19 pandemic influenced access to healthcare and progression of IBD. Reduced compliance to follow-up was noted in all ethnic groups during the pandemic. Greater severity of disease especially in case of CD, and lower compliance to medication in the Black population were noted. No exacerbation of IBD was reported due to SARS-CoV-2 infection.

380 Pancreatic Acinar Metaplasia (PAM) Marks a Distinct Group of Patients with Gastroesophageal Reflux Disease (GERD) Who Are Largely Devoid of Intestinal Metaplasia (IM)

Michael Andersen[1], Bing Ren[2], Anna Bouck[3], Shannon Schutz[2], Richard Rothstein[2], Mikhail Lisovsky[2]
[1]Beth Israel Deaconess Medical Center, Boston, MA, [2]Dartmouth-Hitchcock Medical Center, Lebanon, NH, [3]Dartmouth-Hitchcock Medical Center, Geisel School of Medicine at Dartmouth, Lebanon, NH

Disclosures: Michael Andersen: None; Bing Ren: None; Anna Bouck: None; Shannon Schutz: None; Richard Rothstein: *Grant or Research Support*, Fractyl; *Advisory Board Member*, Allurion; Mikhail Lisovsky: None

Background: PAM is characterized by mucosal glands closely resembling pancreatic acinar tissue. The origin of PAM at the gastroesophageal junction/distal esophagus (GEJ/DE) is uncertain and the significance of PAM at GEJ/DE in patients with GERD is unclear. Anecdotally, we have noticed that PAM and IM overlap infrequently in patients with GERD. The goal of this study was to evaluate the significance of PAM at the GEJ/DE in patients with GERD.

Design: Patient group 1 was derived from 266 patients with established GERD and GEJ/DE biopsies who were evaluated for Nissen fundoplication from 2000-2016. Excluded were biopsies obtained after the Nissen procedure, biopsies showing chronic gastritis, squamous mucosa only or intestinalized mucosa only at the GEJ/DE. The final group 1 consisted of 151 patients. Group 2 consisted of 540 unselected patients from 2004 who had GEJ/DE biopsies with columnar component. It was used for follow-up study of PAM. Overlap of PAM and IM was diagnosed when they were present in the same biopsy specimen.

Results: PAM-only, IM-only or PAM-IM overlap were present in 15.9% (24/151), 31.1% (47/151) and 3.3% (5/151) of all patients with established GERD in group 1, respectively, suggesting PAM-IM dichotomy. Patients with PAM-only were, on average, 12 years younger than patients with IM-only (mean age: 39.2±11.7 vs 51.3± 11.6 years, P=.0099). They were also predominantly female (75%), while patients with IM were predominantly male (68%, P=.0009). Only 6.9% (2/29) of all patients with PAM had Barrett's esophagus of more than 1 cm in extent in comparison to 73% (38/52) of all patients with IM (P<.0001). Pre-surgical pH metry performed in 70.8% (17/24) of patients with PAM-only and 36.2% (14/47) with IM-only showed no significant difference in abnormal acid exposure (13.7±8.9% vs 17.2±11.4, P=.3482). Evaluation of patients of group 2 from 2004 has demonstrated that 30/73 patients with PAM-only had additional later biopsies (mean follow up time 6.6 ± 3.1 year; range 3-12 years). History of GERD was present in 27/30 patients with follow up. Only 6.7% (2/30) of patients demonstrated IM in follow up biopsies.

Conclusions: PAM overlaps with IM only infrequently at GEJ/DE in patients with GERD. Patients with PAM constitute a distinct subgroup of patients with GERD characterized by female predominance and younger age in comparison to patients with IM. Presence of PAM at the GEJ/DE may be indicative of decreased susceptibility to IM in patients with GERD.

381 Effectiveness and Utility of IHC Staining in Mild Chronic Gastritis in Detection of H. pylori Organisms: Practice Trends in General Pathologists and GI Pathologists

Stefen Andrianus[1], Emma Furth[2], Rashmi Tondon[2]
[1]Hospital of the University of Pennsylvania, Philadelphia, PA, [2]Perelman School of Medicine, Hospital of the University of Pennsylvania, Philadelphia, PA

Disclosures: Stefen Andrianus: None; Emma Furth: None; Rashmi Tondon: None

Background: Guidelines suggest implementation of immunohistochemical (IHC) stain for *H. pylori* be used in specific circumstances including defined grades of gastritis. However, the definition of "mild" chronic gastritis is somewhat difficult and subjective. The purpose of this study is to evaluate the effectiveness and utility of *H. pylori* IHC in gastric biopsies showing "mild" chronic gastritis in two practice settings: generalists and GI subspecialists.

Design: Data from reports from three different hospitals under our health care system to evaluate two different practice settings: one subspecialty based GI practice setting at a large academic center, and other general pathology practice setting. Both these settings do not follow reflex/upfront IHC or any other special stain usage. Gastric biopsies reported as showing "mild chronic inflammation/gastritis" were obtained from 1/1/21-3/1/21 for the subspecialty setting and from 1/1/21-4/30/21 for general pathology practice setting. Prior *H. pylori* positive/treated cases and gastric resections were excluded from the study.

Results: A total of 304 cases of mild chronic gastritis were found; 287 cases were of inactive mild chronic gastritis and 17 were of active mild chronic gastritis. Of the 287 cases of inactive mild chronic gastritis, *H. pylori* IHC was ordered on 185 cases (64.5%), of which 3 cases were positive (3/185: 1.62%). Of the 17 cases of active mild chronic gastritis, *H. pylori* IHC was ordered on 15 cases; two of which were found to be positive by IHC (2/17: 13.33%).

Intestinal metaplasia was found in 19 cases (19/304: 6.25%); all of which was found in the inactive category. *H. pylori* IHC was ordered on 14 cases (73.7%; 14/19). However, none of these cases were positive by IHC.

General pathologists ordered IHC on 98.6% of cases in inactive category (141/143) and 90.0% in active category (9/10). In contrast, GI pathologists ordered IHC on 30.5% of cases in inactive category (44/144) and 85.7% (6/7) in active category.

Conclusions: There is a low yield of *H. pylori* IHC positivity in cases of mild chronic inactive gastritis (1.05%; 3/287). Given its low added value, careful consideration for ordering IHC should be given in such cases, even when intestinal metaplasia is present. General pathologists ordered 3 times more IHC than GI pathologists. We advocate the appropriate use of *H. pylori* IHC based on the current recommendations and hypothesize the term "chronic" gastritis may be overused in the generalist setting.

382 Clinicopathological Characteristics of Gastric Well-Differentiated Neuroendocrine Tumors with Oncocytic Features

Alessa Aragao[1], Zongming (Eric) Chen[1], Tsung-Teh Wu[1], Hee Eun Lee[1]
[1]Mayo Clinic, Rochester, MN

Disclosures: Alessa Aragao: None; Zongming (Eric) Chen: None; Tsung-Teh Wu: None; Hee Eun Lee: None

Background: Oncocytic variant of well-differentiated neuroendocrine tumors (WDNETs) has been described previously in the pancreas. However, it has not been systemically evaluated in the stomach. We aimed to reveal the frequency of gastric WDNETs with oncocytic features (oncocytic NETs) and describe their clinicopathologic characteristics.

Design: Surgical pathology files from 2000-2019 were searched for gastric WDNETs. H&E slides were reviewed and cases showing oncocytic features were identified. Medical records were reviewed. Immunostains for trypsin and HepPar-1 were performed on oncocytic NETs, and they were interpreted as 0, 1+ (positive in 1-9% of oncocytic tumor cells), 2+ (10-33%), 3+ (33-67%), and 4+ (>67%). Clinicopathological features were compared between oncocytic and non-oncocytic WDNETs.

Results: Total 243 cases of gastric WDNETs including 176 endoscopic biopsies and 34 endoscopic and 32 surgical resections were included, and 25 (10.3%) of 243 showed at least focal oncocytic features which comprise 10% of tumor area in 3 cases, 30% in 2, 50% in 3, 60% in 3, 70% in 1, 80% in 1, 100% in 12. Compared to non-oncocytic NETs, oncocytic NETs showed a higher M:F ratio (1:1 vs 1:2; p=0.049) and no significant difference in age (average±SD, 57.9±8.6 vs 49.5±8.3; p=0.648) and tumor size (average 0.58 cm vs 0.5 cm; p=0.65). Oncocytic NETs were classified as type 1 (in association with autoimmune atrophic gastritis; n=17, 74%), type 2 (MEN-I or Zollinger-Ellison syndrome; n=3, 13%), and type 3 (sporadic; n=3, 13%), which were not significantly different (p=0.37) from non-oncocytic NETs that included type 1 (n=175, 81%), type 2 (n=12, 6%), and type 3 (n=29, 13%). There is no significant difference in a Ki-67 proliferation index between oncocytic and non-oncocytic NETs [8.7±15.9% (n=16) vs 4.9±4.7% (n=64); p=0.36). In oncocytic NETs, 4 (17%) of 23 cases showed HepPar-1 expression (1+ in 3 cases; 3+ in 1) and 22 (92%) of 24 cases showed trypsin expression (1+ in 9; 2+ in 3; 3+ in 3; and 4+ in 7).

Conclusions: Our study showed oncocytic features can be seen in 10.3% of gastric WDNETs. This variant had a higher male to female ratio and but no difference in Ki-67 proliferation index and types as compared to non-oncocytic NETs. Oncocytic gastric WDNETs can show aberrant expressions of HepPar-1 (17%) and/or trypsin (92%) at least focally. Awareness of the existence of oncocytic variant gastric WDNET and its clinicopathologic features will help make the accurate the diagnosis.

383 Evaluation of Tumor Microenvironment in Anal Squamous Cell Carcinoma and Correlation with PD-L1 Expression

Vaidehi Avadhani[1], Ashley Monsrud[2], Marina Mosunjac[2], Uma Krishnamurti[3]
[1]Emory University Hospital, Atlanta, GA, [2]Emory University, Atlanta, GA, [3]Yale School of Medicine, Yale New Haven Hospital, New Haven, CT

Disclosures: Vaidehi Avadhani: None; Ashley Monsrud: None; Marina Mosunjac: None; Uma Krishnamurti: None

Background: Expression of PD-L1 has been associated with poorer survival in anal squamous cell carcinoma (ASCC). Recent studies have also shown that PD-L1 plays a critical role in regulatory T-cell development and function. Although increases in FOXP3(+) T-cell infiltration and PD-L1 expression have been reported in several malignancies, their correlation in ASCC has not been evaluated. A previous study in our laboratory has shown PD-L1 expression to be an independent adverse prognostic factor for overall survival in ASCC (in press). In this study, we perform immunohistochemical analysis of intratumoral (IT) and peritumoral (ST) FOXP3 and CD8 and correlate that with PD-L1 expression in ASCC.

Design: Whole-tissue FFPE sections from 35 patients with ASCC were examined for FOXP3 (Dako, 1:100) and CD8 (Abcam, 1:100) expression by immunohistochemistry. Expression of FOXP3 was used to identify T-regulatory cells (Tregs). Expression of FOXP3 and CD8 was evaluated within the tumor (IT) and in the peritumoral stroma (ST). For FOXP3 and CD8, scoring of the number of positively stained cells per high power field (40x objective) was done in 25 high power fields and the average score per high power field was recorded (1HPF= 0.237mm^2). In addition, the average percentage of stromal area that was positive for CD8 was also evaluated (ST%). Scoring of FOXP3 and CD8 was done blinded to the PD-L1 results. The expression of FOXP3, CD8, and CD8/FOXP3 ratio was compared in tumors positive (n=18) and negative (n=17) for PD-L1 by Combined positive score; CPS $\geq$ 1% = PD-L1 +. Statistical analysis was performed using the SPSS (version: 27.0; IBM Corporation). The mean, median,

and range were calculated. The median scores were compared using the Mann-Whitney U test. A p-value less than .05 was considered statistically significant.

Results: Median FOXP3 expression (IT and ST) was significantly higher in PD-L1 positive tumors (p<.001). However, the median scores for CD8 expression (IT, ST, and stromal area) and CD8 (IT)/FOXP3 (IT) ratio were not found to be significantly different between the PD-L1 positive and PD-L1 negative tumors. See Table 1. Figure 1. FOXP3 expression in a PD-L1 positive case. Figure 2. FOXP3 expression in a PD-L1 negative case.

	PD-L1 positive (n=18)	PD-L1 negative (n=17)	p-value
FOXP3 (ST)			
Mean	19.9	7.5	
Median	12.0	6.0	<.001 (.00 -.12)
Range	0.5-60.0	0-25.0	
FOXP3 (IT)			
Mean	5.6	1.9	
Median	5.0	1.5	<.001 (.00 -.12)
Range	0-14.0	0-9.0	
CD8 (ST)			
Mean	145.8	127	0.68
Median	80.0	100	0.81
Range	15-450	6-400	
CD8 (IT)			
Mean	13.0	12.1	0.87
Median	9.0	3.0	0.19
Range	0.3-40	0-60	
CD8 (ST%)			
Mean	34.1	42.1	0.36
Median	25.0	40	0.44
Range	2-70	10-80	
CD8 (IT) /FOXP3 (IT)			
Mean	3.7	7.1	.29
Median	2.5	2.0	<.80 (.63-.97)
Range	0.15-25.0	0.30-30.0	

Figure 1 - 383

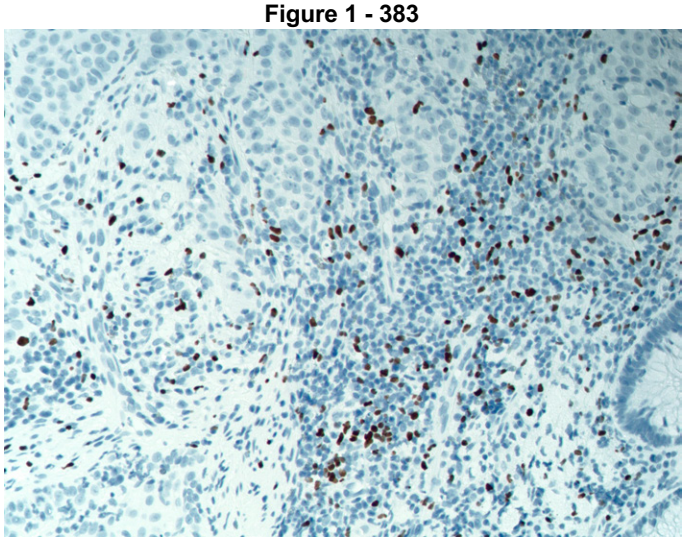

Figure 2 - 383

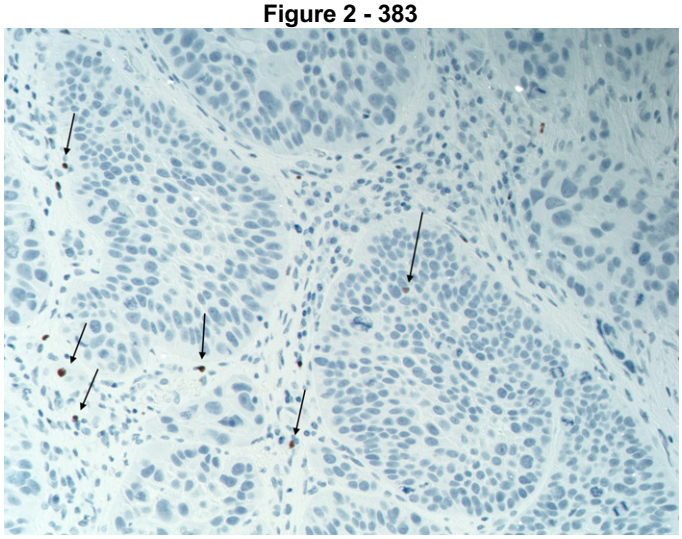

Conclusions: Our study shows that in ASCC, FOXP3 expression is significantly higher in PD-L1 positive tumors and thus may be associated with a poorer prognosis. Combinatorial immunotherapeutic approaches aiming at blocking PD-L1 and depleting Tregs might improve therapeutic efficacy in ASCC patients. A better understanding of the tumor microenvironment in anal squamous cell carcinoma may help to evaluate new immunotherapy treatments.

384 Undetected Dysplasia Found in Colectomy Specimens of Patients with Inflammatory Bowel Disease is Often Associated with Non-Conventional Dysplastic Features, Flat/Invisible Gross Appearance, and Primary Sclerosing Cholangitis

Dorukhan Bahceci[1], Gregory Lauwers[2], Won-Tak Choi[3]
[1]UCSF Pathology, San Francisco, CA, [2]H. Lee Moffitt Cancer Center & Research Institute, University of South Florida, Tampa, FL, [3]University of California, San Francisco, San Francisco, CA

Disclosures: Dorukhan Bahceci: None; Gregory Lauwers: *Consultant*, ALIMENTIV, Inc; Won-Tak Choi: None

Background: Several non-conventional dysplastic subtypes have been described in inflammatory bowel disease (IBD). Hypermucinous (HMD), goblet cell deficient (GCD), and crypt cell (CCD) dysplasias have received most attention, as they often present as flat/invisible dysplasia and develop advanced neoplasia on follow-up. This study aimed to investigate the incidence and characteristics of dysplastic lesions found in colectomy specimens that were undetected on prior colonoscopy.

Design: A cohort of 207 consecutive IBD patients who had at least one colonoscopy prior to total colectomy were analyzed. Dysplasia was classified as undetected, only when there was no corresponding site of dysplasia on previous colonoscopic biopsies.

Results: The cohort included 113 (55%) men and 94 (45%) women with a mean age of 40 years. A mean IBD duration was 10 years with a history of pancolitis in 174 (84%) patients. There were 182 (88%) patients with ulcerative colitis. Fourteen (7%) patients had primary sclerosing cholangitis (PSC). Most patients (84%) underwent a colectomy for medically refractory IBD. Of the 207 patients, 27 (13%) had undetected dysplastic lesions (n = 49). The majority of these lesions showed non-conventional dysplastic features (n = 37; 76%) and low-grade dysplasia (n = 46; 94%), and had a flat/invisible gross appearance (n = 36; 73%). They included 15 (31%) HMD, 7 (14%) GCD, 7 (14%) CCD, 6 (12%) dysplasia with increased Paneth cell differentiation, and 2 (4%) traditional serrated adenoma-like dysplasia. The remaining 12 (24%) lesions represented conventional dysplasia. Twelve (44%) patients had multifocal dysplasia, 10 (83%) of whom had multifocal non-conventional dysplasia. Three (11%) patients also had missed adenocarcinoma. There was a left-sided predilection (n = 27; 55%) for undetected dysplasia. Almost all patients with undetected dysplasia (n = 25; 93%) had a colonoscopy within 1 year of colectomy. Patients with undetected dysplasia were more likely to be older at the time of colectomy (mean: 46 years; p = 0.049) and have PSC (19%; p = 0.009) compared to those without undetected dysplasia (39 years and 5%, respectively).

Conclusions: The incidence of undetected dysplasia was 13%. More than 70% of these lesions were associated with non-conventional dysplastic features and flat/invisible gross appearance. Patients with undetected dysplasia were more likely to be older and have PSC, suggesting that these patients may benefit from more aggressive colonoscopic surveillance.

385 Is PAS Stain Necessary to Exclude Whipple Disease in Duodenal Biopsies?

Ahmed Bakhshwin[1], Lauren Duckworth[2], Thomas Plesec[1]
[1]Cleveland Clinic, Cleveland, OH, [2]Cleveland Clinic Foundation, Cleveland, OH

Disclosures: Ahmed Bakhshwin: None; Lauren Duckworth: None; Thomas Plesec: None

Background: Whipple disease is a rare, multi-system infectious disease caused by the bacterium *Tropheryma whipplei.* It often presents with malabsorptive diarrhea, leading to upper endoscopy and duodenal biopsies. Small bowel biopsies in Whipple disease demonstrate expansion of the lamina propria by foamy macrophages containing *T. whipplei* bacilli that are intensely PAS-positive. Biopsies to rule out Whipple disease are often received with a clinician request for PAS staining, even in histologically normal duodenum; the yield of PAS staining in such biopsies has never been reported to our knowledge.

Design: The anatomic pathology database was searched for all cases of duodenal biopsies stained with PAS from 1993-2021. Cases were categorized by the following histomorphologic features: normal, non-specific changes such as villous blunting or dilation of lacteals, and expansion of the lamina propria by aggregates of foamy histiocytes. Patient follow up information was obtained via the medical record, including microbiology confirmatory testing.

Results: There were a total of 181 cases of duodenal biopsies stained with PAS. Biopsies lacking foamy histiocytes on H&E (n=146) were never PAS-positive. Thirteen biopsies contained PAS-positive histiocytes; 11 out of the 13 PAS-positive cases were subsequently confirmed to be *T. whipplei* (Table 1). One hundred seventeen cases had a clinical request for PAS staining. Three of the 117 (2.6%) cases contained PAS-positive foamy histiocytes, all of which were confirmed positive for *T. whipplei*.

	Normal/Nonspecific changes	Foamy macrophages	p-value
PAS-positive	0	13*	0.0001
PAS-negative	146	22	
	Clinically requested	Pathologist initiated	p-value
PAS positive	3	10	0.0019
PAS Negative	114	54	
*75% PAS-positive, confirmed *T. whipplei* infection			

Figure 1 - 385

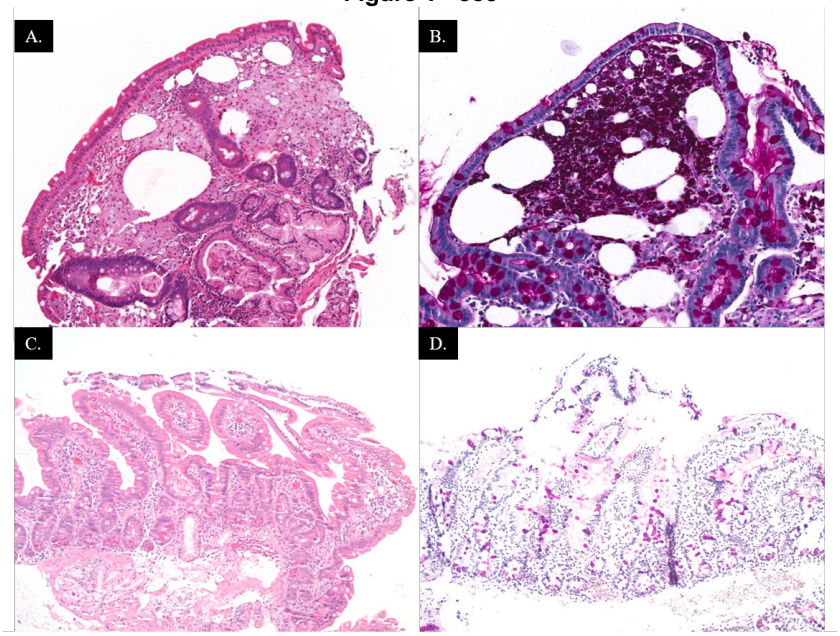

Figure 1. A case of pathologist-initiated PAS staining due to the presence of foamy histiocytes and dilated lacteals (A) that was positive for PAS (B). Clinically requested PAS/D staining on duodenal biopsy with only mild villus intraepithelial lymphocytes (C) that was negative for PAS/D (D).

Figure 2 – 385

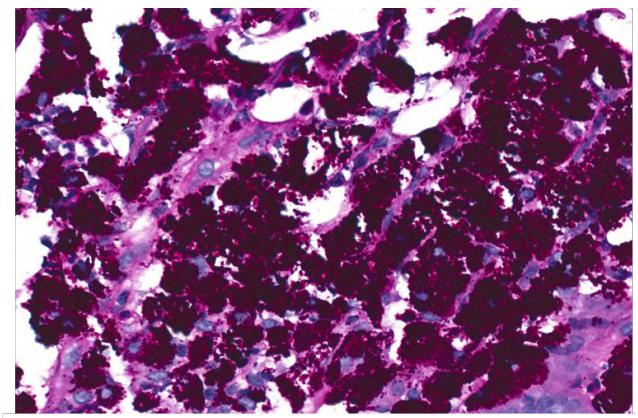

Figure 2. A high power image of a PAS-positive duodenal specimen. The patient subsequently tested positive for T. whipplei organism infection.

Conclusions: PAS staining for *T. whipplei* is not indicated to exclude Whipple disease in duodenal biopsies lacking aggregates of foamy macrophages, regardless of clinical suspicion. Further, biopsies performed for the clinical suspicion of Whipple disease is negative for Whipple disease in the vast majority of cases.

386 Prognostic Performance of Tumor Regression Grading Systems Following Salvage Surgery for Anal Squamous Cell Carcinoma

Ahmed Bakhshwin[1], Neha Khaitan[1], Lauren Duckworth[2], Sarah Elsoukkary[1], Xuefeng Zhang[1], David Liska[1], Ehsan Balagamwala[1], Daniela Allende[3]

[1]Cleveland Clinic, Cleveland, OH, [2]Cleveland Clinic Foundation, Cleveland, OH, [3]Cleveland Clinic, Lerner College of Medicine of Case Western University School of Medicine, Cleveland, OH

Disclosures: Ahmed Bakhshwin: None; Neha Khaitan: None; Lauren Duckworth: None; Sarah Elsoukkary: None; Xuefeng Zhang: None; David Liska: *Consultant*, Olympus; Ehsan Balagamwala: *Speaker*, Carl Zeiss; Daniela Allende: *Advisory Board Member*, Incyte

Background: Anal squamous cell carcinoma (SqCC) is the most common malignancy of the anus and incidence has increased in the last decade. Chemoradiotherapy has replaced surgery as standard of care for anal SqCC. Persistent or recurrent locoregional disease requires treatment with salvage surgery. Tumor regression scoring systems (TRSS) following neoadjuvant therapy are useful in predicting outcomes in various treated gastrointestinal adenocarcinomas. To our knowledge, there is no validated TRSS for anal SqCC. We evaluated 4 TRSS studied in esophageal SqCC plus CAP system in these patients to assess for their ability to predict overall survival (OS).

Design: The pathology database was searched from 2005-2019 for cases of surgically treated anal SqCC. Clinical data and outcomes were obtained from the medical record. All cases had ≥1 section/cm of tumor for visible lesions and were entirely submitted if no gross lesion was seen. Cases with limited sampling, no block/slides for review, or rectal SqCC were excluded. Percent of viable RT in relation to tumor bed was semiquantitatively estimated: 1. As an average of all tumor sections 2. As the highest percentage of RT in a single section. Quantitative determination using scanning slides via Aperio scanner is ongoing. Histologic data and AJCC 8th ed. staging were analyzed. All 4 [Japan Esophageal Society (JES), Chirieac, Hermann, and Schneider systems] and CAP TRSS systems were applied to our data and correlated with OS.

Results: A total of 48 patients were identified: 96% White, 56% women, and the median age was 56.5 years (range: 40-87). Abdominoperineal resection was performed in 79% of patients while 21% underwent pelvic exenteration. Histologic grade is as follows: 60% poorly; 27% moderately; 13 well-differentiated. Margins were negative in 58% of cases, positive in 38%, and 4% were indeterminate. Median OS is 48.5 months. Table 1 demonstrates survival data and OS in months across TRSS. Margin status was the only parameter predictive of OS.

	Residual tumor/score	Survival (months)	Alive	Dead	Lost to Follow-up
JES(1)	0	33 [75.5] (27-124)	1	1	0
	<1/3	37 [62] (16-105)	1	2	0
	1/3-2/3	46 [40.2] (9-81)	1	4	0
	>2/3	48.5 [58.4] (12-194)	14	19	5
Chirieac (2)	0	33 [75.5] (27-124)	1	1	0
	1-50 %	46 [67] (16-105)	1	3	0
	>50 %	48.5 [58.4] (9-194)	15	22	5
Hermann (3)	No	33 [75.5] (27-124)	1	1	0
	Yes	48.5 [58.4] (9-194)	16	25	5
Schneider (4)	1	33 [75.5] (27-124)	1	1	0
	2	Na	Na	Na	Na
	3	48.5 [58.4] (9-194)	14	22	5
	4	37 [39.6] (16-97)	2	3	0
CAP	0	33 [75.5] (27-124)	1	1	0
	1	105	1	0	0
	2	60 [49] (15-97)	4	5	0
	3	48.5 [59] (9-194)	11	20	5
Margin status	Negative	50 [69] (9-194)	15	12	1
	Positive	48.5 [41.6] (12-168)	1	13	4
Lymph node	Negative	51 [61] (9-194)	14	24	5
	Positive	33 [46.2] (18-100)	0	5	0

1. Esophagus 2016;14:1-36, 2. Cancer 2005;103:1347-55, 3. Dis Esophagus 2006;19:329-34, 4. 1:<1% RT without positive lymph nodes (LN), 2: <1% RT with positive LN, 3: >1% RT without positive LN, 4:>1% RT with positive LN (Ann Surg 2005;242:684-92).

Conclusions: Our data set suggests that using semiquantitative methods, known TRSS based on percentage of RT do not correlate with OS in treated anal SqCC. Among all features, margin status was the only parameter predictive of OS (p=0.0028 Fisher's exact test). As opposed to SqCC in other sites, lymph node status was not predictive of outcome. Our findings support the use of a comprehensive approach to assess residual anal SqCC that takes into consideration margin status and does not solely rely on quantifying RT.

387 Epidermoid Metaplasia: A Precursor Lesion to Squamous Neoplasia or Just a Bystander?

Cameron Beech[1], Andrea Barbieri[2], Dhanpat Jain[2], Xuchen Zhang[2]
[1]Yale New Haven Hospital, New Haven, CT, [2]Yale School of Medicine, New Haven, CT

Disclosures: Cameron Beech: None; Andrea Barbieri: None; Dhanpat Jain: None; Xuchen Zhang: None

Background: Epidermoid metaplasia (EM), a rare phenomenon involving the esophagus, is characterized by a prominent granular layer and orthokeratosis or hyperorthokeratosis, resembling epidermis of the skin. Studies have suggested an association with adjacent high-grade squamous dysplasia or squamous cell carcinoma (SCC); thus, patients may be followed with surveillance at a higher frequency if found in isolation. The aim of the study was to further characterize the association between EM and squamous neoplasia.

Design: We retrospectively reviewed all 19 EM cases identified on esophageal biopsy at a large tertiary care center from 2011-2021. Clinical-pathologic variables were tabulated, including patient age, gender, reason for endoscopy, endoscopic impression, location, active health problems and history of SCC, prior biopsies of the esophagus, Barrett's esophagus, and dysplasia. In addition, esophageal resection specimens (17 SCC and 51 adenocarcinoma) were reviewed to identify any associated EM.

Results: The clinical and pathologic features for the 19 EM biopsy cases are listed in Table 1. The median age at diagnosis of EM was 58 yrs (26-90 yrs), with 13/19 (68%) patients being male and 6/19 (32%) being female. Follow-up of patients diagnosed with EM revealed no cases of squamous dysplasia or carcinoma on subsequent surveillance. Of the 17 resection specimens for esophageal SCC, 2 of them showed focal EM. One was adjacent to a focus of high-grade dysplasia and invasive SCC, and another showed no adjacent dysplasia or carcinoma. The EM was wild type for TP53. None of the 51 esophageal adenocarcinoma specimens showed EM.

Reason for Endoscopy	Prior Biopsy Diagnosis	EM Endoscopic Impression	Location	Active problems
Dyspepsia= 1/19	Intestinal metaplasia with low grade dysplasia= 1/19	Plaque= 6/19	Proximal = 1/19	alcohol abuse = 7/19
Dysphagia= 7/19	Intestinal metaplasia with high grade dysplasia= 1/19	Ulcer= 1/19	Mid= 4/19	tobacco use = 1/19
Barretts = 2/19	Candida esophagitis= 1/19	Nodule= 2/19	Distal = 12/19	GERD = 8/19
Varicies= 1/19	Ulcerative esophagitis= 1/19	White exudate = 1/19	Entire = 1/19	
Epigastric pain = 1/19		Erosion = 1/19	Unknown= 1/19	
GI bleed= 1/19		Unknown= 8/19		
GERD= 2/19				
Melana= 2/19				
Unknown= 2/19				

Conclusions: Our cohort demonstrates that EM is a rare entity; no patients developed squamous dysplasia or carcinoma on subsequent follow up. Similar to prior studies, alcohol abuse is common amongst patients with EM (7/19). Although, EM was seen in 2 of 17 resection specimens for SCC, only one specimen showed localization with dysplastic epithelium and carcinoma, which was focal. Whether EM is a true precursor lesion or a histologic bystander remains unclear. Prior study have shown TP53 mutations within EM, however, in our resection specimens, TP53 was wild type within EM. Given its focal presence within resection specimens for SCC and no new onset squamous dysplasia or carcinoma in patients with EM in biopsy specimens, the findings do not suggest a strong association with a stepwise model of carcinogenesis.

388 Eosinophilic Esophagitis-Associated Squamous Papillomas are Inflammatory in Nature

Phoenix Bell[1], Kevin McGrath[2], Jennifer Chennat[2], Asif Khalid[1], Marina Nikiforova[1], Abigail Wald[1], Katelyn Smith[1], Elizabeth Montgomery[3], Aatur Singhi[1]
[1]University of Pittsburgh Medical Center, Pittsburgh, PA, [2]University of Pittsburgh School of Medicine, Pittsburgh, PA, [3]University of Miami Miller School of Medicine, Miami, FL

Disclosures: Phoenix Bell: None; Kevin McGrath: None; Jennifer Chennat: None; Asif Khalid: None; Marina Nikiforova: None; Abigail Wald: None; Katelyn Smith: None; Elizabeth Montgomery: None; Aatur Singhi: None

Background: Esophageal squamous papillomas (ESPs) are solitary, epithelial neoplasms and often located within the distal esophagus. Etiologically, ESPs arise in the setting of gastroesophageal reflux disease or human papillomavirus (HPV) infection. In addition, ESPs are reported in eosinophilic esophagitis (EoE) patients but are limited to case reports. We, therefore, performed a clinicopathologic and molecular analysis of ESPs among EoE patients.

Design: Patients with a history of EoE and ESPs were identified through an electronic medical record search between 2005 to 2021. Among available tissue blocks, RNA in situ hybridization for low- and high-risk HPV, and targeted next-generation sequencing (NGS) of 28 genes associated with squamous neoplasia were performed.

Results: The study consisted of 29 patients with a median age of 35 years and were predominantly male (n=20, 69%). Endoscopically, most ESPs were in the upper-to-mid esophagus (n=20, 69%) and in a background of longitudinal furrows. However, the ESP(s) for each patient varied in number (1 to >50) and size (0.1 to 2.1 cm). Eighteen (62%) patients had >1 papilloma and 5 (17%) patients had >10 papillomas. ESPs were sessile-to-polypoid in appearance and larger lesions (>0.5 cm) had finger-like projections. The histologic features were characterized by a rete-like protuberance of non-dysplastic squamous epithelium with basal hyperplasia. Further, there was an associated eosinophilic infiltrate (median of 29 per high power field). The number of eosinophils within the background esophagus did not differ significantly. HPV testing and NGS were performed for 19 and 12 cases, respectively, and negative for low/high-risk HPV, and genomic alterations, respectively. Follow-up was available for 28 (97%) patients and ranged from 4 to 184 months (median, 40). All patients were treated with proton pump inhibitors (PPI) and 15 patients received topical steroids. Upon treatment, repeat endoscopy was done for 16 patients and at least 1 ESP was identified for 6 (of 16, 38%) patients; however, the ESP(s) were diminutive in size. None of the patients developed esophageal squamous dysplasia or carcinoma.

Conclusions: The pathogenesis of ESPs in EoE remains unknown, but their occurrence in areas of mucosal injury, multiplicity, lack of HPV and genomic alterations, and response to PPI/steroid treatment suggests EoE-related ESPs are inflammatory in nature. Moreover, the presence of ESPs in the setting of EoE does not confer an increased risk of squamous neoplasia.

389 High Frequency of Genomic Alterations in HPV-Associated Anal Cancer Precursors

Swati Bhardwaj[1], Tinaye Mutetwa[1], Jane Houldsworth[1], Paz Polak[1], Michael Gaisa[1], Keith Sigel[1], Yuxin Liu[2]
[1]Icahn School of Medicine at Mount Sinai, New York, NY, [2]Mount Sinai Health System, New York, NY

Disclosures: Swati Bhardwaj: None; Tinaye Mutetwa: None; Jane Houldsworth: None; Paz Polak: None; Michael Gaisa: None; Keith Sigel: None; Yuxin Liu: None

Background: Genomic alterations are characteristic features of HPV-associated cancers. The most frequent alterations are gains of chromosomes 3q, 5p and 20q, regions that contain important genes regulating cell cycle and antiviral response. We aim to examine the frequency of these alterations in HPV-associated anal precancerous lesions (Anal Intraepithelial Neoplasia, AIN 2/3) and to assess their association with treatment response.

Design: Fluorescence in-situ hybridization (FISH)-based HPV-associated cancer test was performed on 63 anal biopsy samples, including 27 AIN 1, 25 AIN 2, and 11 AIN 3. The single hybridization four-color FISH assay targeted four genomic loci: 3q26 (red), 5p15 (green), 20q13 (gold) and the centromere of chromosome 7 (cen7, aqua). FISH results were compared with lesion severity and treatment response.

Results: Among AIN 2/3 lesions, 48% showed genomic gains, specifically, gain of one locus (17%), two loci (6%), three loci (6%) and four loci (19%). 3q26 was the most common gain (47%), followed by 5p15 (30%), 20q13 (30%) and cen7 (19%). AIN 2 revealed a slightly higher genomic gain frequency compared to AIN 3 (52% versus 36%). All AIN 1 lesions were genomically stable except two (8%), which revealed gain 3q26 and 20q13, respectively. Gain of any loci resulted in sensitivity of 47% (95% CI: 30-

65%) and specificity of 93% (95% CI: 76-99%) for the detection of AIN 2/3. AIN 2/3 lesions that resisted or responded to ablative treatment revealed similar frequency of alterations.

Table 1. Correlation between genomic alternations and AIN grade.

* P < 0.002

Morphological grade	FISH result		Chromosome locus			
	Normal	Abnormal	3q26	5p15	20q13	Cen7
LSIL/AIN 1 (n=27)	25 (92%)	2 (8%)	2	0	1	0
HSIL (n=36)	19 (53%)	17 (47%)*	17	11	11	7
AIN 2 (n=25)	12 (48%)	13 (52%)	13	9	9	5
AIN 3 (n=11)	7 (64%)	4 (36%)	4	2	2	2

Figure 1 - 389

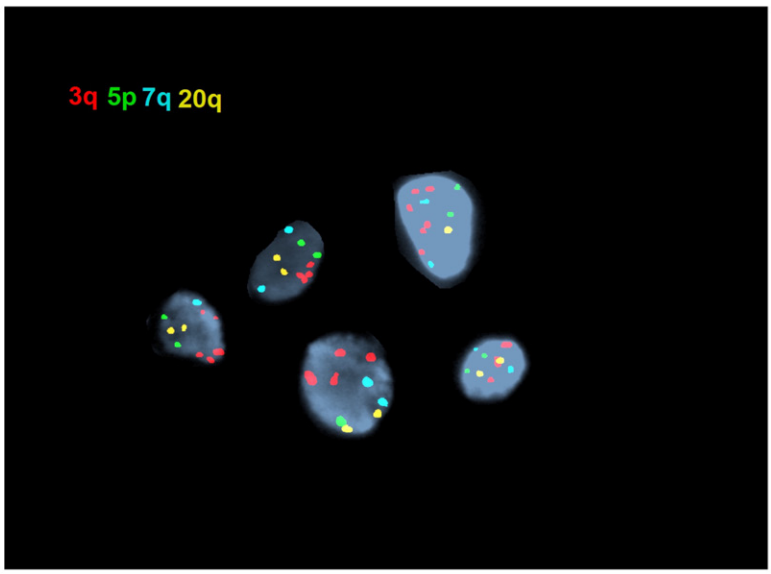

Figure 1. FISH-based HPV-associated cancer test image on an AIN 3 lesion. Five nuclei show gain of 3q26 (red), normal copy number of 5p15 (green), cen7 (aqua) and 20q13 (gold).

Conclusions: Anal precancerous lesions (AIN 2/3) harbor a high frequency of genomic alterations that have been characterized in other HPV-associated cancers. The significant amplification of chromosomal regions containing telomerase genes (3q26 and 5p15) indicates reactivation of telomerase as a major mechanism of HPV-mediated anal carcinogenesis.

390 Injury Patterns and Potential Diagnostic Pitfalls Associated with Radiation and Radio-Chemotherapy in the Stomach and Gastroesophageal Junction

Jacqueline Birkness-Gartman[1], Lysandra Voltaggio[2]
[1]*Johns Hopkins University, Baltimore, MD,* [2]*Johns Hopkins Medical Institutions, Baltimore, MD*

Disclosures: Jacqueline Birkness-Gartman: None; Lysandra Voltaggio: *Grant or Research Support*, Pentax Medical

Background: Chemoradiation-associated gastropathy may be a cause of upper gastrointestinal symptoms in patients undergoing treatment for various malignancies. We have encountered a variety of treatment-related epithelial and stromal changes in our daily practice. The goal of this study was to systematically characterize the histologic features associated with radiochemotherapy as well as potential diagnostic pitfalls. We excluded cases associated with Yttrium-90 radioembolization, as the histologic features of this entity have been previously described.

Design: Nineteen cases of radiochemotherapy-associated gastropathy were identified, including 16 cases from our institution and 3 from consultations. Clinical histories, endoscopy reports, and gross descriptions were reviewed for each case. Histologic features including pattern of inflammation, epithelial atypia, and vascular and stromal changes were documented.

Results: Most patients were men (79%) with a median age of 66 years. All patients had a documented history of radiation and 15 patients had also received chemotherapy. The median time from treatment to biopsy or resection was 2.3 months (range 4 days to 2.5 years). Gross and endoscopic findings included erythematous, hemorrhagic, or ulcerated mucosa and areas of fibrosis. Mucosal eosinophilia was seen in 16 cases (84%) while 10 cases (53%) featured acute inflammation including neutrophilic microabscesses. Epithelial changes included increased apoptosis (6 cases, 32%) and marked epithelial atypia (10 cases, 53%), potentially mimicking malignancy in some cases. Atypical cells lined markedly dilated glands and featured voluminous eosinophilic cytoplasm with low nuclear-to-cytoplasmic ratio, a clue to their benign nature. Neuroendocrine cell nests were seen in 4 cases (21%) and loosely aggregated in 1 case, potentially mimicking a neuroendocrine tumor. Eleven cases (58%) featured vascular changes including fibrin thrombi, vessel dilation with endothelial hobnailing, myointimal hyperplasia, fibrin thrombi, and fibrinoid change of vessel walls. Stromal changes were seen in 11 (58%) and included lamina propria and submucosal fibrosis and myofibroblast atypia.

Conclusions: Injury associated with radiochemotherapy is histologically varied and may affect epithelial, stromal, and vascular compartments. Familiarity with these features is important as a subset of these findings may provoke concern for neoplasia.

391 Despite Simplified Diagnostic Criteria, Observer Variability Remains in Interpretation of Colorectal Serrated Polyps

Adam Booth[1], Emina Torlakovic[2], Runjan Chetty[3], Alton B. (Brad) Farris[4], Emma Furth[5], John Goldblum[6], Teri Longacre[7], Mari Mino-Kenudson[8], Robert Riddell[9], Christophe Rosty[10], Amitabh Srivastava[11], Rhonda Yantiss[12], Brian Cox[13], Raul Gonzalez[14]

[1]Feinberg School of Medicine/Northwestern University, Chicago, IL, [2]University of Saskatchewan, Saskatchewan Health Authority, Saskatoon, Canada, [3]Dublin, Ireland, [4]Emory University, Atlanta, GA, [5]Perelman School of Medicine, Hospital of the University of Pennsylvania, Philadelphia, PA, [6]Cleveland Clinic, Cleveland, OH, [7]Stanford University, Stanford, CA, [8]Massachusetts General Hospital, Harvard Medical School, Boston, MA, [9]University of Toronto, Toronto, Canada, [10]Envoi Specialist Pathologists, Brisbane, Australia, [11]Brigham and Women's Hospital, Harvard Medical School, Boston, MA, [12]Weill Cornell Medicine, New York, NY, [13]Cedars-Sinai Medical Center, Los Angeles, CA, [14]Beth Israel Deaconess Medical Center, Harvard Medical School, Boston, MA

Disclosures: Adam Booth: None; Emina Torlakovic: None; Runjan Chetty: None; Alton B. (Brad) Farris: None; Emma Furth: None; John Goldblum: *Consultant*, Lucid Diagnostics; Teri Longacre: None; Mari Mino-Kenudson: *Consultant*, AstraZeneca, H3 Biomedicine; *Primary Investigator*, Novartis; *Advisory Board Member*, BMS, Sanofi; Robert Riddell: None; Christophe Rosty: None; Amitabh Srivastava: None; Rhonda Yantiss: None; Brian Cox: None; Raul Gonzalez: None

Background: Many studies have highlighted interobserver variability in histologic distinction between colorectal sessile serrated lesion (SSL) and hyperplastic polyp (HP). In 2019, the WHO updated their criteria for diagnosis of SSL, now requiring "≥1 unequivocal architecturally distorted serrated crypt." Even with this streamlined criterion, as well as experience accumulated in recognizing SSL over 25 years, SSL and HP remain difficult to distinguish in some instances. This study aims to assess observer variability and preferred criteria in diagnosing SSL among gastrointestinal pathologists.

Design: We retrospectively identified 60 serrated colorectal polyps, produced uniform H&E recuts, and scanned all cases. They were selected to cover the overall SSL/HP spectrum, as confirmed via review by 4 pathologists who individually interpreted each as SSL, HP, or serrated polyp NOS (SP-NOS). The cases were then reviewed by 9 additional pathologists, who also provided their top 3 criteria for diagnosis of SSL over HP. A second round of review followed after a 5-month washout period. A third round was completed after 5 additional months; polyp size and site were provided for round 3, but not 1 or 2. Fleiss and Cohen's kappa were calculated to determine overall inter- and intra-observer agreement.

Results: Criteria reported by the 9 pathologists focused on crypt distortion (9/9), polyp location (5/9), and exclusion of prolapse (3/9). There was moderate agreement among all 13 pathologists on the 60 cases for rounds 1 and 2, and good agreement for round 3; stratification by location showed agreement was worst for transverse polyps (Table). Twenty-one (35%) cases were called SSL ≥80% of the time (Fig 1A), and 16 (27%) cases HP ≥80% of the time (Fig 1B); 4 (7%) cases were called a particular diagnosis <50% of the time (Fig 1C). Median intraobserver agreement was good from rounds 1 to 2 and rounds 2 to 3 but decreased to moderate in comparing rounds 1 to 3 (Fig 2).

Interobserver overall agreement.			
Round	Overall agreement	Kappa (95% confidence interval)	*P-value*
One	Moderate	0.496 (0.473-0.519)	<0.001
Two	Moderate	0.459 (0.435-0.483)	<0.001
Three	Good	0.630 (0.604-0.655)	<0.001
Round 3 overall agreement by location.			
Location (n)	Overall agreement	Kappa (95% confidence interval)	*P-value*
Left side (31)	Fair	0.374 (0.338-0.411)	<0.001
Right side (21)	Fair	0.229 (0.191-0.267)	<0.001
Transverse colon (8)	Poor	0.171 (0.112-0.231)	<0.001

Kappa results and *P-values* were calculated using Fleiss Kappa reliability test for 2+ raters (inter) and Cohen Kappa for 2 raters (intra). Performed on SPSS statistical software v28.

Figure 1 - 391

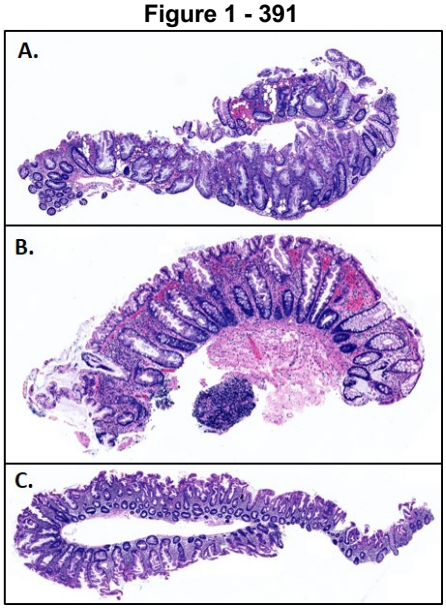

Figure 2 - 391

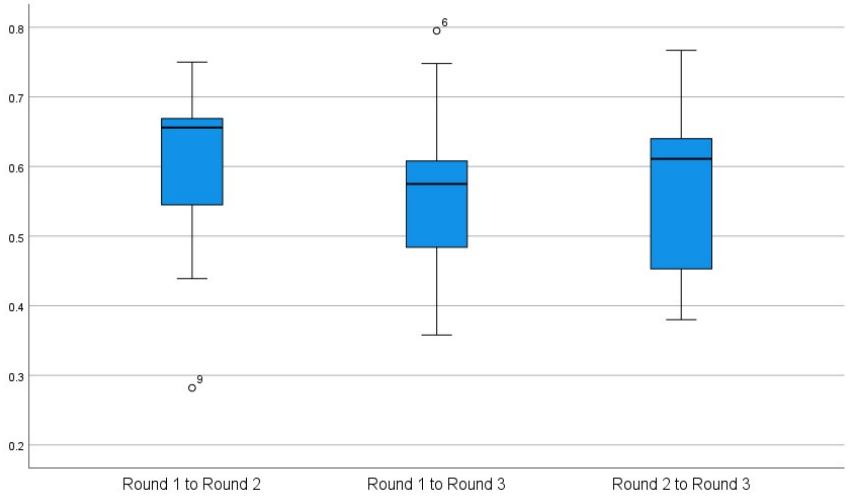

Conclusions: In keeping with current WHO criteria, crypt distortion was the only feature consistently used by each pathologist to diagnose SSL. Overall interobserver agreement improved from moderate to good with size and site included, supporting location as a useful diagnostic aid despite not being a WHO criterion. Transverse polyps had the worst agreement by location, suggesting pathologists struggle with the left/right colon cutoff in this site. Non-histologic criteria may be necessary to reproducibly distinguish SSL from HP, if properly validated.

392 Loss of Beta-2 Microglobulin by Immunohistochemistry in MSI-H Colonic Adenocarcinoma

Brian Brinkerhoff[1], Joseph Kaminsky[2], Benjamin Smith[1], Christian Lanciault[3], Alaaeddin Alrohaibani[1]
[1]Oregon Health & Science University, Portland, OR, [2]Pathology Locums, Montgomery, AL, [3]Portland Providence Medical Center, Portland, OR

Disclosures: Brian Brinkerhoff: None; Joseph Kaminsky: None; Benjamin Smith: None; Christian Lanciault: None; Alaaeddin Alrohaibani: None

Background: Beta-2 microglobulin (B2M) is an essential protein in the class I major histocompatibility complex (MHC-I). Peptides, including abnormal forms generated by tumor cells, are presented in complex with MHC-I to T-cells. One mechanism of immune escape and resistance to immune checkpoint inhibitor therapy is MHC-I downregulation. While microsatellite instability-high (MSI-H) status is one biomarker used to predict response to immune checkpoint inhibitor therapy, previous studies found that MSI-H tumors have increased mutations in B2M, some of which decrease MHC-I formation. We investigated B2M cell surface expression by immunohistochemistry (IHC) in microsatellite stable (MSS) and MSI-H colon adenocarcinomas as a marker of intact MHC-I complex signaling and assessed whether immunostaining for B2M was more often lost in MSI-H tumors.

Design: Institutional archives were searched over a 7-year period for colonic adenocarcinoma biopsy and resection specimens with known mismatch repair protein (MMR) IHC and molecular data, including MSI status. One case with several mutations in the MHC-I pathway served as control. Slides with representative tumor from each case were stained with the anti-B2M antibody (Abnova, 1:2500 dilution). At least 5% circumferential membranous staining of tumor cells were considered to have retained B2M cell surface expression. B2M IHC was evaluated independently by two pathologists.

Results: Twenty-nine total cases were evaluated. Eight cases were identified with B2M loss by IHC, all of which were MSI-H. MMR IHC in these patients showed 6 with MLH1/PMS2 loss and 2 with MSH2/MSH6 loss. Of the cases with MLH1/PMS2 loss, 4 showed *MLH1* hypermethylation (3 with *BRAF* pV600E mutations); gene sequencing of the other 2 cases was notable for *B2M* p.S16fs*27 and *TAP1* p.T352fs*4 mutations in 1 patient, and *MLH1* gene deletion (Lynch syndrome) in the other. The 2 patients with MSH2/MSH6 loss each showed *KRAS* p.G12 mutations. The remaining 21 cases with intact B2M IHC contained 8 MSI-H patients (38%), all showing MLH1/PMS2 IHC loss.

Age	Sex	Site	Specimen	MMR IHC	Beta-2 M IHC	MSS/MSI	MLH Hypermethylation	Lynch	MMR sequencing	Mutations
84	Female	Ascending	Biopsy	MLH1/PMS2 loss	Loss	MSI-H	Positive		MSH6 p.F1088fs*2	BRAF p.V600E, MSH6 p.F1088fs*2
77	Male	Rectum	Resection	Intact	Intact	MSS			No mutation	KRAS p.G12S
64	Male	Jejunum	Resection	MLH1/PMS2 loss	Loss	MSI-H	Negative		MLH1 p.E102D and p.M342fs*20	B2M p.S16fs*27; TAP1 p.T352fs*4
73	Male	Sigmoid	Resection	Intact	Intact	MSS			No mutation	NRAS p.Q61R
42	Female	Sigmoid	Resection	Intact	Intact	MSS				KRAS p.G12D
71	Female	Transverse	Resection	MSH2/MSH6 loss	Intact	MSI-H			No mutation	
85	Male	Transverse	Resection	Intact	Intact	MSS				
39	Female	Rectum	Resection	Intact	Intact	MSI-H			No mutation	KRAS p.G12A
35	Male	Ascending	Resection	MLH1/PMS2 loss	Loss	MSI-H		Yes		MLH1 gene deletion
41	Male	Rectum	Resection	Intact	Intact	MSI-H			No mutation	TP53 p.R282W
75	Female	Ascending	Resection	MLH1/PMS2 loss	Intact	MSS	Positive			BRAF p.V600E
42	Male	Transverse	Resection	MLH1/PMS2 loss	Intact	MSI-H	Negative	Yes	P648L (1943C>T) MLH1	
41	Male	Sigmoid	Resection	Intact	Intact	MSS				
47	Female	Sigmoid	Resection	Intact	Intact	MSS				
42	Female	Sigmoid	Resection	Intact	Intact	MSS			No mutation	KRAS p.G12C
83	Female	Ascending	Resection	MLH1/PMS2 loss	Loss	MSI-H	Positive			
76	Male	Rectum	Resection	Intact	Intact	MSI-H				
71	Female	Ascending	Resection	MLH1/PMS2 loss	Loss	MSI-H	Positive			V600E BRAF
56	Female	Rectosigmoid	Biopsy	MLH1/PMS2 loss	Intact	MSI-H	Negative	Yes	MLH1 C.1852_1854delAAG	
82	Female	Cecum	Resection	MLH1/PMS2 loss	Intact	MSI-H	Negative			
49	Female	Rectosigmoid	Resection	MSH2/MSH6 loss	Loss	MSS				KRAS p.G12A
60	Male	Ascending	Resection	Not performed	Intact	MSI-H		Yes	3957ins19 MSH6	
61	Female	Ascending	Biopsy	MLH1/PMS2 loss	Intact	MSI-H	Positive		MSH2 p.D240V	
54	Male	Sigmoid	Resection	Intact	Intact	MSS				
70	Male	Transverse	Resection	MLH1/PMS2 loss	Loss	MSI-H	Positive			BRAF p.V600E
59	Male	Sigmoid	Resection	MSH2/MSH6 loss	Loss	MSI-H				KRAS p.G12D
69	Male	Transverse	Resection	MLH1/PMS2 loss	Intact	MSI-H				BRAF p.V600E
55	Male	Descending	Resection	MLH1/PMS2 loss	Intact	MSI-H	Negative	Yes	MLH1 N551S (1652A>G)	
76	Male	Ascending	Resection	MLH1/PMS2 loss	Intact	MSI-H				BRAF p.V600E

Figure 1 - 392

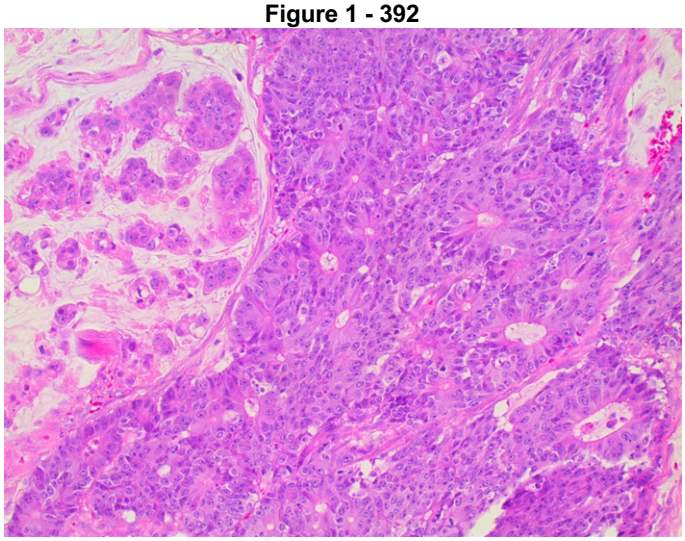

Figure 2 - 392

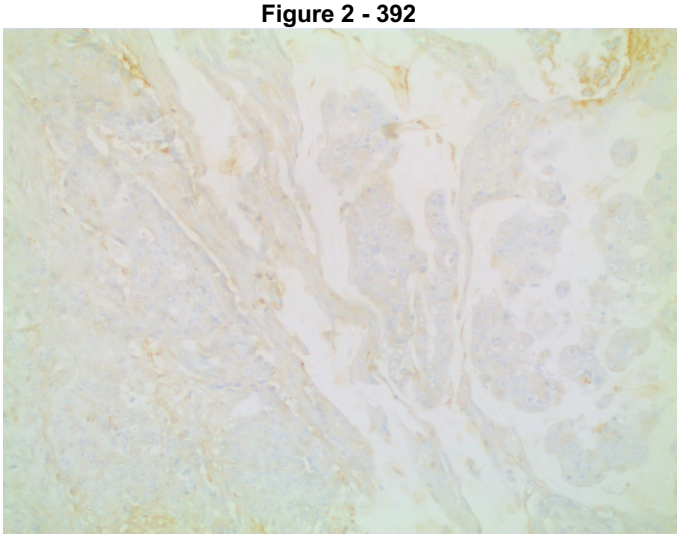

Conclusions: B2M immunohistochemical analysis in colorectal adenocarcinoma is an effective assessment of MHC-1 integrity and correlates with MSH-H status. Integration of this assay is a cost-effective approach to predict responsiveness to immune checkpoint inhibitors.

393 Whole-Slide Digital Quantification of Intraepithelial Gamma/Delta T-Cell Populations Can Distinguish Celiac Disease from Other Etiologies of Duodenal Intraepithelial Lymphocytosis

Nicholas Caldwell[1], Ibrahim Abukhiran[2], Andrew Bellizzi[2]
[1]University of Iowa, Carver College of Medicine, Iowa City, IA, [2]University of Iowa Hospitals & Clinics, Iowa City, IA

Disclosures: Nicholas Caldwell: None; Ibrahim Abukhiran: None; Andrew Bellizzi: None

Background: There is histologic overlap between etiologies of duodenal intraepithelial lymphocytosis (IEL), such as celiac disease, inflammatory bowel disease (IBD), and Helicobacter pylori gastritis (HP). Studies have demonstrated an increased proportion of duodenal T-cell receptor gamma/delta positive intraepithelial (IE) T-cells in patients with celiac disease compared to other etiologies of duodenal IEL. In this study, we sought to quantitate the population of T-cell receptor delta positive (TCRd+) T-cells in etiologies of duodenal IEL using both immunohistochemistry (IHC) and digital image analysis.

Design: CDX2, CD3 plus keratin AE1/AE3, and TCRd plus keratin AE1/AE3 IHC were each performed on a single duodenal biopsy specimen from 54 patients. The patient's age, body mass index (BMI), the degree of villous blunting seen on histology (intact vs. mild-to-severe blunting), and the clinical diagnoses were gathered for each case. Whole-slide digital quantification of CDX2+ enterocytes, whole-tissue (WT) CD3+ T-cells, IE CD3+ T-cells, WT TCRd+ T-cells, and IE TCRd+ T-cells was performed on each biopsy using QuPath v0.3.0's pixel thresholder and positive cell detection functions. The quantity of IE CD3+ and TCRd+ T-cells was counted per 100 CDX2+ enterocytes. The ratios of IE TCRd+ T-cells to IE CD3+ T-cells and WT TCRd+ T-cells to WT CD3+ T-cells were calculated. Relationships were examined using two-sampled T-test and linear regression ($p<0.05$ considered significant).

Results: The cohort consisted of 20 new celiac disease diagnoses, 6 IBD diagnoses, 6 HP diagnoses, and 22 uncertain clinical diagnoses ("Other"). The average IE TCRd+ T-cell count per 100 enterocytes was higher in patients with celiac disease versus patients with non-celiac etiologies (9 vs. 4, $p<0.01$). The average ratio of both IE and WT TCRd+ T-cells to CD3+ T-cells was higher in patients with celiac disease versus patients with non-celiac etiologies (30 vs. 14, $p<0.01$; and 24 vs. 11, $p<0.01$; respectively). The ratio of IE TCRd+ T-cells to IE CD3+ T-cells decreases with increasing age ($p<0.01$) and BMI ($p=0.01$) (depicted in Figure 1). See the Results Table for additional comparisons and Figure 2 for exemplar photomicrographs.

Comparison of Digital Quantification of Lymphocyte Populations

	N	IE CD3+ T-cells per 100 enterocytes			IE TCRd+ T-cells per 100 enterocytes			IE TCRd+ T-cells per 100 IE CD3+ T-cells			WT TCRd+ T-cells per 100 WT CD3+ T-cells		
	#	Mean	(Range)	P&	Mean	(Range)	P&	Mean	(Range)	P&	Mean	(Range)	P&
Full Cohort	**54**	**31**	**(6-79)**		**6**	**(0-21)**		**20**	**(1-82)**		**16**	**(1-59)**	
Celiac	20	35	(18-79)		9	(0-17)		30	(1-82)		24	(1-59)	
Non-Celiac	34	30	(6-79)	0.16	4	(0-21)	<0.01	14	(1-72)	<0.01	11	(1-42)	<0.01
IBD	6	18	(9-31)	0.02	3	(0-14)	0.03	15	(6-44)	0.11	13	(5-40)	0.13
HP	6	29	(16-47)	0.38	4	(0-11)	0.03	11	(8-29)	0.04	11	(1-23)	0.06
Other	22	28	(6-57)	0.13	4	(0-21)	<0.01	14	(1-72)	0.01	11	(1-42)	<0.01
	#	Mean	(Range)	P	Mean	(Range)	P	Mean	(Range)	P	Mean	(Range)	P
Celiac-IVA	7	36	(19-79)	0.89	9	(4-17)	0.96	31	(5-54)	0.78	29	(9-59)	0.32
Celiac-MSVB	13	35	(18-67)		9	(0-16)		29	(1-82)		21	(1-56)	
Non-Celiac-IVA	28	26	(6-57)	0.97	4	(0-21)	0.50	14	(1-72)	0.71	12	(2-42)	0.73
Non-Celiac-MSVB	6	26	(15-54)		2	(0-4)		12	(1-28)		10	(2-23)	

IE = intraepithelial; TCRd = T-cell receptor delta; WT = whole tissue; IBD = inflammatory bowel disease; HP = Helicobacter pylori gastritis; IVA = intact villous architecture; MSVB = mild-to-severe villous blunting

& = compared to celiac disease mean

Figure 1 - 393

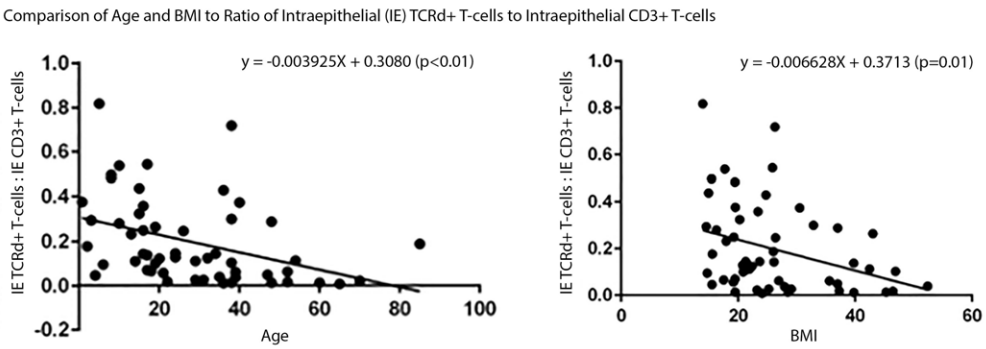

Figure 2 – 393

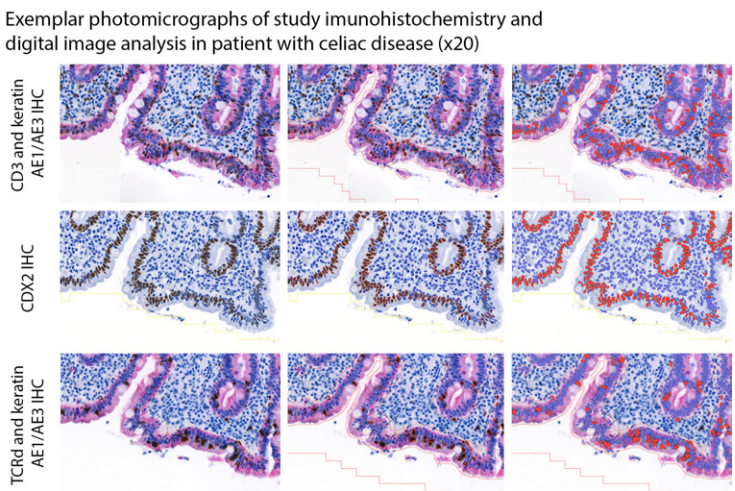

Conclusions: 1. An increased IE TCRd+ T-cell count per 100 enterocytes and increased ratio of either IE or WT TCRd+ T-cells to CD3+ T-cells favors a diagnosis of celiac disease. 2. The degree of villous architectural blunting present does not affect the absolute or relative quantity of TCRd+ T-cells.

394 Pathologic Features of Patients with Celiac Disease and Esophageal Eosinophilia Suggest an Etiologic Link

Carlos Castrodad-Rodríguez[1], Jerome Cheng[2], Maria Westerhoff[2], Guohua Liang[3], Jingmei Lin[3], Ilke Nalbantoglu[4], Shaomin Hu[5], Radhika Sekhri[1], Nicole Panarelli[6]

[1]Albert Einstein College of Medicine, Montefiore Medical Center, Bronx, NY, [2]University of Michigan, Ann Arbor, MI, [3]Indiana University, Indianapolis, IN, [4]Yale School of Medicine, New Haven, CT, [5]Cleveland Clinic, Cleveland, OH, [6]Montefiore Medical Center - Moses Division, Bronx, NY

Disclosures: Carlos Castrodad-Rodríguez: None; Jerome Cheng: None; Maria Westerhoff: None; Guohua Liang: None; Jingmei Lin: *Consultant*, PathomIQ; Ilke Nalbantoglu: None; Shaomin Hu: None; Radhika Sekhri: None; Nicole Panarelli: None

Background: Celiac disease (CD) and eosinophilic esophagitis (EOE) are distinct disorders, but a relationship between the two has been postulated recently. Specifically, increased intestinal permeability due to CD may upregulate global immune response to gluten and other antigens. We performed this study to define the clinical and pathologic features of patients with overlapping CD and EOE.

Design: We evaluated pathologic features of cases with diagnoses of both esophageal eosinophilia that met criteria for EOE and duodenal lymphocytosis with or without villous blunting with positive CD serology from 5 academic centers. Clinical data, when available, were derived from the electronic medical records. Cases with CD or EOE only were used for comparison. Fisher's exact, t, and ANOVA tests were used where appropriate.

Results: The study group comprised 21 males and 7 females (mean age: 15 years). Patients reported symptoms of CD (n=14) or EOE (n=4) only, or both disorders (n=8) (Table). Peak esophageal eosinophil counts in those three study patient subgroups (means: 66, 44 and 49, respectively) did not differ significantly (p=0.8) nor did the histologic severity (modified Marsh score) of CD (p=0.4). Study patients were older (p=0.03) and had significantly lower peak eosinophil counts (p=0.01), but similar rates of eosinophil microabscesses, scale crust, and subepithelial fibrosis compared to controls. CD controls were more likely to have Marsh 3 lesions (p=0.03). Study patients with follow-up (n=23) were all treated with gluten elimination, some with acid suppression (n=9) or steroids (n=4). Combination therapies produced clinical and/or histologic remission of both disorders in 11 cases (73%), whereas gluten elimination alone improved EOE in only 2 (20%) cases, but always resulted in CD improvement.

Table 1. Clinical and Pathologic Features of Study Cases and Controls

Features	Study Cases (n=28)	CD Controls (n=28)	p Values	EOE Controls (n=28)	p Values
Male:Female	21:7	9:19	0.0029	20:8	1.00
Age (years): mean, range	15, 1-56	11, 2-19	0.04	9, 1-47	0.03
Clinical Presentation					
CD symptoms only	14, 50%	24, 86%	N/A	0	N/A
EOE symptoms only	4, 14%	0	N/A	25, 89%	N/A
Both	8, 29%	0	N/A	0	N/A
Unknown	2, 7%	4, 14%	N/A	3, 11%	N/A
Modified Marsh Score					
0	0	0	N/A	28, 100%	N/A
1	4, 14%	3, 11%	1.00	N/A	N/A
2	7, 25%	0	0.01	N/A	N/A
3	17, 61%	25, 89%	0.03	N/A	N/A
Features of Eosinophilic Esophagitis					
Mean peak eosinophil count	55	N/A	N/A	87	0.01
Eosinophil microabscesses	11, 39%	N/A	N/A	17, 61%	0.2
Eosinophil scale crust	5, 18%	N/A	N/A	9, 32%	0.4
Subepithelial fibrosis	14, 50%	N/A	N/A	14, 50%	1.00

Conclusions: The presence of CD symptoms in 79% of study patients, all of whom had combined features of EOE and CD in biopsy samples, supports the hypothesis that gluten may trigger esophageal eosinophilia. Similar esophageal histology among study cases, even in the absence of esophageal symptoms, also supports CD as a possible inciting event. On the other hand, lack of response to gluten elimination suggests that CD-induced dysregulated mucosal immunity may sensitize the esophagus to antigens other than gluten. Some features of CD or EOE were more severe in controls, on average, possibly pointing to milder disease at clinical presentation in study patients, even with symptoms of both disorders.

395 Clinicopathologic Features of Adenocarcinoma Arising in Low-Grade Appendiceal Mucinous Neoplasm

Alexandra Chang-Graham[1], Greg Charville[1]
[1]*Stanford Medicine/Stanford University, Stanford, CA*

Disclosures: Alexandra Chang-Graham: None; Greg Charville: None

Background: Low-grade appendiceal mucinous neoplasm (LAMN) is an uncommon tumor that exhibits a broad spectrum of clinical behavior. Tumors confined to the appendix can be cured by appendectomy, whereas those involving peritoneal surfaces exhibit considerable risk of recurrence and pseudomyxoma peritonei. A rare subset of LAMN exhibits evolution to adenocarcinoma, implying potential for destructive invasion and extraperitoneal metastasis. Given the rarity of adenocarcinoma arising in LAMN, little is known about the clinicopathologic features of this unique diagnostic entity.

Design: We performed an IRB-approved retrospective review of histologic material and clinical data in 11 cases of adenocarcinoma arising in LAMN from our institutional archives. Immunohistochemistry (IHC) was performed using standard techniques. Next-generation sequencing (NGS) was performed using an exon-targeted panel encompassing 130 genes.

Results: Of the 11 cases identified, patients ranged 35-75 years in age (mean=60 years) and 6 were female. Nine cases had direct extension beyond the appendix (pT4), and one case had nodal metastasis (N1a). Nine cases exhibited peritoneal spread (pM1), 2 cases had lung metastases, and 8 cases were associated with pseudomyxoma peritonei. The histologic grade was Grade 1 in 9 cases and Grade 2 in 2 cases, marked cytologic atypia was identified in 7 cases, and 1 case had signet ring cell features. Infiltrative growth was present in 9 cases. By IHC, CK20 and CDX2 were positive, while CK7 and PAX8 were negative, in 4 cases. Mismatch repair proteins MLH1, MSH2, MSH6, and PMS2 showed intact expression by IHC in 5 examined tumors. By NGS, each of the 3 examined cases exhibited *KRAS* mutations: 1 with concurrent *GNAS* mutation, 1 with concurrent *TP53* mutation, and 1 with concurrent *GNAS* and *TP53* mutations. The diagnosis of adenocarcinoma had important clinical implications as 8 patients received at least FOLFOX/XELOX chemotherapy. Among 8 patients with at least 1 year of follow-up, 5 patients required additional debulking surgery for recurrent tumor burden within 2.5 years of primary resection, and 2 had died from disease within 3.5 years of diagnosis.

Conclusions: Adenocarcinoma arising in LAMN is a rare entity with unique clinicopathologic features and important implications for clinical treatment. Further studies are needed to characterize its histologic features, molecular genetic profile, and clinical behavior in comparison to conventional LAMN.

396 Colonic Mucinous Neoplasms: Analogous to Appendiceal Counterparts or A Distinct Entity?

Fengming Chen[1], Tatianna Larman[2], Lysandra Voltaggio[3]
[1]*Johns Hopkins Hospital School of Medicine, Baltimore, MD,* [2]*Johns Hopkins University School of Medicine, Baltimore, MD,* [3]*Johns Hopkins Medical Institutions, Baltimore, MD*

Disclosures: Fengming Chen: None; Tatianna Larman: None; Lysandra Voltaggio: *Grant or Research Support*, Pentax Medical

Background: Appendiceal mucinous neoplasms are characterized by a mucinous epithelial proliferation with pushing borders and an associated densely fibrotic wall. We have recently identified four examples of histologically analogous neoplasms arising in the colon in our consultation service.

Design: All pathology reports and slides were reviewed. Clinical data and follow-up information were obtained.

Results: Our cohort was comprised of two women and two men, with a mean age of 71 years (range, 58-87). Associated conditions included diverticulosis (2), Crohn's disease (1), and sarcoma of terminal ileum (1). Presenting signs/symptoms included obstruction (2) and nausea, vomiting, and abdominal pain (1). One patient was asymptomatic and the tumor was incidentally found on imaging for renal calculi. Colonoscopies, performed in 2 patients, were notable for narrowing and "fullness" without mucosal involvement. Tumors involved the rectosigmoid (2), sigmoid (1), and transverse colon (1) and ranged in size from 1.7 cm to 6.1 cm. One tumor arose in a duplication cyst and another in association with a sessile serrated lesion. All cases showed columnar, variably mucinous epithelium associated with little-to-no lamina propria. All but one case (transverse colon) showed fibrosis of the submucosa. Focal areas interpreted as high-grade dysplasia were seen in 3 cases. Prominent apoptosis was identified in one case. Neoplastic glands and/or mucin dissected through the colonic wall in 3 examples. No extracolonic neoplastic cells/mucin,

infiltrative invasion, or desmoplastic response were identified in any case. Follow-up information was available for three patients, ranging from 5.5 to 28 months. No patient experienced pseudomyxoma peritonei, distant metastases, or tumor-related deaths.

Conclusions: Our series shows that colonic mucinous neoplasms are found predominantly in the rectosigmoid colon, are associated with diverticula or duplication cysts, and show histologic features analogous to appendiceal counterparts. Although limited by our case number, these appear to pursue an indolent course with complete surgical resection. As these examples arose in diverticula or duplication cysts (growth in confined space, diverted from fecal stream), we propose that the pathogenesis of intestinal mucinous neoplasms may overlap with that of appendiceal mucinous neoplasms. Larger, multi-institutional series with long-term follow up and molecular analysis are needed to further characterize these lesions.

397 Evaluation of Enterochromaffin-like Cell Hyperplasia Does Not Help Diagnose or Stratify Patients with Atrophic Gastritis

Feidi Chen[1], Raul Gonzalez[1]
[1]*Beth Israel Deaconess Medical Center, Harvard Medical School, Boston, MA*

Disclosures: Feidi Chen: None; Raul Gonzalez: None

Background: Atrophic gastritis (AG) is characterized by atrophy of gastric glands, in particular oxyntic glands; it is often autoimmune in nature. The histologic diagnosis is confirmed by immunohistochemistry (IHC) for gastrin (to confirm biopsy site), and pathologists often use neuroendocrine IHC to evaluate for enterochromaffin-like cell hyperplasia (ECL-H). The utility of this latter staining is unclear, and we undertook this study to stratify AG patients by ECL pattern and compare clinicopathologic findings.

Design: We identified all patients in our archives with AG (Fig 1A). For available cases, we confirmed the diagnosis by reviewing H&E and gastrin IHC slides. Using Solcia's 1998 criteria, we evaluated ECL patterns using existing chromogranin and/or synaptophysin IHC and divided cases into three groups: AG with ECL-H (qualitative and quantitative criteria met, Fig 1B), AG with focal ECL-H (qualitative but not quantitative criteria met, Fig 1C), and AG without ECL-H (neither met, Fig 1D). We also evaluated intestinal metaplasia (IM), percentage oxyntic gland loss, and *Helicobacter pylori* status. We recorded patient age, sex, MCV, vitamin B12 level, and serologies (anti-parietal cell and/or anti-intrinsic factor antibodies), as available. Findings between groups were compared using Fisher's exact test and the unpaired *t* test, with statistical significance set at $P<0.05$.

Results: The cohort included 223 AG cases (59 men and 143 women). Findings are summarized in the Table. Age distribution was similar between groups, but patients without ECL-H were more often male compared to ECL-H patients (56% vs. 28%, $P=0.028$). Patients with ECL-H were more likely to have serum antibodies those with focal ECL-H (79% vs 0%, $P=0.0003$) or no ECL-H (79% vs 0%, $P=0.014$). Mean MCV was highest in patients with focal ECL-H (91 vs. 86 for ECL-H, $P=0.023$; 91 vs. 84 for no ECL-H, $P=0.031$). However, no H&E histologic findings (percentage of oxyntic gland loss, IM, *H. pylori* status) were significantly different between groups, though patients with ECL-H tended to more commonly show IM than those without ECL-H (76% vs. 56%, $P=0.089$).

	Group 1: AG with ECL-H (n=181)	**Group 2:** AG with focal ECL-H (n=24)	**Group 3:** AIG without ECL-H (n=18)	P-value (1 vs. 2)	P-value (1 vs. 3)	P-value (2 vs. 3)
Male:female ratio	50 M:131 F	9 M:15 F	10 M:8 F	0.34	0.028*	0.35
Mean age	61 years	66 years	59 years	0.081	0.59	0.11
Antibody +	41/52 (79%)	0/6 (0%)	0/3 (0%)	0.0003*	0.014*	1.0
Mean MCV	86	91	84	0.023*	0.29	0.031*
Mean vitamin B12	535	623	523	0.47	0.93	0.54
Intestinal metaplasia	137 (76%)	17 (71%)	10 (56%)	0.62	0.089	0.35
Mean percentage oxyntic gland loss	97%	92%	95%	0.13	0.60	0.60
Helicobacter pylori	6 (3%)	2 (8%)	2 (11%)	0.24	0.16	1.0

Figure 1 - 397

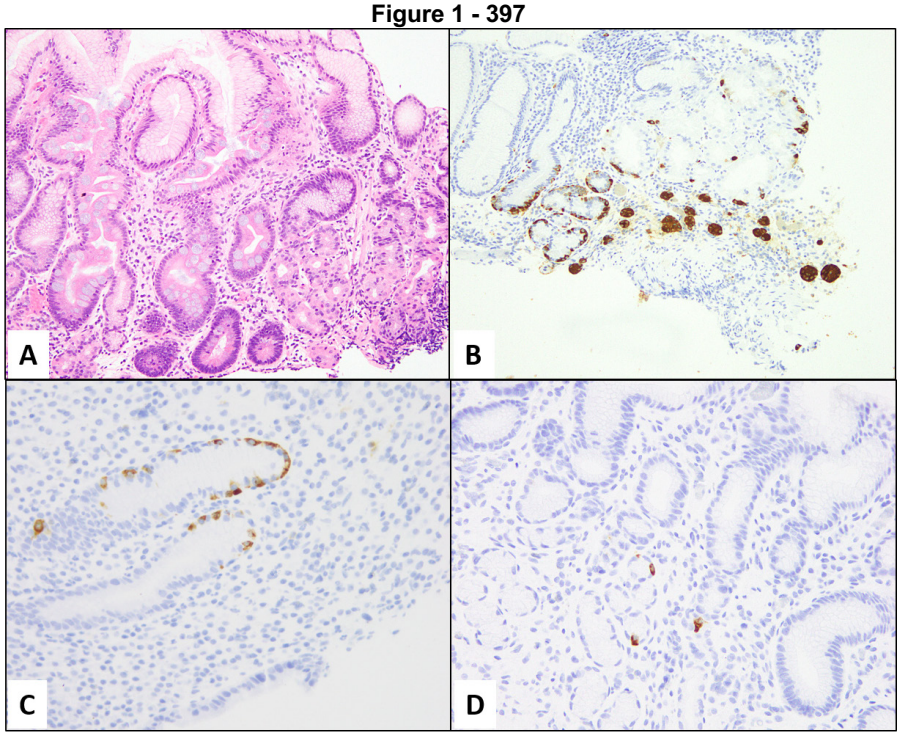

Conclusions: H&E findings in AG were generally similar regardless of ECL-H status, indicating that ECL evaluation has limited utility for diagnostic purposes (outside the setting of a mass lesion). Patients without ECL-H on biopsy were more often male and more often lacked serum antibodies, meaning such cases may be clinically atypical and/or not autoimmune despite classic histologic findings.

398 Feasibility of EPM2AIP1 Immunohistochemistry as Surrogate for MLH1 Promoter Hypermethylation Testing in Colorectal Cancer

Wei Chen[1], Deborah Knight[1], Rachel Pearlman[1], Heather Hampel[1], Wendy Frankel[1]
[1]The Ohio State University Wexner Medical Center, Columbus, OH

Disclosures: Wei Chen: None; Deborah Knight: None; Rachel Pearlman: None; Heather Hampel: *Advisory Board Member*, Promega, Invitae Genetics, Genome Medical; *Consultant*, GI OnDemand; Wendy Frankel: None

Background: *MLH1* promoter hypermethylation (MPH) analysis is an essential step in the universal tumor testing algorithm for Lynch syndrome (LS), the most common inherited predisposition to colorectal cancer (CRC). MPH usually indicates sporadic CRC. *EPM2AIP1* gene shares the same promoter as *MLH1*, therefore MPH should also silence *EPM2AIP1* transcription leading to loss of protein expression on immunohistochemistry (IHC). It has been previously reported that EPM2AIP1 IHC can be used as a surrogate for MPH in endometrial cancer (Mrkonjic & Turashvili, *Lab Invest* 2021; 101 [suppl 1]: page723). Our goal was to evaluate the feasibility of EPM2AIP1 IHC as a surrogate for MPH in CRC.

Design: EPM2AIP1 IHC (Origene, clone OTI2G3, 1:900 dilution, Leica Bond III, Leica Bond Polymer Refine detection system, catalog #DS9800) was evaluated on tissue microarrays of CRC; each case duplicated with two tissue cores of 1.2 mm. Only cases with known results for MPH, MSI, and mismatch repair protein (MMR) IHC were included. Any convincing nuclear staining (>5%) in the tumor as strong as internal positive control (lymphocytes, stroma cells) was considered present. Two pathologists evaluated the IHC without knowing MPH status.

Results: A total of 82 CRC cases were evaluated, 64 with MPH and 18 without MPH. All cases were MSI-high and showed MMR deficiency by IHC. Of the 64 cases with MPH, all showed absent MLH1 by IHC, but only 46 (72%) of the 64 cases with MPH exhibited loss of expression of EPM2AIP1 as expected. The rest (28%) showed retained staining. Of the 18 cases without MPH, 8 (44%) cases had unexpected loss of EPM2AIP1 expression. Of note, 5 cases were MLH1-related Lynch syndrome without MPH,

but only 1 (20%) case showed intact expression of EPM2AIP1 as expected. Various combinations of antibody dilution and blocking agents were tested during antibody optimization, but interpretation of EPM2AIP1 IHC remained challenging. The staining intensity was often weak, and obscuring cytoplasmic, luminal brush border, and heterogeneous staining were occasionally seen.

	Concordant EPM2AIP1 IHC results # (%)	Discordant EPM2AIP1 IHC results # (%)	Total cases
MLH1 promoter methylated	46 (72%)	18 (28%)	64
MLH1 promoter not methylated	10 (56%)	8 (44%)	18
Total cases	56 (68%)	26(32%)	82

Figure 1 - 398

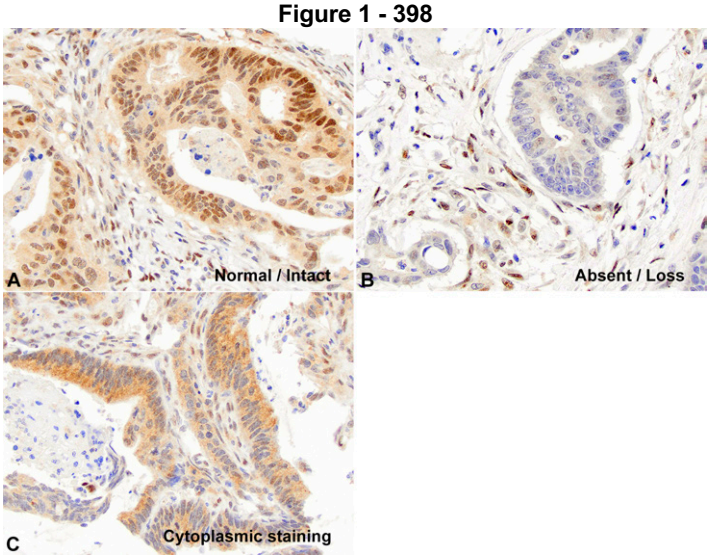

Conclusions: We found EPM2AIP1 IHC was only concordant with MPH status in 68% (47/69) of CRC cases and interpretation of the IHC was challenging. Unless the stain quality improves with different clones or platforms, it will likely not be useful as a surrogate test for MPH in CRC.

399 Neural Colorectal Lesion Incidence Varies by Site, and Multifocal Cases are Often Syndromic: Insights from a Series of 593 Patients

Irene Chen[1], Raul Gonzalez[2], Aaron Huber[1]
[1]University of Rochester Medical Center, Rochester, NY, [2]Beth Israel Deaconess Medical Center, Harvard Medical School, Boston, MA

Disclosures: Irene Chen: None; Raul Gonzalez: None; Aaron Huber: None

Background: Colorectal lesions with neural differentiation include a number of different entities, most of which present as polyps and some of which have histologic overlap or similar immunohistochemical profiles. To date, most studies have focused on a single diagnostic entity. A comprehensive clinicopathologic comparison between different types of colorectal lesions with neural differentiation is lacking, prompting this study.

Design: All patients diagnosed with a neural or neural-related colorectal lesion from 2004 to 2020 (perineurioma, mucosal Schwann cell hamartoma, ganglioneuroma, granular cell tumor, neuroma, neurofibroma, schwannoma, tactoid corpuscle-like bodies) were retrospectively identified at two institutions. The diagnosis of each case was reviewed, and detailed analyses of clinical, histologic, and endoscopic features were performed. Lesion characteristics were compared using statistical analysis on SPSS v25 and GraphPad Prism 9.

Results: Our cohort included 634 lesions from 593 patients (269 males and 324 females) with a median age of 57 (range: 13-85) years. A majority of patients were asymptomatic (n=481, 81%) and presented with a solitary lesion (n=551, 93%). Most lesions (n=615, 97%) appeared polypoid or nodular on colonoscopy. The most common types were perineurioma (n=229, 36%, Fig 1A),

mucosal Schwann cell hamartoma (n=204, 32%, Fig 1B), and ganglioneuroma (n=147, 23%, Fig 2A). They most commonly involved the mucosa (n=544, 94%, $p < 0.0001$) of the sigmoid colon (n=230, 40%, $p < 0.0001$). In contrast, granular cell tumor (n=32, 5%, Fig 2B) most commonly involved the submucosa (n=13, 41%, $p < 0.0001$) of the cecum and ascending colon (n=21, 66%, $p < 0.0001$). Other lesions, such as schwannoma (n=13, 2%) and neurofibroma (n=4, 1%), remained rare and could be seen involving different sites and layers of the colon. A small subgroup (n=42, 7%) had synchronous and/or metachronous lesions. Of these, 23 (55%) had genetic evidence of a syndromic manifestation ($p < 0.0001$), with multiple ganglioneuromas in Cowden syndrome (n=18) being the most common scenario.

Figure 1 - 399

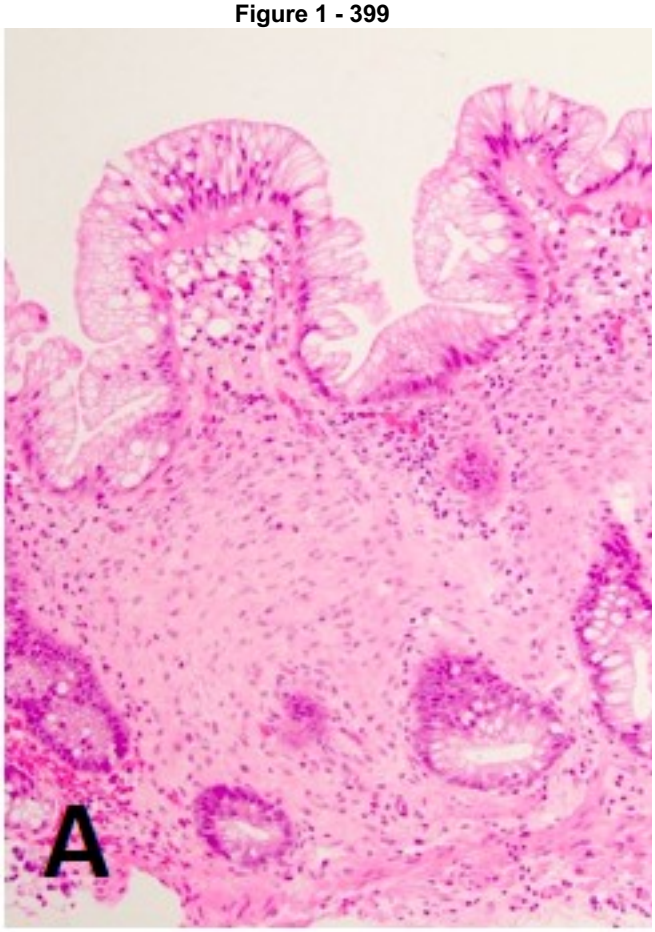

Figure 2 - 399

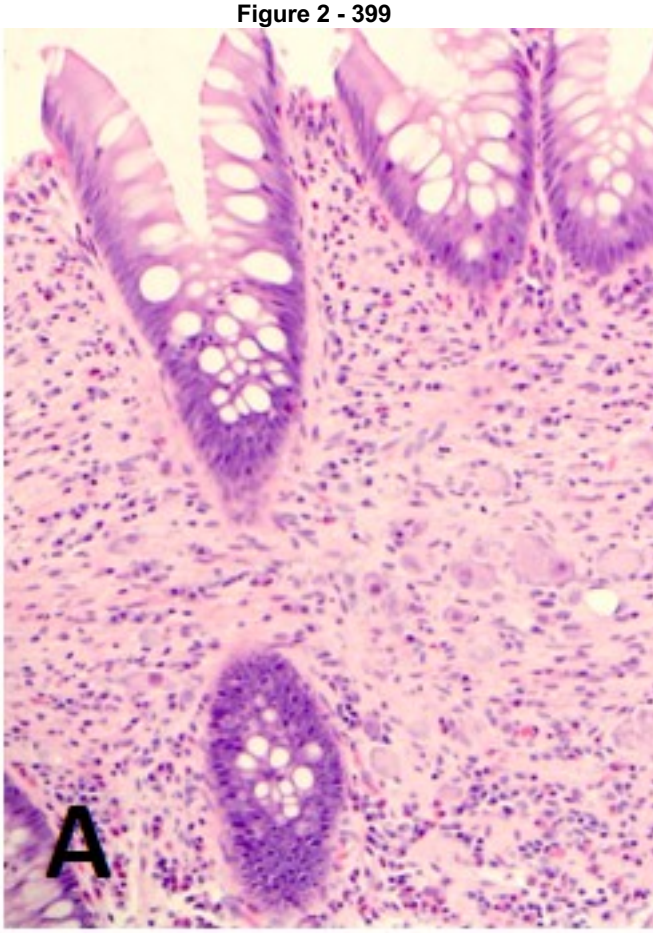

Conclusions: Our cohort is the largest to date comparing different types of neural colorectal lesions, which are commonly found incidentally in asymptomatic patients. Lesion type is significantly associated with colon segment and the layer involved. Multifocal presentation, while uncommon, is typically associated with genetic syndromes.

400 Sessile Serrated Lesions of the Appendix Are Distinct from Their Right-Sided Colonic Counterparts and May Be Precursors for Appendiceal Mucinous Neoplasms

Ksenia Chezar[1], Parham Minoo2

[1]Alberta Precision Laboratories, University of Calgary, Calgary, Canada, [2]University of Calgary, Alberta Precision Laboratories, Calgary, Canada

Disclosures: Ksenia Chezar: None; Parham Minoo: None

Background: Sessile serrated lesions (SSLs) of the appendix have significant morphologic overlap with their colorectal counterparts. Despite a similar histologic appearance, they exhibit a different spectrum of genetic abnormalities. It has been postulated that appendiceal SSLs may serve as precursors to low-grade appendiceal mucinous neoplasms (LAMNs), but this has

not been examined systematically. The aim of this study was to better elucidate the serrated neoplasia pathway in the appendix, and explore the relationship between SSLs and LAMNs through multigene and immunohistochemical characterization of paired and unpaired cases.

Design: A search was made in the laboratory information system over a six-year period (2014-2019) for appendiceal specimens with the diagnoses of low grade appendiceal mucinous neoplasm and/or sessile serrated lesion/adenoma. In our cohort, 21 out of 119 LAMNs (17%) had a concurrent SLL component. In the twelve paired cases selected for the study, the SSL and LAMN components could be microdissected without cross-contamination. In total, we evaluated 62 serrated lesions from 50 appendectomy specimens for hotspot mutations in BRAF, KRAS and GNAS genes. Cases were subdivided into 3 groups: 20 unpaired SSLs, 18 unpaired LAMNs, and 12 with an SSL and concurrent LAMN. β-catenin and Annexin A10 immunostaining were performed on the SSL and LAMN components in the 12 paired cases. Fourteen colonic SSLs served as controls for the immunostaining.

Results: There was no significant difference in KRAS hotspot mutation rates in appendiceal SSLs (17/26; 65%) and LAMNs (16/30; 58%) (p=0.42). BRAF V600E was identified in a single case (1/50; 2%) of SSL and concurrent LAMN (p=1.0). Mutations in GNAS were more common in LAMNs (6/30; 20%) compared to SSLs (1/30; 3%) (p=0.05). The molecular genotypes between paired SSLs and LAMNs were concordant in most cases (10/12; 83%). β-catenin immunostaining was significantly increased in LAMNs (10/12; 83%) compared to their paired appendiceal SSLs (2/12; 17%) (p=0.003). Annexin A10 immunostaining was significantly reduced in appendiceal SSLs (1/12; 8%) compared to colonic SSLs (14/14; 100%) (p<0.0001).

Table 1. Genetic analysis results of the paired and unpaired appendiceal SSL and LAMN cases and IHC results of the β-catenin localization of paired lesions.

Case #	Age/ Gender	Histology	Mutation analysis			IHC
			KRAS c12/13/61	*GNAS* c201	*BRAF* V600E	Nuclear β-catenin
SSLs (unpaired)						
Case 1	59/F	SSL	–*	–	Wild-type	n/a
Case 2	77/F	SSL	–	Wild-type	–	n/a
Case 3	53/M	SSL	–	Wild-type	–	n/a
Case 4	68/F	SSL	*KRAS* p.G12A (c.35G>A)	Wild-type	Wild-type	n/a
Case 5	70/F	SSL	*KRAS* p.G13A (c.38G>A)	Wild-type	Wild-type	n/a
Case 6	40/F	SSL	Wild-type	Wild-type	Wild-type	n/a
Case 7	65/F	SSL	*KRAS* p.G12A (c.35G>A)	Wild-type	Wild-type	n/a
Case 8	78/F	SSL	Wild-type	Wild-type	Wild-type	n/a
Case 9	49/M	SSL	*KRAS* p.G12A (c.35G>A)	Wild-type	Wild-type	n/a
Case 10	46/F	SSL	Wild-type	Wild-type	Wild-type	n/a
Case 11	46/F	SSL	*KRAS* p.G12A (c.35G>A)	Wild-type	Wild-type	n/a
Case 12	74/M	SSL	*KRAS* p.G12V (c.35G>T)	Wild-type	Wild-type	n/a
Case 13	82/M	SSL	Wild-type	Wild-type	Wild-type	n/a
Case 14	56/F	SSL	*KRAS* p.G12A (c.35G>A)	*GNAS* p.R201H (c.602G>A)	Wild-type	n/a
Case 15	37/F	SSL	–	Wild-type	Wild-type	n/a
Case 16	66/F	SSL	*KRAS* p.G12C (c.34G>T)	Wild-type	–	n/a
Case 17	67/F	SSL	*KRAS* p.G12V (c.35G>T)	Wild-type	Wild-type	n/a
Case 18	31/F	SSL	–	Wild-type	Wild-type	n/a
Case 19	78/M	SSL	Wild-type	Wild-type	–	n/a
Case 20	52/F	SSL	–	Wild-type	–	n/a
LAMNs (unpaired)						
Case 21	57/F	LAMN	Wild-type	Wild-type	Wild-type	n/a
Case 22	54/F	LAMN	Wild-type	Wild-type	Wild-type	n/a
Case 23	76/F	LAMN	Wild-type	Wild-type	Wild-type	n/a
Case 24	64/F	LAMN	*KRAS* p.G12A (c.35G>A)	*GNAS* p.R201H (c.602G>A)	Wild-type	n/a
Case 25	73/F	LAMN	*KRAS* p.G12A (c.35G>A)	Wild-type	Wild-type	n/a
Case 26	41/M	LAMN	Wild-type	Wild-type	Wild-type	n/a
Case 27	62/F	LAMN	Wild-type	Wild-type	Wild-type	n/a
Case 28	60/F	LAMN	*KRAS* p.G12A (c.35G>A)	*GNAS* p.R201H (c.602G>A)	Wild-type	n/a
Case 29	61/F	LAMN	*KRAS* p.G13D (c.38G>A)	Wild-type	Wild-type	n/a
Case 30	59/M	LAMN	Wild-type	Wild-type	Wild-type	n/a
Case 31	73/F	LAMN	*KRAS* p.G12A (c.35G>A)	Wild-type	Wild-type	n/a
Case 32	69/M	LAMN	*KRAS* p.G12A (c.35G>A)	Wild-type	Wild-type	n/a
Case 33	50/M	LAMN	*KRAS* p.G12A (c.35G>A)	Wild-type	Wild-type	n/a
Case 34	44/F	LAMN	*KRAS* p.G12A (c.35G>A)	Wild-type	Wild-type	n/a
Case 35	74/M	LAMN	Wild-type	Wild-type	Wild-type	n/a
Case 36	54/F	LAMN	Wild-type	Wild-type	Wild-type	n/a
Case 37	25/M	LAMN	*KRAS* p.G12A (c.35G>A)	Wild-type	Wild-type	n/a
Case 38	52/F	LAMN	Wild-type	Wild-type	Wild-type	n/a
SSLs and LAMNs (paired)						
Case 39	75/M	SSL LAMN	*KRAS* p.G12V (c.35G>T) *KRAS* p.G12V (c.35G>T)	Wild-type Wild-type	Wild-type Wild-type	- -
Case 40	82/M	SSL LAMN	*KRAS* p.G12A (c.35G>A) *KRAS* p.G12A (c.35G>A)	Wild-type Wild-type	Wild-type Wild-type	+ +

Case 41	55/F	SSL LAMN	*KRAS* p.G12V (c.35G>T) Wild-type	Wild-type Wild-type	Wild-type Wild-type	- +
Case 42	76/M	SSL LAMN	*KRAS* p.G12V (c.35G>T) *KRAS* p.G12V (c.35G>T)	Wild-type *GNAS* p.R201H (c.602G>A)	Wild-type Wild-type	- +
Case 43	60/F	SSL LAMN	*KRAS* p.G12A (c.35G>A) *KRAS* p.G12A (c.35G>A)	Wild-type Wild-type	Wild-type Wild-type	+ +
Case 44	46/F	SSL LAMN	*KRAS* p.G12A (c.35G>A) *KRAS* p.G12A (c.35G>A)	Wild-type *GNAS* p.R201H (c.602G>A)	Wild-type Wild-type	- +
Case 45	66/M	SSL LAMN	Wild-type Wild-type	Wild-type Wild-type	Wild-type Wild-type	- +
Case 46	61/F	SSL LAMN	Wild-type Wild-type	Wild-type Wild-type	Wild-type Wild-type	- +
Case 47	51/M	SSL LAMN	Wild-type Wild-type	Wild-type Wild-type	Wild-type Wild-type	- -
Case 48	78/M	SSL LAMN	*KRAS* p.G12V (c.35G>T) *KRAS* p.G12V (c.35G>T)	Wild-type *GNAS* p.R201H (c.602G>A)	Wild-type Wild-type	- +
Case 49	76/M	SSL LAMN	*KRAS* p.G12V (c.35G>T) *KRAS* p.G12A (c.35G>A)	Wild-type Wild-type	Wild-type Wild-type	- +
Case 50	79/F	SSL LAMN	Wild-type Wild-type	Wild-type *GNAS* p.R201H (c.602G>A)	*BRAF* p.V600E (c.1799T>A) *BRAF* p.V600E (c.1799T>A)	- +

*M, male; F, female; SSL, sessile serrated lesion; LAMN, low grade appendiceal neoplasm; n/a, not applicable. *– indicates uninterpretable genetic results.*

Figure 1 - 400

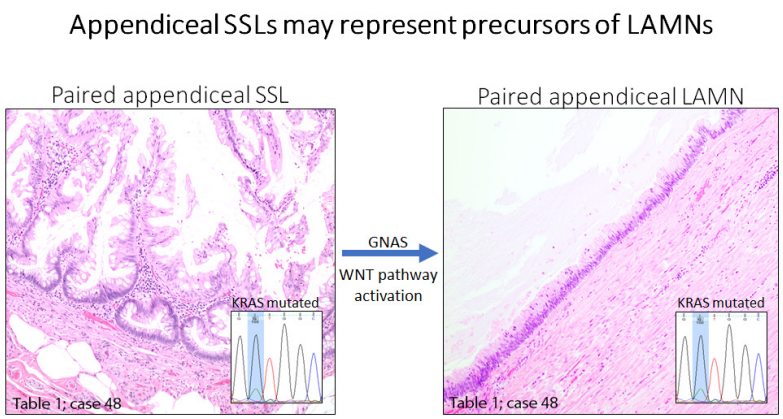

Figure 2 – 400

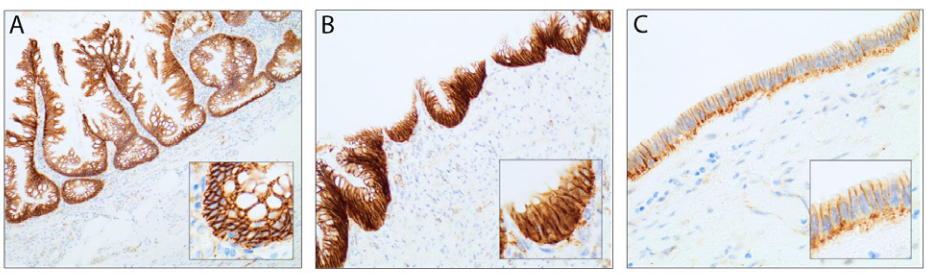

Expression of β-catenin in an appendiceal sessile serrated lesion (SSL) and low grade appendiceal mucinous neoplasm (LAMN). The majority of appendiceal SSLs demonstrate normal membrane-predominant expression of β-catenin (A). A majority of LAMNs demonstrate aberrant nuclear immunohistochemical expression of β-catenin (B), while only a minority of cases show normal membrane-predominant expression (C).

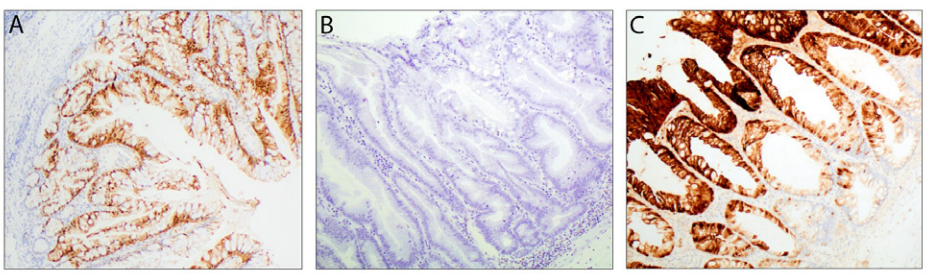

Annexin A10 immunostaining in appendiceal and colonic sessile serrated lesions (SSL). Appendiceal SSLs rarely demonstrate cytoplasmic positivity (A) and are typically negative (B). The majority of right-sided colonic SSLs demonstrate strong cytoplasmic positivity of Annexin A10 (C).

Conclusions: Appendiceal serrated lesions are predominantly driven by KRAS mutations and are not characterized by Annexin A10 immunostaining. At least a subset of LAMNs may arise from a precursor SSL in which GNAS mutation and/or upregulation of the WNT-signaling pathway are likely key events modulating this progression.

401 Clinicopathological and Molecular Characteristics of PIK3CA-mutant Gastric Cancer with Emphasis on its Tumor Immune Microenvironment

Sangjoon Choi[1], Hyunjin Kim[1], Won Ki Kang[2], Kyoung-Mee Kim[1]
[1]Samsung Medical Center, Seoul, South Korea, [2]Samsung Medical Center, South Korea

Disclosures: Sangjoon Choi: None; Hyunjin Kim: None; Won Ki Kang: None; Kyoung-Mee Kim: None

Background: In gastric cancer (GC), PIK3CA mutation is frequently observed in Epstein-Barr virus –associated-GC (EBVaGC). However, the clinicopathological, molecular, and immunophenotypic characteristics of PIK3CA mutated GC are not fully explored.

Design: We investigated 133 GC cases harboring PIK3CA mutations and categorized them into three groups; E542K, E545X, and H1047R. Clinicopathological parameters including EBV, microsatellite instability (MSI), PD-L1 combined proportion score (CPS), and stromal TIL were evaluated. Concurrent genomic alterations were analyzed using targeted sequencing. Nanostring GeoMx Digital Spatial Profiling (DSP) was used to assess multiple immunooncology protein expressions.

Results: Of 133 PIK3CA mutated GC, E542K, E545X, H1047R, and others were found in 21 (15.8%), 36 (27.1%), 26 (19.5%), and 46 (34.6%) cases. Four GC (3.0%) had co-mutations (3 E542K and E545K, 1 E545K and H1047R). H1047R-mutation was significantly frequent in MSI-high GC (p=0.009) while EBV positivity did not affected mutation subtypes with even distribution. Exon 9 (E542K and E545X) mutated GC was significantly associated with poorly differentiated histology and advanced pN stage (p<0.04) compared to Exon 20 (H1047R) mutated GC. There was no significant difference on survival and concurrent molecular alterations between E542K, E545X, and H1047R subgroups. However, in subgroup analysis for EBV+ GC, H1047R-mutant GC showed a trend toward longer survival than E542K and E545X mutated GC (p=0.090 and 0.062). Clustering analysis showed immunologically distinct 3 subtypes of immune-low (42.9%), immune-medium (54.0%), and immune-high (3.1%) tumors. Immune-high groups showed significant association with undifferentiated histology, PD-L1 negativity, and E542K/E545X mutation. Multivariable analysis showed that CD11c, Ki-67, Tim-3, GITR, and IDO expressions were independent prognostic factors for worse survival, while HLA-DR, CTLA4, CD45, and CD4 were associated with better prognosis.

		Exon 9 (E542K)	Exon 9 (E545X)	Exon 20 (H1047X)	Significance between E542K, E545X, H1047X	Significance between Exon 9 and 20
	Total	n=21	n=36	n=26	p value	p value
Sex					0.105	0.053
male	48	12	25	11		
female	35	9	11	15		
Histology					0.145	0.031
WD,MD	30	6	10	14		
PD	42	12	20	10		
SRCC	4	1	1	2		
Others	7	2	5	0		
AJCC T stage					0.945	1
2	2	0	1	1		
3	24	6	10	8		
4	28	5	14	9		
AJCC N stage					0.076	0.028
0	3	0	1	2		
1	14	3	6	5		
2	12	3	2	7		
3	25	5	16	4		
Lauren					0.184	0.062
Intestinal	30	5	11	14		
Diffuse	41	13	17	11		
Mixed	5	1	3	1		
Others	7	2	5	0		
Stromal TIL (cut-off=25%)					0.305	0.115
(-)	24	4	9	11		
(+)	28	7	14	7		
PD-L1 CPS					0.017	0.752
0	34	9	5	4		
>=1	56	6	21	12		
Immune checkpoint inhibitor response					0.111	0.103

Non-responder	6	1	4	1		
Responder	7	1	1	5		
MSI					0.009	0.001
Stable	66	19	31	16		
Unstable	15	2	3	10		
EBV					0.502	0.406
(-)	54	14	21	19		
(+)	20	4	11	5		
TP53					0.721	0.484
(-)	63	16	26	21		
(+)	20	5	10	5		
ERBB2 (SNV, Amp)					0.183	0.419
(-)	61	12	29	20		
(+)	8	4	3	1		
KRAS (SNV, Amp)					1.000	1.000
(-)	68	17	29	22		
(+)	15	4	7	4		
PTEN					0.107	0.427
(-)	62	16	26	20		
(+)	7	0	6	1		
FGFR2					1.000	1.000
(-)	65	16	29	20		
(+)	5	1	3	1		
ARID1A					0.189	0.740
(-)	56	15	23	18		
(+)	13	1	9	3		
CCNE1 (SNV, Amp)					1.000	1.000
(-)	67	16	30	21		
(+)	2	0	2	0		

Figure 1 - 401

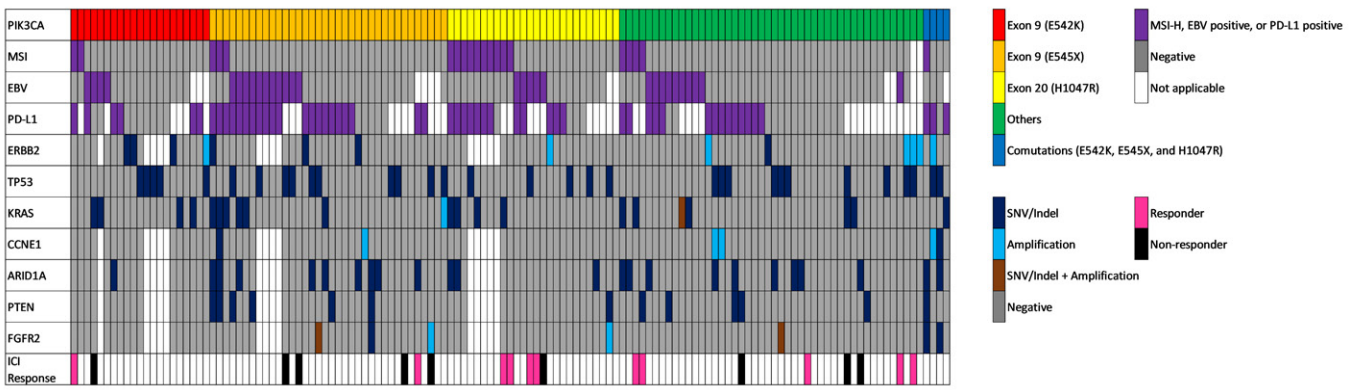

Figure 2 – 401

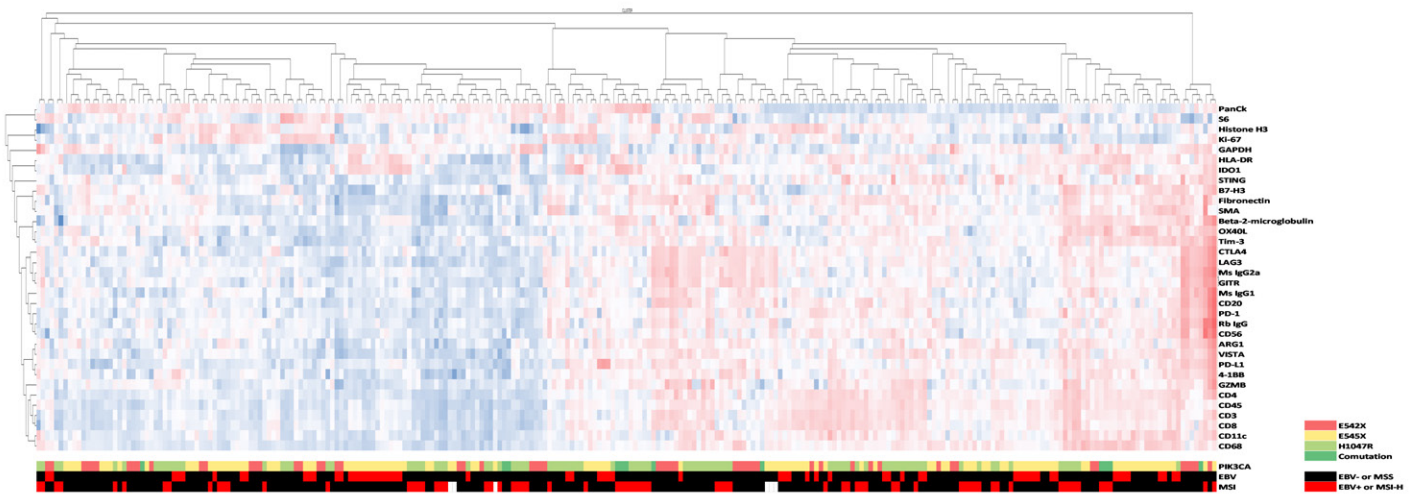

Conclusions: PIK3CA mutations of GC are clinicopathologically and immunologically heterogenous group. EBV status, PIK3CA mutation subtype, various immune-related protein expressions and their interactions should be considered as factors of clinical significance.

402 Higher Rate of Late Recurrence of Colorectal Carcinoma in Patients with Malignant Polyp Managed with Polypectomy and Local Excision versus Segmental Colectomy

Min Cui[1], Wei Xin[2]
[1]University Hospitals Cleveland Medical Center, Cleveland, OH, [2]Case Western Reserve University/University Hospitals Cleveland Medical Center, Cleveland, OH

Disclosures: Min Cui: None; Wei Xin: None

Background: Malignant polyps (MP) are polypoid lesions that appear benign endoscopically but harbor adenocarcinoma invasion into submucosa microscopically. Current practice generally recommends following up with endoscopic surveillance after polypectomy if there are no high-risk factors in the malignant polyp, such as positive margin, angiolymphatic invasion, and high-grade components. Current guidelines recommended intervals of 1, 3, and 5 years if colonoscopy findings are normal. Whether this management is sufficient for the long-term follow-up is uncertain with very little literature on follow-up data of MP managed by polypectomy beyond 5 years. We aim to address this knowledge gap in the study.

Design: Consecutive MP cases between 1995-2019 from a single institute were retrieved, and only cases with follow-up periods over one year were included (n=76, age 39-89, F/M:30/46). Among these patients, 28 patients had endoscopic polypectomy, some cases with local re-excision followed by endoscopic surveillance (group 1), while 48 patients underwent segmental colectomy (group 2).

Results: In Group 1, during the follow-up period (varying from 1.0 to 10.3 years, median 4.1 years), three patients presented with local recurrent T3 adenocarcinoma (5.9 to 9.7 years), one patient developed liver metastasis (7.3 years), and one patient presented with MP in another segment of the colon (4.0 years). Two of the local recurrence cases did not have known high risk features. All three local recurrent cases were negative for KRAS mutation and two of them harbored P53 mutation. In Group 2, during the follow-up period (1.0-21.8 years, median 9.3 years), none of the patients developed local recurrence. One patient developed metastases in the liver and lung one and three years respectively after surgery.

Conclusions: Our study showed that patients managed by endoscopic polypectomy and local excision had a higher local late recurrence rate (10.7%) than patients managed by surgical resection (0%). These findings suggest that patients with malignant polyp managed by endoscopic polypectomy and local excision, even without high-risk indicators, have a higher chance of late recurrence and may require more intense surveillance than suggested by the current guideline. Further study is needed to explore whether certain molecular alteration, such as P53 mutation, is high risk factor for late recurrence.

403 Prospective HER2/neu Testing in Invasive Colorectal Cancer: A Real-World Experience

Armando del Portillo[1], Huaibin Mabel Ko[2], Anne Koehne de Gonzalez[2], Michael Lee[2], Ladan Fazlollahi[2], Helen Remotti[3], Stephen Lagana[2]
[1]Columbia University Irving Medical Center, New York, NY, [2]New York-Presbyterian/Columbia University Medical Center, New York, NY, [3]Columbia University Medical Center, New York, NY

Disclosures: Armando del Portillo: None; Huaibin Mabel Ko: None; Anne Koehne de Gonzalez: None; Michael Lee: None; Ladan Fazlollahi: None; Helen Remotti: None; Stephen Lagana: *Consultant*, GATT Technologies, Organ Recovery Systems; *Stock Ownership*, Doc Vita; *Consultant*, SpringTide Ventures; *Stock Ownership*, Biotech stocks: BFLY, DNA, EDIT, GH, NAUT, QSI

Background: Approximately 3% of colorectal cancers (CRC) are *HER2/neu* amplified. This percentage increases in tumors which are wild type for RAS and BRAF. Following the successful HERACLES and MyPathway studies, and following discussion with colleagues in gastrointestinal oncology, our institution began a program of reflexively testing all invasive or metastatic CRC for *HER2/neu* amplification by immunohistochemistry (IHC) and silver in-situ hybridization (SISH) for equivocal cases.

Design: We test all invasive or metastatic CRC in whatever form we first encounter it (e.g. biopsy of the primary tumor, resection of the primary, biopsy or resection of a metastasis). We do not repeat testing on subsequent samples unless requested. We use the

same IHC protocol for breast and upper GI cancer (Ventana) and report IHC according to the criteria described in the HERACLES trial. In brief, negative for HER2 includes 0-1+ staining (faint any cellularity), 2+ staining <50% of tumor cells, or 3+ <10% of tumor cells; equivocal staining includes 2+ in >50% of tumor cells or 3+ in >10% and <49% of tumor cells; and positive *HER2/neu* expression is for tumors with 3+ staining in ≥50% of tumor cells. Staining includes lateral, basolateral, and circumferential. Positive SISH criteria includes HER2:CEP17 ratio ≥2 in ≥50% of tumor cells, with counting a minimum of 100 tumor cells. Herein, we summarize our experience to date.

Results: Between 5/2019 - 9/2021, we tested 168 patients with CRC (105 bx, 64 resection), 3 of which had 2 synchronous primaries, for a total of 172 tumors. The HER2 positivity rate was 4% (7/172), 3 positive cases were identified on biopsy, whereas 4 were identified on resection. The positive cases consisted of six 3+ IHC and one which was 2+ by IHC and required positive SISH. Of the 165 negative cases, 161 (98%) were negative by IHC criteria, two were 2+ with negative SISH, and one was negative by SISH only. Mismatch repair status was preserved in all HER2+ cases, and of the 5 cases tested for molecular alterations, one had a *PIK3CA* mutation, and none had *RAS* or *BRAF* mutations.

Case	Location	Procedure	Differentiation	pT stage	pN stage	pM stage
1	Rectosigmoid	Biopsy	Moderate	3	1a	
2	Hepatic flexure	Biopsy	Minute, not stated	Unknown	Unknown	1
3	Rectum	Resection	Moderate	3	0	
4	Descending	Resection	Moderate	2	0	
5	Liver	Biopsy	Moderate	Unknown	Unknown	1
6	Right	Resection	Moderate	3	0	
7	Sigmoid	Resection	Moderate to poor	3	2b	

Conclusions: Prospectively testing CRC for *HER2/neu* has yielded the anticipated results, i.e. the positivity rate is similar to what was identified in retrospective studies and clinical trials. Performing the testing is a trivial matter if the laboratory is experienced evaluating *HER2/neu* in other cancers, and the results can increase the therapeutic options for the patient. We will monitor whether patients are treated with and respond to anti-HER2 therapy.

404 Mesenchymal Neoplasms of the Gastrointestinal Tract: A Single Institution Clinicopathologic Analysis of Over 2500 Cases

Julio Diaz-Perez[1], Domenika Ortiz Requena[2], Jaylou Velez Torres[1], Monica Garcia-Buitrago[3], Andrew Rosenberg[4], Julio Poveda[1], Elizabeth Montgomery[1]

[1]University of Miami Miller School of Medicine, Miami, FL, [2]University of Miami Miller School of Medicine/Jackson Memorial Hospital, Miami, FL, [3]University of Miami Miller School of Medicine/Jackson Health System, Miami, FL, [4]University of Miami Health System, Miami, FL

Disclosures: Julio Diaz-Perez: None; Domenika Ortiz Requena: None; Jaylou Velez Torres: None; Monica Garcia-Buitrago: None; Andrew Rosenberg: None; Julio Poveda: None; Elizabeth Montgomery: None

Background: Mesenchymal neoplasms arising in the gastrointestinal tract (GI) encompass a group of diverse, distinctive and often rare tumors. The correct identification of these neoplasms is important in the identification of syndromic diseases, clinical management and prognostication. In this study we aim to determine the distribution of mesenchymal tumors by site, the clinicopathologic parameters of each type, and asses the utility of endoscopic biopsies in their accurate diagnosis.

Design: We retrospectively queried our surgical pathology database for cases of mesenchymal neoplasms of the gastrointestinal tract between 2013 to 2021. Clinical data were retrieved for each case through the electronic medical record for each case, when available.

Results: Between 2013 to 2021, we identified 2511 patients with mesenchymal tumors involving the GI tract. Of these patients, 1280 were males (51%) and 1231 were females (49%) with median age of 57.6 years (range: 9-98 years). Tumors locations included the esophagus (n=168, 6.66%), stomach (n=841, 33.49%), duodenum (n=126, 5%), ileum and jejunum (n=169, 6.73%), GE junction (n=19, 0.75%), cecum (n=115, 4.57%), appendix (n=9, 0.35%), ascending colon (n=365, 14.52%), transverse colon (n=146, 5.8%), descending colon (n=155, 6.17%), sigmoid colon (n=238, 9.47%), and rectum (n=160, 6.37%). Tumors measured from 0.15 up to 20 cm (mean: 3.3 cm). The tumor distribution and the percentage of tumors diagnosed by endoscopic biopsy are shown in Table 1.

Tumor	Total Number	Percentage	Percentage of Endoscopic diagnosis
Gastrointestinal stromal tumor	1292	51.45	14.81
Lipoma	479	19.07	65.17
Leiomyoma	370	14.73	51
Inflammatory fibroid polyp	109	4.34	100
Perineurioma/Benign fibroblastic polyp of colon	47	1.87	100
Leiomyosarcoma	38	1.51	0
Schwann cell hamartoma	29	1.15	100
Lymphangioma	20	0.79	
Hemangioma	19	0.75	
Schwannoma	18	0.71	
Fibromatosis	17	0.67	
Ganglioneuroma	16	0.63	100
Granular cell tumor	13	0.51	
Kaposi sarcoma	10	0.39	100
Inflammatory myofibroblastic tumor	6	0.23	0
Multiple leiomyomata	5	0.19	80
Liposarcoma	5	0.19	0
Xanthoma	4	0.15	100
Smooth muscle tumor of indeterminate potential	3	0.11	0
Plexiform Angiomyxoid Myofibroblastic Tumor/angiomyxoma	3	0.11	100
Pleomorphic fibroblastic/myofibroblastic sarcoma	2	0.07	0
Kaposiform hemangioendothelioma	1	0.03	0
Mucosal Neuroma	1	0.03	100
Lipomatosis	1	0.03	100
Dedifferentiated liposarcoma	1	0.03	0
Arteriovenous malformation	1	0.03	100
Angiosarcoma	1	0.03	0
Total	2511	100	

Conclusions: To our knowledge, this is the largest single institution series on GI mesenchymal tumors to date. We highlight the various tumor subtypes and prevalence amongst the various anatomic sites within the GI tract. Our study underscores the effectiveness of endoscopic biopsy in the diagnosis of GI-associated mesenchymal neoplasms.

405 Optimizing Detection of Colorectal Adenocarcinoma Micrometastases Using Deeper Sections and Immunohistochemistry

David Dodington[1], Keegan Guidolin[2], Fayez Quereshy[3], Stefano Serra[4], Klaudia Nowak[5]
[1]University of Toronto, Toronto, Canada, [2]Toronto General Hospital, Research Institute (UHN), Toronto, Canada, [3]University Health Network, Toronto, Canada, [4]University Health Network, University of Toronto, Toronto, Canada, [5]Toronto General Hospital, University Health Network, Toronto, Canada

Disclosures: David Dodington: None; Keegan Guidolin: None; Fayez Quereshy: None; Stefano Serra: None; Klaudia Nowak: None

Background: Micrometastases are defined as a cluster of tumor cells measuring 0.2-2.0 mm on cut section. The presence of micrometastases in colorectal adenocarcinoma is a significant poor prognostic factor and an important indication for adjuvant therapy. Currently, there is a lack of studies determining optimal methods for detection of micrometastases. The objective of this study was to determine if additional deeper levels and immunohistochemical stains would help detect micrometastases in patients that were initially staged as lymph node (LN) negative and subsequently developed a recurrence.

Design: Among a cohort of patients diagnosed with stage 2A colorectal adenocarcinoma (pT3, pN0) between 2014 and 2019, five patients who subsequently developed local or distant recurrence were selected for the study. None had received neoadjuvant chemotherapy. All LNs from primary surgical specimens were retrospectively evaluated for the presence of micrometastases. For each block containing LNs, three deeper levels (separated by 20 microns) were cut and stained with hematoxylin & eosin (H&E). This was followed immediately by one section stained by immunohistochemistry (IHC) for pancytokeratin (AE1/AE3 antibody); cells having strong immunoreactivity with membranous accentuation were identified as tumor cells (Figure 1).

Results: Patient demographics, tumor characteristics and results are summarized in Table 1. There was a median of 21 LNs identified per patient, and these were submitted in a median of 9 blocks. Micrometastesis were not identified in any of the evaluated

LNs; however, isolated tumor cells (ITCs), defined as single cells or clusters <0.2mm, were identified in 3 of 5 patients. ITCs were seen in 2/21, 2/20 and 5/23 of the respective LNs. Of note, ITCs were only seen initially on H&E-stained sections in one of the positive LNs and the remaining were identified only after IHC. Retrospective review of H&E-stained sections revealed single atypical cells in areas highlighted by IHC in only two of the positive LNs (Figure 1A), while ITCs were only seen by IHC in the remaining six LNs (Figure 1B).

Table 1.

	Patient 1	Patient 2	Patient 3	Patient 4	Patient 5
Patient demographics					
Age	51	63	48	38	88
Sex	Female	Male	Male	Male	Female
Tumor recurrence data					
Recurrence type	Clinical	Pathological	Pathological	Clinical	Clinical
Recurrence site	Adnexa	Liver	Liver	Lung	Lung
Months to recurrence	27	9	0	16	0
Tumor histopathological features					
Tumor location	Sigmoid	Ascending	Sigmoid	Rectum	Cecum
Tumor size (cm)	2.8	4.2	6.5	4.2	8.5
Tumor differentiation	Moderate	Moderate	Moderate	Moderate	Moderate
Small vessel invasion	Yes	No	Yes	No	No
Large vessel invasion	Yes	No	Yes	No	No
Perineural invasion	No	No	No	Yes	No
Tumor budding	High	High	Int	Int	High
Tumor deposits	No	No	No	No	No
Margin status	Negative	Negative	Negative	Negative	Negative
Total number of lymph nodes	20	21	25	20	23
Blocks with lymph nodes	6	9	11	8	10
Results (number of lymph nodes with)					
Micrometastesis after deepers	0	0	0	0	0
Micrometastesis after IHC	0	0	0	0	0
Isolated tumor cells after deepers	0	1	0	0	0
Isolated tumor cells after IHC	0	2	0	2	5

Figure 1 - 405

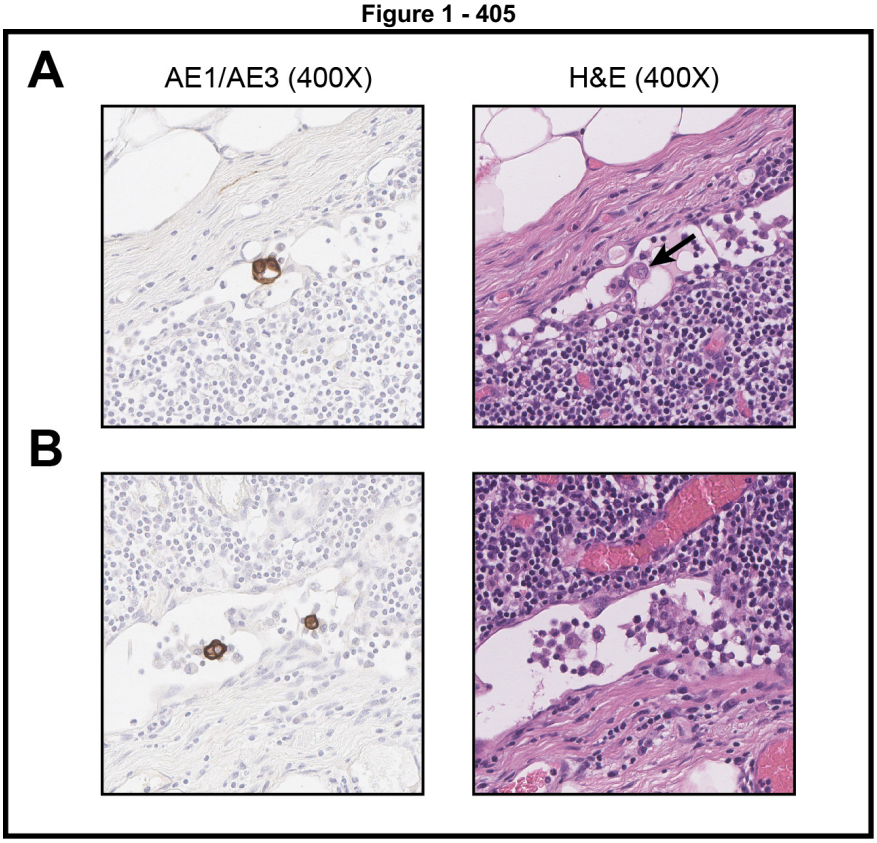

Conclusions: Additional deeper levels and IHC did not identify micrometastases in patients diagnosed with stage 2 colorectal adenocarcinoma with subsequent recurrence. ITCs, however, were identified in a significant proportion of these patients by IHC. These findings have important implications for staging of colorectal cancer, however, the clinical significance of ITCs requires further investigation.

406 Distinguishing Gastrointestinal Leiomyoma from Muscularis Propria in Biopsies by Differential Expression of S100 Immunohistochemical Stain

Zachary Dong[1], Gonzalo Barraza[2], Kajsa Affolter, Benjamin Witt[3], Jolanta Jedrzkiewicz[1]
[1]The University of Utah, Salt Lake City, UT, [2]Salt Lake City VA Medical Center, Salt Lake City, UT, [3]Huntsman Cancer Hospital, Salt Lake City, UT

Disclosures: Zachary Dong: None; Gonzalo Barraza: None; Kajsa Affolter: None; Benjamin Witt: None; Jolanta Jedrzkiewicz: None

Background: Interpreting small biopsies or fine needle aspirations of gastrointestinal tract (GI) smooth muscle lesions may be challenging when the differential diagnosis includes leiomyoma versus muscularis propria (MP), which can appear similar histologically. S100 immunohistochemical staining is often performed as part of the work up for spindle cell lesions and it has been reported to stain nerve fibers within the MP. Therefore, we decided to evaluate the utility of S100 staining in distinguishing GI leiomyomas from MP.

Design: A search was conducted in our laboratory electronic system for cases of leiomyomas arising within the GI tract (2004-2021). All included cases had an available S100 stain or tissue blocks. Site-matched controls containing MP were selected (2018-2020) to include esophagus, stomach, and colon. Five high power fields were counted on S100 immunohistochemical stains by two pathologists in the resections and by three different blinded pathologists in the biopsies and analyzed in STATA 17.0 MP (StataCorp LLC, College Station, TX). The statistical significance was set as $p<0.05$.

Results: The median S100 counts were 2.5/5 HPF in leiomyoma resection cases (n=38) (Figure 1A), which was significantly lower than the median counts of 548/5 HPF in MP (n=19) (Figure 1B) with p value <0.0001. The median S100 counts in biopsies (n=17) was 1.3/5 HPFs and were within the expected range of 1 to 104/5 HPFs (min-max value) of evaluated leiomyoma resections (Table 1).

	Leiomyoma resections (n=38)	Tumor biopsies (n=17)	Muscularis propria controls (n=19)
Mean Age (years)	48.7	57.2	55.1
Male gender, n (%)	17 (44.7)	10 (58.8)	10 (52.6)
Resection site, n (%)			
Esophagus	19 (50)	6 (35.3)	5 (26.3)
Stomach	17 (44.7)	8 (47.1)	5 (26.3)
Colon and rectum	2 (5.3)	3 (17.6)	9 (47.4)
Tumor size in cm, median and range (minimum to maximum)	2.45 (0.3 to 15)	1.9 (0.4-7.6)	N/A
S100 IHC stain, median positive cells/5 HPF, range (minimum to maximum)	2.5 (1 to 104)	1.3 (0-13.3)	548 (297 to 2878)
IHC - Immunohistochemistry, HPF- high power field			
Table 1. Clinicopathologic characteristics of our cohort (n=74)			

Figure 1 - 406

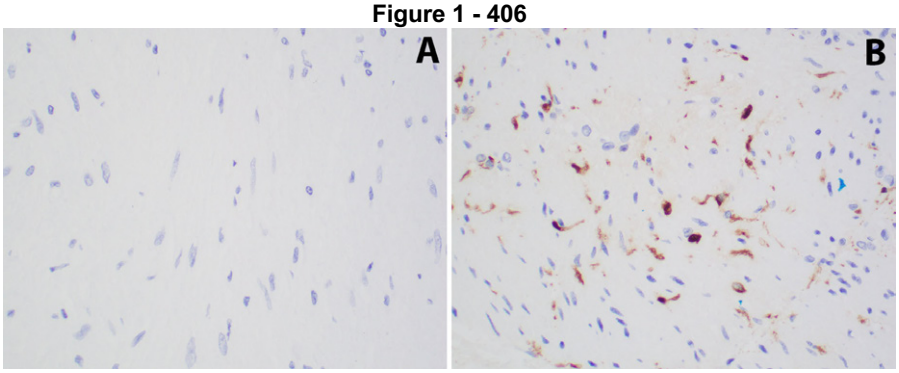

Conclusions: S100 counts within the normal MP are significantly higher than those observed in leiomyomas (p<0.001). Therefore, S100 staining can aid in distinguishing leiomyoma from MP in the GI tract, which is especially helpful when evaluating cases with limited sampling. This simple observation can help pathologists ensure a targeted lesion was sampled so that patients avoid unnecessary repeated procedure.

407 Is Duodenal Biopsy a Useful Tool for Detecting Unsuspected Celiac Disease?

Zhe Ran Duan[1], Christine Orr[2], Rhonda Yantiss[3]
[1]New York-Presbyterian/Weill Cornell Medical Center, New York, NY, [2]Queen's University, Kingston Health Sciences Centre, Kingston, Canada, [3]Weill Cornell Medicine, New York, NY

Disclosures: Zhe Ran Duan: None; Christine Orr: None; Rhonda Yantiss: None

Background: Although duodenal lymphocytosis supports a diagnosis of celiac disease in the appropriate setting, it is not specific for this condition. In fact, approximately 3-4% of duodenal biopsy samples show intraepithelial lymphocytosis that is usually unrelated to gluten sensitivity. For this and other reasons, the American Gastroenterological Association recommends against biopsy of normal-appearing duodenum when patients lack signs and symptoms of celiac disease. However, we have noted that many gastroenterologists routinely sample the duodenum when there are no clinical findings that might raise concern for celiac disease. The purpose of this study is to assess the value of this practice by determining the frequency with which detection of duodenal lymphocytosis leads to a diagnosis of previously unsuspected celiac disease.

Design: We retrospectively identified all patients with non-targeted duodenal biopsy samples obtained at our institution during a 24-month period. Cases that showed intraepithelial lymphocytosis with, or without, villous architectural abnormalities were reviewed. Patients who underwent biopsy analysis to evaluate for malabsorptive symptoms, positive serologic studies, or a family history of celiac disease were excluded from further analysis. The remaining patients with duodenal lymphocytosis were followed to determine whether any of them developed celiac disease.

Results: We identified 6337 patients with at least one non-targeted duodenal biopsy. Of these, 189 (3%) showed intraepithelial lymphocytosis with, or without, villous architectural abnormalities and plasma cell-rich inflammation of the lamina propria. After eliminating patients who underwent endoscopy to evaluate for possible celiac disease, 65 (34%) patients with duodenal lymphocytosis remained. Of these, 32 (49%) were not further evaluated with serologic studies. Thirty-two (49%) patients underwent serologic evaluation with negative results. Only one patient with incidentally discovered duodenal lymphocytosis was found to have serologic findings supporting a diagnosis of celiac disease. That individual, an older male with refractory dyspepsia and abdominal pain, had elevated serum tissue transglutaminase antibodies.

Table 1. Clinical features of 65 patients with duodenal lymphocytosis and no clinical suspicion for celiac disease.

Age (mean)	47 years
Male/Female ratio	13:51
Presenting Symptoms	
GERD	
Dysphagia	
Abdominal pain	
Dyspepsia	
Crohn disease	
Eosinophilic esophagitis	
Gastritis	
Barrett esophagus	
Morbid obesity	

Conclusions: We conclude that routine sampling of endoscopically normal duodena rarely identifies celiac disease when patients lack signs, symptoms, or family history to suggest that diagnosis. This practice should be discouraged, as it often leads to expensive work-ups that provide limited benefit.

408 Anal Canal Melanin and Melanoma - Demographic Characteristics

Melissa Duarte[1], Elizabeth Montgomery[2], Monica Garcia-Buitrago[3], Nemencio Ronquillo[1], Clara Milikowski[4], Satyapal Chahar[5], Abhilasha Ghildyal[6], Khaled Algashaamy[4], Oliver McDonald[2], Julio Poveda[2]
[1]University of Miami/Jackson Health System, Miami, FL, [2]University of Miami Miller School of Medicine, Miami, FL, [3]University of Miami Miller School of Medicine/Jackson Health System, Miami, FL, [4]University of Miami/Jackson Memorial Hospital, Miami, FL, [5]Memorial Sloan Kettering Cancer Center, New York, NY, [6]Jackson Memorial Hospital, Miami, FL

Disclosures: Melissa Duarte: None; Elizabeth Montgomery: None; Monica Garcia-Buitrago: None; Nemencio Ronquillo: None; Clara Milikowski: None; Satyapal Chahar: None; Abhilasha Ghildyal: None; Khaled Algashaamy: None; Oliver McDonald: None; Julio Poveda: None

Background: Anal canal melanoma is rare and presumably arises in association with anal melanocytes. SEER data indicate a female predominance and a predominance in Whites. We assessed the prevalence and demographic distribution of melanin in anal transitional mucosa without melanoma and compared it with the demographic distribution of melanoma in our population.

Design: We prospectively assessed anal biopsies from sequential patients seen in a specialized clinic for persons at risk for HPV-associated anal canal neoplasia. Samples were interpreted as “positive for melanocytes” or “negative for melanocytes”. Self-reported race and gender were recorded. To assess the demographic distribution of anal melanoma, we queried the pathology database from our hospital system for patients with anal melanoma seen from January 2003 to August 2021

Results: Anal transitional biopsies from 64 consecutive patients were analyzed for melanocytes and pigmented squamous cells. Twenty nine patients self reported as Black (17/29 female) including one woman self-reported as Black/Hispanic, 2 as Asian (both male) and 31 as White (7/31 female), amongst whom 24 self-reported as White/Hispanic. Anal transitional melanocytes were identified in 8/31 (26%) of the White patients (2/7 [28%] women, 6/24 [25%] men and in 19/29 (65%) of the Black patients (11/17 [65%] women, 8/12 [66%] men), in the single Hispanic patient, and in one of the two Asian patients. Twenty nine separate patients had anal melanomas, arising in the anal canal (24) and anal verge (5). The self-reported race of the patients with anal canal melanomas was recorded for 19 patients, including 14 White patients (74%; 11 women and 3 men) and 5 Black patients (26%; 4 women, one man). The overall demographic profile of patients in our specialized clinic for anal transitional biopsies differed from that of persons in our Institution’s catchment area, which, based on local government records, consists of 76 % White and 16.3% Black citizens.

Figure 1 - 408

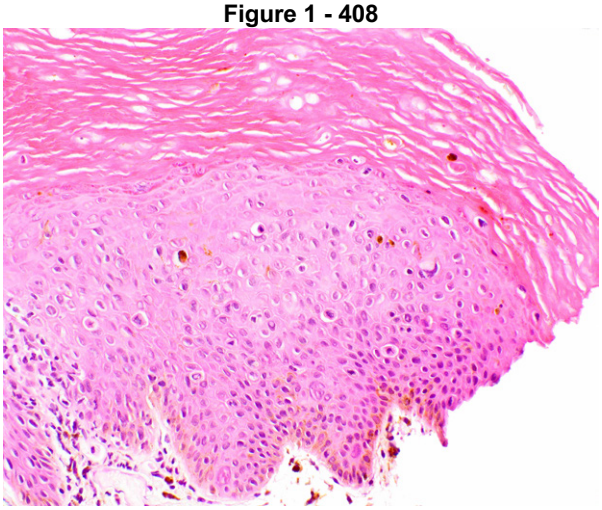

Figure 2 - 408

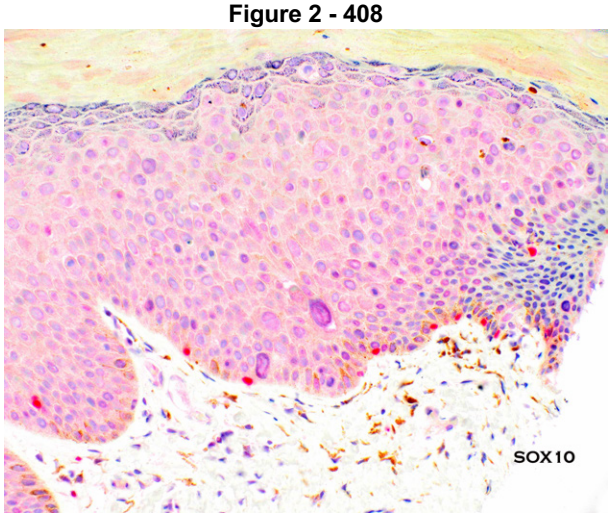

Conclusions: Anal canal transitional zone melanocytes are more abundant (and thus were more likely to be detected on small biopsies) in patients who self-report as Black than those who self-report as White (65% v 26%) with gender parity regardless of reported race, whereas anal canal melanomas predominate in women, but are probably over-represented in Blacks. Their greater density of anal canal melanocytes might explain an over-representation of anal melanoma in Blacks, but the etiology for the female predominance is unclear.

409 Is That a Steak Dinner in Your Appendix?- Does Undigested Animal Meat Contribute to Development of Appendicitis?- A Study on 2100 Consecutive Appendixes

Basma Elhaddad[1], Civan Altunkaynak[1], Ibraheem Javeed Mohammed[1], Ketav Desai[1], Sandra Siller[2], Noor Marji[3], Amal Shukri[4], Darren Brow[5], Raafat Makary[1], Ahmad Alkhasawneh[6], Brett Baskovich[3], Reeba Omman[1], Arun Gopinath[7]
[1]University of Florida College of Medicine, Jacksonville, FL, [2]University of South Florida, Tampa, FL, [3]UF Health Jacksonville, Jacksonville, FL, [4]Jackson Memorial Hospital/ University of Miami Hospital, Miami, FL, [5]Mayo Clinic College of Medicine and Science, Mayo Clinic Florida, Jacksonville, FL, [6]UF Health Jacksonville, FL, [7]University of Florida College of Medicine

Disclosures: Basma Elhaddad: None; Civan Altunkaynak: None; Ibraheem Javeed Mohammed: None; Ketav Desai: None; Sandra Siller: None; Noor Marji: None; Amal Shukri: None; Darren Brow: None; Raafat Makary: None; Ahmad Alkhasawneh: None; Brett Baskovich: None; Reeba Omman: None; Arun Gopinath: None

Background: Obstruction of the appendiceal lumen is considered one of the major factors leading to the development of appendicitis. Many factors contribute to the development of obstruction, particularly fecaliths, foreign bodies, and fibrous strictures. Omer et al. demonstrated that fruit seeds were found in 0.05% of cases, and undigested plant residuals were found in 0.35% of appendicitis cases. Occasionally, we see skeletal muscle tissue and bone in the lumen of appendectomy specimens. Patients with animal-bone-induced small and large bowel perforation mimicking appendicitis have also been reported. However, meat particles have seldom been implicated in the development of appendicitis. We speculate that these undigested meat particles also serve as a nidus for the development of the fecalith, eventually leading to appendicitis.

Design: Retrospective slide review of 2,100 consecutive appendixes was done for presence of meat particles (skeletal muscle or skeletal muscle and bone) in the lumen. The clinicopathologic and histologic features of these cases were analyzed.

Results: Out of 2,100 consecutive appendixes, 200 (9.5%) had animal meat particles present in the lumen (figures 1 & 2). Out of these, 105 (52.5%) cases were females and 95 (47.5%) were males. There were 115 (57.5%) of these 200 patients who presented clinically as appendicitis and microscopically showed evidence of acute inflammation. Another 49 (24.5%) presented as abdominal pain, but no evidence of acute inflammation was seen in the appendix. The remaining 36 (18%) were incidentally removed appendixes as a part of other procedures. There were 185 (92.5%) appendixes that had an outer diameter of more than 6 mm, and most had some organization of the undigested residue. We identified 83 (41.5%) cases that had meat as a significant component (more than 20% of luminal contents). Additionally, 4 (2%) also had bone particles in association with skeletal muscle tissue.

Figure 1 - 409

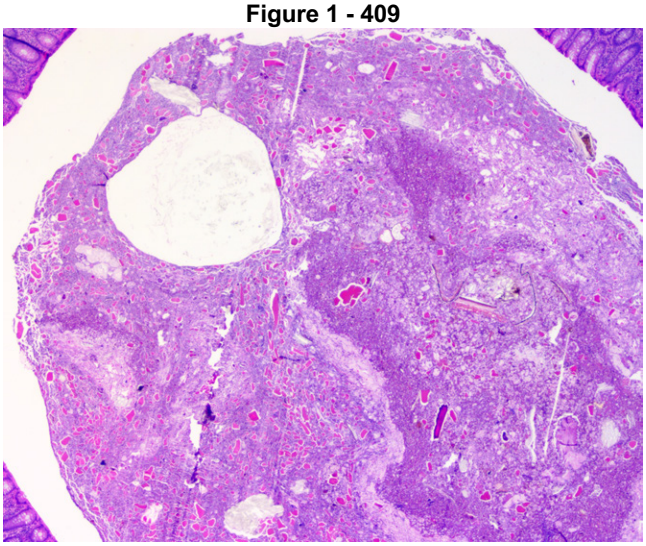

Figure 2 - 409

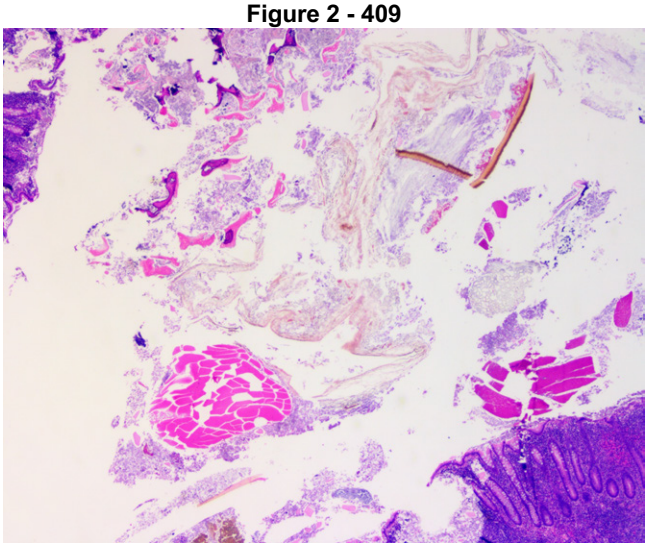

Conclusions: In addition to vegetable matter, meat particles are also associated with fecalith formation. In our patient population, undigested meat particles were seen in approximately 10% of the appendectomies. Based on our findings, similar to vegetable matter, meat particles also are likely factors which contribute to fecalith formation and eventual development of appendicitis.

410 Analysis of Clinical and Histologic Features That May Predict Response to Radiofrequency Ablation in Patients with Barrett's Esophagus

Sarah Elsoukkary[1], Prashanthi Thota[1], Prabhat Kumar[1], Mrinal Sarwate[2], Ahmed Bakhshwin[1], John Goldblum[1], Xuefeng Zhang[1]
[1]Cleveland Clinic, Cleveland, OH, [2]Cleveland Clinic Foundation, Cleveland, OH

Disclosures: Sarah Elsoukkary: None; Prashanthi Thota: None; Prabhat Kumar: None; Mrinal Sarwate: None; Ahmed Bakhshwin: None; John Goldblum: *Consultant*, Lucid diagnostics; Xuefeng Zhang: None

Background: Barrett's esophagus (BE) is a pre-malignant process, diagnosed by the presence of endoscopic changes in the distal esophagus and histologic confirmation of intestinal metaplasia (IM). Endoscopic eradication therapy, including radiofrequency ablation (RFA), is the cornerstone of treatment for BE. Although RFA is safe and effective, resistance to RFA does occur. We aim to identify clinical and histologic features that may predict resistance to RFA in patients with BE.

Design: We retrospectively identified esophageal biopsies from patients with BE who underwent RFA during a 4-year period. Demographic and clinical data was obtained from the institutional BE registry database. Responders were defined as patients with endoscopic and histologic evidence of complete eradication of BE after 3 or less RFA procedures. Pre-ablation biopsies obtained at baseline endoscopy were evaluated for various histologic features. Statistical analysis were performed using chi-square test and univariate/multivariate logistic regression model.

Results: Fifteen patients were responders and 46 patients were resistant to RFA (Table 1). There was no statistical difference in gender, smoking use, or alcohol use between the 2 groups. Histologic features, including the presence of buried BE, density and depth of buried IM glands, the presence, focality and type of dysplasia, the presence and density of Paneth cells, and overall depth of IM glands, were not statistically different between the 2 groups. Patients who were resistant to RFA had significantly longer BE than responders (7.3 cm versus 4.1 cm, p<0.01). Univariate logistic regression showed BE length was related to decreased probability of response to RFA (odds ratio=0.66, p=0.0004). Multivariate logistic regression model identified BE length as the only significant factor between the 2 groups. Using recursive partition analysis, the optimal cutoff point for BE length was identified as 3.5 cm. Among the 15 responders, 8 (53%) had BE length >=3.5 cm, in contrast, 40 of the 46 non-responders (83%) had BE length >=3.5 cm. The specificity, sensitivity, and accuracy were 87%, 47% and 77%, respectively.

Table 1. Clinical and Histologic Features of Patients Resistant and Responders to RFA

Feature	Responder (n=15)	Resistant (n=46)	p-Value
Gender			
Female	1 (7%)	11 (24%)	0.17
Male	14 (93%)	35 (76%)	
Smoking			
Current¥	1 (7%)	0	0.99
Former¥	9 (60%)	32 (70%)	0.71
Never	5 (33%)	14 (30%)	
Alcohol Use			
Current¥	11 (73%)	21 (46%)	0.31
Former¥	0	10 (22%)	0.99
Never	4 (27%)	15 (32%)	
Mean Length of BE (cm)	4.1 ± 2.3	7.3 ± 3.4	<0.01
Mean Biopsy Pieces per Length of BE	1.3 ± 1.3	0.7 ± 0.6	0.13
Mean Depth of IM Glands (microns)	710 ± 306	771.7 ± 410.8	0.53
Presence of Dysplasia			0.25*
Indefinite‡	0	4 (9%)	0.99
LGD‡	7 (47%)	12 (26%)	0.90
HGD‡	3 (20%)	20 (43%)	0.18
IMC‡	3 (20%)	7 (15%)	0.70
NDBE	2 (13%)	3 (7%)	
Type of Dysplasia			0.47*
Foveolar	2 (13%)	2 (4%)	0.27
Intestinal	13 (87%)	41 (89%)	
NA	0	3 (7%)	
Focality			0.25*
Multifocal	2 (13%)	15 (33%)	0.16
Unifocal	13 (87%)	31 (67%)	
Buried IM			0.82*
Absent	8 (53%)	23 (50%)	0.82
Present	7 (47%)	23 (50%)	

Mean Depth of Buried IM (microns)	442.9 ± 214.9	447.8 ± 220.8	0.95
Mean Density of Buried IM /HPF	3.3 ± 1.7	5.5 ± 5.2	0.08
Paneth Cells			0.81*
Absent	12 (80%)	38 (83%)	0.82
Present	3 (20%)	8 (17%)	
Mean Density of Paneth Cells /HPF	18.3 (3-29)	7.4 (2-20)	0.29

BE, Barrett's esophagus; IM, intestinal metaplasia; NDBE, non-dysplastic Barrett's esophagus; LGD, low-grade dysplasia; HGD, high-grade dysplasia; IMC, intramucosal carcinoma; HPF, high power field.

¥ Univariate logistic regression model performed versus "Never". ‡ Univariate logistic regression model performed versus "NDBE" * Chi-square test

Figure 1 - 410

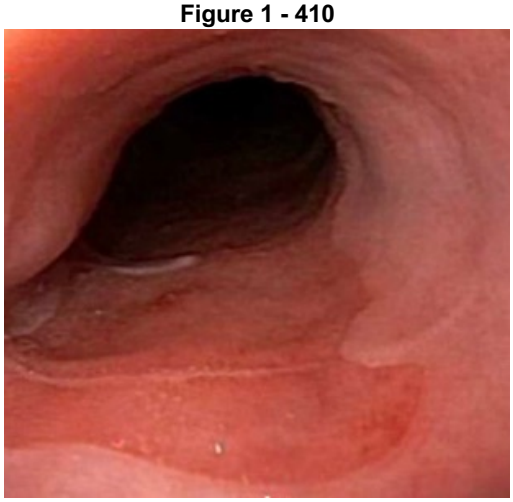

Conclusions: In conclusion, long segment BE increases the risk of resistance to RFA treatment. Histological parameters on pre-ablation biopsies show no statistical difference between responders and patients who were resistant to RFA.

411 Clinical Significance of Equivocal Cytomegalovirus (CMV) Staining by Immunohistochemistry in Colorectal Mucosal Biopsies from 526 Patients- Four-year Experience from a Large Academic Institution

Shaimaa Elzamly[1], Albina Joldoshova[2], Michaelangelo Friscia[3], Aswathi Chandran[1], Ana Meza[1], Jimmy Pham[4], Mamoun Younes[5], Andrew DuPont[6]

[1]McGovern Medical School at UTHealth, The University of Texas Health Science Center at Houston, Houston, TX, [2]Baylor College of Medicine/University of Houston, Houston, TX, [3]The University of Texas at Houston, Houston, TX, [4]The University of Texas Health and Sciences Center at Houston, Houston, TX, [5]George Washington University School of Medicine and Health Sciences, Washington, DC, [6]The University of Texas Health Science Center at Houston McGovern Medical School

Disclosures: Shaimaa Elzamly: None; Albina Joldoshova: None; Michaelangelo Friscia: None; Aswathi Chandran: None; Ana Meza: None; Jimmy Pham: None; Mamoun Younes: None; Andrew DuPont: None

Background: The diagnosis of CMV colitis by histopathologic examination alone can be accurately performed in only 50% of case, as morphology can resemble ischemia, drug-induced colitis, inflammatory bowel disease (IBD), and bacterial or other viral infections. In suspicious cases, confirmation by the gold standard immunohistochemical (IHC) staining for CMV is mandatory. However, some cases reveal only a single rare small positive nucleus and is so called "equivocal" for CMV. The clinical significance of the equivocal IHC-CMV is not yet confirmed. The aim of this study is to determine the clinical significance and response to antiviral medications of so called "equivocal" IHC-CMV staining in colorectal mucosal biopsies in a large series of patients.

Design: A retrospective review of the colorectal biopsies that were stained for CMV by IHC between the years of 2016 and 2019 revealed 526 cases. IHC staining results were recorded as negative, unequivocal, or equivocal. Data analysis included correlation of both unequivocal and equivocal IHC results for CMV with the clinicopathological characteristics, available molecular test results,

response to antiviral medications, clinical outcome, and the recurrence rate after 1 year of follow up was performed using standard statistical analysis.

Results: Within our population, we found that the equivocal positive CMV staining to be more common than unequivocal staining, The IHC staining results were unequivocal in 67 (12.7%) cases, equivocal in 239 (45.5%) cases, and negative in 220 (41.8%) cases. Out of the 239 equivocal cases, 217 case had follow-up information of whom 164 (75.5%) of the cases had improved or complete resolution of clinical symptoms and 53 (24.4%) had no change of symptoms. Out of those 164 cases, 126 (76.8%) cases received or increased the dose of antiviral medications, and only 38 (23.1%) cases did not receive antiviral medication with p value = 0.01 (graph 1). PCR was performed largely on blood samples in 209 cases and was not found to be sensitive for the detections of CMV proctocolitis; sensitivity of 20% (8.44 -36.94, 95% CI). There was no statistically significant difference between the equivocal and unequivocal CMV cases in terms of recurrence.

Follow Up Information of Equivocal CMV Cases				
Antiviral treated (n= 158)		**Not treated (n=59)**		**P value**
No change	**Improved/complete resolution**	**No change**	**Improved/complete resolution**	**0.019**
32 (20.25%)	**126 (79.75%)**	**21 (35.6)**	**38 (64.4%)**	

Figure 1 - 411

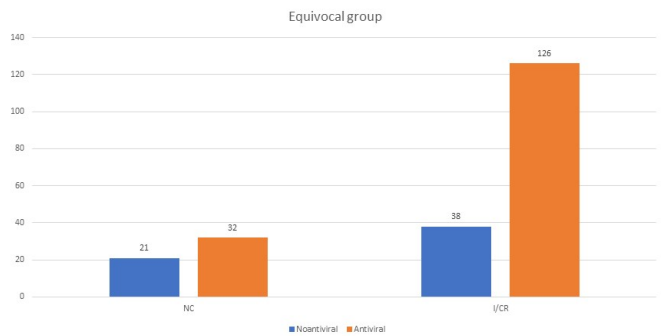

(Figure 1): The response to adding/ increasing the dose of antiviral medications in the CMV equivocal group.

Conclusions: Most of the equivocal cases respond well to antiviral therapy, and therefore, it is crucial that pathologists recognize this pattern of CMV staining and report it to the clinicians to initiate appropriate treatment. Equivocal CMV staining likely represents true CMV proctocolitis.

412 Unique Molecular and Histopathologic Features of Rectal Adenocarcinoma Stratified by Tumor Regression Score After Neoadjuvant Chemo-Radiation Therapy

David Escobar[1], Juehua Gao[2], Lawrence Jennings[3], Guang-Yu Yang[4]
[1]Northwestern University Feinberg School of Medicine, Chicago, IL, [2]Northwestern Memorial Hospital, Chicago, IL, [3]Northwestern University, Feinberg School of Medicine, Chicago, IL, [4]Northwestern University, Chicago, IL

Disclosures: David Escobar: None; Juehua Gao: None; Lawrence Jennings: None; Guang-Yu Yang: None

Background: Therapy for locally advanced anorectal cancer consists of neoadjuvant chemo-radiation therapy (CRT) followed by total excision. The response to neoadjuvant CRT is mixed, with ~35% of patients achieving complete pathologic remission. The use of molecular profiling to identify patients who may not benefit from CRT remains underreported in the literature. In this study, we report the molecular profile of rectal cancer, and correlate the findings to tumor regression score, clinical parameters, and histologic findings.

Design: Cases of rectal adenocarcinoma status-post chemo-radiation therapy were identified. Tumor regression score (TRS), DNA mismatch repair protein status and pre-resection next generation sequencing was reported for each case. Demographic and clinical data were extracted from the electronic medical record.

Results: The clinicopathologic parameters of 87 cohort cases are shown in Table 1. 25.3% of cases were classified as therapy "responders" (TRS 0 or 1), and 74.7% of cases were classified as "poor responders" (TRS 2 or 3). The majority of cases were high stage at the time of resection, and all but one case were microsatellite stable (Table 1).

The most commonly mutated genes in the cohort were *TP53, KRAS, FBXW7, NRAS, and PIK3CA* (Figure 1A). A gene cluster analysis was performed and showed significantly high rates of mutation in the *RAS/RAF* (Cluster 1) and *TP53* (Cluster 2) pathways. Clusters 1 and 2 together accounted for the majority (71%) of mutations in complete responders (TRS 0). Mutations in other gene clusters, especially *WNT* pathway (Cluster 3), *PIK3CA* pathway (Cluster 4) and *TSC/MTOR/STK11* pathway (Cluster 6), were rare/absent in complete responders, and conversely showed high rates of mutation in poor responders (77%, 87%, and 100%, respectively, $p<0.05$). A subset of tumors were evaluated on H&E slides and categorized by being predominantly mucinous (10%), senescent (48%), proliferative (34%), or a mixture of senescent and early proliferative (7%).

Cohort Demographics	
Total Number	87
Age, y (mean, range)	55 (24-83)
Sex	
Male	53 (60.9%)
Female	34 (39.1%)
Median Tumor size, cm (mean, range)	2.8 (0-8.8)
Tumor Regression Score (TRS)	
Complete Response (Score 0)	8 (9.2%)
Near Complete Response (Score 1)	14 (16.1%)
Partial Response (Score 2)	51 (58.6%)
Poor or No Response (Score 3)	14 (16.1%)
Tumor Grade	
Low	3 (3.4%)
Mod	67 (77.0%)
High	15 (17.2%)
Not reported	2 (2.3%)
Histology Subtypes	
Adenocarcinoma, NOS	82 (94.3%)
Mucinous	4 (4.6)
Signet ring	1 (1.1%)
T Stage	
ypT0	8 (9.2%)
ypT1	5 (5.7%)
ypT2	20 (23.0%)
ypT3	44 (50.6%)
ypT4	10 (11.5%)
Lymph Node	
ypNX	2 (2.3%)
ypN0	42 (48.3%)
ypN1	32 (36.8%)
ypN2	11 (12.6%)
Metastases	
ypMX	64 (73.6%)
ypM1	23 (26.4%)
Lymphovascular Invasion	
Present	28 (32.2%)
Absent	51 (58.6%)
N/A	8 (9.2%)
Perineural Invasion	
Present	15 (17.2%)
Absent	64 (73.6%)
N/A	8 (9.2%)

MSI	
Intact - Stable	86 (98.9)
Absent - Unstable	1 (1.1%)

Figure 1 - 412

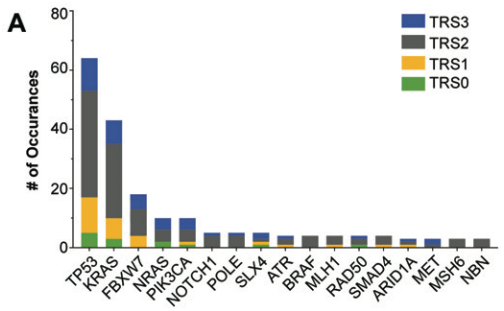

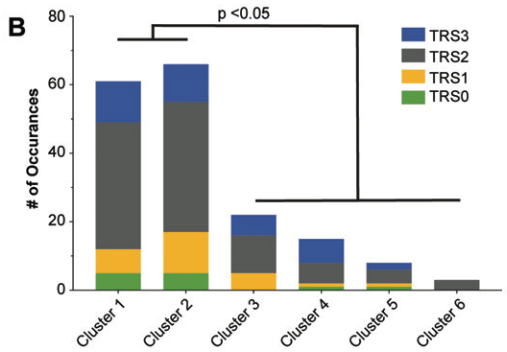

Cluster #1 RAS-RAF	Cluster #2 TP53	Cluster #3 WNT	Cluster #4 PIK3CA	Cluster #5 Homologous Recombination	Cluster #6 TSC/MTOR
KRAS	ATM	CTNNB1	PIK3CA	FANCA	STK11
NRAS	TP53	FBXW7	PTEN	FANCD2	TSC1
BRAF		MYC	PIK3R1	FANCI	TSC2
ERBB2		ARID1A	AKT	SLX4	MTOR
ERBB3					
EGFR					

Conclusions: Our results show that the molecular profiles of CRT responders are unique compared to poor responders. Cluster analysis suggests that mutations in *WNT*, *PIK3CA*, and *TSC/MTOR/STK11* pathways are more resistant to CRT. Demonstrating of mutations in these gene clusters prior to neoadjuvant chemotherapy may serve to identify patients who will benefit from a shortened CRT regimen and faster progression to surgical resection.

413 Clinicopathologic Characterization of Polyps in Patients with AXIN2-Associated Polyposis: A Rare Emerging Familial Polyposis Syndrome

Ashwini Esnakula[1], Heather Hampel[2], Rachel Pearlman[2], Peter Stanich[2], Archana Shenoy[3], Wei Chen[2], Wendy Frankel[2]
[1]The Ohio State University Wexner Medical Center/James Cancer Hospital, Columbus, OH, [2]The Ohio State University Wexner Medical Center, Columbus, OH, [3]Nationwide Children's Hospital - The Ohio State University, Columbus, OH

Disclosures: Ashwini Esnakula: None; Heather Hampel: *Advisory Board Member*, Promega; *Advisory Board Member*, Invitae Genetics; *Advisory Board Member*, Genome Medical; *Consultant*, GI OnDemand; Rachel Pearlman: None; Peter Stanich: *Grant or Research Support*, Pfizer Inc, PTEN Research foundation, Freenome; *Consultant*, UpToDate Inc; *Grant or Research Support*, Jannsen Pharma; *Grant or Research Support*, Emtora Biosciences; Archana Shenoy: None; Wei Chen: None; Wendy Frankel: None

Background: Germline heterozygous mutations in the *AXIN2* gene have been described in association with oligodontia, features of ectodermal dysplasia, and a variable incidence of colorectal polyps/cancer in a few families. AXIN2 is a regulator of β-catenin degradation in the WNT-signaling pathway and is functionally related to APC. These patients show an autosomal dominant inheritance with variable penetrance. Recently, a single family without features of ectodermal dysplasia and phenotype of attenuated polyposis was reported. Here we report the gastrointestinal polyp burden in six patients from two families with inherited novel truncating mutations in the *AXIN2 gene*.

Design: Six patients from two families were identified with heterozygous germline mutations for *AXIN2* during genetic counseling and testing for personal or family history of colon polyps/cancer or other cancers. We reviewed charts for clinical history,

endoscopic findings, genetic testing results, and pathology reports, and reviewed polyp slides to determine the types, location, and number of polyp(s).

Results: Two members from one family had a novel pathogenic *AXIN2* mutation c.1594G>T; p.Glu532*. The proband is an 86 year old woman with at least 212 polyps throughout the colon identified on multiple colonoscopies including 202 tubular adenomas (TA), 6 sessile serrated lesions (SSL), and 4 hyperplastic polyps (HP). She also had a fundic gland polyp of the stomach. The daughter has one missing adult tooth and 26 polyps (17 TAs, 3 SSL, 6 HPs; 22 proximal and 4 distal) by 61 years. The second family had a novel pathogenic *AXIN2* c.1036C>T, p.Gln346* mutation in 4 members. The proband is a man with family history of colon and ovarian cancer and personal history of metastatic renal cell carcinoma diagnosed at 64 years. He reportedly had 10-15 polyps and had one confirmed HP in the proximal colon at 66 years. The three daughters have had one colon polyp each including HP, TA, and SSL of proximal colon diagnosed at 38, 34, and 27 years respectively. None of the patients had colon cancer.

Conclusions: Patients with germline *AXIN2* mutations show high variability in colon polyp burden and can develop polyps at early adulthood. Although adenomas are most common, patients can have HPs and SSLs. *AXIN2*–associated polyposis should be considered in patients with a personal and family history of colon polyps with or without the features of ectodermal dysplasia.

414 NTHL1-Associated Tumor Syndrome: Expanding the Neoplastic Spectrum of a Rare Tumor Predisposition Syndrome

Ashwini Esnakula[1], Heather Hampel[2], Kate Shane[2], Rachel Pearlman[2], Peter Stanich[2], Archana Shenoy[3], Wendy Frankel[2]
[1]The Ohio State University Wexner Medical Center/James Cancer Hospital, Columbus, OH, [2]The Ohio State University Wexner Medical Center, Columbus, OH, [3]Nationwide Children's Hospital - The Ohio State University, Columbus, OH

Disclosures: Ashwini Esnakula: None; Heather Hampel: *Advisory Board Member*, Promega; *Advisory Board Member*, Invitae Genetics; *Advisory Board Member*, Genome Medical; *Consultant*, GI OnDemand; Kate Shane: None; Rachel Pearlman: None; Peter Stanich: *Grant or Research Support*, Pfizer Inc; *Grant or Research Support*, PTEN Research foundation; *Grant or Research Support*, Freenome; *Consultant*, UpToDate Inc; *Grant or Research Support*, Jannsen Pharma; *Grant or Research Support*, Emtora Biosciences; Archana Shenoy: None; Wendy Frankel: None

Background: *NTHL1*-Associated Tumor Syndrome (NATS) is a rare, recently described recessive tumor predisposition syndrome caused by biallelic mutations in *NTHL1,* a DNA glycosylase gene of the base excision repair pathway. It was initially described as a polyposis and colorectal cancer predisposition syndrome but is now associated with multi-organ benign and malignant tumors. In this study, we characterize the phenotypic spectrum of extracolonic tumors and colon polyp burden in three patients with biallelic germline *NTHL1* mutations.

Design: We identified 3 patients from two unrelated families with NATS at our institution based on genetic counseling and testing for personal and family history of colon polyps and other tumors. The clinical information, and available slides from biopsy/excision specimens were reviewed.

Results: Two patients from one family included male and female siblings. The female reportedly had ductal carcinoma in situ at age 36 and confirmed left breast invasive ductal carcinoma, grade 1, at age 47. She had multiple colon polyps starting at 57, including 20 tubular adenomas (TA), 2 sessile serrated lesions (SSL), 10 hyperplastic polyps (HP) in the colon and rectum, and 1 duodenal TA. The male sibling was diagnosed with left breast invasive ductal carcinoma, grade 3, at age 58 with subsequent extensive metastasis. He had left frontal meningioma at age 58. He reportedly had colon cancer in his 50s and confirmed four TAs of the left colon at age 61. He died at age 64 prior to his sister's genetic testing so it is assumed he had NAP based on his phenotype. The third patient was diagnosed with multifocal dysembryoplastic neuroepithelial tumor (DNT) of the brain at age 19 and basal cell carcinoma of the face at age 25. At age 33, he underwent colectomy for multiple polyps (>50) and distal transverse colon mass. TAs were the common polyps followed by HPs. The mass was a traditional serrated adenoma (TSA) with prominent high-grade dysplasia. Also, 1 SSL and 1 TSA were identified in the right colon.

Conclusions: We report the first case of male breast cancer, DNT, and TSA in patients with NATS and highlight the incidence of extracolonic tumors. Our patients showed varying colorectal polyp incidence and burden, with the most common being TAs, followed by HPs, and rarely SSLs and TSAs. Thus, our series contributes to emerging literature of tumor phenotype associated with this rare tumor predisposition syndrome, critical for cancer risk assessment and management.

415 BRG1 Loss by Immunohistochemistry as an Emerging Prognostic Biomarker in Esophageal, Junctional and Gastric Adenocarcinomas with SWI/SNF Complex Alterations

Gertruda Evaristo[1], Mina Farag[2], Amit Katz[3], Marianne Issac[4], Duc-Vinh Thai[5], Veena Sangwan[6], Jose Ramirez-GarciaLuna[6], Carmen Mueller[3], Jonathan Cools-Lartigue[3], Alfred Cuellar[3], Nick Bertos[4], Dongmei Zuo[6], Morag Park[6], Marie-Christine Guiot[3], Sophie Camilleri-Broët[7], Victoria Marcus[3], Lorenzo Ferri[6], Pierre Fiset[3]
[1]McGill University, Montreal, Canada, [2]McGill University Health Centre, Glen site, Montreal, Canada, [3]McGill University Health Centre, Montréal, Canada, [4]McGill University, Research Institute of the McGill University Health Network, Montréal, Canada, [5]Trillium Health Partners, Credit Valley Hospital, Mississauga, Canada, [6]McGill University, Montréal, Canada, [7]McGill University Health Centre, McGill University, Montréal, Canada

Disclosures: Gertruda Evaristo: None; Mina Farag: None; Amit Katz: None; Marianne Issac: None; Duc-Vinh Thai: None; Veena Sangwan: None; Jose Ramirez-GarciaLuna: None; Carmen Mueller: None; Jonathan Cools-Lartigue: None; Alfred Cuellar: None; Nick Bertos: None; Dongmei Zuo: None; Morag Park: None; Marie-Christine Guiot: None; Sophie Camilleri-Broët: None; Victoria Marcus: None; Lorenzo Ferri: None; Pierre Fiset: *Advisory Board Member*, Amgen, AstraZeneca, Bristol Myers Squibb; *Grant or Research Support*, Bristol Myers Squibb; *Advisory Board Member*, Merck, Pfizer, Hoffmann-La Roche; *Speaker*, EMD Serono

Background: The SWI/SNF chromatin remodeling complex is an important epigenetic regulator disrupted in 20% of cancers. Recent genetic studies have linked dysregulation of the complex with Mismatch Repair deficiency (MMR-D) in upper GI carcinomas. Screening for SWI/SNF complex disruption has shown conflicting results with respect to prognosis and upper GI anatomical sites. This study aims to assess with IHC esophageal, junctional (GEJ), and gastric adenocarcinoma SWI/SNF complex protein expression, the association with MMR-D and the associated clinical significance.

Design: We performed IHC for MLH1, MSH2, MSH6, PMS2, BRG1, ARID1A and ARID1B on tissue microarrays constructed from 235 cases of esophageal (62), GEJ (97) and gastric (76) adenocarcinomas resected at our institution from 2011-2019. Patterns of SWI/SNF complex proteins H-scores were correlated with MMR status and overall survival (OS) using Kaplan-Meier method and log rank test.

Results: MMR-D immunophenotype was identified in 29/235 tumors (12%). Loss of expression (H-Score<100) in at least one component of SWI/SNF pathway was identified in 186 cases (79% overall): 18% (BRG1), 73% (ARID1A), 30% (ARID1B) and 10% (all three proteins). No significant difference was seen between esophageal, GEJ and gastric groups (p=0.47). MMR-D tumors (28/29, 97%) showed significantly higher SWI/SNF complex loss compared to MMR stable tumors (48/206, 23%), p=0.01. No prognostic significance was identified with ARID1A/B, but loss of BRG1 was associated with a trend for longer mean OS compared to BRG1-retained cases in the overall cohort (mean[CI] 4.68[3.50-5.86] versus 3.39[2.91-3.87] years, respectively; p=0.06). BRG1 expression status did not show any difference in the MMR-D subgroup with mean OS of 5.64[3.86-7.41] versus 4.38[2.67-6.08] years (p=0.37). In univariate analysis, increasing age, higher pathological staging, and MMR-proficient status were significant predictors of poor outcome among patients with BRG1 loss; all three associations remained significant in multivariable analysis (p=0.001, p=0.001, p=0.03, respectively).

Conclusions: High frequencies of SWI/SNF complex component expression deficiency highlight its pathogenic importance in all anatomical compartments of the upper GI tract, particularly in cases with MMR-D. Screening for BRG1 loss by IHC, irrespective of MMR status, may have prognostic significance in the upper GI tract and may help guide therapeutic decision making.

416 Processing Rectal Cancer Resection Specimens: A Laborious Cross Sectioning-Wholemount Approach Detects Closer Radial Margin and More Lymph Nodes Than the Regular Approach but Does Not Change the Final Margin Positive/Negative Status or the pN Staging Status

Canan Firat[1], Hannah Thompson[1], Jasme Lee[1], Jonathan Yuval[1], Chiyun Wang[1], Peter Ntiamoah[1], Efsevia Vakiani[1], Mithat Gonen[1], Julio Garcia-Aguilar[1], Jinru Shia[1]
[1]Memorial Sloan Kettering Cancer Center, New York, NY

Disclosures: Canan Firat: None; Hannah Thompson: None; Jasme Lee: None; Jonathan Yuval: None; Chiyun Wang: None; Peter Ntiamoah: None; Efsevia Vakiani: None; Mithat Gonen: None; Julio Garcia-Aguilar: *Consultant*, Ethicon Johnson & Johnson; *Stock Ownership*, Intuitive Surgical; Jinru Shia: None

Background: In managing rectal cancer patients, the importance of accurate pathological assessment of the resected cancer specimens is well recognized. A long-debated question has been whether the current regular approach (RA) of processing the specimen with regular-size sections is optimal in capturing all the features, or should the more thorough cross-sectioning approach

(CSA) be adopted widely. We had previously shown data suggesting that RA was likely effective when compared to CSA [Mod Pathol 33(Suppl. 2): 661, 2020]. Here we present our updated results on a much-expanded case series comparing the performance of the two approaches.

Design: Rectal cancer resection specimens with comparable clinical features (including treatment modalities and operating surgeons) that were processed by either RA or CSA over a 3-year period were used for this analysis. CSA included 1)fixing the rectal specimen with tumor region intact/not-opened for >= 48hours, 2)cross sectioning at 4mm-interval of the entire tumor region and the portion distal to it, 3)wholemount blocks and slides of each cross section, and 4)digitization of both gross and microscopic wholemounts. RA was according to routine protocol with regular-size sections of the entire tumor region upon visualization of the opened specimen.

Results: Three-hundred-and-nineteen primary rectal cancer resections were evaluated, 148 by CSA and 171 by RA. No difference was detected between the 2 groups in mesorectal intactness (97% complete in CSA vs 97% in RA, p>0.9), distal margin-clearance (median for CSA vs RA, 30 vs 35mm, p=0.2), greatest-tumor-dimension (median, 30 vs 30mm, p=0.14), and rate of any vascular invasion (43% vs 47%, p=0.4). Of the tumors treated with neoadjuvant-therapy, no difference was detected between treatment responses (38% grade-3 vs 36%, p=0.8); however, CSA detected a significantly closer CRM-clearance (mean/median, 10mm/8mm vs 16mm/14mm, p<0.001), although the rates of positive CRM did not differ significantly [CRM<=1mm, 18/148(12%) vs 15/171(8.8%), p=0.3]. CSA yielded a higher LN-count than RA (median, 28 vs 16, p<0.001), but no difference was detected in the number of positive LNs (mean, 1.28 vs 1.17, p=0.3) or pN stage (pN+: 40% vs 43%, p=0.5). pT stage was similarly not different (p=0.5).

Conclusions: Our results confirm the data from our initial analysis and indicate that the laborious cross-sectioning approach with wholemount detects a closer CRM-clearance in rectal cancer resections when compared to the regular-approach but does not impact the final CRM positive/negative status or the pN status. Collection of clinical follow-up information is ongoing to evaluate whether the differences in pathology parameters between the 2 approaches translate to different management and/or different outcome.

417 End-to-End Risk Stratification Model to Predict Progression from Barrett's Esophagus to Esophageal Adenocarcinoma

Daniel Franklin[1], Tara Pattilachan[2], F. Scott Corbett[3], Anthony Magliocco[4], Domenico Coppola[5]
[1]Protean Bio Diagnostics Inc, Orlando, FL, [2]University of Central Florida College of Medicine, Orlando, FL, [3]Florida Digestive Health Specialists, Sarasota, FL, [4]Protean Bio Diagnostics Inc, Tampa, FL, [5]FDHS, Bradenton, FL

Disclosures: Daniel Franklin: None; Tara Pattilachan: None; F. Scott Corbett: None; Anthony Magliocco: None; Domenico Coppola: None

Background: Esophageal adenocarcinoma (EAC) surfaces from dysplastic progression of Barrett's esophagus (BE), with 8% of patients with BE developing EAC; however, there is no current model that directly predicts risk of progression from image tiles from biopsy slides. Herein, we designed an end-to-end model stratification model to predict BE progression to EAC without the need to triage patient data and instead, directly predict progression from whole slide images. Non-progressors (BEN) did not develop dysplasia or carcinoma upon follow up of > 7 years, progressors (BEP) developed carcinoma upon follow up of 3-4 years

Design: Whole slide images of H&E stained BE tissue scanned at 20x were tiled into 512 x 512 pixel (256 x 256 µm) .jpeg images using OpenSlide, and tiles without metaplasia were discarded. Images were augmented by rotating in 90° increments and mirroring. From 29 non-progressor (BEN) and 17 progressor (BEP) this created 24,552 BEN and 31,002 BEP tiles for training. Pixel values were normalized by dividing the mean and subtracting the standard deviation of the entire dataset for each channel.

The parameters of an EfficientNet-B0 model trained on a separate project involving H&E stained whole slide images were used as a starting point to predict BE progression to improve sensitivity to cellular features. The model was trained with a batch size of 30 and a learning rate of 1x10-7 for 39 epochs before the validation loss continued to increase for 5 epochs.

Results: The test dataset consisted of 4,000 BEN tiles and 4,248 BEP tiles from 6 slides. The model achieved an AUC of 0.83 when averaging all predictions of a slide together, and 0.76 when all tiles are considered separately.

Conclusions: Risk of EAC development from BE can effectively be predicted from our end-to-end stratification model. Our results support our model as a novel method for screening patients with BE and may be paired with various endoscopic treatments.

418 Correlation of NTRK Genetic Fusions and Mismatch Repair Protein Deletion of Patients with Colorectal Cancer

Yao Fu[1], Xiangshan Fan[2], Xiaohong Pu[3]
[1]Affiliated Drum Tower Hospital Nanjing University Medical School, Nanjing, China, [2]Nanjing Drum Tower Hospital, Nanjing, China, [3]Nanjing Drum Tower Hospital, The Affiliated Hospital of Nanjing University Medical School, Nanjing, China

Disclosures: Yao Fu: None; Xiangshan Fan: None; Xiaohong Pu: None

Background: In this study, the MMR status of primary colorectal cancer and NTRK gene fusion were analyzed, and the NTRK gene fusion partner and scission mode of primary colorectal cancer were analyzed, hoping to provide new ideas and basis for clinical screening of NTRK positive in colorectal cancer.

Design: Immunohistochemical and fluorescence in situ hybridization method was used respectively to detect the expression of MMR proteins and the break-apart of NTRKs in 830 cases of CRC, and the relationship between the expression of mismatch repair proteins and the NTRK genetic fusions were analyzed.

Results: The total deletion rate of mismatch repair protein expression was 9.88%(82/830), the total deletion rate of hMLH1 protein was 9.04% (75/830), hPMS2 protein deletion rate was 9.04% (75/830), hMSH2 protein deletion rate was 2.53% (21/830), the deletion rate of hMSH6 protein was 4.10% (34/830), the deletion rate of synchronous hMLH1 and hPMS2 were 8.67% (72/830) and the deletion rate of synchronous hMSH2 and hMSH6 were 2.17% (18/830). The mismatch repair proteins deficiency(dMMR) group was tend to right location, different histological subgroup, poor differentiation, AJCC stage and N stage. More importantly, NTRK fusion was enriched in dMMR group（7.32% vs. 0.94%）.

Clinicopathological features and ntrk gene fusion results of dMMR group and pMMR group

Clinicopathological features		**pMMR (n= 748)**	**dMMR (n= 82)**	***P***
Year（mean）		62.16(22-89)	62.88(22-83)	1.000
Sex	Male	441	48	1.000
	Female	307	34	
Location	Left	569	33	0.000*
	Right	179	49	
Diameter (cm)		2.69(0.1-9.0)	2.46(0.7-9.0)	1.000
Histological classification	Adenocarcinoma Mucinous adenocarcinoma	719 29	74 8	0.041*
Growth pattern	Ulcerative type Elevated type Infiltrative type Ulcerative -Elevated	491 229 6 22	48 30 2 2	0.316
Differentiation	Well	15	2	0.017*
	Moderate	564	50	
	Poor	169	30	
AJCC	Ⅰ-Ⅱ	324	56	0.000*
	Ⅲ-Ⅳ	424	26	
T	1-2	98	12	0.697
	3-4	650	70	
N	0	326	56	0.000*
	1-2	422	26	
M	0	717	81	0.357
	1	31	1	
NTRK fused	Pos	7	6	0.001*
	Neg	741	76	

Conclusions: In conclusion, this study shows that in primary colorectal cancer, the probability of NTRK fusion in dMMR patients is relatively high. Therefore, a detection strategy for the key screening of NTRK gene fusion detection for tumor dMMR status can be established, which is useful for judging colorectal cancer. The molecular pathological characteristics of new cases and the development of individualized treatment strategies are of great significance.

419 Evaluation of Tumor Budding and Poorly Differentiated Clusters as Independent Predictors of Clinical Outcome in Ampulla of Vater Carcinoma

Haijuan Gao[1], Whayoung Lee[2], Vishal Chandan[1], Xiaodong Li[2]
[1]University of California, Irvine, Orange, CA, [2]UCI Medical Center, Orange, CA

Disclosures: Haijuan Gao: None; Whayoung Lee: None; Vishal Chandan: None; Xiaodong Li: None

Background: Tumor budding (TB) and poorly differentiated clusters (PDC) are known to correlate significantly with nodal metastasis and recurrence of colon cancers. However, these two features have not been examined in detail within Ampulla of Vater Carcinoma (AVC).

Design: 105 resection cases of AVC (none had presurgical neoadjuvant therapy) from 2001 to 2019 were reviewed. TB and PDC were scored as per the 8th edition AJCC and a prior study (PMID: 32358792) respectively. TB and PDC scores in each case was correlated with pathological features (histologic grade, perineural invasion (PNI), lymphovascular invasion (LVI), margin status, tumor site and size), and patient survival.

Results: Mean age: 66.8 years (range: 31-86), M/F: 1.56. Average clinical follow-up time: 39 months. 44(41.9%) tumors showed low (0-4), 20 (19.0%) intermediate (5-9), and 41 (39.05%) high TB (>10) score. The tumors with high TB were more significantly staged (per 8th AJCC) as pT3a and pT3b tumors (46.15%) while tumors with low TB score were more significantly pT1 and pT2 tumors (59.26%) (p=0.035). High TB score was also associated with high grade histology (p<0.001). Although tumors with high TB were also more commonly associated with larger tumor size, intra-ampullary location, higher PNI and LVI, these results are not statistically significant. 78 (74.29%) tumors showed grade 1 PDC (0-4), 13 (12.4%) grade 2 (5-9) and 14 (13.33%) grade 3 PDC (>10). Grade 1PDC was significantly prevalent in the well or moderately differentiated (83.08%) than poorly or undifferentiated carcinomas (61.54%) (p=0.045). There was no significant association between PDC and tumor site, PNI, LVI, margin and lymph node metastasis. Only six tumors showed both grade 3 PDC and high TB score. Univariate Cox proportional Hazard Regression analysis showed that TB (p=0.03), age, pancreatic invasion (>0.5 cm), margin status and lymph nodes metastasis are significant associated with overall disease free survival. Multivariate regression analysis also showed that TB and pancreatic invasion (>0.5 cm) were independent predictors of disease free survival (p=0.036 and p=0.030 respectively).

Conclusions: The results of our study showed that both high TB and PDC are significantly associated with high histologic grading of AVC. Multivariate regression analysis showed TB to an independent predictor of survival in patients with AVC.

420 CD8+ T cell Density but not Mismatch Repair Protein Expression is an Independent Predictor of Survival in Colonic Adenocarcinoma with Mucinous Differentiation

Paulo Garcia[1], Douglas Hartman[1], Reetesh Pai[2]
[1]University of Pittsburgh Medical Center, Pittsburgh, PA, [2]UPMC Presbyterian Hospital, Pittsburgh, PA

Disclosures: Paulo Garcia: None; Douglas Hartman: *Speaker*, Philips; *Consultant*, Iqvia; Reetesh Pai: *Consultant*, Alimentiv (formerly Robarts Clinical Trials)

Background: Colonic adenocarcinoma with mucinous differentiation includes mucinous adenocarcinoma (>50% mucin) and adenocarcinoma with a mucinous component (≤50% mucin) and represents the most common subtype of colon cancer. Prognosis of this histologic subtype is variable; however, emerging evidence suggests immune cell infiltration in the tumor microenvironment may affect prognosis. The aim of this study was to evaluate the prognostic value of CD8+ T cell density in stage II and III colonic adenocarcinomas with mucinous differentiation.

Design: Clinicopathologic data of 117 patients from 2011 to 2015 with resected stage II and III primary colonic adenocarcinoma with mucinous differentiation were evaluated for CD8+ T cell density, mismatch repair protein status, adjuvant chemotherapy treatment, development of tumor recurrence, and histopathologic features. CD8 immunohistochemistry was performed on a whole tissue tumor section containing the deepest extent of invasion. The CD8 slides were then digitally scanned, and a digital image recognition algorithm was used to quantify the CD8+ T cells present at the invasive edge and tumor core and scored as either high/intermediate or low CD8+ T cell density, as previously described (Hartman DJ, et al. PMID 32205483).

Results: Of the 117 colonic adenocarcinomas with mucinous differentiation, 88 had high/intermediate CD8+ T cell density and 29 had low CD8+ T cell density. Compared to tumors with low CD8+ T cell density, tumors with high/intermediate CD8+ T cell density were more often stage II (66% vs. 41%, p=0.02) and more often exhibited areas with medullary differentiation (13% vs. 0%,

p=0.04). Both low and high/intermediate CD8+ T cell density categories had similar rates of MMR deficiency (41% vs 52%, p=0.3). There were no differences between CD8+ T cell density categories with respect to venous invasion, lymphatic invasion, perineural invasion, tumor budding, or KRAS or BRAF mutations. Multivariate analysis of disease-free survival showed that high/intermediate CD8+ T cell density was an independent predictor of disease-free survival (p<0.001). The only other variables independently associated with survival were stage (p=0.006) and perineural invasion (p=0.003). MMR protein expression status was not associated with prognosis in the multivariable model.

Table 1: Correlation of CD+ T cell density with clinicopathologic variables in tumors with mucinous differentiation

Clinical and Pathologic Features	Low CD8-Positive T-cell Density N (%)	High/Intermediate CD8-Positive T-cell Density N (%)	*p*-value
No. of Patients (%)	29 (25)	88 (75)	NA
Gender, Male/Female	14 (12) / 15 (13)	40 (34) / 48 (41)	0.8
Median Age in Years (IQR)	71 (13)	73 (17)	0.03
Location*	11 (9)	32 (27)	1.0
Cecum	11 (9)	32 (27)	
Right / Transverse colon	7 (6)	22 (19)	
Left colon			
Stage	12 (41)	58 (66)	0.02
II	17 (59)	30 (34)	
III			
High grade (WHO 5th edition criteria)	7 (6)	19 (16)	0.8
MMR Status	12 (41)	46 (52)	0.3
MMR Protein Deficient	17 (15)	42 (36)	
MMR Protein Proficient			
***KRAS* Exon 2 or 3 Mutation Present**	6/14 (5/12)	10/30 (9/26)	0.5
***BRAF* V600E Mutation / MMR proficient Present**	9 / 21 (8/18)	30 / 53 (26/45)	0.3
Mucinous Differentiation	11 (9)	69 (59)	<0.001
1-50%	18 (15)	19 (16)	
>50%			
Signet Ring Cell Differentiation	5 (4)	10 (9)	0.4
Medullary Differentiation	0	11 (9)	0.04
Venous Invasion	4 (3)	13 (11)	0.9
Lymphatic Invasion	15 (13)	38 (32)	0.4
Perineural Invasion	5 (4)	20 (17)	0.5
High tumor budding score	2 (2)	10 (9)	0.5

IQR, interquartile range

Figure 1 - 420

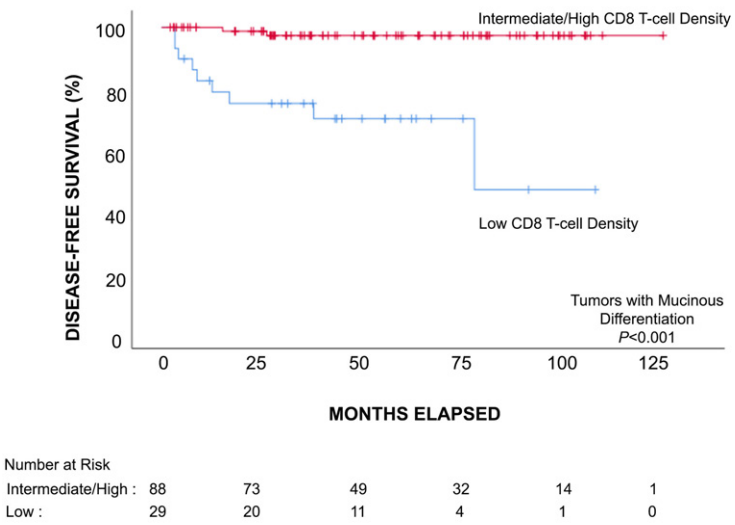

Conclusions: Prognostic outcome for stage II/III colonic adenocarcinomas with mucinous differentiation is strongly associated with CD8+ T cell density and stage and not MMR protein expression status. CD8+ T cell density in colonic adenocarcinomas with

mucinous differentiation is an important prognostic biomarker that should be incorporated into routine pathologic evaluation of this colon cancer subtype.

421 CD8+ T-cell Density is an Independent Predictor of Survival and Response to Adjuvant Chemotherapy in Stage III Colon Cancer

Paulo Garcia[1], Douglas Hartman[1], Reetesh Pai[2]
[1]University of Pittsburgh Medical Center, Pittsburgh, PA, [2]UPMC Presbyterian Hospital, Pittsburgh, PA

Disclosures: Paulo Garcia: None; Douglas Hartman: None; Reetesh Pai: None

Background: Treatment and prognosis of colon cancer is primarily determined by TNM staging; however, emerging evidence suggests that T cell infiltration in the tumor microenvironment is a significant prognostic factor. The aims of this study were to: (1) evaluate the prognostic value of CD8+ T cell density in stage II and stage III colon cancer and (2) analyze its association in stage III patients with the effect of adjuvant chemotherapy on time to recurrence.

Design: Clinicopathologic data of 351 patients from 2011 to 2015 with consecutively resected stage II and III primary colonic adenocarcinoma were evaluated for CD8+ T cell density, mismatch repair protein status, adjuvant chemotherapy treatment, development of tumor recurrence, and histopathologic features. CD8 immunohistochemistry was performed on a whole tissue tumor section containing the deepest extent of invasion for each case. The CD8 slides were then digitally scanned and a digital image recognition algorithm was used to quantify the CD8+ T cells present at the invasive edge and tumor core and score as either high/intermediate CD8+ T-cell density or low CD8+ T-cell density, as previously described (Hartman DJ, et al. PMID 32205483).

Results: For all stage II-III tumors, 70% had high/intermediate and 30% had low CD8+ T-cell density. Compared to low CD8+ T-cell density, high/intermediate CD8+ T-cell density was significantly associated with MMR deficiency (28% vs. 13%, p=0.003) and mucinous differentiation (36% vs. 27%, p<0.001) and less frequently displayed adverse histologic features including venous invasion (22% vs. 35%), lymphatic invasion (54% vs. 65%), perineural invasion (23% vs. 33%), and high tumor budding (16% vs. 27%) (all with p<0.05). Multivariate analysis demonstrated that high/intermediate CD8+ T cell density was an independent predictor of improved disease-free survival (HR 0.39, 0.21-0.71 95% CI, p=0.002). The only other variable independently predictive of improved disease-free survival for stage III patients was adjuvant chemotherapy (HR 0.52, 0.27-0.98 95% CI, p=0.04). For stage III patients, adjuvant chemotherapy was significantly associated with improved survival in the high/intermediate CD8+ T-cell density group (HR 0.28, 0.11-0.74 95% CI, p=0.01) but not in the low CD8+ T-cell density group, indicating that high/intermediate CD8+ T-cell density selects stage III patients that most benefit from adjuvant chemotherapy. CD8+ T cell density was not predictive of disease-free survival in patients with stage II colon cancer (p=0.9), but the analysis was limited by low numbers of patients with tumor recurrence.

Table 1: Univariate and multivariate analysis of disease-free survival in patients with the study cohort stratified by stage

Clinicopathologic Factor	Stage II-III (Entire Cohort, N=351)		Stage III (N=164, 52 recurrences)	
	Multivariable Hazard Ratio (95% CI)	*p*-value	Multivariable Hazard Ratio (95% CI)	*p*-value
Stage III (vs. II)	2.20 (1.08-4.48)	0.03	NA	NA
High/intermediate CD8-positive T-cell density	0.50 (0.30-0.82)	0.006	0.39 (0.21-0.71)	0.002
Chemotherapy given (vs. not given)	0.60 (0.34-1.06)	0.08	0.52 (0.27-0.98)	0.04
MMR protein deficient	0.53 (0.22-1.28)	0.2	0.73 (0.22-2.47)	0.6
Venous invasion	1.17 (0.68-2.02)	0.6	1.09 (0.58-2.06)	0.8
Lymphatic invasion	1.92 (0.92-4.00)	0.08	1.05 (0.42-2.61)	0.9
Perineural invasion	1.60 (0.92-2.80)	0.09	1.31 (0.69-2.49)	0.4
High tumor budding	1.42 (0.83-2.42)	0.2	1.50 (0.82-2.75)	0.2
High-risk stage III (vs. low-risk stage III)	NA	NA	1.23 (0.65-2.34)	0.5

MMR, DNA mismatch repair; NA, not applicable

Figure 1 - 421

Figure 1: Patient survival stratified by CD8+ T cell density

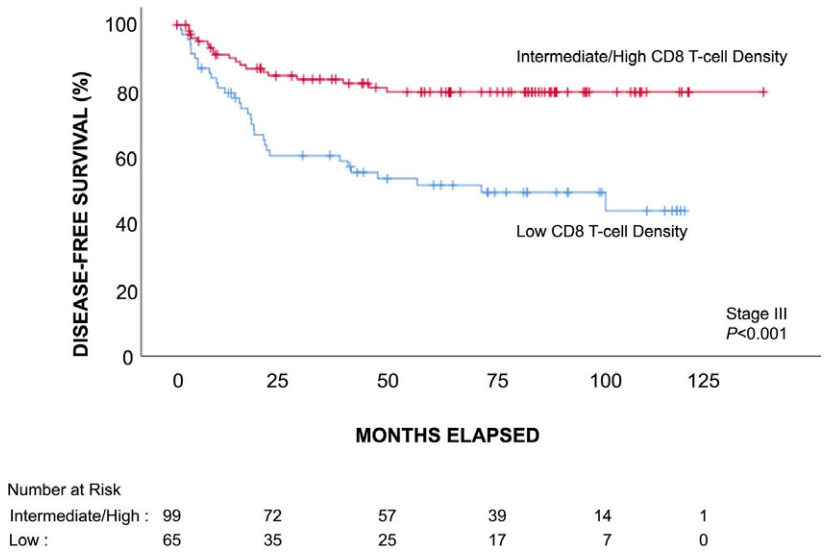

Conclusions: In stage III colon cancer, high/intermediate CD8+ T cell density is associated with improved disease-free survival and selects patient that most benefit from adjuvant chemotherapy in terms of recurrence risk. In contrast, stage III patients with a low CD8+ T cell density have increased risk of disease recurrence and do not appear to benefit from current adjuvant chemotherapy regimens.

422 KRAS, NRAS and BRAF Mutation Prevalence and its Clinicopathological Association in Colorectal Carcinoma with Emphasis on Tumor Budding

Mariam Ghafoor[1], Namra Ajmal[1], Zixuan Wang[2], Babar Bashir[3], Daniel Lin[3], Stephen Peiper[4], Wei Jiang[1], Manju Ambelil[2]
[1]Thomas Jefferson University Hospital, Philadelphia, PA, [2]Thomas Jefferson University, Philadelphia, PA, [3]Sidney Kimmel Medical College, Thomas Jefferson University, Philadelphia, PA, [4]Sidney Kimmel Medical College, Philadelphia, PA

Disclosures: Mariam Ghafoor: None; Namra Ajmal: None; Zixuan Wang: None; Babar Bashir: None; Daniel Lin: *Consultant*, Exelixis; *Stock Ownership*, Bionano Genomics; Stephen Peiper: None; Wei Jiang: None; Manju Ambelil: None

Background: Tumor-Node-Metastasis (TNM) staging system in colorectal cancer (CRC) provides valuable but incomplete prognostic information. Accumulating evidence suggests that tumor budding (TB) is a complementary prognostic factor in predicting the aggressive behavior of the tumor. RAS and RAF oncogene mutations are among the common mutations in CRC with therapeutic and prognostic significance. Systematic studies comparing the correlation between mutational status and tumor budding are rare.

Design: 172 primary sporadic CRCs were retrospectively analyzed from 2016-2019, for which the H&E slides were available and a Next Generation Sequencing multigene mutation analysis for *KRAS*, *NRAS,* and *BRAF* was performed. 2-5 representative sections per case were reviewed by two pathologists and TB was scored as per the International Tumor Budding Consensus Conference recommendations. Neoadjuvant treated cases with near-complete and partial responses were excluded. Demographic, tumor characteristics, and follow-up data were obtained from electronic medical records. Statistical analysis utilized Chi-Square and Fisher's exact test.

Results: The salient clinicopathologic features of null vs mutated CRCs are detailed in Table 1. Mutated tumors showed a significantly high proportion among female patients (p=0.037), tumors located on right side (p=0.003), and those with high histologic grade (p=0.030). There were no significant differences among the groups in terms of tumor depth, nodal status, lymphovascular, perineural space invasion, and recurrence/metastasis. Significantly high TB score was present in the mutated CRC cohort (p=0.045). Mutated (n=110) CRCs distribution in our cohort was 72 *KRAS* (65.5%), 11 *NRAS* (10%) and 27 *BRAF* (24.5%). *KRAS* mutated tumors showed significant distribution on right side (p=0.017), increased lymphovascular

(p=0.037) and perineural (p=0.035) space invasion and high TB score (p=0.018). Significant right-sided distribution and high histologic-grade were present in *BRAF* mutated tumors (p <0.00001 and 0.0005 respectively). CRCs with high TB scores in both cohorts showed increased rate of recurrence/metastasis.

	Null (n=62)	**Mutated (n=110)**	p-value	*KRAS* (n=72)	*NRAS* (n=11)	*BRAF* (n=27)
Gender						
Male (%)	34 (54.8)	41 (37.3)	**0.037**	32	4	5
Female (%)	28 (45.2)	69 (62.7)		40	7	22
Age						
Mean	62.9	67.5		66.1	62.5	74.1
Range	27-94	30-99		30-89	35-82	48-99
Location						
Right (%)	18 (29)	66 (60)	**0.003**	38	5	23
Left (%)	28 (45.2)	32 (29.1)		24	4	4
Rectum (%)	16 (25.8)	12 (10.9)		10	2	0
T stage						
T1 (%)	8 (12.9)	10 (9.1)	0.110	5	2	3
T2 (%)	15 (24.2)	13 (11.8)		8	0	5
T3 (%)	31 (50)	65 (59.1)		44	5	16
T4 (%)	8 (12.9)	22 (20)		15	4	3
N stage						
N0 (%)	32 (51.6)	61 (55.5)	0.96	38	7	16
N1-N2	25 (40.3)	47 (42.7)		33	4	10
WHO grade						
Low (%)	55 (88.7)	82 (74.5)	**0.030**	59	9	14
High (%)	7 (11.3)	28 (25.5)		13	2	13
LVI						
Present (%)	25 (40.3)	60 (54.5)	0.082	43	7	13
Absent (%)	37 (59.6)	50 (45.5)		29	4	14
PNI						
Present (%)	20 (32.3)	53 (48.2)	0.053	37	8	10
Absent (%)	42 (67.7)	57 (51.8)		35	3	17
Tumor Budding						
Low TB1 (%)	36 (58.1)	58 (52.7)		36	4	18
Intermediate TB2 (%)	19 (30.6)	25 (22.7)		15	5	5
High TB3(%)	7 (11.3)	27 (24.5)		21	2	4
TB1+TB2 vs TB3			**0.045**			

Table 1. Clinicopathological characteristics of total colorectal cancers analyzed

Conclusions: Tumor budding in CRC is an important prognostic marker and our study linking its association with the commonly mutated *KRAS*, *NRAS* and *BRAF* genes. Deepening the knowledge on these significant associations will disclose novel interventional opportunities in CRC.

423 5-hydroxymethylcytosine (5-hmC) Loss is a Marker of Malignancy in Biliary Tree Neoplasms

Miguel Gonzalez Mancera[1], Kevin Waters[1], Maha Guindi[1], Danielle Hutchings[1], Brent Larson[1], Andrew Siref[2]
[1]Cedars-Sinai Medical Center, Los Angeles, CA, [2]Baylor Scott & White Health, Temple, TX

Disclosures: Miguel Gonzalez Mancera: None; Kevin Waters: None; Maha Guindi: None; Danielle Hutchings: None; Brent Larson: None; Andrew Siref: None

Background: 5-methylcytosine is the methylated form of the nucleoside base cytosine, and its oxidation product, 5-hydroxymethylcytosine (5-hmC), is thought to be an intermediate form in the active demethylation process back to cytosine. Isocitrate dehydrogenase 1 and 2 (IDH1/2) are Krebs cycle enzymes that are thought to drive oxidization to 5-hmC when they are mutated in some neoplasms. Loss of 5-hmC expression and immunoreactivity has been observed in a variety of malignancies, though has not been thoroughly investigated in biliary neoplasms. Because intrahepatic cholangiocarcinomas (IHCs) are known to be enriched for alterations in IDH1/2, it was hypothesized that 5-hmC loss could serve as a diagnostic marker of biliary malignancies.

Design: Forty-six consecutive cases of biliary malignancies from 2010 to 2021 were retrieved from departmental archives, including 13 IHCs, 17 distal common bile duct cholangiocarcinomas (CBDCs), 10 perihilar cholangiocarcinomas (PHCs) and 6 gallbladder adenocarcinomas (GBCs). Histological mimics were selected as controls, including 8 biliary microhamartomas (BMHs), 9 bile duct adenomas (BDAs), 1 biliary intraductal papillary neoplasm (IPN), 2 biliary intraductal tubulopapillary neoplasms (ITPNs), 9 intracholecystic papillary neoplasms (ICPNs), and 3 biliary mucinous cystic neoplasms (MCNs). Immunohistochemical staining of 5-hmC was evaluated as a percentage of lesional nuclei staining, and the intensity of staining was graded semiquantitatively as 0-3+ compared to control tissue. Loss of 5-hmC was defined as >70% cells with negative (0) or 1+ staining. Groups were compared by Fisher's exact test, with a *p* value of <0.05 considered significant. Sensitivity and specificity were calculated.

Results: Loss of 5-hmC was 89% sensitive and 100% specific for biliary adenocarcinomas compared to benign biliary lesions (*p*=<0.0001). IHC showed loss of 5-hmC in 85% of cases, not significantly different from the 90% of other biliary adenocarcinomas with loss (*p*=0.6). 5-hmC was lost in significantly fewer pre-invasive neoplasms than in invasive biliary adenocarcinomas (26% vs. 89%, *p*=<0.0001).

Lesion	5-hmC Loss, n (%)	*p value*
Biliary adenocarcinomas (n=46)	41/46 (89%)	
Intrahepatic cholangiocarcinoma (n=13)	11/13 (85%)	0.6*
Perihilar cholangiocarcinoma (n=10)	10/10 (100%)	
Distal common bile duct cholangiocarcinoma (n=17)	15/17 (88%)	
Gallbladder adenocarcinoma (n=6)	5/6 (83%)	
Benign biliary lesions (n=17)	0/17 (0%)	<0.0001**
Bile duct adenoma (n=9)	0/9 (0%)	
Biliary hamartoma (n=8)	0/8 (0%)	
Mass-forming pre-invasive neoplasms (n=15)	4/15 (27%)	<0.0001***
Intraductal papillary neoplasm of bile duct (n=1)	1/1 (100%)	
Intraductal tubulopapillary neoplasm of bile duct (n=2)	0/2 (0%)	
Intracholecystic papillary neoplasm (n=9)	2/9 (22%)	
Mucinous cystic neoplasm of bile duct (n=3)	1/3 (33%)	

P* = intrahepatic cholangiocarcinoma vs. all other biliary adenocarcinomas. P** = biliary adenocarcinomas vs. benign biliary lesions

P*** = biliary adenocarcinomas vs. mass-forming pre-invasive neoplasms

Conclusions: 5-hmC loss is a sensitive and specific marker of invasive adenocarcinomas in the biliary tract compared to benign/non-invasive histological mimics. Similarly high rates of loss between IHC and other biliary adenocarcinomas suggest that 5-hmC loss is due to factors other than IDH1/2 alterations. Retention of 5-hmC staining in pre-invasive neoplasms suggests that 5-hmC loss may be a late development in malignancy coinciding with invasion.

424 Regression Grading and Pathologic Staging in Neoadjuvantly Treated Gastric Adenocarcinomas

Suntrea Hammer[1], Matthew Porembka[2], Sam Wang[1], John Karalis[2], Rodrigo Alterio[1]
[1]UT Southwestern Medical Center, Dallas, TX, [2]The University of Texas at Southwestern, Dallas, TX

Disclosures: Suntrea Hammer: None; Matthew Porembka: None; Sam Wang: None; John Karalis: None; Rodrigo Alterio: None

Background: Use of neoadjuvant therapy (NAT) in advanced gastric cancer is increasingly common. Very few studies address the effect of NAT on the relevance of AJCC 8th ed. pathologic staging, or the Ryan regression score, currently endorsed by the College of American Pathologists. In our study, we evaluate outcomes in a series of NAT treated gastric adenocarcinomas in relation to pathologic staging and Ryan's regression scoring.

Design: Data was collected from a prospectively created database of gastric carcinoma patients. Inclusion criteria were diagnosis of gastric adenocarcinoma, history of NAT, availability of recurrence and survival data, and pathologic staging and regression grading. Cases with non-curative intent or unusual histology (adenosquamous, mixed adeno-neuroendocrine carcinoma) were excluded.

Pathologic data and slides were reviewed by a gastrointestinal pathologist for site of carcinoma, differentiation, Lauren classification, lymphovascular invasion, perineural invasion, pathologic TNM classification, margin status, and tumor size. Clinical data collected included demographic information, NAT regimen, recurrence site and date, and all cause death and date.

Results: Results data can be found in Table 1. The cohort consists of 50 cases with a predominance of minority patients. Tumor locations include cardia: 12, body: 12, antrum/pylorus: 19, diffuse: 8. There were 12 recurrences (mean time 23 mos). There were 13 deaths (mean time 19.9 mos).

T stage correlated with patient outcome, demonstrating more recurrences and deaths with increasing T-stage. Pathologic N-stage demonstrated similar numbers of recurrences and deaths in each group. Mean follow up time did not differ significantly between T or N staging groups. Modified Ryan's score demonstrated a higher rate of recurrence and death in patients with a grade 3 (poor, 33%) than for grade 0 (0%) and grades 1 and 2 (20% and 20%). Tumor size showed a trend toward risk of recurrence, but not for overall survival.

Table 1. Cohort Characteristics

Demographics	Total number (%)				
Female	17 (34)				
Race					
AA	12 (24)				
H	25 (50)				
C	9 (18)				
O	5 (10)				
Age (yrs)					
mean	58.3				
range	26-90				
		Recurrence	p-value	Mortality	p-value
pT-stage					
T0	2	0	0.074	0	0.2925
T1a	1	0		0	
T1b	5	0		0	
T2	8	1		2	
T3	22	6		6	
T4a	10	5		5	
T4b	2	0		0	
pN-stage					
N0	16	2	0.0788	3	0.5075
N1	9	0		3	
N2	13	5		3	
N3a	10	3		4	
N3b	2	2		0	
Regression grade					
0	2	0		0	
1	5	1		1	
2	25	5		6	
3	18	6		6	0.3088
Mean size					
yes		6.4 cm	0.2295	5.0 cm	0.8156
no		4.8 cm		5.3 cm	

Conclusions: We demonstrate a trend towards higher risk of recurrence and death with increasing T-stage. N stage shows a trend toward recurrence free survival in patients with N0 disease, but not with overall survival. No recurrence or death was seen with complete regression, while poor response had higher rates of recurrence and mortality, showing some utility to the Ryan's regression grading in NAT treated gastric carcinomas. Additional studies are needed to clarify the role of TNM and regression grading in NAT cases.

425 Clinical and Pathologic Features of Colorectal Adenocarcinomas in Patients Under 50 Years of Age Undergoing Resection

Naomi Hardy[1], Pauline Shih[2], Maggie Sundel[1], Allen Burke[2], Andrea Bafford[2], Kristen Stashek[2]
[1]University of Maryland Medical Center, Baltimore, MD, [2]University of Maryland School of Medicine, Baltimore, MD

Disclosures: Naomi Hardy: None; Pauline Shih: None; Maggie Sundel: None; Allen Burke: None; Andrea Bafford: None; Kristen Stashek: None

Background: Colorectal adenocarcinoma (CRC) is the 3rd leading cause of death for both men and women in the US. While the overall incidence of CRC has decreased since 1975, the incidence of CRC in patients < 50 years of age has increased. In this study, clinicopathologic and molecular features and disease-free and overall survival were assessed in CRC patients <50 y and compared with the >50 subgroup.

Design: Slides, pathology reports and clinical data for 504 resections performed for CRC between 2013-2021 were reviewed, including confirmation of staging, mismatch repair status by IHC, and assessment for morphologic variants. The medical record was searched for past medical history, germline mutational status, molecular testing and outcomes. Fisher's Exact Test and Kaplan-Meier disease-free and overall survival analyses were performed.

Results: 86/504 (17%) CRCs were in patients < 50 y, with 50% between the ages of 45-49. Of patients < 50, 31% had a background predisposition (confirmed/suspicion for germline mutation or history of IBD), compared to 7% of patients > 50 (p=.001). 58% of patients < 50 were female (compared to 45% in >50 group, p=.031), and this uneven gender ratio persisted when excluding patients with a predisposition. Compared to the > 50 group, younger patients had smaller tumors (4 vs. 4.8cm), higher rates of perforation (17 vs 12%, p=.007), and were more likely to be left-sided with fewer right-sided tumors (38 vs 24% and 15 vs 33%, respectively, p=.006). They also had a greater likelihood of metastatic disease at diagnosis (19 vs 13%), regional lymph node positivity (56 vs 42%) and margin positivity (19 vs 9%, p=.02), and lower likelihood of MMR deficiency (MMR-D) (6 vs 17%, p=.004). All patients <50 with MMR-D were confirmed Lynch cases and none of the tested cases had a BRAF mutation. 31% showed variant morphology, with mucinous and micropapillary variants most common in both <50 and >50 groups (17 and 8%; 18 and 5%, respectively). Outside of the absence of medullary in the younger patients, all other variants occurred in similar frequencies in both groups. No difference in disease-free or overall survival was found in patients younger or older than 50.

Figure 1 - 425

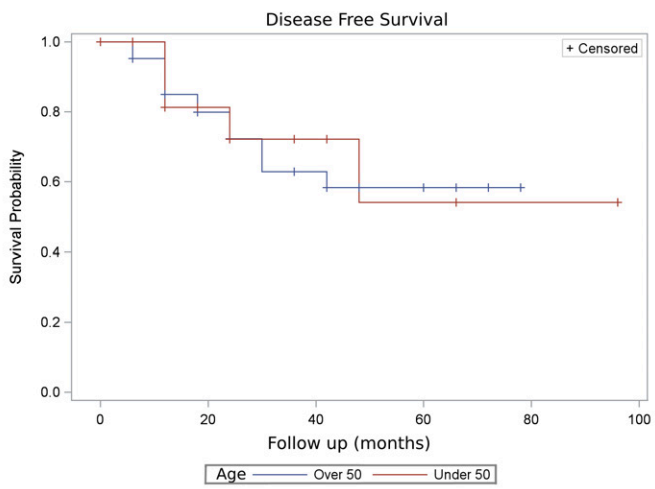

Figure 2 - 425

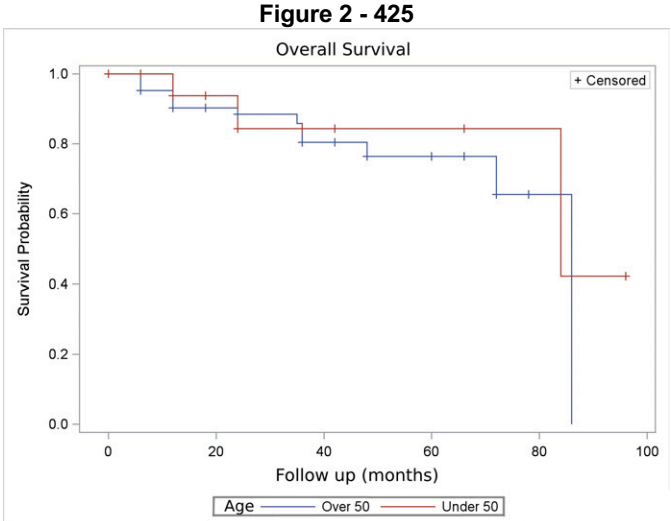

Conclusions: CRCs in patients <50 y may occur more often in females and be more advanced, left-sided, and MMR proficient. Although younger CRC patients were more likely to have a background predisposition, in particular IBD, almost 3/4 of those aged 45-49 lacked an identifiable predilection and would not have received colonoscopic screening under the previous guidelines.

426 Tumor Budding in Non-Treated, Node-Negative Colorectal Adenocarcinoma Resection Specimens: What is the Association with Isolated Tumor Cells?

Naomi Hardy[1], Autumn Larocque[1], Rachel Fanaroff[2], Allen Burke[3], Andrea Bafford[3], Kristen Stashek[3]
[1]University of Maryland Medical Center, Baltimore, MD, [2]University of Maryland, Baltimore, MD, [3]University of Maryland School of Medicine, Baltimore, MD

Disclosures: Naomi Hardy: None; Autumn Larocque: None; Rachel Fanaroff: None; Allen Burke: None; Andrea Bafford: None; Kristen Stashek: None

Background: Tumor buds (TB) are clusters of four or fewer cells at the invasive edge of a colorectal adenocarcinoma (CRC) and are considered an adverse prognostic indicator in clinical stage I/II tumors. Isolated tumor cells (ITCs) are defined as single tumor cells within lymph nodes and are currently categorized as N0 by CAP cancer staging protocols. In this study, the relationship between TB and node positivity as well as TB and the presence of ITCs in node negative resection specimens were assessed.

Design: H&E stained slides, immunohistochemical stains (IHC), pathology reports, and clinical data were reviewed for resection specimens performed for CRC between 2013-2021. Cases with neoadjuvant treatment, transmural invasion of entire bowel wall (pT4), and non-conventional morphologies (mucinous, signet ring, sarcomatoid, medullary) were excluded, leaving 182 cases for TB assessment. A representative H&E stained slide for each case was digitally scanned using the Aperio slide scanner and bud counts were assessed in a single "hot spot" at the invasive edge in a .785 μm^2 boxed field. All lymph nodes from 23 node negative cases with varying degrees of TB [low (LTB, 0-4 buds), intermediate (ITB, 5-9 buds), high (HTB, >10 buds)] were stained with pancytokeratin to assess for ITCs. Statistical analysis using independent T-Test was performed in SPSS to assess statistical significance.

Results: TB was greater in node negative compared to node positive CRC resections (64% vs. 44% LTB, 19% vs. 28% ITB, 18% vs. 28% HTB, and 4.87 vs 7.06 average bud count in node negative cases vs. node positive cases, respectively, p=0.03). In node negative resections, cases with high TB were more likely to be mismatch repair proficient (5.57 vs 2.40 average bud count, respectively, p = .015). Pancytokeratin immunostaining on a select number of pT3N0 cases revealed ITCs present only in cases categorized as high TB (6/12 cases versus 0/8 LTB and 0/3 ITB). Of these six cases, two developed distant metastatic disease.

Conclusions: High TB is associated with node positivity and in node negative cases, mismatch repair proficiency in non-neoadjuvant treated resections for CRC. In stage IIA cases, ITCs were found only when high TB was also present. Further studies are necessary to determine the role ITCs play in disease outcomes in the non-neoadjuvant, node negative setting.

427 Intestinal "Piggybacking Polyp": a Unique Polyp Composed of Lipoma and Overlying Lesions

Ana Hernandez Caballero[1], Xiaoyan Liao[2], Yansheng Hao[2]
[1]University of Rochester School of Medicine and Dentistry, Rochester, NY, [2]University of Rochester Medical Center, Rochester, NY

Disclosures: Ana Hernandez Caballero: None; Xiaoyan Liao: None; Yansheng Hao: None

Background: Lipomas are rare but the most common benign mesenchymal lesions of the gastrointestinal (GI) tract, composed of mature adipose cells. Lipomas more commonly occur on the right colon. The "piggybacking polyp" formed by lipoma with overlying polypoid epithelial lesions, are only mentioned in very limited case reports. In this case series, we systematically investigated the clinicopathological characteristics of these unique polyps.

Design: GI lipomas diagnosed at our institution from 2016-2021 were reviewed and only those with concurrent polypoid epithelial or mesenchymal lesions during the same endoscopic episode were included in this study. The concurrent lesion may occur at the same site as the lipoma forming a "piggybacking polyp", or located at a different intestinal site. Clinical and demographic data were obtained from medical records.

Results: A total of 400 GI lipomas were diagnosed, among which 100 (25%) lipomas from 98 patients had concurrent polypoid epithelial lesions, including sessile serrated lesion (SSL, n=29), Tubular adenoma (TA, n=92), Hyperplastic polyp (HP, n=43), inflammatory polyp (n=4), and tubulovillous adenoma (n=2), as well as mesenchymal lesions such as ganglioneuroma (n=2), and mucosal schwann cell hamartoma (n=1). The lipomas most commonly occurred at the right colon (58%), followed by the left colon (36%) and small bowel (6%). Most of them were located in submucosa, with rare cases located in mucosa (4%) (Fig D). Up to 35% of these lipomas had multiple concurrent polypoid lesions and 21% presented as “piggybacking polyps” with overlying epithelial lesions. The average age of patients did not differ between the ones with “piggybacking polyps” and the rest (61.8 vs 64.4, p=0.152). However, there was a significant difference with the ratio of females to males (17F:4M and 34F:43M respectively) (p=0.003). There was no significant difference in the mean size of the polyps between the two groups (10.7 mm vs 10.1 mm, p=0.410). Histologically, the “piggybacking polyps” showed overlying SSL (76.2%), TA (19%) and HP (4.8%) (Fig A, B and C), whereas the “non-piggybacking” group showed different concurrent preferences with SSL (9.9%), TA (52.9%), and HP (27.3%).

Figure 1 - 427

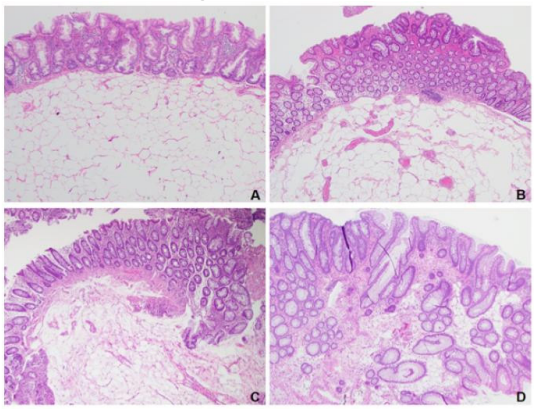

Conclusions: GI “piggybacking polyps” are rare lipomas with overlying polypoid epithelial lesions, most commonly SSL. They present with different clinicopathological features, compared to “non-piggybacking” lipomas, suggesting a unique underlying pathogenesis process that warrants further studies.

428 Mixed Neuroendocrine-acinar Neoplasms of the Stomach: A Contemporary Clinicopathologic Analysis of Seven Cases with Molecular Profile Studies

Wen Yu Hsiao[1], Shu Kwun Lui[1], Hanlin Wang[2], Linsheng Zhang[1], Alyssa Krasinskas[3], Wei Zheng[3]
[1]Emory University Hospital, Atlanta, GA, [2]David Geffen School of Medicine at UCLA, Los Angeles, CA, [3]Emory University, Atlanta, GA

Disclosures: Wen Yu Hsiao: None; Shu Kwun Lui: None; Hanlin Wang: *Advisory Board Member*, Astellas; *Grant or Research Support*, Bristol Meyers Squibb; *Consultant*, NGM Bio; *Consultant*, PathAI; Linsheng Zhang: None; Alyssa Krasinskas: None; Wei Zheng: None

Background: Gastric mixed neuroendocrine-non-neuroendocrine neoplasms consisting of extrapancreatic acinar and endocrine differentiation are very rare. Although limited cases have been reported in the pathology literature, their clinicopathologic features and mutation profiles are not yet understood.

Design: A search was made through multi-institutional electronic databases of GI pathology files and consult cases for mixed neuroendocrine-acinar neoplasms of the stomach. Seven cases were identified. Adequate immunohistochemical stains were performed to confirm the pancreatic acinar and neuroendocrine differentiation with each component >30% of the neoplasm. Immunostains for RB1, p53, ATRX, and DAXX were also performed in cases of high-grade carcinoma. Clinicopathologic parameters and whole-exome sequencing data were analyzed.

Results: The mean patient age at diagnosis was 61.9 years (ranging from 37 to 90 years). Five (71%) patients were male. Endoscopically, the tumor was located at gastric body in six (86%) cases and was described as a submucosal lesion/nodule or a large ulcerated mass. Autoimmune atrophic gastritis was noted in five cases. The mean size of the tumor was 5.2 cm (ranging from 1.1 to 8.5 cm). Four (57%) cases were grade 2 well-differentiated neuroendocrine tumors with pancreatic acinar features with a

mean Ki67 score of 7.2% (range: 6.1 to 8.7%) and tumor stage of pT1 or pT2. Mutations in MEN1, PIK3CB, PRKACA, NOTCH1, MED12, PTPN11, TERT, XRCC1, and XRCC2 were identified in these cases. Three (43%) cases were high-grade acinar-endocrine carcinoma with a mean Ki67 of 41.3% (range: 30.6-67.2%). The acinar component appeared to account for the majority of proliferation index while neuroendocrine component did not show definite high-grade features. All three tumors had advanced tumor stage (pT4) and positive lymph nodes. Mutations in CTNNB1, SMAD4, BRCA2, TSC2, FGR3 and NTRK1 were reported in these cases.

Conclusions: This study provides the largest contemporary analysis of clinicopathologic features of gastric mixed neuroendocrine-acinar neoplasms and broadens the molecular landscape of these rare tumors with implications for therapeutic options. In addition, recognition of pancreatic acinar differentiation in gastric acinar-endocrine carcinoma with detailed immunohistochemical workup is critical to avoid practice pitfalls such as misdiagnosing it as large cell neuroendocrine carcinoma or well-differentiated grade 3 neuroendocrine tumor.

429 Diagnostic Challenges of Grading Goblet Cell Adenocarcinoma

Ingold Huang[1], Dana Balitzer[2], Soo-Jin Cho[1], Won-Tak Choi[1], Ryan Gill[1], Nancy Joseph[1], Grace Kim[1], Hsiang-Chih (Sean) Lu[3], Aras Mattis[1], Sarah Umetsu[1], Sanjay Kakar[1], Kwun Wah Wen[1]

[1]University of California, San Francisco, San Francisco, CA, [2]San Francisco VA Health Care System, San Francisco, CA, [3]Diagnostic Pathology Medical Group, Inc, Sacramento, CA

Disclosures: Ingold Huang: *Stock Ownership*, ThermoFisher Scientific; *Stock Ownership*, BioMarin Pharmaceutical; Dana Balitzer: None; Soo-Jin Cho: *Stock Ownership*, BHB Therapeutics; *Grant or Research Support*, BHB Therapeutics; *Advisory Board Member*, Virta Health, Inc.; Won-Tak Choi: None; Ryan Gill: None; Nancy Joseph: None; Grace Kim: *Stock Ownership*, Senti Biosciences Inc.; *Stock Ownership*, Adicet Bio; Hsiang-Chih (Sean) Lu: None; Aras Mattis: *Consultant*, Hepatx, Ambys Medicines, Biomarin; Sarah Umetsu: None; Sanjay Kakar: None; Kwun Wah Wen: None

Background: A new grading scheme for appendiceal goblet cell adenocarcinoma (GCA) was adopted in the 2019 WHO classification based on the percentage of low- and high-grade components. The earlier Tang scheme (PMID 18685490) divided GCA into 3 grades (A, B, C) based on different morphologic criteria. Both schemes have been shown to stratify patients by clinical outcomes. This study compares the WHO and Tang schemes, and determines their diagnostic reproducibility.

Design: Clinicopathologic data were obtained for 34 GCA cases. Grading using 2019 WHO vs. Tang scheme was compared by 2 GI pathologists. To assess interobserver variability, 10 GI-trained pathologists blindly graded 5 selected GCA cases using the 2019 WHO vs. Tang grading schemes.

Results: Among 34 GCA cases, the grading was concordant in 19 (56%) cases using WHO and Tang schemes. Of the 15 discrepant cases (44%), 7 were WHO G1 and Tang B, while 8 were WHO G3 and Tang B. (Table 1). Among the 10 GI pathologists reviewing 5 selected GCA cases, the overall agreement was 54.7% agreement (kappa=0.32) for the WHO scheme (Figure 1) and 53.3% agreement (kappa=0.3) for the Tang scheme (Figure 2). Case 2 (G3/Tang B) and Case 5 (G1/Tang B) showed the most disagreement amongst 10 GI pathologists, highlighting the challenge in assigning Tang B cases that did not correspond to the respective WHO grades.

	Tang A	Tang B	Tang C
WHO 1	7	7	0
WHO 2	0	3	0
WHO 3	0	8	9

Figure 1 - 429

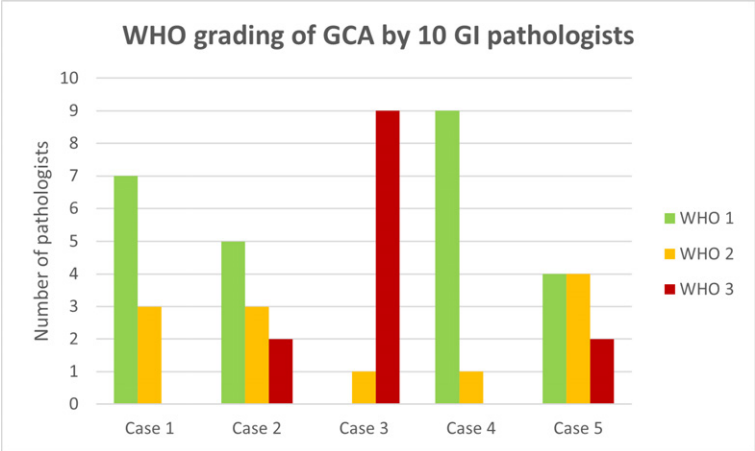

Figure 2 – 429

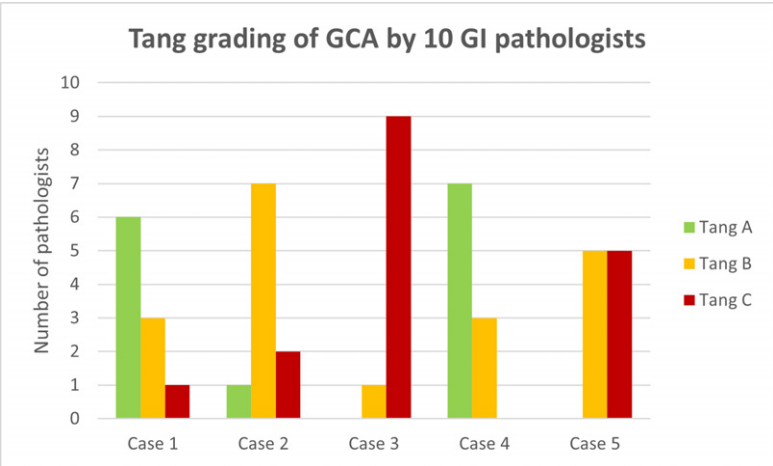

Conclusions: There is high discrepancy in WHO G1 cases and Tang A vs B as high grade component of <25% is regarded as WHO G1 even if this component is poorly differentiated or shows features of frank signet ring cell adenocarcinoma. There is high interobserver variability in GCA grading even among GI pathologists. Detailed definitions of WHO grades and long term outcome studies to examine the prognostic effect of poorly differentiated component <25% are necessary for a more robust grading scheme.

430 Is this Lymphoid Aggregate Neoplastic? Five Years of Data on Hematopathology Workup in Endoscopic Gastrointestinal Biopsies

Ammoura Ibrahim[1], Hwajeong Lee[2], Mahmoud Aldyab[2], Anne Chen[2]
[1]Albany Medical College, Albany, NY, [2]Albany Medical Center, Albany, NY

Disclosures: Ammoura Ibrahim: None; Hwajeong Lee: None; Mahmoud Aldyab: None; Anne Chen: None

Background: While benign lymphoid aggregates are commonly encountered in endoscopic gastrointestinal (GI) biopsies, the GI tract is also the most common site for extranodal lymphomas. Hematopathology (HP) workup can be costly and prolong turnaround time. Investigation into case features associated with lymphoma diagnoses versus benign tissue in GI biopsies is warranted.

Design: The departmental database was searched for in-house endoscopic GI biopsy cases, accessioned from January 2016 to December 2020, with final report text containing either HP attendings' last names or "CD20." For the resulting cases, electronic medical records were reviewed for demography, clinical history, and final diagnoses. The associations between the parameters and diagnoses were analyzed, with significance defined as $p<0.05$.

Results: Out of 31,020 GI endoscopic biopsy cases in the study period, 192 (0.6%) received HP workup. Among those receiving HP workup, there were 22 new lymphoma diagnoses (11%), 10 recurrent/persistent lymphomas (5%), 1 large cell transformation with prior history of small B-cell lymphoma (1%), 1 myeloid sarcoma with history of acute myeloid leukemia (1%), 10 benign cases with prior lymphoma history (5%) and 148 cases negative for hematopoetic malignancy (HPM) and without prior history of such (77%) **(Figures 1-2, Table 1)**. Total number of containers submitted by endoscopist per case was significantly less for new lymphomas compared to recurrent/persistent lymphomas (mean 2.5 vs. 5.6; p=0.002).

Table 1

Patient Age	Diagnosis	Prior History?	Site(s)
67	Chronic Lymphocytic Leukemia/Small Lymphocytic Lymphoma (CLL/SLL)	Yes	Colon, Rectum
59	Marginal Zone Lymphoma (Mucosa-Associated Lymphoid Tissue/MALT)	Yes	Stomach
61	Marginal Zone Lymphoma (Mucosa-Associated Lymphoid Tissue/MALT)	Yes	Stomach
62	Marginal Zone Lymphoma (Mucosa-Associated Lymphoid Tissue/MALT)	Yes	Gastroesophageal Junction, Stomach
59	Chronic Lymphocytic Leukemia/Small Lymphocytic Lymphoma (CLL/SLL)	Yes	Terminal Ileum, Colon, Rectum
54	Follicular Lymphoma, Grade 1-2	Yes	Colon
58	Unspecified clonal small B-cell population	Yes	Stomach
70	Chronic Lymphocytic Leukemia/Small Lymphocytic Lymphoma (CLL/SLL)	Yes	Anus, Perianus
77	Transformed High Grade B-cell Lymphoma with MYC, BCL6 and BCL2 Rearrangements; Follicular Lymphoma, Low Grade	Yes	Colon
60	Myeloid Sarcoma	Yes	Esophagus
56	Marginal Zone Lymphoma (Mucosa-Associated Lymphoid Tissue/MALT)	No	Stomach
65	High Grade B-cell Lymphoma with MYC and BCL6 Rearrangements	No	Stomach, Duodenum
82	Diffuse Large B-cell Lymphoma, Germinal Center B-cell Type	No	Stomach
67	Diffuse Large B-cell Lymphoma, Activated B-cell Type	No	Stomach
91	Diffuse Large B-cell Lymphoma, Activated B-cell Type	No	Esophagus
53	Marginal Zone Lymphoma (Mucosa-Associated Lymphoid Tissue/MALT)	No	Stomach
53	Marginal Zone Lymphoma (Mucosa-Associated Lymphoid Tissue/MALT)	Yes	Stomach
80	Chronic Lymphocytic Leukemia/Small Lymphocytic Lymphoma (CLL/SLL)	No	Colon
57	Chronic Lymphocytic Leukemia/Small Lymphocytic Lymphoma (CLL/SLL)	No	Terminal Ileum, Colon
76	Diffuse Large B-cell Lymphoma, Germinal Center B-cell Type	No	Esophagus
63	Follicular Lymphoma, Grade 1-2	No	Colon
66	Diffuse Large B-cell Lymphoma, Activated B-cell Type; Follicular Lymphoma, Low Grade	No	Stomach
67	Mantle Cell Lymphoma, Classic Type	No	Colon
44	Follicular Lymphoma, Grade 1-2	No	Duodenum
47	Marginal Zone Lymphoma (Mucosa-Associated Lymphoid Tissue/MALT)	No	Stomach, Duodenum
63	Diffuse Large B-cell Lymphoma, Activated B-cell Type	No	Jejunum
65	High Grade B-cell Lymphoma with MYC and BCL2 Rearrangements	No	Stomach
32	T-cell Lymphoma (Peripheral T-cell Lymphoma, Not Otherwise Specified versus Extranodal NK/T-cell Lymphoma)	No	Jejunum
77	Diffuse Large B-cell Lymphoma, Activated B-cell Type	No	Jejunum
71	Diffuse Large B-cell Lymphoma, Germinal Center B-cell Type	No	Stomach
74	Diffuse Large B-cell Lymphoma, Activated B-cell Type	No	Duodenum
48	Marginal Zone Lymphoma (Mucosa-Associated Lymphoid Tissue/MALT)	Yes	Stomach, Duodenum
71	Unspecified clonal small B-cell population	No	Colon
60	Marginal Zone Lymphoma (Mucosa-Associated Lymphoid Tissue/MALT)	No	Stomach

Figure 1 - 430

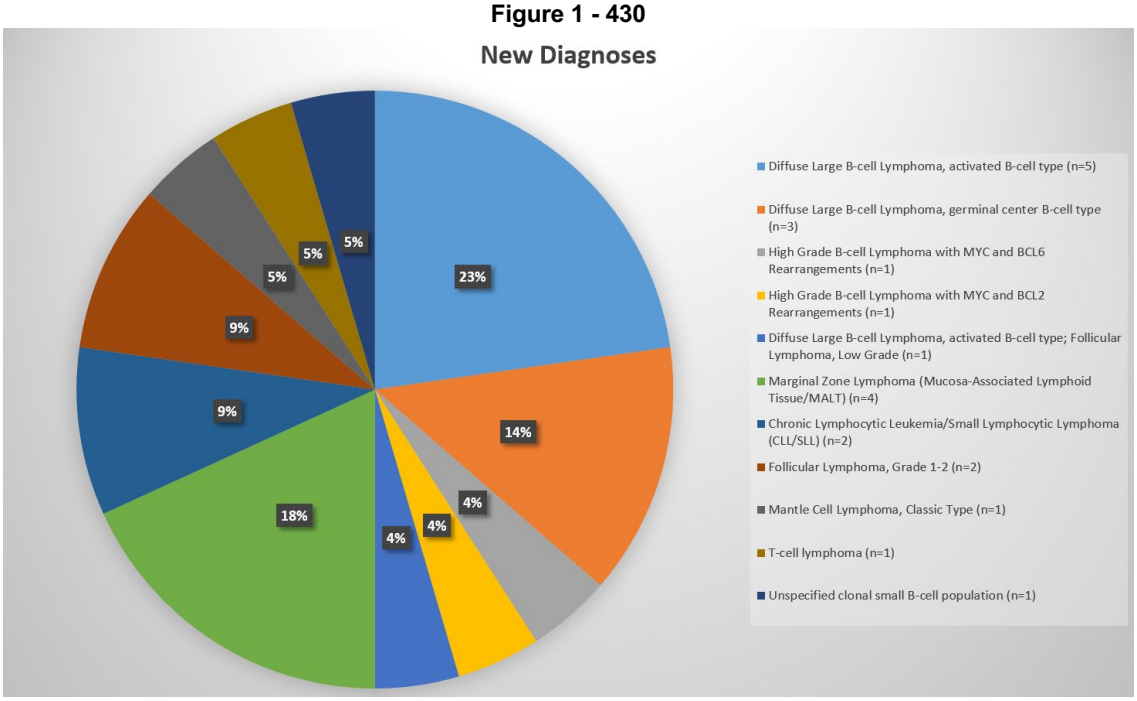

Figure 2 – 430

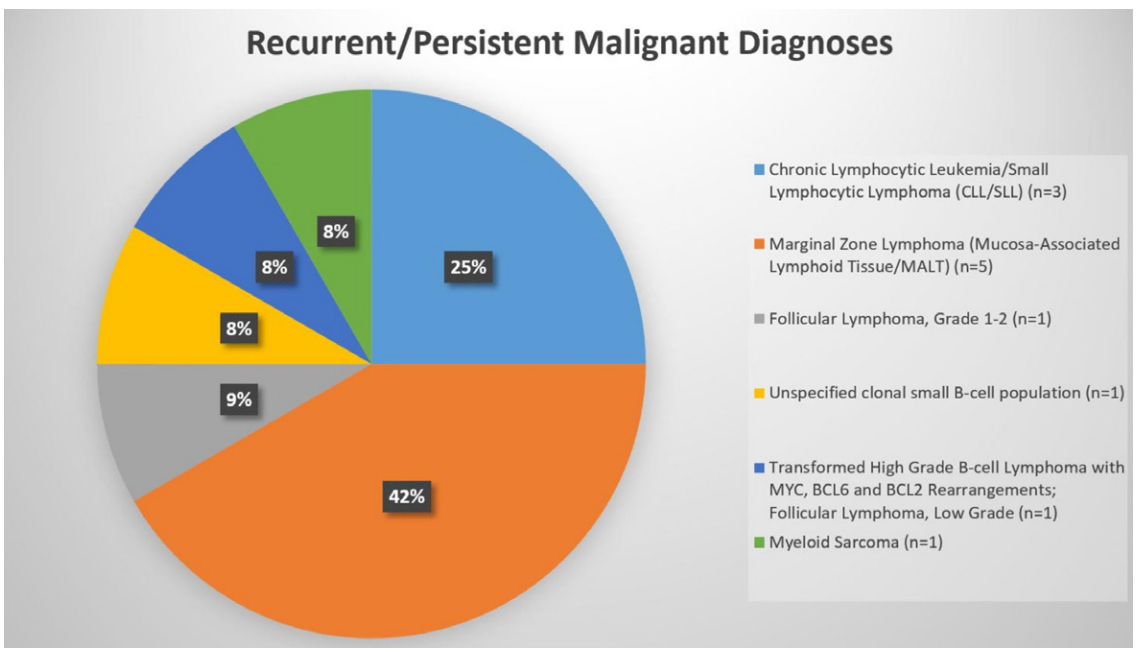

Conclusions: Within this limited data set, large B-cell lymphomas were more often diagnosed in patients with no prior history of any lymphoma. New lymphoma diagnoses occurred for cases with a smaller number of total containers per case compared to recurrent/persistent lymphoma. This sheds light on new lymphoma diagnoses certainly occurring in single-part cases opposed to the “multiple lymphomatous polyposis” scenario often taught for GI tract lymphoma.

431 Evaluation of Annexin A10, Claudin-18, and SOX2 Expression in 545 Gastrointestinal and Pancreaticobiliary Adenocarcinomas

Raymond Isidro[1], Ibrahim Abukhiran[2], Robert Humble[2], Matthew Gosse[2], Alexandra Isaacson[2], Joyce Arnouk[2], Andrew Bellizzi[2], Jason Hornick[3]

[1]Brigham and Women's Hospital, Harvard Medical School, Brookline, MA, [2]University of Iowa Hospitals & Clinics, Iowa City, IA, [3]Brigham and Women's Hospital, Harvard Medical School, Boston, MA

Disclosures: Raymond Isidro: None; Ibrahim Abukhiran: None; Robert Humble: None; Matthew Gosse: None; Alexandra Isaacson: None; Joyce Arnouk: None; Andrew Bellizzi: None; Jason Hornick: *Consultant*, Aadi Biosciences, TRACON Pharmaceuticals

Background: Primary tumor site determination for gastrointestinal (GI) tract carcinomas that present as metastasis of unknown primary can be problematic. Annexin A10 (ANXA10), a calcium-dependent phospholipid-binding protein, and claudin-18 (CLDN18), a tight junction protein, have been identified through expression profiling as markers of gastric lineage commitment. Expression of the transcription factor SOX2 has been reported in several tumor types, including gastric adenocarcinomas. The purpose of this study was to evaluate immunohistochemistry (IHC) for ANXA10, CLDN18, and SOX2 in adenocarcinomas of the GI tract to determine potential diagnostic utility.

Design: IHC for ANXA10, CLDN18, and SOX2 was performed on tissue microarrays including 545 GI tract tumors. Staining was scored based on the intensity (0-3) and the extent (percentage) of tumor cells showing expression (0-100%). H-scores were calculated as the product of the intensity and extent of staining. Positive staining was defined as greater than 5% staining.

Results: Table 1 summarizes the results by marker and primary tumor site. ANXA10 expression was strongest and most frequent in pancreatic adenocarcinomas when compared to all other tumors (96.5% vs 48.9%, p<0.001; strong staining 70.2% vs 13.1%, p<0.001). Strong staining for ANXA10 can discriminate between tumors of pancreatic and colorectal origin (70.2% vs 0%, p<0.001). Claudin-18 was least frequently positive in colorectal adenocarcinomas compared to all other GI tumors (18.8% vs 56.7%, p<0.001). SOX2 was least frequently expressed in tumors of the pancreas and small intestine; strong staining was not observed in tumors from these sites. All sites evaluated can potentially stain with all three markers; however, triple positivity is more frequent in the upper tubular GI tract (esophagus, GEJ, and stomach, 23.9% vs other sites 4.4%; p<0.001).

Location	Total Number	Annexin A10					Claudin-18					SOX2					% Triple Positive	% Double Positive	% Single Positive
		Positive	Median H*	% H ≥ 50	% H ≥ 100	% H ≥ 200	Positive	Median H*	% H ≥ 50	% H ≥ 100	% H ≥ 200	Positive	Median H*	% H ≥ 50	% H ≥ 100	% H ≥ 200			
Esophagus	89	58.4 %	145	46 %	39 %	16 %	69.7 %	215	62 %	55 %	40 %	51.7 %	160	45 %	34 %	19 %	31.5 %	61.8 %	87.6 %
GEJ	83	54.2 %	155	45 %	35 %	20 %	56.6 %	215	48 %	45 %	33 %	41.0 %	117	31 %	23 %	12 %	21.7 %	51.8 %	79.5 %
Stomach	58	51.7 %	119	40 %	31 %	19 %	58.6 %	193	43 %	38 %	26 %	39.7 %	45	28 %	22 %	9%	15.5 %	55.2 %	79.3 %
Small Bowel	70	55.7 %	169	43 %	34 %	24 %	45.7 %	108	40 %	24 %	14 %	8.6%	46	4%	3%	0%	2.9%	37.1 %	70.0 %
Pancreas	57	96.5 %	270	88 %	82 %	70 %	66.7 %	173	63 %	47 %	30 %	10.5 %	28	4%	0%	0%	7.0%	70.2 %	96.5 %
Cholangiocarcinoma	103	40.8 %	84	25 %	17 %	5%	46.6 %	120	39 %	33 %	12 %	15.5 %	63	10 %	7%	1%	4.9%	34.0 %	64.1 %
Colorectal	85	12.9 %	58	7%	2%	0%	18.8 %	123	13 %	11 %	6%	25.9 %	38	9%	6%	2%	4%	16%	38%

* If positive (intensity score ≥1 and extent >5%)

Conclusions: Staining for ANXA10, CLDN18, and SOX2 as part of a panel may aid in distinguishing adenocarcinomas from the upper tubular GI tract from other GI primary sites. ANXA10 staining may be particularly useful in distinguishing between adenocarcinomas of the pancreas and colorectum.

432 Artificial Intelligence (AI) for Evaluating the Risk of Gastric Cancer; A High Quality AI System for Detecting and Scoring Intestinal Metaplasia Was Constructed Successfully Using Deep Learning

Mai Iwaya[1], Yuichiro Hayashi[2], Yasuhiro Sakai[3], Akihiko Yoshizawa[4], Takeshi Uehara[5], Yugo Iwaya[5], Hiroyoshi Ota[6], Kensaku Mori[2]
[1]Shinshu University Hospital, Matsumoto, Japan, [2]Nagoya University, Nagoya, Japan, [3]Fujita Health University, Toyoake, Japan, [4]Kyoto University Hospital, Kyoto, Japan, [5]Shinshu University School of Medicine, Matsumoto, Japan, [6]Shinshu University School of Health Sciences, Matsumoto, Japan

Disclosures: Mai Iwaya: None; Yuichiro Hayashi: None; Yasuhiro Sakai: None; Akihiko Yoshizawa: None; Takeshi Uehara: None; Yugo Iwaya: None; Hiroyoshi Ota: None; Kensaku Mori: *Grant or Research Support*, Cybernet System, Morita Mfg, Ziosoft, Olympus

Background: The majority of gastric cancers (GC) are associated with chronic gastritis. To evaluate the degree of gastritis universally, the Updated Sydney System (USS) was developed, and based on the USS, the Operative Link on Gastric Intestinal Metaplasia Assessment (OLGIM) system was constructed. Further studies with the OLGIM system showed a higher gastric cancer risk in stage III or IV patients, which is determined by the degree of intestinal metaplasia (IM). While the OLGIM system is useful to evaluate the risk of GC, the scoring system used in the USS is subjective, and the OLGIM system requires at least four gastric biopsies for each case. Thus, scoring has been a huge burden on gastrointestinal (GI) pathologists. Whole-slide imaging (WSI) is becoming a routine procedure for the clinical diagnosis of many diseases; however, most artificial intelligence (AI) systems in the pathology field are focused on neoplastic lesions. The development of an AI system to evaluate IM with high accuracy could decrease pathologists' workloads and provide universal assessment of the risk of GC.

Design: We examined 963 cases of gastric biopsies, which were collected according to the USS protocol. IM was scored as: 0 (no IM), 1 (mild IM), 2 (moderate IM), and 3 (severe IM) by two experienced GI pathologists. H&E slides were scanned using a WSI scanner, and each gastric biopsy specimen image was labelled with a USS IM score. WSIs were divided according to the gastric biopsy tissue. Each gastric biopsy tissue image was resized to 1500 × 1500 pixels for inputting to the AI system; 5753 gastric tissue images were prepared, and 5-fold cross validation was performed for evaluation.

Results: In the 5753 images, pathologists diagnosed 3894 (69%) images with no IM and 1766 (31%) images with IM. AI classified 3990 (69%) images without IM and 1763 (31%) images with IM, with a sensitivity of 97.6% and specificity of 94.7%. IM score 2 and 3, those are involved as a criteria of stage III or IV OLGIM was classified by pathologists in 290 (5%) and 750 (13%) images, respectively, compared with AI with 263 (5%) and 801 (14%) images, respectively. The sensitivity and specificity of classifying IM between scores 0, 1 and scores 2, 3 was 99.0% and 93.0%, respectively.

Conclusions: Our AI system grades IM scores based on the USS criteria within the performance range of experienced GI pathologists and is useful for evaluating the risk of GC in practice.

433 Stromal Desmoplastic Reaction is Associated with Recurrence Free Survival in Post-Neoadjuvant Esophageal Adenocarcinoma Resection Specimens

Krishna Iyer[1], Iván González[2], Dhanpat Jain[3], Xuchen Zhang[3]
[1]Yale New Haven Hospital, New Haven, CT, [2]Children's Hospital of Philadelphia, Philadelphia, PA, [3]Yale School of Medicine, New Haven, CT

Disclosures: Krishna Iyer: None; Iván González: None; Dhanpat Jain: None; Xuchen Zhang: None

Background: Pathological tumor regression and various histological features have been evaluated as predictors of survival in locally advanced esophageal adenocarcinomas (EAC). These systems are largely based on extent of tumor regression, depth of invasion and pathological staging, but recent studies have suggested the tumor microenvironment could also be important. In this study we investigated the significance of the stromal desmoplastic reaction (DR) in post-neoadjuvant EAC (NAT-EAC) as a predictor of survival.

Design: A total number of 126 NAT-EAC cases from 2005 to 2016 were included in the study. Various demographics, clinical variables (e.g. smoking status, BMI, and age) and histopathological features (e.g. tumor depth of invasion, grade, acellular mucin, neuroendocrine differentiation) were analyzed. In addition, DR was evaluated and classified as "immature" (presence of myxoid

stroma involving at least one high-power field (40x)) or “mature” stroma (more mature collagen fibers, sometimes with keloid-like changes without any myxoid changes).

Results: Nineteen cases showed complete treatment response and 107 cases had residual tumor. Of the 107 cases with residual tumor, 7 (6.5 %) had an immature and 100 showed (93.4%) a mature DR. Immature DR was associated with full thickness tumor invasion into the adventitia (6/39 cases, 15.4%; p< 0.01), but not with any of the clinical variables or histopathological features. The tumor extending to adventitia had a significantly lower post-neoadjuvant recurrence free survival (RFS) than tumor confined to submucosa and muscularis propria (Fig. 1). Immature DR was also associated with a worse RFS (p<0.01) compared to mature DR. More importantly, in multivariate analysis immature DR was the only parameter significantly associated with RFS (HR 2.68, 95%CI; p=0.02).

Figure 1 - 433

Figure 1: A) Comparison of survival differences for tumors with different depths of invasion (CR=complete response, M=mucosa, SM=submucosa, MP=muscularis propria, AD=adventitia). **B)** RFS is worse for cases with immature vs. mature stromal reaction.

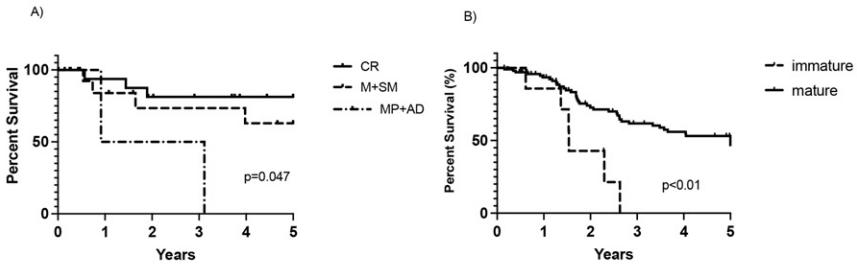

Conclusions: Our study show that immature DR is an independent predictor of survival in NAT-EAC. Immature DR likely represents an active ongoing tumor to stromal interaction, and needs further studies to understand underlying molecular mechanisms. Our results also suggest that the nature of DR should be incorporated into pathology report of NAT-EAC.

434 Screening at the Scope: Can Review of Prior Pathology Reports Accurately Predict Gastrointestinal Polyposis Syndromes?

Pari Jafari[1], Namrata Setia[2], Christine Drogan[2], Sonia Kupfer[1], John Hart[2]
[1]University of Chicago Medicine, Chicago, IL, [2]University of Chicago, Chicago, IL

Disclosures: Pari Jafari: None; Namrata Setia: None; Christine Drogan: None; Sonia Kupfer: None; John Hart: None

Background: While the diagnosis of gastrointestinal (GI) polyposis syndromes relies on family history and genetic testing, screening for polyposis syndromes currently incorporates polyp count/phenotype and associated medical conditions. The pathologist’s contribution has generally been limited to classification of polyp phenotype; the extensive chart review involved in evaluating family history and pedigree analysis typically precludes a more active role in the screening process. In this study, we assess a set of time-efficient parameters for polyposis syndrome screening that draws on information readily available to pathologists at the point of sign-out.

Design: A set of parameters was developed for identification of patients with a high suspicion for GI polyposis syndromes (Fig. 1), based solely on a review of current and prior pathology reports and intended to be applied during case sign-out. The parameters were drawn from a review of the polyposis-related literature and consensus among GI pathologists at our institution and were optimized for time-efficiency and ease of access. These criteria were validated by a blinded review of pathology reports for a cohort of patients followed at our institution’s GI Cancer Risk Clinic. The overall sensitivity of the criteria for identifying the presence of a polyposis syndrome was calculated. In each suspected syndromic case, an attempt was made to identify the most likely syndrome cluster (adenomatous, hamartomatous, serrated, or mixed polyposis).

Results: A total of 106 patients (3-79y, median 36y; M:F 1:1) with an established clinical diagnosis of a germline polyposis syndrome and one or more GI pathology reports available within our pathology information system were identified. Of these, 96 met

criteria for one of the four categories of polyposis syndromes (Table 1), with a resultant sensitivity of 90.6%. Specific syndrome clusters were correctly predicted in 95 of 96 instances (99.0%). Within the hamartomatous polyposis category, specific syndromes were accurately predicted in 15 of 16 cases (93.8%). Cumulative number of polyps was the most frequently met criterion across syndromes (Fig. 1); among cases with insufficient diagnostic polyps, the most commonly met criterion was the presence of upper tract adenomas.

Table 1. Validation of Criteria Against Clinically Confirmed Polyposis Cases.

	Category of polyposis syndrome, per application of criteria	Number of cases meeting criteria (blinded review)	Underlying diagnosis per cancer risk clinic records			Predicted N (blinded pathologist review) / True N with underlying diagnosis
			Underlying clinical diagnosis	Number of patients with underlying clinical diagnosis	Germline mutations (number with mutation / number undergoing multigene testing)	
Cases meeting criteria	Adenomatous polyposis syndromes (APS)	78	Familial adenomatous polyposis (FAP)	67	APC, 28/28	78/78
			MUTYH-associated polyposis (MAP)	8	MUTYH, 8/8	
N=96			Colonic polyposis of unknown etiology (CPUE)	2	MUTYH, 1/2	
					Second case with negative genetic testing	
			Other	1	POLE, 1/1	
	Hamartomatous polyposis syndromes (HMS)	16				16/16
	JPS	9	JPS	10	SMAD4, 4/4	9/10
	PJS	3	PJS	3	STK11, 2/2	3/3
	CS	4	CS	3	PTEN, 2/2	4/3
	Serrated Polyposis Syndrome (SPS)	1	FAP	1	No testing performed	1/0
	Mixed Polyposis Syndrome (MPS)	1	MAP	1	MUTYH, 1/1	1/1
Cases not meeting criteria	APS (N=8)		FAP	7	APC, 2/2	
			MAP	0		
N=10			CPUE	1	Genetic testing negative	
	HPS (N=2)					
	JPS		JPS	1	No testing performed	
	PJS		PJS	0		
	CS		CS	1	PTEN, 1/1	
	SPS		0			
	MPS		0			

Figure 1 - 434

Figure 1. Screening Criteria for Germline Polyposis Syndromes. The number of cases in which each finding represented the pivotal diagnostic criterion is given in red italics. Four patients exhibited n concurrent diagnostic findings.

		Germline Polyposis Syndromes – Diagnostic Clusters			
		APS (FAP, aFAP, NAP, MAP, LS)	**SPS**	**HPS** (JPS/HHT, CS, PJS)	**MPS** (*GREM1, BMPR1,* [rarely] MAP)
Screening Criteria for Identi-fication of GI Polyposis Syndromes *Fulfilment of any single criterion constitutes a positive screen.	**Criteria based on polyp count**	≥10 cumulative adenomas *N=38*	≥5 cumulative serrated polyps, proximal to rectum (all measuring >0.5 cm *or* 2 measuring >1 cm) *N=1*	≥3 cumulative hamartomatous polyps *N=11* - *Presence of ≥1 juvenile-type polyp: favor JPS*	≥10 cumulative adenomas and serrated/hamar-tomatous polyps *N=1*
			>20 cumulative serrated polyps, 5 located proximal to rectum	≥1 Peutz-Jeghers-type polyp [*sub-classify as PJS*] *N=3*	
	Criteria based on additional endoscopic findings/ patient history	Colorectal carcinoma diagnosed at <50y *N=8*		≥1 hamartomatous polyp and >2 primary cancers (any site) *N=0*	
				≥3 nondescript polyps of the upper tract *N=0*	
		Multiple colorectal carcinomas *N=2*		*Favor CS* — History of breast cancer and lipoma *N=0*	
		≥5 cumulative adenomas and >2 primary cancers (any site) *N=0*		*Favor CS* — Multiple glycogenic acanthoses *N=0*	
		Upper tract (including small bowel) adenomas: ≥1 if <50y, ≥3 if ≥50y *N=22*		*Favor CS* — ≥1 hamartomatous polyp and ≥1 follicular adenoma of thyroid *N=1*	
		≥1 fundic gland polyp with dysplasia *N=7*		*Favor JPS/ HHT* — Cutaneous vascular lesions (e.g., angioectasia, angiokeratoma) *N=0*	
		History of endometrial cancer and *either* >5 cumulative adenomas *or* ≥1 advanced adenoma measuring >1 cm *N=1*			
		History of papillary thyroid carcinoma, cribriform-morular variant *N=2*			
		History of desmoid tumor *N=4*			

Abbreviations: APS, adenomatous polyposis syndromes; FAP, familial adenomatous polyposis; aFAP, attenuated familial adenomatous polyposis; NAP, *NTHL1*-associated polyposis; MAP, *MUTYH*-ass polyposis; LS, Lynch syndrome; SPS, serrated polyposis syndrome; HPS, hamartomatous polyposis syndromes; JPS, juvenile polyposis syndrome; HHT, hereditary hemorrhagic telangiectasia; CS, Cowc syndrome; PJS, Peutz-Jeghers syndrome; MPS, mixed polyposis syndromes

Conclusions: Here, we show that structured review of prior pathology reports, guided by accessible, time-efficient parameters, offers a highly sensitive screening mechanism for flagging potential GI polyposis syndrome patients.

435 Intestinal Xanthomatosis: A Clinicopathologic Analysis of 17 Cases

Sebastian Jofre[1], James Lapinski[2], Erica Savage[2], Lei Zhao[3], Kenan Sauder[4], Namrata Setia[5], Vikram Deshpande[6], Deepa Patil[3]

[1]Brigham and Women's Hospital, Boston, MA, [2]Cleveland Clinic, Cleveland, OH, [3]Brigham and Women's Hospital, Harvard Medical School, Boston, MA, [4]Newton-Wellesley Hospital, Newton, MA, [5]University of Chicago, Chicago, IL, [6]Massachusetts General Hospital, Harvard Medical School, Boston, MA

Disclosures: Sebastian Jofre: None; James Lapinski: None; Erica Savage: None; Lei Zhao: None; Kenan Sauder: None; Namrata Setia: None; Vikram Deshpande: None; Deepa Patil: None

Background: Xanthomatous lesions occur in patients with hyperlipidemia and are characterized by accumulation of lipid-laden foamy histiocytes (FH). Gastrointestinal tract involvement usually manifests as gastric or colorectal polyps. In rare instances, the bowel shows diffuse accumulation of bland FH within the mucosa, with or without transmural involvement. The aim of this study was to describe pathologic features of 17 such cases of intestinal xanthomatosis and explore their clinical associations.

Design: Seventeen cases (16 small bowel resections, 1 colon biopsy sample) from 15 patients at 3 institutions were identified. All were incidental; polypoid xanthomas were excluded. Age, gender, history of dyslipidemia/metabolic syndrome, inborn errors of metabolism, immune status, and clinical symptoms were recorded. Pathologic features assessed were mucosal architecture, FH distribution, vessel morphology and distribution, muscularis propria (MP) thickness and serosal findings.

Results: The mean age of patients (M:F: 1.1) was 70 yrs (range: 16 - 92). Most patients presented with symptoms of obstruction (13; 73%) followed by hernia/ischemia (3; 20%) and mesenteric mass (1; 7%). The mean length of resected bowel was 31 cm

(range: 3.5 - 84). A mucosal-predominant pattern of FH was seen in 15 (88%) cases while 2 (12%) had infiltration of the submucosa and MP. Villous blunting/necrosis was noted in 6 (35%) cases; 12 (70%) showed a normal architecture with a diffuse band-like distribution of FH in the basal lamina propria (Fig 1, 2). Dilated lymphatics (6 mucosal, 1 serosal) containing FH were seen in 7 (41%) cases. Other findings included thickened MP (2; 13%), serosal adhesions (15; 94%) and dilated submucosal and subserosal vessels (14; 88%). Coexisting clinical conditions included dyslipidemia/metabolic syndrome (3; 20%), immunosuppression (3; 20%), Crohn's disease (1; 7%), Sjogren's syndrome (1; 7%), carnitine deficiency (1; 7%), idiopathic and unknown (3 each; 20%). An infectious workup was negative in all cases.

Figure 1 - 435

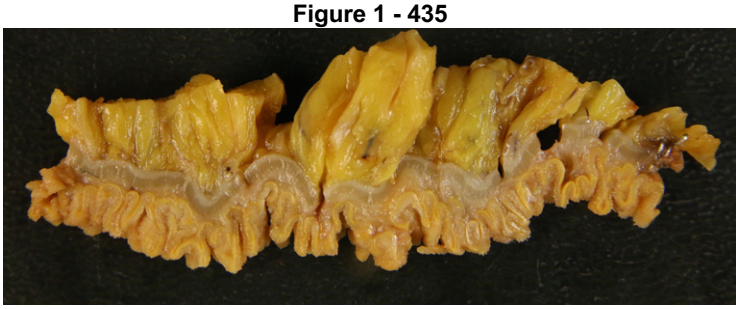

Figure 2 - 435

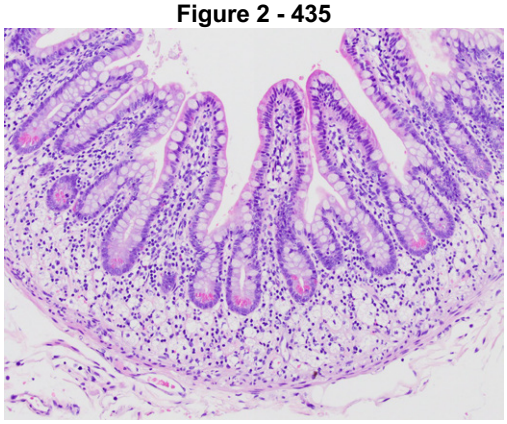

Conclusions: Intestinal xanthomatosis is a benign condition that tends to affect older patients and has a predilection to involve the small bowel in a mucosal-predominant pattern. In addition to altered lipid metabolism, it can be associated with other immunologic conditions. As most patients present with bowel obstruction, but with minimal/no mucosal injury, it either represents a unique response to prior mucosal injury or a consequence of altered motility and impaired lymphatic drainage.

436 Hamartomatous Polyps in Patients with Tuberous Sclerosis Complex

Richard Judelson[1], Stuti Shroff[2], Vikram Deshpande[3], Rory Crotty[1]
[1]Massachusetts General Hospital, Boston, MA, [2]Massachusetts General Hospital, Watertown, MA, [3]Massachusetts General Hospital, Harvard Medical School, Boston, MA

Disclosures: Richard Judelson: None; Stuti Shroff: None; Vikram Deshpande: None; Rory Crotty: None

Background: Tuberous sclerosis complex (TSC) is an inherited tumor susceptibility syndrome resulting from mutations in *TSC1* or *TSC2* genes. Rare case reports have identified hamartomatous polyps in the gastrointestinal tract (GIT), primarily the colorectal region in patients with TSC. Our objective is to evaluate the morphological features of TSC related gastrointestinal polyps.

Design: Patients with a clinical history of TSC (1990-2021) and at least one surgical pathology specimen were identified, and all gastrointestinal polyps were documented. The polyps were evaluated by two gastrointestinal pathologists. Selected cases with available paraffin blocks were stained with HMB-45 (n=3) and desmin (n=2).

Results: 13 patients were identified with a total of 19 GIT polyps. The median age = 29, mean age = 28 (age at time of endoscopy) and gender = 54% female. These included specimens from the stomach (n=7) and colon (n=12). All 19 polyps show prominent mucosal arborizing smooth muscle-like cells, thus mimicking mucosal prolapse polyps. In addition, 3 of 7 gastric polyps showed lobular growth pattern with lobules surrounded by desmin positive smooth muscle cells in the one gastric polyp stained. In the colon the smooth muscle-like cells showed pale eosinophilic cytoplasm with vacuolar change, resembling the appearance seen in PEcomas. On immunohistochemistry the colonic smooth muscle-like cells were focally positive for HMB-45 in 1 of 3 cases evaluated.

Conclusions: GIT polyps in patients with TSC are characterized by arborizing smooth muscle-like cells. Gastric polyps in patients with TSC show a lobulated appearance with perilobular smooth muscle cells. A proportion of colonic polyps in TSC patient that resemble mucosal prolapse polyps represent TSC-related hamartomas.

437 Submucosal Duct Involvement in Esophageal Squamous Cell Carcinoma: A Case Series

Savas Kanaroglou[1], Corwyn Rowsell[2], Christopher Teshima[3], Catherine Streutker[1]
[1]Unity Health Toronto, Toronto, Canada, [2]St. Michael's Hospital, Toronto, Canada, [3]St. Michael's Hospital/University of Toronto, Toronto, Canada

Disclosures: Savas Kanaroglou: None; Corwyn Rowsell: None; Christopher Teshima: None; Catherine Streutker: None

Background: Submucosal duct involvement (DI) in superficial squamous cell carcinomas of the esophagus (SSCCE) has been investigated in Taiwanese and Japanese populations yet there is a paucity of North American literature on the topic. While it has been shown that DI alone does not qualify as submucosal invasion, DI remains a potential risk factor for recurrence following radiofrequency ablation (RFA) or mucosal resection (EMR/ESD). Our goal is to present cases of DI in SSCCE within a North American population.

Design: The study was approved by the Research Ethics Board of our facility. The pathology database was queried for intramucosal carcinoma cases spanning 2011 to 2021; cases of SSCCE were investigated for the presence of DI. Outcome was investigated from the clinical database.

Results: 24 of 712 EMR/ESD cases contained SSCCE of which 5 had DI. Cases with DI displayed squamous intraepithelial lesion (4 HSIL, 1 LSIL) involving submucosal ducts and/or glands without invasion through basement membranes. Of these, 1 was an ESD and 4 were EMRs. 1 EMR displayed pure squamous carcinoma in situ (HSIL). 2 had submucosal invasion with tumour sizes of 2.0 cm and 0.5 cm, both grade 2. 2 had intramucosal squamous carcinoma; 1 grade 1 and the other grade 2. With follow-up for 0.5-4 years, 3 patients had biopsies with low grade dysplasia (LSIL) while no patients had recurrent or metastatic carcinoma.

Of the 19 cases lacking DI, 12 had intramucosal SCC while 7 had submucosal invasion. Cases were graded as 1-2 with a single case of submucosal invasion that was grade 3. Cases of intramucosal SCC with follow up of 0.3 – 3 years had no evidence of recurrence or metastases with 1 patient receiving chemotherapy/radiation. Of the cases with submucosal invasion, 4 had 0.6 – 7 year follow-up; 2 had residual dysplasia, 1 was negative for dysplasia and malignancy and one had recurrent disease with suspicion of nodal involvement. 2 patients received chemotherapy/radiation.

Conclusions: DI within SSCCE at our institution displays comparable pathological characteristics to DI described in studies of Taiwanese and Japanese populations. The presented cases lacked basement membrane invasion at foci of DI. Outcome for patients with DI was comparable to those without. This is compatible with the understanding that DI does not constitute submucosal invasion, therefore patients should not reflexively be referred for surgery or chemo/radiation therapy when DI is identified in mucosal resection specimens.

438 Practice Patterns for Reporting Digestive System Neuroendocrine Neoplasms: Results from a Large, Comprehensive International Survey

Dipti Karamchandani[1], Brian Cox[2], Stefano La Rosa[3], Andrew Bellizzi[4], Chanjuan Shi[5], Raul Gonzalez[6]
[1]UT Southwestern Medical Center, Dallas, TX, [2]Cedars-Sinai Medical Center, Los Angeles, CA, [3]University of Insubria, Varese, Italy, [4]University of Iowa Hospitals & Clinics, Iowa City, IA, [5]Duke University Medical Center, Raleigh, NC, [6]Beth Israel Deaconess Medical Center, Harvard Medical School, Boston, MA

Disclosures: Dipti Karamchandani: None; Brian Cox: None; Stefano La Rosa: None; Andrew Bellizzi: None; Chanjuan Shi: None; Raul Gonzalez: None

Background: Criteria for diagnosis and grading of digestive system neuroendocrine neoplasms (NENs) continue to evolve. Although there are some literature recommendations regarding workup and diagnosis of these lesions, we have encountered different practice patterns among pathologists when signing out these specimens. The aim of this study was to assess practice trends among pathologists worldwide when encountering digestive system NENs.

Design: We created an online survey with multiple questions pertaining to workup and diagnosis of digestive system NENs. It was circulated among pathologists, and the results were analyzed based on type of practice setting, years of sign-out experience, and practice location using SPSS v27 software.

Results: Respondents included 384 practicing pathologists with the following characteristics: 70% academic, 30% private practice; 63% gastrointestinal (GI) pathology-subspecialized, 37% not; North American 39%, European 42%, other 19%; <10 years in

practice 45%; ≥10 years 55%. Some responses were chosen by the majority (eg, 85% use both mitotic count and Ki67 index for grading NENs, 91% distinguish between large cell and small cell neuroendocrine carcinoma on histologic grounds, 82% complete a synoptic and Ki67 stain even for small incidental appendiceal neuroendocrine tumors (NETs), 96% utilize the diagnosis of grade 3 NET). However, some questions showed significantly varying responses (Table 1), including how to count mitotic figures (GI and North American pathologists preferred a gestalt, with true counting if needed), Ki67 stain interpretation (academic pathologists preferred counting even weakly staining nuclei, Figure 1, Table 1), and pancreatic grade 3 NEN workup (European pathologists preferred always using ancillary stains for diagnosis). Pathologists had some variability in interpreting local metastatic foci of small bowel NETs (eg, positive node vs. tumor deposit, Figure 2, Table 1), and in choosing block(s) for Ki67 staining in multifocal lesions.

Table 1: Selected survey questions with responses and practice patterns

Representative Survey Questions	Responses	% of respondents	Practice Patterns
How do you count mitotic figures when grading digestive tract neuroendocrine neoplasms?	a. Ignore and go straight to Ki67	7%	- GI pathologists (p<0.001) and North American pathologists (p<0.001) preferred response “b” - General pathologists preferred response “c” (p<0.001)
	b. A quick glance to get the gestalt, then count if it seems high	20%	
	c. I carefully count 10 high-power fields (or 2 mm^2)	41%	
	d. I carefully count 50 high-power fields (or 10 mm^2), then divide by 5 to get an average	32%	
When counting Ki67 index, what approach do you use?	a. Eyeballing only	7%	- General pathologists preferred response “b” (p=0.001) - GI pathologists preferred response “e” (p=0.001) - North American pathologists preferred response “c” (p=0.001) - European pathologists preferred response “d” (p<0.001)
	b. Eyeballing first and if borderline between grades, manual counting at the microscope	23%	
	c. Eyeballing first and if borderline between grades, manual counting on a printed image	22%	
	d. Manual counting at the microscope only	23%	
	e. Manual counting on a printed /computer image only	20%	
	f. Counting using computer software	5%	
When calculating Ki67 index, how many cells do you include in your denominator?	a. Exactly 500	14%	No significant difference based on practice patterns
	b. Exactly 2000	3%	
	c. 500 to 1000	26%	
	d.1000 to 2000	13%	
	e. Whatever number is in my field of vision / the photograph	18%	
	f. Whatever number is in my field of vision / the photograph, but if < 500, add in another field	26%	
When counting Ki67 index, what is your criterion for calling a cell positive? (**Figure 1**)	a. Dense dark diffuse nuclear staining (i.e. A’s in the figure)	23%	- Academic pathologists preferred response “c” (p=0.001) - Private practitioners preferred response “b” (p=0.001)
	b. At least convincing moderate nuclear / nucleolar staining (i.e. A’s and B’s in the figure)	55%	
	c. Any evidence of nuclear / nucleolar staining, even if faint and/or spotty (i.e. A’s, B’s, and C’s in the figure)	22%	
A small bowel resection was received containing multiple discrete foci of well-differentiated neuroendocrine tumor within the bowel wall. Which primary tumor do you stain for Ki67? (**Check all that apply)**	a. All foci	19%	- Academic (p=0.033), GI (P=0.007), and European (p<0.001) pathologists preferred response “a” - American pathologists preferred response “c” (p=0.006)
	b. Largest focus	24%	
	c. Most mitotically active focus	61%	
	d. Focus with highest T-category stage	20%	
A small bowel resection containing one primary well-differentiated neuroendocrine tumor with lymph node and liver metastases was received. Which tissue do you stain for Ki67? (**Check all that apply)**	a. The small bowel primary	89%	- GI (p<0.001) and European (p=0.007) pathologists more often included response “c.” - Academic (p=0.049) and GI (p=0.013) pathologists more often ordered 2 stains (compared to 1 stain).
	b. The lymph node metastases	21%	
	c. The liver metastases	46%	
For mesenteric tumor deposits ≤2 cm (i.e., not used in AJCC staging) encountered during segmental resection of small bowel for a well-differentiated neuroendocrine tumor, do you add an additional comment	a. Yes, only regarding their presence	77%	- North American pathologists preferred response “a” (p=0.019)
	b. Yes, regarding both their presence and prognosis	16%	
	c. No	7%	
	d. No to Ki67 stain, no to synoptic report	4%	

about their presence and/or prognosis?			
Would you call this figure a positive lymph node or a mesenteric tumor deposit (**Figure 2**)?	a. Positive lymph node	35%	No significant difference based on practice patterns
	b. Mesenteric tumor deposit	65%	
You receive a pancreatic resection that contains a low-grade well-differentiated neuroendocrine tumor. Do you perform stains to assess for hormone production by the tumor (insulin, glucagon, somatostatin, etc.)?	a. Yes, always	9%	- Private practitioners (p<0.001), general pathologists (p<0.001), and non-Europeans and Non-American pathologists (p<0.001) preferred response "c" - European pathologists (p<0.001) and pathologists with >10 years of experience (p=0.005) preferred response "a" - North American pathologists (p<0.001) preferred response "b"
	b. No, no added value	23%	
	c. No, stains not available at our institution	37%	
	d. Sometimes, if the clinical team asks	19%	
	e. Sometimes, if there is a known clinical hormone syndrome	12%	
In the pancreas, do you use immunohistochemical stains (e.g., p53, Rb) to distinguish grade 3 well-differentiated neuroendocrine tumors from poorly differentiated neuroendocrine carcinomas?	a. Yes, always	2%	- European pathologists preferred response "a" (p<0.05)
	b. Yes, but only on difficult cases	32%	
	c. No, only H&E histology	14%	
	d. No, only H&E histology and Ki67 index	39%	
You receive a gastric corpus biopsy from a patient with a known history of atrophic autoimmune gastritis. It lacks oxyntic mucosa and shows intestinal metaplasia. There are no gross or microscopic masses. Do you perform a neuroendocrine stain to evaluate for neuroendocrine hyperplasia/dysplasia?	a. Yes	56%	- Academic pathologists (p=0.002), GI pathologists (p=.024), and European pathologists (p<0.001) preferred response "a"
	b. No	44%	
Do you attempt to classify gastric neuroendocrine tumors into types 1, 2, and 3 in your report?	a. Yes	54%	No significant difference based on practice patterns
	b. No	46%	

Figure 1 - 438

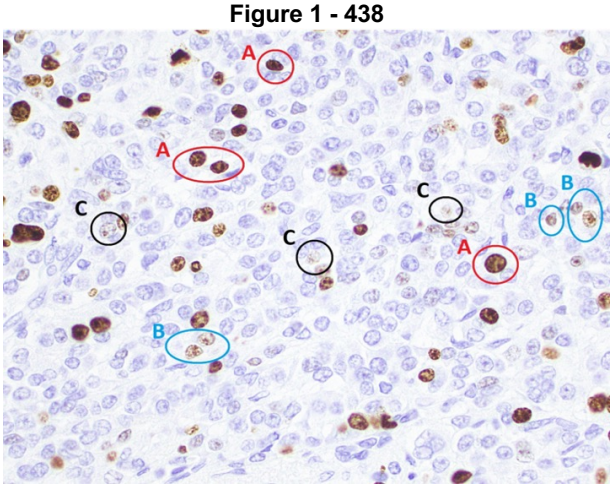

Figure 2 - 438

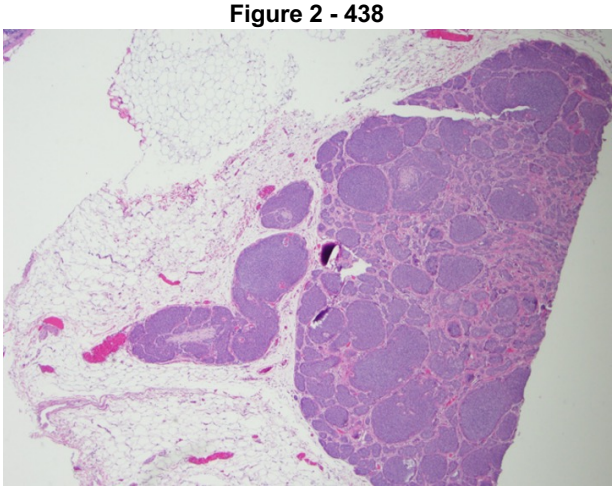

Conclusions: There exist many scenarios wherein pathologist practice patterns vary in evaluating digestive system NENs, sometimes despite recommendations in the literature. However, there were also certain common scenarios (e.g., number of tumor foci to be stained for Ki67 in case of multiple or metastatic NENs) where pathologists used varying judgement, as there remain no clear guidelines. This survey highlights key gray areas in digestive system NEN evaluation where more studies would be helpful to ensure consistency in work-up and diagnosis.

439 Distribution and Significance of T cell Phenotypes in Immune Microenvironment of Esophageal Adenocarcinoma and Barrett's Esophagus

Isha Khanduri[1], Arlene Correa[1], Renganayaki Krishnaramanujam[1], Riham Katkhuda[2], Anuj Verma[3], Alicia Mejia[1], Zhimin Tong[1], Akash Mitra[4], Luisa Solis Soto[1], Ignacio Wistuba[1], Wayne Hofstetter[1], Edwin Parra[1], Dipen Maru[1]
[1]The University of Texas MD Anderson Cancer Center, Houston, TX, [2]University of Chicago Medical Center, Chicago, IL, [3]Yale School of Medicine, New Haven, CT, [4]Guardant Health, Redwood City, CA

Disclosures: Isha Khanduri: None; Arlene Correa: None; Renganayaki Krishnaramanujam: None; Riham Katkhuda: None; Anuj Verma: None; Alicia Mejia: None; Zhimin Tong: None; Akash Mitra: *Employee*, Guardant Health; *Stock Ownership*, Guardant Health; Luisa Solis Soto: None; Ignacio Wistuba: *Advisory Board Member*, Genentech/Roche, Bayer, Bristol-Myers Squibb, AstraZeneca, Pfizer, HTG Molecular, Merck, GlaxoSmithKline; *Consultant*, Flame; *Advisory Board Member*, Novartis, Sanofi, Daiichi Sankyo, Amgen, Oncocyte; *Speaker*, Platform Health, AstraZeneca, Genentech/Roche; *Grant or Research Support*, Genentech, HTG Molecular, Merck, Bristol-Myers Squibb, Medimmune/Astra Zeneca, Adaptimmune, Adaptive, EMD Serono, Pfizer, Takeda, Amgen, Karus, Johnson & Johnson, Bayer, Iovance, 4D, Novartis, Akoya; Wayne Hofstetter: None; Edwin Parra: None; Dipen Maru: None

Background: T cell composition of immune microenvironment of esophageal adenocarcinoma (EAC) in comparison to Barrett's esophagus (BE) and in the context of clinicopathologic features and patient outcome is unknown. The aim of this study was to analyze costimulatory, coinhibitory, regulatory and activation T cell subtypes in EAC and BE using multiplex immunofluorescence (mIF) platform and correlate them with clinicopathologic features.

Design: mIF was performed on a tissue microarray (TMA) of EAC samples from 54 patients (M:F;6.7:1, median age: 65 years) who underwent esophagogastrectomy without neoadjuvant therapy and on a separate TMA with matched non dysplastic BE from 21 patients. The mIF markers were grouped into two panels: panel 1 for T cell activation and regulation: pan cytokeratin, CD3, CD8, CD45RO, Granzyme B, and FOXP3 and panel 2 for T cell costimulatory and inhibitory immune checkpoint markers: pan cytokeratin, CD3, TIM3, LAG3, VISTA, ICOS and OX40. Image analysis software (InForm) was used to segment each tissue core into intraepithelial and stromal compartments. This software identifies each cell separately for one of the phenotypes. To obtain co-expression of markers (cell phenotypes), the individual markers analyzed from each panel using the x and y coordinates of each cell were merged with the phenoptr script from R Studio. Final report of cell phenotype density in the intraepithelial and stromal compartments was expressed as number of cells per mm^2.

Results: We observed higher densities of T cell phenotypes in EAC as compared to BE, predominantly in the stroma (Table 1). Higher densities of intraepithelial and stromal immunosuppressive T cell phenotypes, regulatory T cells and memory regulatory T cells, were identified in pT1 than pT2-4 EAC. Higher total T cells and regulatory T cells were observed in tumors without lymphovascular invasion. Only intraepithelial total T cells were significantly higher in node negative tumors (p=0.04) and there was no correlation of T cell distribution with tumor histologic grade. Higher than median intraepithelial and stromal T cell TIM3 expression was associated with shorter disease-free survival in univariate (Figure 1 and 2) and multivariate analysis.

	Intraepithelial			Stroma		
Cell subtype, mean (SD) n/mm²	**BE**	**EAC**	**p**	**BE**	**EAC**	**p**
T cells (CD3+)	182 (92)	223 (241)	0.5	460 (259)	1295 (1236)	**0.009**
Cytotoxic T cells (CD3+ CD8+)	37 (45)	47 (56)	0.5	34 (33)	191 (218)	**0.005**
Activated cytotoxic T cells (CD3+ CD8+ Granzyme B+)	4 (6)	2 (2)	**0.047**	4 (6)	7 (12)	0.256
Memory T cells (CD3+ CD45RO+)	26 (28)	49 (47)	0.084	83 (93)	523 (917)	**0.041**
Effector Memory T cells (CD3+ CD8+ CD45RO+)	7 (12)	9 (11)	0.3	9 (19)	88 (148)	**0.031**
Regulatory T cells (CD3+ FOXP3+ CD8-)	25 (19)	36 (48)	0.3	85 (67)	163 (161)	0.065
Memory Regulatory T cells (CD3+ FOXP3+ CD45RO+ CD8-)	4 (6)	17 (23)	**0.021**	14 (18)	97 (119)	**0.006**
TIM3 expressing T cells (CD3+ TIM3+)	5 (6)	5 (10)	0.8	8 (10)	25 (24)	**0.002**
LAG3 expressing T cells (CD3+ LAG3+)	91 (66)	119 (107)	0.3	214 (127)	869 (544)	**0.001**
VISTA expressing T cells (CD3+ VISTA+)	<1 (1)	<1 (1)	0.66	3 (4)	10 (18)	0.11
ICOS expressing T cells (CD3+ ICOS+)	15 (22)	23 (33)	0.28	64 (41)	170 (167)	**0.009**
OX40 expressing T cells	<1 (1)	<1 (1)	0.081	2 (3)	10 (18)	0.11

(CD3+ OX40+)						
Pathologic tumor stage						
Cell subtype	**pT1**	**pT2-4**	**p**	**pT1**	**pT2-4**	**p**
T cells	160 (171)	188 (196)	0.92	1435 (1144)	805 (825)	**0.008**
Memory T cells	40 (42)	41 (49)	0.88	595 (817)	271 (359)	**0.021**
Regulatory T cells	27 (32)	14 (32)	**0.002**	214 (209)	72 (77)	**0.001**
Memory Regulatory T cells	12 (18)	5 (13)	**0.016**	124 (141)	39 (54)	**0.003**
TIM3 expressing T cells	4 (9)	8 (11)	**0.019**	19 (22)	26 (35)	0.56
Lymphovascular invasion						
Cell subtype	**LVI+**	**LVI-**	**p**	**LVI+**	**LVI-**	**p**
T cells	134 (155)	239 (207)	**0.008**	1005 (1073)	1531 (1000)	**0.02**
Cytotoxic T cells	28 (40)	47 (61)	**0.04**	135 (147)	214 (240)	0.18
Memory T cells	32 (41)	10 (47)	0.05	401 (741)	595 (587)	**0.02**
Regulatory T cells	18 (31)	30 (36)	**0.01**	126 (174)	218 (190)	**0.01**
Memory Regulatory T cells	7 (13)	14 (22)	0.21	63 (96)	142 (148)	**0.002**

Figure 1 - 439

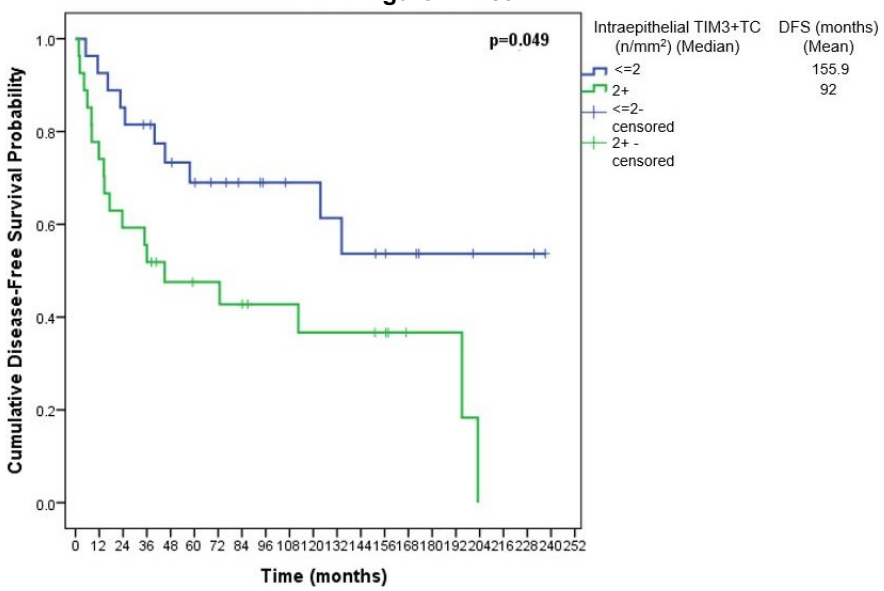

Figure 2 – 439

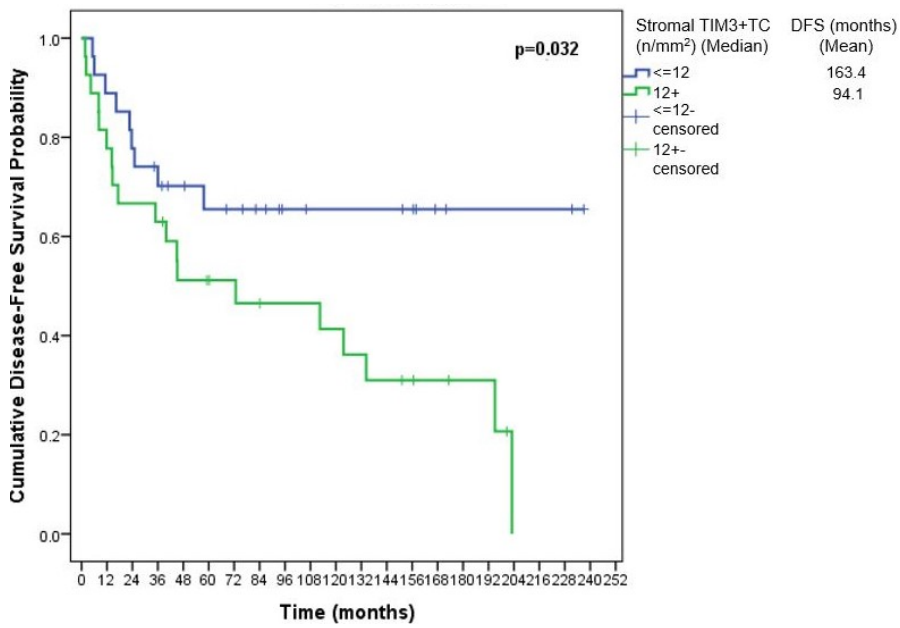

Conclusions: Compared to BE, there is increase in heterogenous T cell infiltrate in EAC, predominantly in the stroma. Higher T regulatory cells and memory regulatory T cells are associated with favorable histologic features and T cell TIM3 expression is a candidate marker of poor prognosis in EAC.

440 Patients with SM3-massive pT2 Gastric Cancer Have Worse Prognosis than Conventional pT2 Patients

Hyunjin Kim[1], Soomin Ahn[1], Kyoung-Mee Kim[1]
[1]Samsung Medical Center, Seoul, South Korea

Disclosures: Hyunjin Kim: None; Soomin Ahn: None; Kyoung-Mee Kim: None

Background: Submucosal massive and nodular growth pattern of invasion (SM3-massive) into the muscularis propria of the stomach have been described by the Japanese Gastroenterological Society. However, their clinical implications have not been reported due to their rarity. In this study, we collected 168 cases of SM3-massive gastric cancer and analyzed the prognostic significance.

Design: From the archive of pathologic reports at Department of Pathology and Translational Genomics of Samsung Medical Center in Seoul, Korea, we identified 1671 pT2 gastric carcinomas from March 2008 to May 2021. Out of 1671, we identified 168 SM3-massive cases and their survivals were compared to those of patients with conventional pT2 gastric cancer.

Results: In 168 SM3-massive gastric cancer patients, ages ranged from 35 to 93, with median age at 65. 117 cases (69.6%) were male, and 51 cases (30.4%) were female with median follow up period of 60 months. Six cases were N3 disease, 17 were N2, 41 were N1, and 104 (61.9%) were N0. Nine patients (5.36%) were dead 5 years after the diagnosis. In 1502 conventional pT2 patients, age ranged from 25 to 91, with median age at 62. Median follow up period was 60 months likewise. 87 cases were N3, 224 were N2, 343 were N1, and 848 (56.5%) were N0. 87 patients (5.8%) were dead at 5 years from diagnosis. When SM3-massive pT2 cases were compared to the conventional pT2 cases, survival difference was not observed. However, when patients under 60 years of age were separately analyzed, we found significant survival difference; unexpectedly, worse prognosis was found in SM3-massive gastric cancer patients compared to conventional pT2 patients ($p<0.001$).

Figure 1 - 440

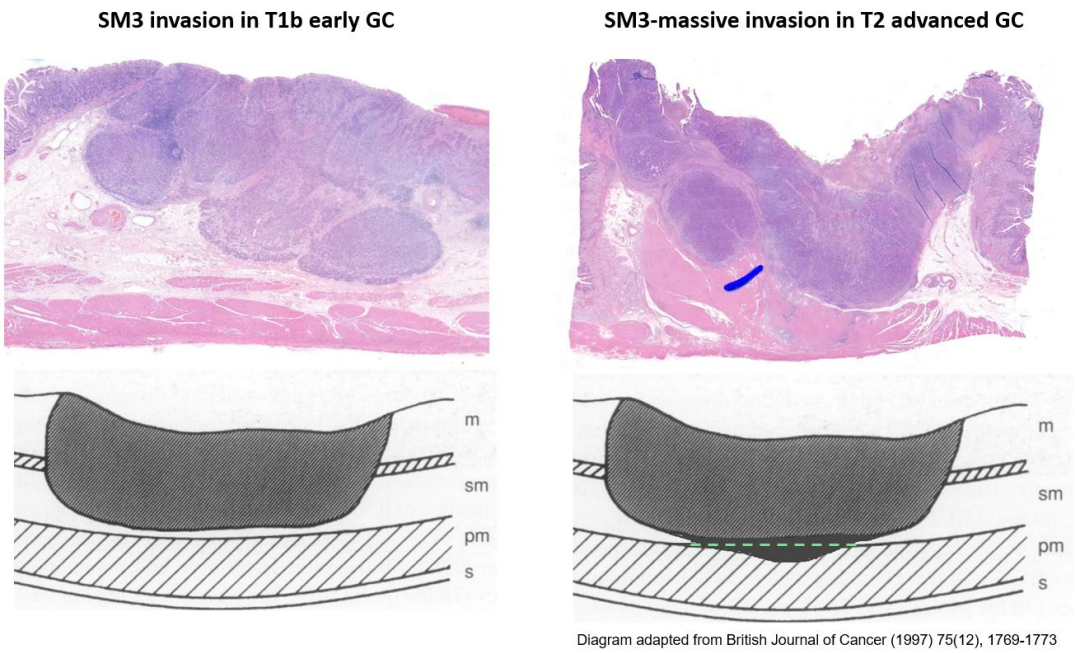

Diagram adapted from British Journal of Cancer (1997) 75(12), 1769-1773

Conclusions: SM3-massive gastric cancer is associated with worse prognosis in young pT2 gastric cancer patients.

441 Peritoneal seeding is more common in gastric cancer patients with FGFR2 amplification or high tumor mutation burden

Hyunjin Kim[1], Soomin Ahn[1], Kyoung-Mee Kim[1]
[1]Samsung Medical Center, Seoul, South Korea

Disclosures: Hyunjin Kim: None; Soomin Ahn: None; Kyoung-Mee Kim: None

Background: Fibroblast growth factor receptor (FGFR) translates downward signals for cell proliferation, migration, differentiation, and angiogenesis. Different genetic modifications were found in cancers of various organs. In particular, FGFR2 amplification has been identified in endometrial and gastric cancers (GC), and associated with poor prognosis. In GC, the incidence has been reported in 2-9%, and more frequently in the diffuse types. Moreover, it is associated with resistance to chemotherapy and sensitivity to FGFR-targeting tyrosine kinase inhibitors. Despite its clinical significance, FGFR2 amplification has not been studied with respect to peritoneal seeding, which is the most frequent mode of recurrence and metastasis associated with death in GC. We explored the association between the two factors.

Design: The results of mass parallel sequencing in 360 patients with advanced (stage III and IV) GC were reviewed. All patients received systemic chemotherapy at Samsung Medical Center from October 2019 to June 2021. Genomic profiling was done in the paraffin-embedded blocks with TruSight Oncology 500 (TSO500) panel and bioinformatics pipeline (Illumina, San Diego, CA, USA). Statistical analysis was performed using SPSS (Version 25.0; IBM, Armonk, NY, USA).

Results: In 360 cases, 222 (61.7%) were male, 246 (73.7%) were poorly differentiated, and 175 (48.6%) presented with peritoneal seeding. FGFR2 amplification was found in 26 (7.2%), where 14 (53.8%) were male and 22 (84.6%) poorly differentiated. Among the 26 FGFR2-amplified cases, 18 showed peritoneal seeding, and this association was statistically significant (18/26=69.2% versus 157/334=47%; p=0.023). At 95% confidence interval, the odds ratio (OR) was 2.54 (1.07-6.00). TMB-high cases were also statistically significant with p=0.028 and OR=1.83 (1.02-3.30). The difference in sex distribution was also significant with p<0.001. Due to the short follow-up period, prognostic significance was not evaluable.

		FGFR2 amplification		Total
		Pos	Neg	
Seeding	Pos	18	157	175
	Neg	8	177	185
Total		26	334	360

Conclusions: In patients with advanced GC, FGFR2 amplification, TMB-high, and female sex are more likely to develop peritoneal seeding.

442 Hypermucinous Dysplasia in Inflammatory Bowel Disease: A Heterogeneous Condition with Frequent Foveolar Differentiation

Bence Kővári[1], Till Clauditz[2], Katerina Kamaradova[3], Agnes Bathori[4], Fanni Hegedűs[1], Gregory Miller[5], Marcela Salomao[6], Anita Sejben[1], Magali Svrcek[7], Masato Yozu[8], Priyanthi Kumarasinghe[9], Rish Pai[6], Won-Tak Choi[10], Gregory Lauwers[11]
[1]University of Szeged Faculty of Medicine, Szeged, Hungary, [2]University Medical Center Hamburg-Eppendorf, Hamburg, Germany, [3]University Hospital and Faculty of Medicine Hradec Kralove, Charles University, Hradec Kralove, Czech Republic, [4]H. Lee Moffitt Cancer Center & Research Institute, Tampa, FL, [5]Envoi Specialist Pathologists, Brisbane, Australia, [6]Mayo Clinic, Scottsdale, AZ, [7]Sorbonne University, Assistance Publique Hôpitaux de Paris, Paris, France, [8]Middlemore Hospital, Auckland, New Zealand, [9]Queen Elizabeth II Medical Centre, Nedlands, Australia, [10]University of California, San Francisco, San Francisco, CA, [11]H. Lee Moffitt Cancer Center & Research Institute, University of South Florida, Tampa, FL

Disclosures: Bence Kővári: None; Till Clauditz: None; Katerina Kamaradova: None; Agnes Bathori: None; Fanni Hegedűs: None; Gregory Miller: None; Marcela Salomao: None; Anita Sejben: None; Magali Svrcek: None; Masato Yozu: None; Priyanthi Kumarasinghe: None; Rish Pai: *Consultant*, Alimentiv Inc, Allergan, Verily, Eli Lilly, AbbVie, PathAI; Won-Tak Choi: None; Gregory Lauwers: *Consultant*, ALIMENTIV, Inc

Background: Several types of non-conventional dysplasia (NCD) have been associated with inflammatory bowel disease (IBD). To date, some of their morphologic and clinicopathologic characteristics have yet to be elucidated. Hypermucinous dysplasia shows a

tubulovillous/villous architecture with mild nuclear atypia and prominent mucinous differentiation. Recently, we observed that hypermucinous dysplasia can demonstrate foveolar differentiation and may be surrounded by mucosal foveolar metaplasia, a recently reported feature of chronicity in IBD.

Design: A series of hypermucinous lesions from 64 IBD patients from 10 institutions were analyzed, including 49 lesions classified as hypermucinous dysplasia and 19 non-dysplastic mucinous proliferative lesions [NDMPL] (i.e., mucinous proliferative lesions not fulfilling all criteria of hypermucinous dysplasia). The phenotype of mucinous differentiation was evaluated in all cases. Intestinal differentiation was characterized by the presence of back-to-back goblet cells, whereas foveolar differentiation was defined by the presence of a supranuclear mucin cap. The presence, location, and phenotype of concurrent adenocarcinoma, conventional dysplasia, and other NCD types (if present) were also documented.

Results: Among the 49 hypermucinous dysplasia lesions, 19 (39%) showed intestinal, 6 (12%) foveolar, and 24 (49%) mixed differentiation. Concurrent adenocarcinoma was noted in 25 (51%) cases (16 mucinous, including 12 with at least focal foveolar differentiation and 9 non-mucinous). Coexisting non-hypermucinous dysplasia was present in 33 (67%) cases, including 15 conventional, 9 NCD, and 9 mixed (conventional and NCD) dysplasias. In the NDMPL category (n=19), 8 (42%) demonstrated intestinal, 7 (37%) foveolar, and 4 (21%) mixed phenotypes. Furthermore, when available for review, the adjacent mucosa of all but one case of foveolar hypermucinous dysplasia lesions showed a spectrum of non-dysplastic lesions with a foveolar phenotype including NDMPL (n=4) and foveolar metaplasia (n=5).

Conclusions: Our results highlight the heterogeneous nature of IBD-related hypermucinous dysplasia, with intestinal, foveolar, or mixed differentiation. The recent description of non-neoplastic mucinous lesions such as foveolar metaplasia can lead to diagnostic confusion. Awareness of a spectrum (i.e., from metaplastic to dysplastic) of hypermucinous lesions with foveolar differentiation in IBD may increase their detection and help determine their biological potential.

443 Modified Ulcerative Colitis Activity Scoring Methods Offer Good Reproducibility in Grading the Severity of Immune Checkpoint Inhibitors Colitis

Bence Kővári[1], Rish Pai[2], Barbara Centeno[3], Won-Tak Choi[4], Zhiyan Fu[3], Masoumeh Ghayouri[3], Kun Jiang[3], Yukihiro Nakanishi[3], Michael Vieth[5], Gregory Lauwers[6]

[1]University of Szeged Faculty of Medicine, Szeged, Hungary, [2]Mayo Clinic, Scottsdale, AZ, [3]H. Lee Moffitt Cancer Center & Research Institute, Tampa, FL, [4]University of California, San Francisco, San Francisco, CA, [5]Institut fur Pathologie, Bayreuth, Germany, [6]H. Lee Moffitt Cancer Center & Research Institute, University of South Florida, Tampa, FL

Disclosures: Bence Kővári: None; Rish Pai: *Consultant*, Alimentiv Inc; *Consultant*, Allergan; *Consultant*, Verily; *Consultant*, Eli Lilly; *Consultant*, AbbVie; *Consultant*, PathAI; Barbara Centeno: None; Won-Tak Choi: None; Zhiyan Fu: None; Masoumeh Ghayouri: None; Kun Jiang: None; Yukihiro Nakanishi: None; Michael Vieth: None; Gregory Lauwers: *Consultant*, ALIMENTIV, Inc

Background: Colitis is a common complication of immune checkpoint inhibitors (ICI). Recently, histologic activity grading using the Robarts histopathological index (RHI), an index developed for ulcerative colitis (UC), has been reported as an independent predictor of adverse clinical outcomes in ICI patients. However, RHI might be overly complex for daily clinical use. The aim of this study was to modify two simpler activity scoring methods originally developed for the assessment of UC and investigate their feasibility and reproducibility in evaluating ICI colitis.

Design: The cohort included 40 patients with ICI colitis. Biopsies were evaluated for various histologic features: active inflammation, chronicity features, and apoptotic injury. All the cases were independently reviewed and assessed by a total of 10 gastrointestinal pathologists from 4 institutions. For each case, the disease activity was assessed using a modified version of the Nancy and Erlangen DCA (D=distribution; C=chronicity; A=activity) activity scores, both originally developed for UC. To increase uniformity, all the participants were provided with illustrative diagrams of the modified Nancy and Erlangen scoring systems (i.e., taking the presence of apoptotic bodies and withering crypts into account as part of active injury). Interobserver agreement for both scoring systems was measured using Cohen's kappa.

Results: The average weighted kappa for all raters was 0.65 (moderate agreement) for the Nancy scoring system. Regarding the Erlangen DCA scoring system, interobserver agreement was first evaluated separately for each of the 3 parameters, resulting in only weak agreement among the 10 raters with average weighted kappa coefficients of D: 0.42, C: 0.46, and A: 0.48. However, the kappa coefficient for the average of all 3 parameters yielded a higher average weighted kappa of 0.67 (moderate agreement).

Conclusions: The modified Nancy and Erlangen DCA histologic indexes can provide simple and reproducible scoring of ICI colitis activity.

444 Pediatric Crohn's disease: Histologic Findings at Initial Presentation

Melanie Kwan[1], M Lisa Zhang[1], Jess Kaplan[1], Christopher Moran[1], Deepa Patil[2], Vikram Deshpande[3], Smiljana Spasic[1]
[1]Massachusetts General Hospital, Boston, MA, [2]Brigham and Women's Hospital, Harvard Medical School, Boston, MA, [3]Massachusetts General Hospital, Harvard Medical School, Boston, MA

Disclosures: Melanie Kwan: None; M Lisa Zhang: None; Jess Kaplan: None; Christopher Moran: None; Deepa Patil: None; Vikram Deshpande: None; Smiljana Spasic: None

Background: The histologic diagnosis of pediatric Crohn's disease (CD) can be challenging. This study evaluated the histological spectrum of treatment-naïve biopsies in a consecutive cohort of children with established CD and assessed the diagnostic and predictive value of these findings.

Design: Three cohorts were identified from prospective databases: 1) 138 patients with CD, 2) 116 patients with UC, and 3) 50 patients without inflammatory bowel disease (IBD) (control IBD cohort). Biopsies from the entire gastrointestinal tract were reassessed for active and chronic inflammation (including specifically lymphocyte-pattern esophagitis and focal enhancing gastritis) and histological changes of chronicity. We enumerated granulomas, microgranulomas (defined as a cluster of 4-9 epithelioid histiocytes), and giant cells.

Results: Lymphocyte-pattern esophagitis was noted in 15% (n=20) of esophageal biopsies while esophageal subepithelial chronic inflammation was identified in 10.5% (n=14) of cases. 68 gastric biopsies (50.4%) showed moderate to severe diffuse gastritis, while focal enhancing gastritis was noted in only 15 cases (11.1%). In terminal ileum biopsies, 56% showed activity while only 5.2% had features of chronicity. Active colitis was identified in 58% (n=80 cases) of cases while chronic colitis was observed in 11.7% of cases (n= 16). Granulomas and microgranulomas were seen in 27.7% and 43.4% of patients, respectively. Of these, 21 patients with microgranulomas lacked granulomas, and none of these microgranulomas were identified at the time of the original evaluation. Microgranulomas were identified in 2.5% of patients with UC and 0% of patients with clinically suspected IBD (control cohort). Lymphocyte-pattern esophagitis was identified in one UC patient. Lymphocyte-pattern esophagitis predicted need for anti-TNF therapy (p=0.03).

Conclusions: Gastrointestinal microgranulomas are frequently overlooked but are a specific and sensitive feature of CD. Esophageal lymphocytosis and subepithelial acute and chronic inflammation are additional features that discriminate between CD and UC. Esophageal lymphocytosis may predict more aggressive disease. We highlight some of the less emphasized features of CD including esophageal subepithelial inflammation, diffuse gastritis (as opposed to focal enhancing gastritis), the frequent lack of terminal ileitis, and the low incidence of chronic colitis in children with CD at initial biopsy.

445 Low Grade Appendiceal Mucinous Neoplasm (LAMN): The M Stage is a Significant Predictive Factor for Disease Recurrence, Irrespective of the T Stage

Whayoung Lee[1], Jack Guccione[2], Kapitolina Semenova[1], Cary Johnson[3], Xiaodong Li[1], Vishal Chandan[4]
[1]UCI Medical Center, Orange, CA, [2]UC Irvine Health, Orange, CA, [3]University of California, Irvine, Irvine, CA, [4]University of California, Irvine, Orange, CA

Disclosures: Whayoung Lee: None; Jack Guccione: None; Kapitolina Semenova: None; Cary Johnson: None; Xiaodong Li: None; Vishal Chandan: None

Background: Low-grade appendiceal mucinous neoplasm (LAMN) has been increasingly recognized in both appendectomy and pseudomyxoma peritonei (PMP) patients. The aim of this study was to determine the prognostic significance of the 8th edition AJCC staging system for LAMNs.

Design: All LAMN cases from 2000-2020 were reviewed and the diagnosis was confirmed using PSOGI criteria and re-staged according to AJCC 8th edition. Clinicopathologic data was collected from chart review. Each component was analyzed by Pearson correlation analysis.

Results: Total 60 cases of LAMN were identified (M:F 1:1.9, median age of 57.4 (ranges 29-82) years). 24 (40%) cases were confined to appendiceal muscularis propria (pTis), 8 (13.3%) cases had invasion into mesoappendix or subserosa (pT3), 23 (38.4%) cases had acellular mucin or epithelium on the serosa (pT4a), and 5 (8.3%) cases had direct invasion into adjacent structure (pT4b). PMP was identified in 21 (35%) cases; 6 cases with acellular mucin in the peritoneum (pM1a), 2 cases with epithelium in the peritoneum (pM1b), and 13 cases with other organs involvement (pM1c). Clinical follow up was available in 42 patients (average follow up 4.7 years). Of these, all the 24 cases (100%) without PMP (pM0) did not develop recurrent disease, regardless of T stage (15 pTis, 5 pT3, 2 pT4a, and 2 pT4b). In contrast, 15 out of 18 cases (83.3%) with initial presentation of PMP developed peritoneal or pleural recurrence within 5 years and 1 died from disease ($p<0.01$). The recurrence rate was not significantly different depending on T stage (16 pT4a v/s 2 pT4b) or M stage (5 pM1a v/s 13 pM1b/c), $p>0.05$.

Conclusions: Results of our study show that LAMN without peritoneal dissemination have a very low to negligible likelihood of peritoneal recurrence. Disease recurrence significantly correlates with the presence of PMP, indicating that M stage is a significant predictive factor of disease recurrence, irrespective of the T stage.

446 Presence of Clonal T-cell Receptor Gene Rearrangement is Specific for Refractory Celiac Disease Type 2

Hee Eun Lee[1], Rok Seon Choung[1], David Viswanatha[1], Joseph Murray[1], Tsung-Teh Wu[1]
[1]Mayo Clinic, Rochester, MN

Disclosures: Hee Eun Lee: None; Rok Seon Choung: None; David Viswanatha: None; Joseph Murray: None; Tsung-Teh Wu: None

Background: Refractory celiac disease type 2 (RCD2) is defined as RCD with presence of clonal T-cell populations of intraepithelial lymphocytes (IELs), which is demonstrated by an abnormal phenotype by immunostains and/or clonal T-cell receptor gene rearrangement (TCRGR). However, it has been reported TCRGR analysis is prone to false positivities. This study was aimed to evaluate the accuracy of TCRGR for the diagnosis of RCD2.

Design: Small bowel (SB) biopsies of CD patients on which TCRGR was performed were searched in surgical pathology files, and cases were classified as non-RCD, RCD1, and RCD2 after correlation with clinical presentation. Immunostains (CD3 and CD8) and TCRGR results were evaluated. Loss of CD8 expression in >50% of CD3+ IELs was considered an abnormal phenotype. TCRGR was interpreted as negative, equivocal, or positive for clonal TCRGR. As a control, initial and paired follow-up biopsies from 8 newly diagnosed CD patients; 5 duodenal biopsies with increased IELs associated with H. pylori (HP) gastritis; and 4 normal duodenal biopsies were included.

Results: Total 66 CD patients underwent TCRGR on SB biopsies, and 10, 15, and 41 were RCD2, RCD1, and non-RCD, respectively. In RCD2, 9 (90%) cases showed clonal TCRGR with a normal (n=7) or abnormal (n=2) phenotype of IELs and 1 (10%) showed equivocal clonal TCRGR with an abnormal phenotype. In RCD1, 4 (27%) and 11 (73%) cases showed equivocal and negative clonal TCRGR, respectively, all with a normal phenotype. In non-RCD, 32 (78%), 6 (15%), and 3 (7%) cases showed negative, equivocal, and positive clonal TCRGR, respectively, all with a normal phenotype. In 8 newly diagnosed CD patients, all initial and follow-up biopsies showed no clonal TCRGR with a normal phenotype. 5 duodenal biopsies with increased IELs associated with HP gastritis and 4 normal duodenal biopsies showed no clonal TCRGR in all but one case with HP gastritis had an equivocal result. Sensitivity and specificity of an abnormal phenotype of IELs for RCD2 were 30% and 100%, respectively, and those of clonal TCRGR were 90% and 96.3% when an equivocal result was considered negative.

Conclusions: Our study showed clonal TCRGR detected in our clinical laboratory is quite sensitive (90%) and specific (96.3%) for RCD2 and can be reliably used to detect clonal T-cell populations of IELs in patients with RCD. Discrepancy between the current and previous studies regarding its specificity might be due to difference in regions of TCR gene covered and interobserver variability.

447 Clinicopathologic Features of Patients with Sporadic and Syndromic Gastrointestinal Peutz-Jeghers Polyps

Bella Liu[1], Shengjie Cui[1], Nazire Albayrak[1], Swati Bhardwaj[1], Stephen Ward[1], Alexandros Polydorides[1]
[1]*Icahn School of Medicine at Mount Sinai, New York, NY*

Disclosures: Bella Liu: None; Shengjie Cui: None; Nazire Albayrak: None; Swati Bhardwaj: None; Stephen Ward: None; Alexandros Polydorides: None

Background: Peutz-Jeghers syndrome (PJS) is an autosomal dominant genetic disorder associated with *STK11/LKB1* mutations and characterized by gastrointestinal (GI) hamartomatous polyps, mucocutaneous pigmentation, and increased cancer risk. Histologically identical sporadic Peutz-Jeghers-type polyps (PJP) can also occur in patients without any PJS stigmata, but their significance and prognosis, particularly in terms of their malignant potential and in identifying new PJS probands, is still debated.

Design: We identified 98 cases with PJPs over 20 years (2001-2021) and reviewed patient demographics (including personal history of GI and other neoplasia) and polyp parameters (including number, size, location, and presence of metaplasia and/or dysplasia). Patients with PJS were defined as having 2 of the following: family history of PJS, mucocutaneous pigmentation, and any GI PJPs or, alternatively, as having 3 or more GI PJPs.

Results: As expected, compared to patients with sporadic PJPs, patients with PJS were significantly younger (37.9±20.3 vs. 55.3±14.8; p<.001) and had more (median number: 8 [IQR: 3.3-15.8] vs. 1 [IQR: 1-2]; p<.001) and larger (median size [cm]: 3.1 [IQR: 1.7-4.5] vs. 1.4 [IQR: 1.0-1.9]; p<.001) PJPs, that were more often small intestinal (76.7% vs. 29.4%; p<.001) and multifocal (40.0% vs. 0%; p<.001). Importantly, syndromic PJPs were more likely to show histologic metaplasia (16.7% vs. 4.4%; p=.055), which was most often gastric, and dysplasia (26.7% vs. 5.9%; p=.007), compared to sporadic PJPs. In multivariate analysis, PJS patients were more likely to present with additional GI (p=.019; OR: 12.6 [CI: 1.5-105.2]) and non-GI (p=.016; OR: 10.3 [CI: 1.5-68.9]) neoplasia. Relaxing the criteria for PJS by including patients with only 2 GI PJPs, revealed that sporadic solitary PJPs were still significantly less likely to contain dysplasia than syndromic PJPs (p=.009, OR: 18.5 [CI: 2.1-163.5]).

Conclusions: Regardless of the strictness of diagnostic criteria, sporadic PJPs remain clinicopathologically distinct from syndromic PJPs, particularly in terms of presenting in older patients, being smaller in size, and occurring in locations other than the small bowel. In addition, while sporadic PJPs can contain dysplasia and be associated with GI and other neoplasia, they do so at significantly lower rates compared to syndromic PJPs. Thus, sporadic PJPs may be less likely to identify syndrome patients or at least signal those with a forme fruste of PJS.

448 Extramammary Paget's Disease of the Esophagus: Clinicopathologic, Immunohistochemical and Molecular Features of 8 Cases

Xiaoqin Liu[1], Xiaoyan Liao[1], Dongwei Zhang[1]
[1]*University of Rochester Medical Center, Rochester, NY*

Disclosures: Xiaoqin Liu: None; Xiaoyan Liao: None; Dongwei Zhang: None

Background: Extramammary Paget's disease (EMPD) of the esophagus is a rare entity and may be indicative of an underlying malignancy. The aim of this study was to investigate the clinicopathologic, immunohistochemical and molecular features of EMPD of the esophagus.

Design: Eight cases of EMPD from the esophagus were identified from our institution between 2005-2021. Relevant clinical information was retrieved and analyzed.

Results: The cohort included 6 males and 2 females with a median age of 67 (range 52-85) years. Common clinical presentations included dysphagia and melena. Underlying invasive adenocarcinoma was identified in all 8 cases, and all (including the Paget cells) were located in the distal esophagus. Immunohistochemistry (IHC) showed that the Paget cells were universally positive for CK7, variably positive for CAM5.2, CK20, CDX2, GATA3, and CEA, but negative for p63, BRST2, and SOX10. Intracellular mucin was identified in 7 of 8 (87.5%) cases. The expression levels of epithelial marker E-cadherin and mesenchymal marker vimentin were compared between Paget cells and underlying adenocarcinoma cells. E-cadherin expression was retained in adenocarcinoma cells but partially lost (faint expression) in Paget cells in 6 of 7 (85.7%) cases, whereas vimentin expression was detected in Paget cells but not in adenocarcinoma cells in 6 of 7 (85.7%) cases. P53 overexpression was identified in 4 (50%) cases, positive PD-L1 (Combined Positive Score [CPS] ≥1) in 3 (37.5%) cases, and HER2 amplification in 2 (25%) cases. All adenocarcinomas showed

retained nuclear expression of mismatch repair proteins, suggestive mismatch repair proficiency. Lymph node and distant metastasis were present in 6 (75%) cases. Four patients received esophagectomy, and 4 patients received chemotherapy or chemoradiation therapy. After a median follow-up of 29 (range 5-43) months, 2 patients died of disease, 6 patients were still alive (median survival 36 months, range 5-43 months).

Conclusions: Esophageal EMPD is an aggressive disease frequently associated with underlying adenocarcinoma. CK7 and mucin stain are helpful in detecting the Paget cells. P53 overexpression, positive PD-L1, and HER2 amplification are not uncommon in the underlying adenocarcinoma. Partial E-cadherin expression loss and gained vimentin expression in Paget cells suggest a role of epithelium-mensenchymal-transition in the development of EMPD.

449 PD-L1 Immunohistochemical Comparability Multi-Institutional Study in Esophageal Squamous Cell Carcinoma

Yueping Liu[1], Xinran Wang[1], Jiankun He[1]
[1]The Fourth Hospital of Hebei Medical University, Shijiazhuang, China

Disclosures: Yueping Liu: None; Xinran Wang: None; Jiankun He: None

Background: Immunocheckpoint of PD-1/PD-L1 inhibitor treatment have shown promising clinical efficacy of patients with advanced esophageal squamous cell carcinoma(ESCC). Accurate assessment of PD-L1 as companion diagnosis is significantly important to screen patients for PD-1/PD-L1-targeted immunotherapy. Given real-world limitations in programmed death-ligand 1 (PD-L1) testing in ESCC, concordance studies between PD-L1 assays are needed. We firstly undertook comparisons of four PD-L1 assays (DAKO22C3, Ventana SP263, Ventana SP142, E1L3) among observers in ESCC and analyze reasons influencing consistency of PD-L1 interpretation.

Design: Paraffin embedded samples of 50 cases of esophageal squamous cell carcinoma from January 2019 to December 2019 were obtained, stained with all four PD-L1 assays (22C3, SP263, SP142 and E1L3). PD-L1 was evaluated by 68 pathologists who had received training from 19 different hospitals through whole slide image. PD-L1 expression was assessed for combined positive score(CPS) and the numbers of positive tumor cells (TCPS) and positive lymphocytes and macrophages (ICPS) were respectively interpreted.

Results: The expression sensitivity of SP263 was the highest in esophageal squamous cell carcinoma, followed by 22C3, E1L3 and SP142. Taking CPS 10 as the critical value, the overall consistency (OPA) of CPS scores of 22C3, SP263, SP142 and E1L3 in 68 doctors were 0.777 (0.773-0.780), 0.790 (0.786-0.793), 0.758 (0.754-0.762) and 0.782 (0.778-0.785), respectively. The overall consistency of the number of positive tumor cells was 0.799 (0.796-0.802), 0.762 (0.759-0.765), 0.845 (0.842-0.848) 0.857 (0.854-0.860), and the overall consistency rates of the number of positive immune cells were 0.609 (0.604-0.614), 0.578 (0.572-0.583), 0.628 (0.624-0.633) and 0.634 (0.630-0.639), respectively. The overall consistency rates of 22C3, SP263, SP142 and E1L3 CPS scores were 0.896 (0.882-0.910), 0.833 (0.813-0.853) and 0.853 (0.840-0.867), respectively. 22C3 and SP263 have high consistency, with OPA of 0.896, while E1L3 and SP142 have the highest consistency, with OPA of 0.908 (0.896-0.919).

Figure 1 - 449

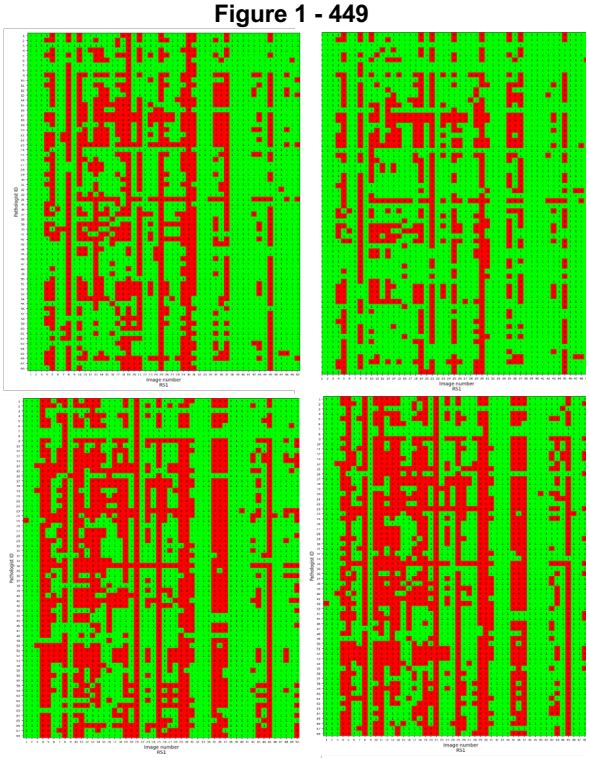

Figure 2 - 449

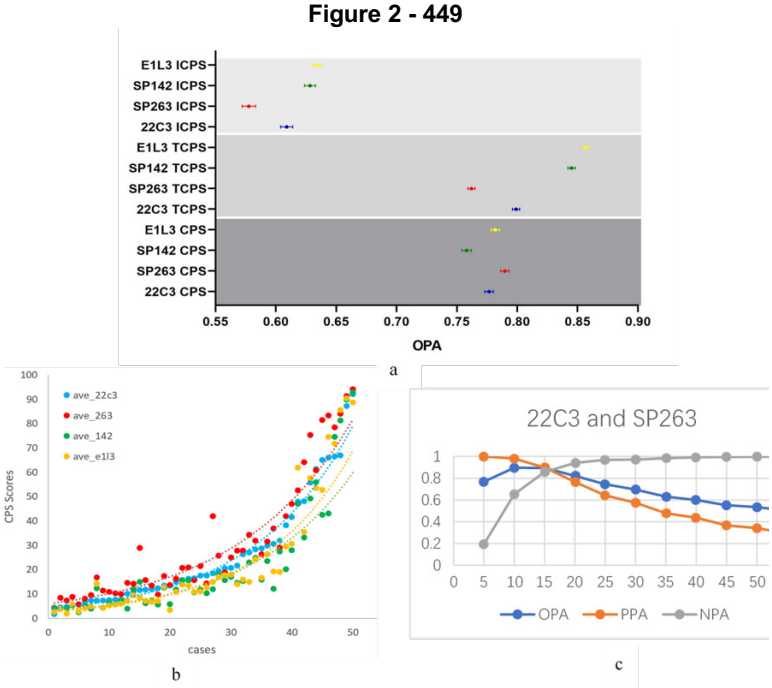

Conclusions: In esophageal squamous cell carcinoma, the consistency of PD-L1 evaluation among observers is good, and the immune cell score is still an important factor affecting the consistency of interpretation among observers. Cases near the specific threshold are still the difficult problem of interpretation. SP263 cannot identify all 22C3 positive cases.

450 Preoperative Prediction of Lymph Node Metastasis in Colorectal Cancer Through Multimodal Multiple Instance Learning

Hailing Liu[1], Yu Zhao[2], Fan Yang[3], Xiaoying Lou[4], Jianhua Yao[5], Xinjuan Fan[1]
[1]The Sixth Affiliated Hospital of Sun Yat-sen University, Guangzhou, China, [2]Technical University of Munich, Munich, Germany, [3]China, [4]The Six Affiliated Hospital of Sun Yat-sen University, Guangzhou, China, [5]Shenzhen, China

Disclosures: Hailing Liu: None; Yu Zhao: None; Fan Yang: None; Xiaoying Lou: None; Jianhua Yao: None; Xinjuan Fan: None

Background: Preoperative diagnosis of lymph node metastasis (LNM) status is essential for deciding treatment strategy for patients with colorectal cancer (CRC). Existing approaches for evaluating the LNM status based on preoperative radiology imaging or genomic tests are either unreliable or too costly. In the present study, we developed an artificial intelligence (AI) system to predict LNM status by integrating information of pathological images from colonoscopy biopsy and serum tumor-specific biomarkers.

Design: A total of 1338 patients with CRC from three hospitals were recruited in this study, among of them, 1128 patients from one center were designed as a discovery cohort and 210 patients from the other two centers as an external validation cohort. We developed a Multimodal Multiple Instance Learning (MMIL) model based on the deep neural network to learn latent features from whole-slide images (WSIs) and then jointly integrate the clinical biomarker features for predicting LNM status. The initial model was developed and validated in the discovery cohort and then tested in the external validation cohort. The heatmaps of the obtained MMIL model were constructed for model interpretation.

Results: The MMIL model outperformed preoperative CT imaging-based diagnosis and yielded high areas under the curve (AUCs) of 0.926 (95% CI: 0.864-0.988), 0.878 (95% CI: 0.824-0.933), 0.809 (95% CI: 0.775-0.843), and 0.857 (95% CI: 0.799-0.915) for patients with stage T1, T2, T3 and T4 CRC, respectively, in the discovery cohort. The model was further validated in the external cohort. It obtained AUCs of 0.855 (95% CI: 0.678-1.00), 0.832 (95% CI: 0.628-1.00), 0.691 (95% CI: 0.602-0.780) and 0.792 (95%

CI: 0.538-1.00) for stage T1, T2, T3 and T4, respectively, which indicates its prediction accuracy and potential adaptability among multiple centers.

Conclusions: Our MMIL model can effectively predict LNM by integrating H&E histology and tumor-specific biomarkers, which is ubiquitously available cross different institutes. Furthermore, we revealed the potential features that determined the LNM status in subregions of each WSI. These results indicate that the MMIL-based AI method could learn the latent specific histomorphologic features to determine LNM status. The findings could assist clinical professionals in the early diagnosis of LNM and potentially offers a time window for the early treatment of CRC patients.

451 Clinicopathologic Features of Non-Type 1 and Non-Type 2 Gastric Neuroendocrine Tumors and Their Associated Mucosal Changes

Kristen Logan[1], Chanjuan Shi[2]
[1]Duke University Health System, Durham, NC, [2]Duke University Medical Center, Raleigh, NC

Disclosures: Kristen Logan: None; Chanjuan Shi: None

Background: Gastric neuroendocrine tumors (NETs) are subclassified into 3 groups, each with distinct clinical, pathologic, and prognostic features. The pathogenesis underlying Type 1 and 2 gastric NETs is better understood than the “sporadic” type 3 NETs. Two additional provisional groups, type 4 (functional defective parietal cells with hypergastrinemia) and type 5 (PPI-associated), have recently been proposed. The aim of this study was to examine clinicopathologic features of non-type 1 and non-type 2 gastric NETs and their associated mucosal changes.

Design: A search of this institution’s archives for gastric NET from 04/2003 to 07/2021 was performed, excluding cases associated with atrophic gastritis or MEN1 syndrome. The medical records of all included cases were retrospectively reviewed. All H&E stained slides were reviewed for pathologic features and associated mucosal changes. Two-sample t tests and $\chi 2$ were used for statistical analysis.

Results: The cohort included 36 cases from 30 patients, which were assigned to Group 1 or Group 2. Group 1 (n=20) included patients with a history of proton pump inhibitor (PPI) use, and/or increased gastrin levels, and/or significant PPI effect on H&E slides. All other patients were assigned to Group 2 (n=10). Group 2 tumors were significantly larger (mean: 1.95 cm vs 1.04 cm, p= 0.013), occurred in younger (mean age: 53 vs 60) male patients (80% vs 55%), had a higher T stage, and more frequently developed metastases (30% vs 0%, p=0.029) than Group 1. Group 2 patients died from disease progression more frequently than Group 1 patients (20% vs 0%). Group 1 had 3 patients with cirrhosis, and they tended to have a larger tumor size than the non-cirrhotic Group 1 cases (mean: 1.63 cm vs 0.92 cm). Mucosa overlying and/or adjacent to tumor showed a loss of oxyntic glands in 21 (70%), foveolar hyperplasia in 22 (73.3%), and intestinal metaplasia in 8 (26.6%) of the total cases. In addition to PPI effect, atypical neuroendocrine hyperplasia in background oxyntic mucosa was present in 3/20 (15%) Group 1 patients.

Conclusions: Group 1, including provisional type 4 and type 5 gastric NETs, tended to be more indolent. Cirrhosis was associated with a larger tumor size in Group 1 patients. Associated mucosal changes included loss of oxyntic glands and intestinal metaplasia, which can mimic atrophic gastritis. Considering type 1 gastric NETs have a better prognosis than other subtypes, it is recommended that biopsies of background mucosa away from the mass are performed.

452 CXCR2 is Highly Expressed in Gastroenteropancreatic Neuroendocrine Tumors

Kristen Logan[1], Jiaoti Huang[2], Michael Morse[1], Chanjuan Shi[3]
[1]Duke University Health System, Durham, NC, [2]Duke University, Durham, NC, [3]Duke University Medical Center, Raleigh, NC

Disclosures: Kristen Logan: None; Jiaoti Huang: *Consultant*, Kingmed; *Advisory Board Member*, MoreHealth; *Advisory Board Member*, OptraScan; *Advisory Board Member*, Genetron; *Consultant*, Omnitura; *Consultant*, Vetonco; *Stock Ownership*, York Biotechnology; *Consultant*, Genecode, VIVA Biotech; *Stock Ownership*, Sisu Pharma; Michael Morse: None; Chanjuan Shi: None

Background: Chemokine receptor CXCR2 has been shown in several cancer types to play a key role in tumor development and progression. In addition, CXCR2 is a potential therapeutic target for some cancers, including hormone-resistant prostate cancers. Studies on the role of CXCR2 in gastroenteropancreatic neuroendocrine tumors (GEP-NETs) are limited. Our previous study

demonstrated heterogeneous expression of somatostatin receptor type 2, a molecular target for peptide receptor radionuclide therapy (PRRT) in treating GEP-NETs, which may contribute to the limited efficacy of PRRT. In this study, we explored the frequency and pattern of CXCR2 expression in GEP-NETs.

Design: De-identified tissue microarrays containing 68 pancreatic NETs and 15 small intestinal NETs (SI-NETs) as well as tumor sections from 37 gastric and 24 ampullary/duodenal NETs were immunohistochemically studied for the expression of CXCR2. The intensity of the immunostaining was scored as negative, weak, moderate, or strong, and the extent was graded as focal, patchy, or diffuse.

Results: Sixty-four of 68 (94.1%) PanNETs expressed CXCR2. Among them, 61 (95.3%) showed diffuse strong labeling, and 3 (4.7%) displayed weak and patchy staining. All 15 (100%) SI-NETs and 24 (100%) ampullary/duodenal NETs had diffuse strong CXCR2 expression. In addition, 28 of 37 (76%) gastric NETs showed CXCR2 expression, with 26 (96.4%) showing diffuse strong labeling and 1 (3.6%) displaying only weak expression. These included 9 of 14 (64.3%) type 1 and 19 of 23 (82.6%) non-type 1 gastric NETs. Strong CXCR2 expression was seen in islets cells of the pancreas and scattered neuroendocrine cells in intestinal and gastric mucosa. CXCR2 also highlighted enterochromaffin-like cell hyperplasia in atrophic gastritis. Interestingly, scattered positive cells were also present in duodenal Brunner glands adjacent to tumor. The expression of CXCR2 in GEP-NETs was mainly localized to the cell membrane of tumor cells (including apical and circumferential expression), with or without cytoplasmic staining.

Conclusions: CXCR2 expression in most GEP-NETs is homogeneously diffuse and strong. In addition to serving as a novel neuroendocrine marker, CXCR2 is a potential therapeutic target for GEP-NETs since clinical grade CXCR2 inhibitors have been used in clinical trials for various diseases.

453 Deep Learning Model for Predicting the Pathological Complete Response to Neoadjuvant Chemoradiotherapy of Locally Advanced Rectal Cancer

Xiaoying Lou[1], Niyun Zhou[2], Lili Feng[1], Zhenhui Li[3], Yuqi Fang[4], Xinjuan Fan[1], Hailing Liu[1], Jianhua Yao[2], Yan Huang[1]
[1]The Sixth Affiliated Hospital of Sun Yat-sen University, Guangzhou, China, [2]Shenzhen, China, [3]Yunnan Cancer Hospital, Kunming, China, [4]The Chinese University of Hong Kong, Hong Kong

Disclosures: Xiaoying Lou: None; Niyun Zhou: *Employee*, Tencent; Lili Feng: None; Zhenhui Li: None; Yuqi Fang: None; Xinjuan Fan: None; Hailing Liu: None; Jianhua Yao: None; Yan Huang: None

Background: Neoadjuvant chemoradiotherapy (nCRT) followed by total mesorectal excision (TME) is recommended as a standard treatment strategy for patients with locally advanced rectal cancer (LARC). The aim of the present study was to develop an artificial intelligence model for predicting the pathological complete response (pCR) to nCRT of LARC using digital pathological images.

Design: A total of 842 LARC patients treated with standard nCRT from three medical centers were retrospectively recruited and subgrouped into the training, testing and external validation sets. Treatment response was classified as pCR and non-pCR based on the pathological diagnosis after surgery as the ground truth. The hematoxylin & eosin (H&E)-stained biopsy slides were manually annotated and used to develop a deep pathological complete response (DeepPCR) prediction model by deep learning. In our study, four models, including the *hematology model*, *patch-based individual* model, *patch-based combined* model and DeepPCR model, were constructed based on clinical and pathological characteristics. Univariate and multivariate logistic regression analyses were performed and the area under the receiver operating characteristic curve (AUC-ROC) values of the prediction models were calculated to evaluate their predictive efficacy.

Results: Our results showed that the proposed DeepPCR model achieved an AUC-ROC of 0.710 (95% CI: 0.595, 0.808) in the testing cohort, which was significantly higher than that of the *hematology model* (AUC-ROC of 0.403, 95% CI: 0.274, 0.534; $P<0.001$), *patch-based individual* model (AUC-ROC of 0.544, 95% CI: 0.432, 0.653; $P<0.001$), and *patch-based combined* model (AUC-ROC of 0.627, 95% CI: 0.516, 0.733; $P<0.001$). Similarly, in the external validation cohort, the DeepPCR model achieved an AUC-ROC of 0.723 (95% CI: 0.591, 0.844). The sensitivity and specificity of the DeepPCR model were 72.6% and 46.9% in the testing set and 72.5% and 62.7% in the external validation cohort, respectively. Multivariate logistic regression analysis showed that the output of the DeepPCR model was an independent predictive factor of nCRT ($P=0.008$ and $P=0.004$ for the testing set and external validation set, respectively).

Table 1. Results of DeepPCR and the comparative models in the (a) primary and (b) external validation cohorts. The CI value is inside the parentheses. Sen: sensitivity; Spe: specificity; PPV: positive predictive value; NPV: negative predictive value. In this

work, we used a probability threshold of 0.7 (that is, any patient with a pCR prediction probability greater than 0.7 was reported as a pCR candidate).

(a) Model/Outcome	AUC-ROC	AUC-PR	Sen (%)	Spe (%)	PPV (%)	NPV (%)
Hematology model	0.403 (0.274, 0.534)	0.698 (0.591, 0.805)	72.6 (64.1, 80.3)	27.2 (18.8, 36.2)	61.7 (60.0, 71.1)	37.7 (30.8, 51.2)
Patch-based individual model	0.544 (0.432, 0.653)	0.805 (0.717, 0.885)	68.4 (59.8, 76.9)	25.8 (17.0, 34.7)	57.2 (45.2, 69.6)	27.0 (15.4, 46.8)
Patch-based combined model	0.627 (0.516, 0.733)	0.842 (0.762, 0.909)	69.2 (60.7, 77.8)	30.4 (20.7, 40.7)	61.6 (50.5, 73.1)	37.6 (18.0, 59.4)
DeepPCR model	0.710 (0.595, 0.808)	0.875 (0.795, 0.935)	72.6 (64.1, 80.3)	46.9 (32.6, 61.0)	70.4 (61, 79.9)	54.0 (35.8, 70.9)
(b) Model/Outcome	**AUC-ROC**	**AUC-PR**	**Sen (%)**	**Spe (%)**	**PPV (%)**	**NPV (%)**
Hematology model	0.420 (0.293, 0.548)	0.737 (0.623, 0.846)	70.6 (61.8, 79.4)	21. 7 (14.2, 30.0)	57.4 (48.5, 67.4)	17.6 (14.3, 20.4)
Patch-based individual model	0.527 (0.402, 0.657)	0.810 (0.712, 0.895)	73.5 (64.7, 81.4)	22.6 (15.3, 31.4)	57.9 (62.6, 72.4)	17.8 (17.4, 18.1)
Patch-based combined model	0.599 (0.474, 0.726)	0.832 (0.732, 0.919)	69.6 (60.8, 78.4)	27.2 (16.3, 38)	62.3 (49.9, 74.5)	31.7 (14.8, 54.1)
DeepPCR model	0.723 (0.591, 0.844)	0.887 (0.805, 0.949)	72.5 (63.7, 81.4)	62.7 (46.3, 77.3)	75.8 (67.1, 84.7)	53.6 (36.8, 68.8)

Conclusions: The DeepPCR model showed high accuracy in predicting pCR and served as an independent predictive factor for pCR. The model can be used to assist in clinical treatment decision making before surgery for LARC.

454 Early Lesions Seen in Colonoscopic Surveillance Biopsies Prior to Development of Colorectal Carcinomas in Patients with Inflammatory Bowel Disease (IBD) are Often Not Overtly Dysplastic

James Malleis[1], Konstantin Koro[2], Jose Ferraz[2], Scott Lee[3], Xianyong (Sean) Gui[4]
[1]University of Washington, Seattle, WA, [2]University of Calgary, Calgary, Canada, [3]University of Washington School of Medicine, Seattle, WA, [4]University of Washington Medical Center, Seattle, WA

Disclosures: James Malleis: None; Konstantin Koro: None; Jose Ferraz: None; Scott Lee: None; Xianyong (Sean) Gui: None

Background: Colonoscopic surveillance for neoplasia in patients with long-standing IBD has been a standard practice. However, failure of early detection of precursors and prevention of carcinoma development is not uncommon in those who comply to surveillance, which raises question about the effectiveness of current surveillance and whether some lesions shown in prior biopsies escaped from our attention.

Design: We retrieved 91 patients (M 67/F24, 33-94 yo, UC 59/CD 32, 5-20 ys of disease) with IBD-CRC encountered at 2 institutions in the USA and Canada over the past 20 years. Their entire pathology records of CRC resections and prior colonoscopic biopsies were reviewed. 40 patients who had ≥1 colonoscopies performed >1 year prior to cancer diagnosis were regarded as "*surveillanced*" (SURV), and 51 patients who had no prior biopsy as "*non-surveillanced*" (NSURV). The reported characteristics of CRCs and findings in all biopsies were analyzed, focusing on the nonreactive changes/lesions detected in bowel region(s) corresponding to carcinoma site(s) for each patient.

Results: In the SURV group, tumors were significantly smaller and less deeply invasive, with more T2 and less T3 ($p < 0.05$) but similar N stage as compared to NSURV. 73% of SURV patients had at least 1 lesion in prior biopsies (×1-15), in which 33 lesions were firstly identified in the region where CRCs developed 49.7±48.4 mons later ('*index lesions*'), and 32 lesions found lastly in the same areas at 36.1±44.4 mons prior to CRC diagnosis ('*latest lesions*'). The detection rate of index lesion was 80% for all SURV patients and, on average, 1.14 lesions per carcinoma within the positive SURV subgroup. Of the index lesions, 37% were conventional low-grade dysplasia (LGD), 33% indefinite for dysplasia (IND), 27% inflammatory polyp (IP), and 3% serrated epithelial change (SEC, including some called as hyperplastic polyp). Of the latest lesions, 38% were LGD, 34% IND, 19% IP, and 9% SEC. Additional and similar lesions were also seen in adjacent and distant regions.

Conclusions: In patients who had surveillance, IBD-CRCs were diagnosed at an earlier stage, and precancerous lesions were detected by endoscopic biopsies in >70% of patients. Among lesions found previously in the same area where CRCs developed, >60% were not overtly dysplastic and were described as IND, IP and SEC, which in retrospect may at least partly represent newly recognized nonconventional dysplastic lesions.

455 POLE and POLD1 Variant Detection: Potential Immune-Checkpoint Inhibitor Biomarker

Sepideh Besharati[1], Ladan Fazlollahi[2], Helen Remotti[1]
[1]Columbia University Medical Center, New York, NY, [2]New York-Presbyterian/Columbia University Medical Center, New York, NY

Disclosures: Sepideh Besharati: None; Ladan Fazlollahi: None; Helen Remotti: None

Background: Mutation in DNA polymerase epsilon (POLE) and delta 1(POLD1) genes has been shown as a useful marker for selecting patients who could benefit from check point inhibitor therapy in malignant neoplasms such as colorectal cancer (CRC).

Design: In this study we analyzed a real-world data set of 33 patients with nonsynonymous mutations of POLE/POLD1 between Jan 1, 2020 and June 30, 2021. Additional collected data included type of cancer, type of mutated gene, gene alteration significance, microsatellite instability status (stable (MSS) vs unstable (MSI)) and programmed cell death ligand-1 (PD-L1) immunostaining, if it was performed. PDL-1- Tumor proportion score (TPS) is calculated as the number of positive tumor cells divided by the total number of viable tumor cells multiplied by 100%; PDL-1-combined positive score(CPS) as the number of positive tumor cells, lymphocytes and macrophages, divided by the total number of viable tumor cells multiplied by 100.

Results: Distribution of POLE and POLD1 mutations identified in different cancer types in this cohort is shown in figure 1. Among 8 CRC cases, POLE and POLD1 genes were detected in 4(50%) and 3(37.5%) of patients respectively and one case (12.5%) had a variant in both POLE&POLD1 genes. Four CRC cases (50%) were MSS and had POLE variants with predicted pathologic alteration. Other than CRC, only hepatocellular carcinoma (2/2) and cholangiocarcinoma (1/3) cases had POLE variants with predicted pathologic alteration. The remaining tumors had POLE variants of uncertain significance (VOUS). All POLD1 mutations in cholangiocarcinoma tumors (3/3) and 1 of 3 POLD1 mutations in CRC cases were variants with predicted pathologic alteration. MSI was detected in 7 of 27 tumors (26%). PD-L1 immunostain data was available on 9 cases with positive staining in 7 cases. Esophagogastric tumors (2/2) had high PD-L1 with CPS >50. The two lung tumors (2/2) had PD-L1 TPS of 90% and 95%.

Figure 1 - 455

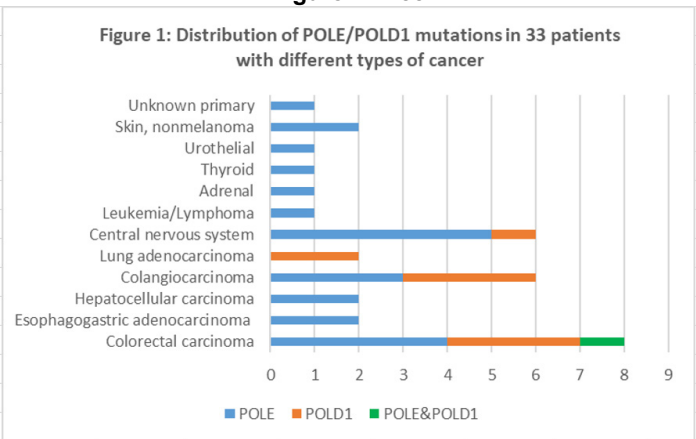

Conclusions: The most common tumors identified in our cohort include CRC and cholangiocarcinomas which in our institution undergo reflex MSI testing; additional testing of POLD1 and POLE variants may detect several additional tumors annually that would potentially qualify for immune check point inhibitors therapy. This is a pilot study based on clinically available data in this small cohort; there appears to be increased PD-L1 immunoreactivity and higher percentage of MSI (26%) in tumors with POLE and POLD1 mutations.

456 Loss of Mismatch Repair Protein Expression Occurs in Lynch Syndrome-Associated Gastric Polyps That Harbor Dysplasia and Rarely in Normal Gastric Pit Epithelium

Tiffany Miller[1], Paige Parrack[1], Dan Feldman[2], Daniel Chung[2], Matthew Yurgelun[3], Vikram Deshpande[4], Deepa Patil[5]
[1]Brigham and Women's Hospital, Boston, MA, [2]Massachusetts General Hospital, Boston, MA, [3]Dana-Farber Cancer Institute, Boston, MA, [4]Massachusetts General Hospital, Harvard Medical School, Boston, MA, [5]Brigham and Women's Hospital, Harvard Medical School, Boston, MA

Disclosures: Tiffany Miller: None; Paige Parrack: None; Dan Feldman: None; Daniel Chung: None; Matthew Yurgelun: None; Vikram Deshpande: None; Deepa Patil: None

Background: The incidence of gastric cancer in Lynch syndrome (LS) patients ranges from 0.3 - 3%. Unlike colorectal cancer where there is abundant data on loss of mismatch repair (MMR) proteins in precursor lesions, gastric polyps in LS patients are morphologically heterogeneous, and there is limited data on MMR immunohistochemistry (IHC). The aim of our study was to explore MMR protein expression in gastric polyps and adenocarcinoma (ADCA) identified during routine screening.

Design: Eighty-four polyps (157 procedures) and 4 gastrectomies from 32 patients were identified from LS registry and pathology databases at two academic centers. Demographics, genotype, endoscopy findings, polyp subtype, grade, and type of cancer were recorded. The presence or absence of MMR protein expression was assessed in lesional cells and normal epithelium, when available.

Results: The mean age of patients (7 M, 25 F) was 57 yrs (range: 33-86). Most (37%) harbored MSH2 mutation, followed by MSH6 (19%), MLH1 (25%), and PMS2 (16%). One patient had pathogenic mutations in both PMS2 and MSH6(3%). Of the 84 polyps, 63 (75%) showed intact MMR expression. All remaining 21 (25%) polyps with dysplasia or ADCA demonstrated MMR protein loss specific for the patients' known germline mutation within the lesional epithelium, including 7/7 HPs with dysplasia (6 low grade, 1 high grade), 3/3 foveolar adenomas, 4/4 mixed polyps (2 low-grade, 2 high-grade), 7/7 ADCAs. All 5 non-dysplastic HPs and 63 fundic gland polyps (FGPs) showed intact staining, including 11 FGPSs from the patient with PMS2 and MSH6 mutation. MSH2 mutations accounted for the majority (19/21) of dysplastic cases, including all HPs with dysplasia, foveolar adenomas, mixed polyps, IMC, and 4/6 ADCAs. The remaining 2 ADCAs occurred in MLH1 mutation carriers and showed MLH1 loss. Within two resections with ADCA (1 MSH2 loss, 1 MLH1 loss), there were multiple small intestinal-type adenomas with MMR loss. One of these specimens also showed multifocal aggregates (average of 4-5 glands) of normal pit epithelium with loss of MMR protein expression.

Conclusions: In our cohort, all FGPs and HPs without dysplasia had intact MMR expression, while only those polyps with dysplasia and ADCA had diffuse loss of MMR protein expression. Most dysplastic lesions and ADCAs were identified in patients with MSH2 mutations. Identification of MMR-deficient normal gastric pits may represent an early detectable marker of LS, which requires further exploration.

457 Pagetoid Spread of Esophageal Squamous Cell Carcinoma and Esophageal Adenocarcinoma: A Clinical and Histopathologic Comparison

Tiffany Miller[1], Xuchen Zhang[2], Huaibin Mabel Ko[3], Stephen Lagana[3], Namrata Setia[4], Lindsay Yassan[4], Maria Westerhoff[5], Mark Redston[1], Lei Zhao[6]
[1]Brigham and Women's Hospital, Boston, MA, [2]Yale School of Medicine, New Haven, CT, [3]New York-Presbyterian/Columbia University Medical Center, New York, NY, [4]University of Chicago, Chicago, IL, [5]University of Michigan, Ann Arbor, MI, [6]Brigham and Women's Hospital, Harvard Medical School, Boston, MA

Disclosures: Tiffany Miller: None; Xuchen Zhang: None; Huaibin Mabel Ko: None; Stephen Lagana: *Consultant*, GATT Technologies; *Consultant*, Organ Recovery Systems; *Stock Ownership*, Doc Vita; *Consultant*, SpringTide Ventures; *Stock Ownership*, Biotech stocks: BFLY, DNA, EDIT, GH, NAUT, QSI; Namrata Setia: None; Lindsay Yassan: None; Maria Westerhoff: None; Mark Redston: None; Lei Zhao: None

Background: Pagetoid spread in esophageal squamous epithelium associated with underlying esophageal adenocarcinoma (EAC) have been well studied. Case reports describing pagetoid spread of esophageal squamous cell carcinomas (ESCC) also exist in the literature. The latter, however, has not been systematically studied. In this study, we report three cases of pagetoid spread associated with ESCC. The clinical, morphologic and immunophenotypic profiles of pagetoid spread in the context ESCC and EAC are compared.

Design: Cases of pagetoid cells associated with ESCC and EAC were identified through systematic search of pathology archives at five institutions. Clinical history was collected via chart review. H&E slides of all cases were reviewed. Immunostains including CK7, CK20, CDX-2, P53, CAM5.2, P63, P40, CEA and GCDFP-15 were performed on selected cases.

Results: Two of the three index cases of pagetoid spread associated with ESCC had both in situ and invasive ESCC. A third case had in situ disease only. The tumors were located in the mid (2patients) or distal esophagus (1 patient). The pagetoid tumor cells (Figure) were focal in one case and diffuse/multifocal in two other cases. They demonstrated enlarged, hyperchromatic nuclei with variable amounts of eosinophilic cytoplasm. The cytoplasm was often condensed to the perinuclear area, creating peripheral clearing. By immunohistochemistry, the pagetoid cells were positive for CK5/6, CAM5.2, P40, P63; and negative for CEA, CDX2 and GCDFP-15. They also showed immunoreactivity to CK7 in one of two cases tested. One of the patients had pagetoid tumor cells on the resection margin and subsequently had recurrent disease 2 years later. Two other patients had negative resection margins and did not have recurrent disease. Four cases of pagetoid spread in the context of EAC were used as a comparison group. These tumors were all located in distal the esophagus or GE junction. All cases were associated with underlying invasive EAC. Pagetoid spread associated with EAC often had cytoplasmic vacuoles or mucin. They were positive for CK7, and negative for P40, P63 and CDX-2.

Figure 1 - 457

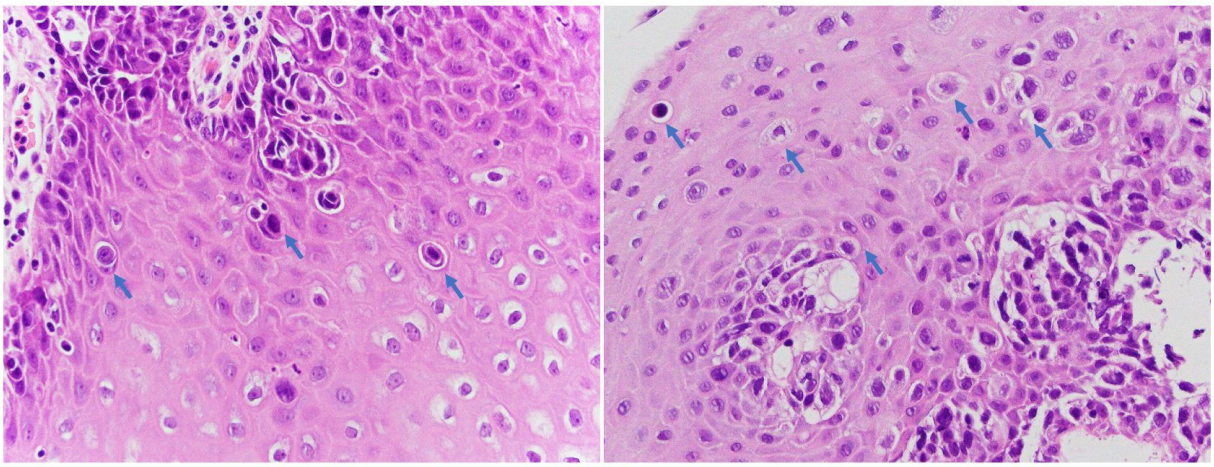

Conclusions: Both ESCC and EAC may give rise to pagetoid spread of tumor cells within surface squamous epithelium. Pagetoid cells from ESCC and EAC have overlapping histologic and immunohistochemical profiles. Understanding their overlapping pathologic features will help pathologists avoid pitfalls and diagnose these lesions correctly on biopsy specimens.

458 How Do Clinicians Handle New Diagnoses of Unsuspected Autoimmune Gastritis?

Maria Mostyka[1], Rhonda Yantiss[2]
[1]New York-Presbyterian/Weill Cornell Medical Center, New York, NY, [2]Weill Cornell Medicine, New York, NY

Disclosures: Maria Mostyka: None; Rhonda Yantiss: None

Background: Autoimmune gastritis is an immune-mediated condition affecting the body/fundus. It may present with iron deficiency or pernicious anemia and is often accompanied by other autoimmune diseases, as well as autoantibodies to H+/K+ ATPase and/or intrinsic factor. Patients with extensive intestinal metaplasia are at increased risk for post-inflammatory adenocarcinoma. Low-quality data suggest risk may be higher for incomplete intestinal metaplasia. Thus, some clinicians ask pathologists to subclassify intestinal metaplasia whenever it is encountered. However, we have noted that many patients with newly diagnosed autoimmune gastritis do not undergo surveillance. We performed this study to determine the nature and frequency of clinical assessment following an initial diagnosis of autoimmune gastritis.

Design: We identified 300 patients with newly diagnosed autoimmune gastritis defined by the presence of mononuclear cell-rich inflammation centered on oxyntic glands, oxyntic gland destruction, and antral sparing. Cases with concurrent dysplasia or adenocarcinoma were excluded, as were those undergoing surveillance for established autoimmune gastritis. Electronic medical records were reviewed for data regarding the indication for biopsy, surveillance endoscopy, and laboratory workup.

Results: There were 227 women and 73 men (mean age: 59 years) in the study group. Common indications for endoscopy included iron deficiency anemia (21%), dyspepsia (18%), and pain (15%). Post-biopsy evaluation of vitamin B12 levels, intrinsic and parietal antibody titers, and iron stores was performed in 228 (76%) cases; 99 (33%) patients received vitamin B12 therapy. Only 121 (40%) patients underwent endoscopic surveillance, including 40% (68/169) of patients with intestinal metaplasia and 40% (53/131) of patients without intestinal metaplasia (p=0.07). None of the patients developed dysplasia or adenocarcinoma during endoscopic surveillance (mean: 57 months, range: 6-167). No patients in the entire group developed signs or symptoms of adenocarcinoma during clinical follow-up (mean: 53 months, range: 0-167).

Figure 1 - 458

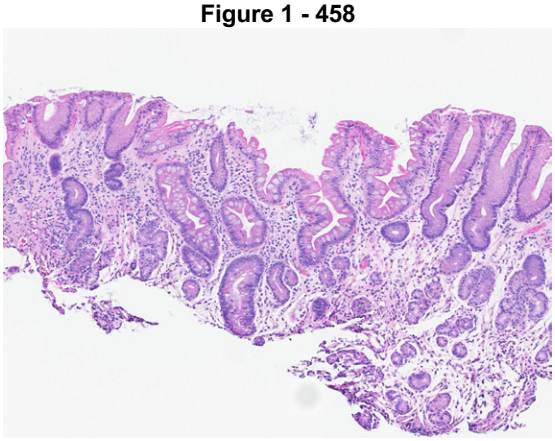

Figure 2 - 458

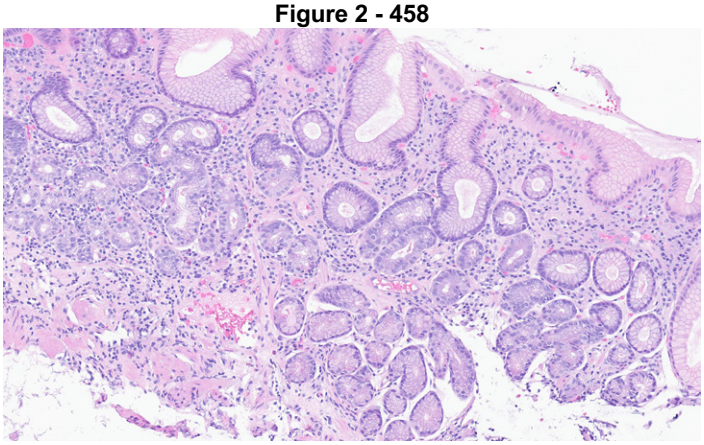

Conclusions: Many patients with clinically unsuspected autoimmune gastritis do not undergo surveillance endoscopy, even when intestinal metaplasia is extensive. Given the low risk of neoplasia and frequent lack of follow-up when intestinal metaplasia is detected, subtyping intestinal metaplasia has not yet been shown to be a clinically meaningful exercise.

459 Machine Learning-Based Quantitative Evaluation of Histological Disease Severity in Ulcerative Colitis

Fedaa Najdawi[1], Michael Drage[2], Kathleen Sucipto[1], Archit Khosla[1], Victoria Mountain[1], Stephanie Hennek[1], Ilan Wapinski[1], Richard Kinsey[3], Andy Beck[1], Murray Resnick[1]
[1]PathAI, Boston, MA, [2]PathAI, Rochester, NY, [3]Poplar Healthcare, Memphis, TN

Disclosures: Fedaa Najdawi: None; Michael Drage: *Employee*, PathAI; *Employee*, PathAI; Kathleen Sucipto: None; Archit Khosla: None; Victoria Mountain: *Employee*, PathAI; *Employee*, PathAI; Stephanie Hennek: *Employee*, PathAI, Ultivue; Ilan Wapinski: *Employee*, PathAI; Richard Kinsey: None; Andy Beck: *Employee*, PathAI; Murray Resnick: *Employee*, PathAI

Background: Emerging evidence supports the adoption of histologic improvement as a therapeutic goal and clinical trial endpoint for patients with ulcerative colitis (UC), including reports that show relapse has been associated with residual histologic disease activity in patients who achieved endoscopic endpoints.

Here we show sensitive and reproducible machine learning (ML)-based pixel-level identification and quantification of histological features of UC, and concordance with expert manual pathologist scoring of disease severity.

Design: ML models, based on convolutional neural networks, were trained to predict histologic features and generate quantitative, slide-level read-outs using 368 whole-slide images (WSI) of hematoxylin and eosin (H&E) stained biopsies (N=133 cases) covering the spectrum of disease severity in UC. WSI included >130k region- and point-based annotations indicating relevant tissue (e.g., erosion/ulceration, crypt abscesses, epithelium with neutrophil infiltration, normal epithelium, granulation tissue, basal plasmacytosis) and cell (e.g., neutrophils, plasma cells, lymphocytes, and eosinophils) features. The models were applied to the validation and test set of 148 H&E images, and concordance with consensus expert manual pathologist scoring of UC (Nancy Histology Index, NHI) was evaluated using Spearman correlation and Wilcoxon rank sum test statistics.

Multivariate analysis was performed to predict the NHI using 16 selected histologic features. The best model, Random Forest classifier, was selected based on the performance of 4-fold cross validation measure by weighted kappa.

Results: ML-generated image overlays indicated the predictions of key UC histologic features at the pixel level (Figure1). ML quantitation of histological features that are indicative of chronicity or degree of disease activity correlated with consensus NHI score (Table1).

For the ML-prediction of NHI score, a Random Forest classifier model yielded a weighted kappa (k= 0.92) and Spearman correlation (ρ=0.94, p<0.001).

Table 1. ML Feature Correlation with Nancy Histologic Index

Histological feature name	Feature type	Spearman Correlation	p-value	Correlation
Mucosal epithelium with neutrophilic infiltration	Area proportion	0.78	<0.001	Grouped NHI scores (0-1 vs 2 vs 3-4)
Crypt abscess	Area proportion	0.80	<0.001	Grouped NHI scores (0-2 vs 3-4)
Mucosal epithelium with neutrophilic infiltration and crypt abscess combined	Area proportion	0.88	<0.001	Grouped NHI scores (0-1 vs 2 vs 3-4)
Goblet cell cytoplasm	Area proportion	-0.62	<0.001	Individual NHI score
Basal plasmacytosis	Area proportion	0.69	<0.001	Individual NHI score
Erosion/ulceration	Area proportion	0.70	<0.001	Grouped NHI scores (0-2 vs 3-4) Discriminated NHI score 3 vs 4
Granulation tissue	Area proportion	0.80	<0.001	Discriminated NHI score 3 vs 4
Neutrophils in tissue	Count proportion	0.79	<0.001	Individual NHI score
Neutrophil in epithelium	Cell density	0.58	<0.001	Individual NHI score
Neutrophils in lamina propria	Count proportion	0.66	<0.001	Individual NHI score
Neutrophil in lamina propria	Cell density	0.76	<0.001	Individual NHI score
Plasma cell	Count proportion	0.58	<0.001	Individual NHI score
Eosinophils	Count proportion	-0.10	0.215	Individual NHI score However, it discriminated NHI score 0 vs 1 (p=0.002)
Intraepithelial lymphocytes	Count proportion	0.32	<0.001	Individual NHI score
lymphocytes within lamina propria	Count proportion	0.01	0.897	Individual NHI score

Figure 1 - 459

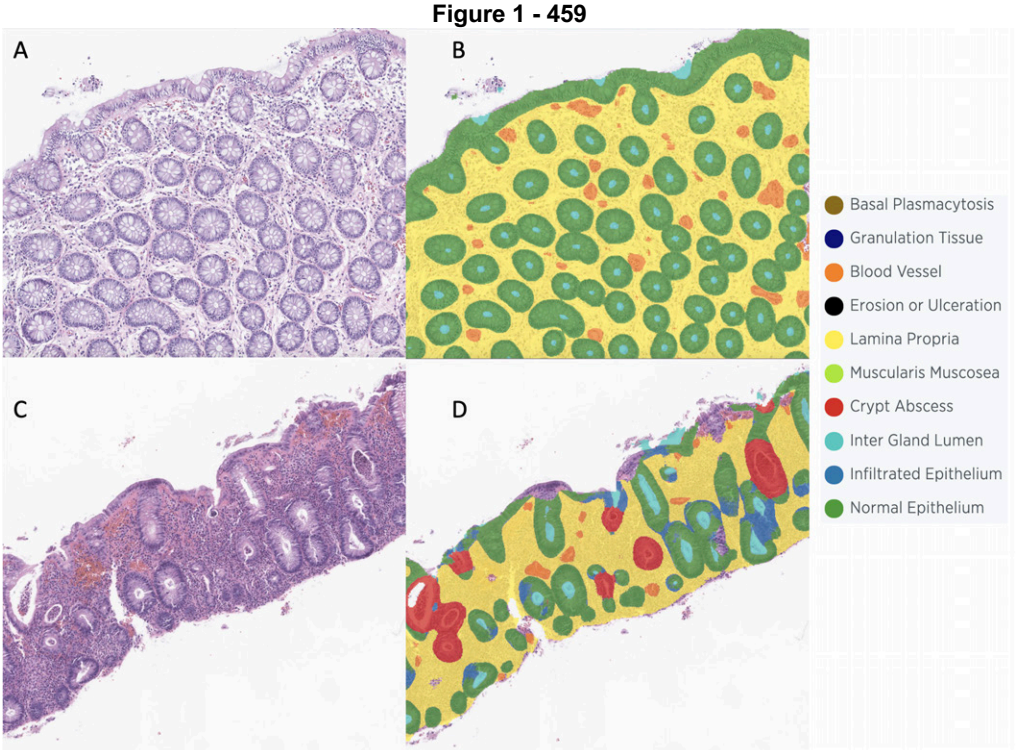

Figure 1. Representative fields from biopsies with corresponding ML tissue overlay. NHI score 0 (A/B) and NHI score 3 (C/D)

Conclusions: ML model predictions show high concordance with pathologist scoring of UC histological features and assessment of disease severity. This highlights the potential of a robust and reproducible ML-based image analysis for quantitative characterization of UC histology to better guide management decisions.

460 Altered Distribution of Duodenal Pou2F3 Positive Tuft Cells in Pediatric Patients with Celiac Disease

Mehran Najibi[1], Li Juan Wang[2], Paola Uriona Gamboa[3], Ripley Bassett[3], Yihong Wang[3], Evgeny Yakirevich[4]
[1]Brown University, Rhode Island Hospital, Lifespan, Providence, RI, [2]Alpert Medical School of Brown University, Providence, RI, [3]Brown University, Rhode Island Hospital, Providence, RI, [4]Rhode Island Hospital, Providence, RI

Disclosures: Mehran Najibi: None; Li Juan Wang: None; Paola Uriona Gamboa: None; Ripley Bassett: None; Yihong Wang: None; Evgeny Yakirevich: None

Background: Tuft cells are unique chemosensory cells in the intestinal epithelium. Their function remained unclear until recent discoveries of their central role in intestinal immunity. POU domain, class 2, transcription factor 3 (Pou2F3) is the master regulator of tuft cells and its expression is restricted to tuft cells within the intestinal epithelium. In this study, we evaluated Pou2F3 IHC expression to investigate the role of this transcription factor and tuft cells in celiac disease (CD).

Design: Immunostains for Pou2F3 were performed on second portion, and duodenal bulb endoscopic biopsies from thirteen patients with CD, nine control patients (CT) with no significant pathological findings in duodenal biopsy, and ten patients with increased intraepithelial lymphocytes but no villous blunting (IEL). Pou2F3+ cells were counted in five high power fields with the most frequent positive cells, and the average numbers were used for statistical analysis.

Results: The average age of patients with CD was 11y (range: 2-16y; 4M, 9F), of CT group, 11y (range: 1-17y; 3M, 6F), of IEL, 13y (range: 12-15y; 3M, 7F). Among CD group four patients showed more severe villous blunting as compared to the other nine patients. Pou2F3 demonstrated nuclear staining with positive cells predominantly in crypt epithelium and only rare cells in villi. The number of Pou2F3+ cells was significantly lower in the duodenal bulb (8.9) as opposed to second portion of the duodenum (14.5) in CT group (p=0.008), but no significant difference was observed in the CD and IEL groups. The number of Pou2F3+ cells in second portion of the duodenum were significantly decreased in CD group (7.6) as compared to CT (14.5, p=0.002) and IEL groups (15.9, p=0.001) (Figure 1D). While not statistically significant, the average numbers in the duodenal bulb were also decreased in the CD group as opposed to other groups (Figure 1A-C). CD patients with more severe villous blunting showed significant reduction in Pou2F3+ cells in duodenal bulb as compared to CD patients with less severe villous blunting (p=0.006), and CT group (p=0.009) (Figure 1E).

Figure 1 - 460

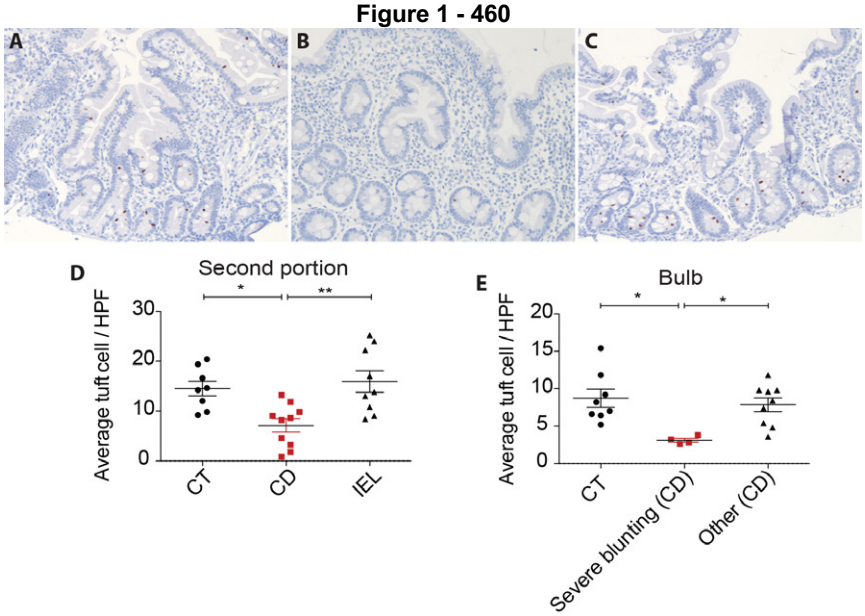

Conclusions: The number of Pou2F3+ tuft cells showed significant reduction in the duodenum of pediatric patients with CD. This reduction is associated with villous blunting, and patients with more severe blunting showed less tuft cells in their duodenum. These findings suggest the possible role of tuft cells and their distribution in CD and may help to further elucidate the pathogenesis of this disease.

461 Metastatic Endometrioid Adenocarcinoma to the GI tract: A Histologic and Immunohistochemical Review

Ilke Nalbantoglu[1], Natalia Buza[1]
[1]Yale School of Medicine, New Haven, CT

Disclosures: Ilke Nalbantoglu: None; Natalia Buza: None

Background: Cases of endometrioid adenocarcinoma metastatic to gastrointestinal (GI) tract with histologic features mimicking a GI tract primary have been described in the literature. Diagnosis can be challenging especially in biopsy (bx) samples. We studied the histologic and immunohistochemical (IHC) features of these tumors.

Design: All cases of endometrioid adenocarcinoma of ovarian and endometrial primary (1999-2021) with metastasis to GI tract were included and reviewed. Some of the histologic features included: site and depth of involvement, mucosal ulceration, mimicry of a GI primary, squamous differentiation, and dirty necrosis. IHC panel of CK7, CK20, PAX8, CDX2, SATB-2, and ER were performed. Cases with serous histology were excluded.

Results: 24 patients (pts) were included (18 endometrial, 6 ovarian primary). Average age: 64 (range 47-93). Average time to recurrence: 55 months (mos), range (0-191). Average follow-up: 93 mos, range (0.3-242). GI tract was involved more than once in 5 pts (21%), in another 5 pts (21%) the primary tumor and metastasis were diagnosed simultaneously. Most common site of involvement was rectosigmoid (22 pts, 92%). Most common symptom was rectal bleeding in 5 pts (21%).

Total of 40 samples, 35 resections (88%) and 5 bxs (12%) were reviewed. Mucosal involvement was seen in 60% (24/40), ulceration was present in 53% (21/40). 51% (18/35) of resections had transmural involvement. Squamous differentiation was identified in total of 16 (40%), “dirty necrosis” was noted in 24 (63%). In 10 samples (25%) the tumor was thought to have focal features resembling a GI primary: 4 with features similar to tubular adenoma, 6 to colon ca (Fig1A&B).

CK7 was positive (+) in 87% (20/23), PAX8 was (+) in 95% (21/22, focal & weak in 2). ER was (+) in 100% (22/22). CK20 was (+) in 2 (2/23, 8.6%) was focal, weak. CDX2 was negative in all (23). SATB2 was (+) in 3 (3/20, 15%), it was focal, weak in 2, and strong in 1 case of dedifferentiated ca (Fig 2A&B).

Figure 1 - 461

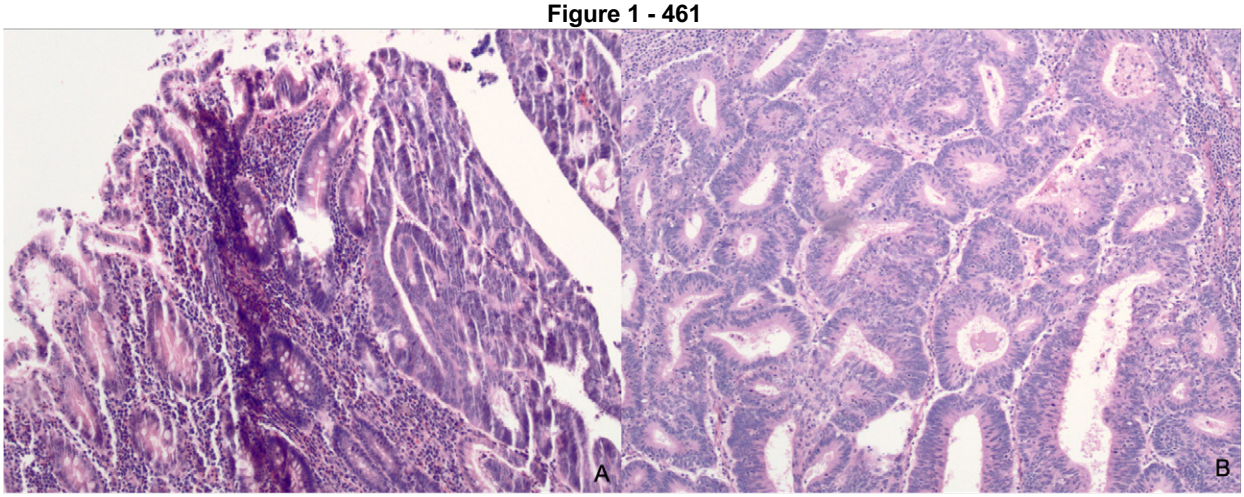

Figure 2 – 461

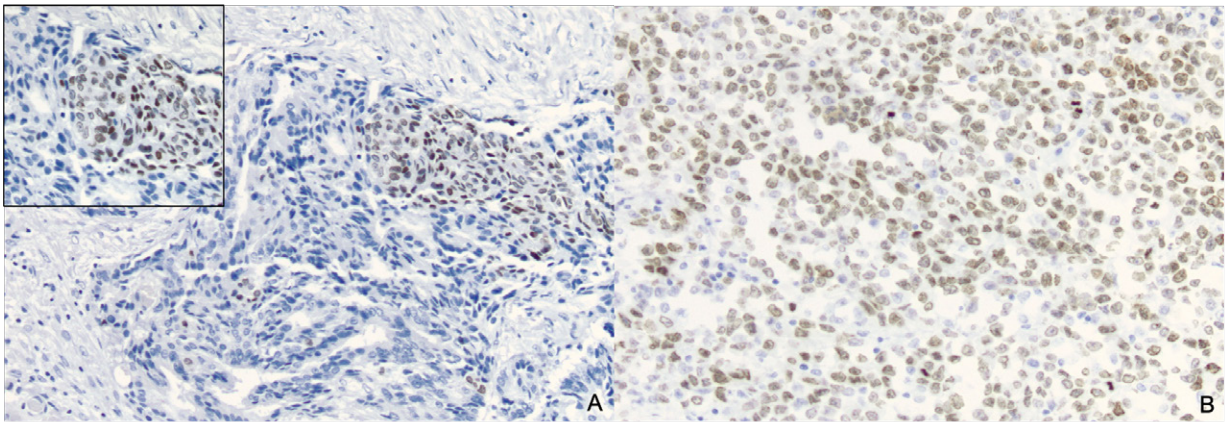

Conclusions: Diagnosis of metastatic endometrioid adenocarcinoma to GI tract can be challenging on bxs especially in pts with long period of remission or unknown clinical history. In our cohort, dirty necrosis, a feature shared by colorectal carcinoma was noted in 63% of all samples and can be misleading in pts with no prior history. Focal SATB2 (+) in a small subset of cases is also noteworthy and should be taken into account.

462 Spectrum of SMARCA4 Mutations in Esophagogastric Carcinomas: Molecular Analysis and Immunohistochemical Correlation

Alexander Neil[1], Fei Dong[1]
[1]Brigham and Women's Hospital, Boston, MA

Disclosures: Alexander Neil: None; Fei Dong: None

Background: SMARCA4 mutations have been described in a subset of undifferentiated esophagogastric carcinomas with aggressive clinical course. However, the full spectrum and overall frequency of SMARCA4 mutations in esophagogastric cancer and how those mutations relate to histologic and immunohistochemical findings remains poorly characterized.

Design: We interrogated our institutional database and identified 1174 esophagogastric carcinomas that underwent panel next generation sequencing. We interpreted the pathogenicity of SMARCA4 mutations, assessed histological features, and when possible, correlated SMARCA4 mutation with SMARCA4 protein expression by immunohistochemistry.

Results: SMARCA4 mutation was identified in carcinomas from 107 of 1174 patients (9.1%). Mutations from 41 of 107 (38%) were interpreted as pathogenic, based on published functional characterization of SMARCA4. 21 of 41 pathogenic variants were missense variants, and the others were truncating variants, including nonsense, frameshift, and splice site variants. 78% of carcinomas with pathogenic SMARCA4 mutation were poorly differentiated, with the rest being moderately differentiated. 31% of esophageal carcinomas with SMARCA4 pathogenic variants were associated with Barrett's esophagus. All 7 carcinomas with pathogenic SMARCA4 missense variants demonstrated retained SMARCA4 protein expression by immunohistochemistry, while 8 of 13 carcinomas with truncating SMARCA4 variants showed loss of SMARCA4 expression. Mutations involving genes implicated in esophagogastric cancer development, including TP53 (29/41; 71%) and ARID1A (13/41; 32%) , were often concurrently mutated in the SMARCA4-mutated cohort.

Conclusions: Pathogenic SMARCA4 mutations are identified in 3.5% of an unselected cohort of 1174 esophagogastric carcinomas. SMARCA4 mutations are observed in carcinomas with a spectrum of histological grade but are correlated with poor differentiation. Loss of SMARCA4 expression by immunohistochemistry is associated with pathogenic truncating mutations. These data demonstrate the wide spectrum of SMARCA4 mutations in esophagogastric cancers.

463 Increased Histologic Inflammation is an Independent Risk Factor for Non-Conventional Dysplasia in Ulcerative Colitis

Eric Nguyen[1], Dongliang Wang[2], Gregory Lauwers[3], Won-Tak Choi[1]
[1]University of California, San Francisco, San Francisco, CA, [2]SUNY Upstate Medical University, Syracuse, NY, [3]H. Lee Moffitt Cancer Center & Research Institute, University of South Florida, Tampa, FL

Disclosures: Eric Nguyen: *Stock Ownership*, Moderna, Inc.; Dongliang Wang: None; Gregory Lauwers: *Consultant*, ALIMENTIV, Inc; Won-Tak Choi: None

Background: Patients with ulcerative colitis (UC) are at increased risk of colorectal neoplasia. Several different types of non-conventional dysplasia (NCD) have been described in inflammatory bowel disease, and some of them appear to be more frequently associated with advanced neoplasia than conventional dysplasia (CD). Also, hypermucinous (HMD), goblet cell deficient (GCD), and crypt cell (CCD) dysplasias often have molecular features characteristic of advanced neoplasia (e.g. aneuploidy). This study aimed to investigate if increased inflammation is a risk factor for NCD.

Design: A cohort of 125 patients with UC-associated dysplasia were analyzed. Sixty-nine (55%) patients had CD only, while the remaining 56 (45%) patients had NCD, including 36 with high-risk NCD (HMD, GCD, CCD) and 20 with dysplasia with increased Paneth cell differentiation or traditional serrated adenoma-like dysplasia. Fifty control patients without neoplasia were also analyzed. For each patient, all biopsies prior to the detection of dysplasia were scored by using a 4-point scale (0, normal; 1, cryptitis; 2, crypt abscess; and 3, ulceration). Each biopsy was designated a score, and both mean and maximum scores for that colonoscopy were derived. Inflammation burden was calculated by multiplying average maximum score between each pair of surveillance episodes by length of surveillance interval in years. The average scores of all colonoscopies for each patient were used to calculate the overall mean, maximum, and inflammation burden scores. Adjusted odds ratios (OR) from multivariate logistic regressions were used to compare between dysplasia and control groups, CD and NCD, and CD and high-risk NCD.

Results: Higher maximum (OR 3.4, p=0.001) and inflammation burden (OR 4.2, p=0.014) scores were significantly associated with the detection of dysplasia. Similarly, higher mean and maximum scores increased the odds of NCD by 2.7 (p=0.020) and 4.9 (p=0.003), respectively. There was an even stronger association between these two scores and the risk of high-risk NCD (OR 4.0, p=0.008 and 7.5, p=0.006, respectively). Primary sclerosing cholangitis was also a risk factor for high-risk NCD (OR 6.4, p=0.036). Although higher inflammation burden showed a trend toward an increased risk (ORs 4.0 for NCD and 2.5 for high-risk NCD), it did not reach statistical significance.

Conclusions: The risk of NCD is significantly associated with increased inflammation, which may contribute to higher rates of aneuploidy and malignant transformation in NCD.

464 PD-L1 Scoring In Esophageal Cancers: Comparison of Immunohistochemistry and Multiplex Immunoprofile Assay

Igor Odintsov[1], Paige Parrack[1], Harvey Mamon[2], Peter Enzinger[2], Kee-Young Shin[3], Lei Zhao[4], Vikram Deshpande[5], Scott Rodig[1], Deepa Patil[4]
[1]Brigham and Women's Hospital, Boston, MA, [2]Brigham and Women's Hospital, Dana-Farber Cancer Institute, Harvard Medical School, Boston, MA, [3]Dana-Farber Cancer Institute, Boston, MA, [4]Brigham and Women's Hospital, Harvard Medical School, Boston, MA, [5]Massachusetts General Hospital, Harvard Medical School, Boston, MA

Disclosures: Igor Odintsov: None; Paige Parrack: None; Harvey Mamon: *Advisory Board Member*, Merck; Peter Enzinger: None; Kee-Young Shin: None; Lei Zhao: None; Vikram Deshpande: None; Scott Rodig: *Grant or Research Support*, Bristol Myers Squibb, Merck, Affimed; *Advisory Board Member*, Immunitas; *Grant or Research Support*, KITE/Gilead; Deepa Patil: None

Background: PD-L1 is a useful, yet imperfect, predictive biomarker of response to immunotherapy. Although immunohistochemistry (IHC) is widely used to determine treatment eligibility, the significant variability in sensitivity and reproducibility across assays and samples calls for a more standardized assessment. Multiplex immunofluorescence (mIF) assay identifies several markers on a single specimen and uses image analysis algorithms to generate biomarker scores based on cell density. The goal of our study was to compare PD-L1 IHC scores from esophageal cancer specimens with those generated by the mIF assay.

Design: Whole tissue sections from 87 specimens (86 patients; 70 adenocarcinoma, 8 squamous cell carcinoma) were analyzed by mIF using these markers: PD-L1, PD-1, CD8, FOXP3, cytokeratin and DAPI. IHC was performed on the corresponding specimens used for mIF assay in 50 cases. Combined Positive Score (CPS) ≥1 was considered positive.

Results: The mean age of cohort was 65 yr (range: 33-88; M:75, F:11). Of the 87 cases analyzed by mIF, there were 37 (42%) pre-treatment biopsies, 26 (30%) post-treatment resections and 24 (28%) metastases. Overall, PD-L1 positivity by mIF was seen in 70/87 (80%) cases. Among the 50 cases tested by both mIF and IHC, 40 (80%) were positive by mIF and 31 (62%) were IHC positive. Compared to mIF, a higher proportion of biopsies were positive by IHC (44% vs 62%), while more resections were positive by mIF compared to IHC (32% vs 19%). CPS scores were concordant in 33/50 (66%) cases with 27 positive and 6 negative cases. Among the 17 (34%) discordant cases, 13 were positive by mIF but IHC negative, and 4 were IHC positive but mIF negative. Most cases (11/13) that were PD-L1 IHC negative but positive by mIF were biopsies; the positive mIF CPS scores were due to more positive immune cells detected by the mMIF assay. Of the 4 IHC positive, mIF negative cases, 3 were biopsies with immune cell-only expression (CPS 1, 3 and 5) and one was an untreated pT1b resection (CPS 19).

Conclusions: Multiplex immunoflourescence assay had a higher rate of PD-L1 positivity compared to IHC, with a concordance rate of 66% between the two assays. Most discrepancies were seen in biopsy specimens from primary or metastatic location, with mIF assay detecting more immune cells compared to IHC. Multiplex immunoflourescence and digital image analysis is a feasible, precise, and quantitative approach for PD-L1 assessment but needs prospective clinical validation across all treatment settings.

465 Capecitabine Induced Gastrointestinal Injury Shows Graft Versus Host Disease (GVHD)-like pattern

Kenechukwu Ojukwu[1], Brian Cox[1], Brent Larson[1], Maha Guindi[1], Stacey Kim[1], Kevin Waters[1], Danielle Hutchings[1]
[1]Cedars-Sinai Medical Center, Los Angeles, CA

Disclosures: Kenechukwu Ojukwu: None; Brian Cox: None; Brent Larson: None; Maha Guindi: None; Stacey Kim: None; Kevin Waters: None; Danielle Hutchings: None

Background: Capecitabine is an orally administered pyrimidine analog prodrug of 5-fluorouracil (5-FU), commonly used in the treatment of various malignancies. Gastrointestinal (GI) side effects are clinically well known, however, there are only rare case reports describing the histopathologic features. Herein, we present the largest case series characterizing the histopathology of capecitabine-induced GI injury.

Design: A search of the departmental database (2011-2021) identified eight patients on capecitabine with GI biopsies. Clinical information was obtained from the electronic medical record. All available slides were reviewed for each patient.

Results: All patients were adults (median age 64.5 years, range 61-76) and there was gender parity. Patients were receiving treatment for malignancy of the colorectum (n=5), breast (n=1), pancreas (n=1), and appendix (n=1). All patients had GI symptoms, including seven with nausea, vomiting, diarrhea, and/or abdominal pain and one with melena. Five of eight (63%) showed graft-versus-host disease (GVHD)-like changes in small intestinal and/or colonic biopsies characterized by architectural distortion, crypt atrophy, regenerative epithelial changes, and increased crypt apoptosis in one or more specimens. Acute inflammation was minimal-mild, though rare crypt abscesses were seen in one case. All showed patchy prominence in lamina propria eosinophils. Endocrine cell aggregates were present in three of five cases. All had negative cytomegalovirus immunostains. One case showed a small intestinal biopsy with an ischemic injury pattern. This patient was receiving concomitant radiation. Two cases were normal. On follow-up, capecitabine was discontinued or dose-reduced in all patients. Three of five patients with a GVHD-like pattern had improvement of clinical symptoms, whereas two died shortly after biopsy. The patient with ischemic pattern showed improvement after drug discontinuation and radiation dose reduction. The two patients with normal biopsies improved symptomatically with dose reduction.

Conclusions: We report the largest case series describing the histopathology of capecitabine-induced GI injury. Capecitabine shows a GVHD-like pattern of injury in the small intestine and colon. One case showed an ischemic pattern, though this patient was also receiving radiation therapy. Patients improve clinically after discontinuation or dose reduction of the drug.

466 Comparison of Histologic Changes in Inflammatory Bowel Disease Patients With and Without Cytomegalovirus Infection: Crypt Abscesses are More Common in Noninfected Patients, While Apoptosis is Not a Helpful Feature

Yuho Ono[1], Raul Gonzalez[2]
[1]Beth Israel Deaconess Medical Center, Boston, MA, [2]Beth Israel Deaconess Medical Center, Harvard Medical School, Boston, MA

Disclosures: Yuho Ono: None; Raul Gonzalez: None

Background: Cytomegalovirus (CMV) colitis superimposed on inflammatory bowel disease (IBD) can be challenging to diagnose. While immunohistochemistry (IHC) is the gold standard for detecting CMV, staining may appear equivocal. Marked apoptosis is a hallmark of isolated CMV colitis but has not been evaluated in CMV complicating IBD. This study aimed to determine what histologic clues, if any, can help diagnose CMV superinfection in IBD.

Design: H&E and CMV IHC slides of colon biopsies were reviewed from all patients with CMV colitis (with and without IBD) between 2010 and 2021 at our institution. IBD patients with negative CMV IHC from 2020 and 2021 were also identified. Biopsies were assessed for architectural distortion, crypt dropout, lamina propria (LP) expansion, LP neutrophils, cryptitis, crypt abscesses, ulceration, Paneth cell metaplasia, phlebitis, fibrin thrombi, basal crypt apoptosis, CMV viral cytopathic effect (VCE), and CMV IHC positivity. Features between groups were compared, with statistical significance set at $P<0.05$. Cases with multiple concurrent biopsies were analyzed using cumulative findings.

Results: The study included 224 biopsies from 147 cases (22 CMV only, 47 CMV+IBD, 78 IBD only). Compared to the CMV group, the CMV+IBD group was significantly more likely to show distortion, dropout, LP expansion, cryptitis, ulceration, Paneth cell metaplasia, and phlebitis (Table). Compared to the IBD group, the CMV+IBD group was less likely to show crypt abscesses (77% vs. 56%, $P=0.016$). The CMV group was more likely to show ≥5 apoptotic bodies per high-power field compared to the CMV+IBD group (43% vs. 13%, $P=0.012$, Fig 1), but apoptosis was similar in CMV+IBD and IBD-only cases. CMV was detected by IHC in 21 CMV+IBD cases without VCE on H&E. Three of these showed equivocal IHC staining on a concurrent biopsy (Fig 2). Four additional CMV+IBD cases had a biopsy with equivocal IHC staining, one of which had a positive viral load and a concurrent biopsy with CMV VCE on H&E. In the 56 cases where IHC was performed on multiple concurrent biopsies, IHC was positive on at least one in 21, seven (33%) of which were positive in all biopsies. Eighteen (47%) CMV+IBD cases with positive CMV IHC showed VCE on H&E.

Table. Comparison of histologic features present in CMV, CMV+IBD, and IBD groups

	CMV-only				**CMV+IBD**				**IBD-only**			**CMV-only vs. CMV+IBD**	**IBD-only vs. CMV+IBD**
	(n=22)		n*		(n=47)		n*		(n=78)		n*	***P*-value**	***P*-value**
Distortion	7	33%	21		29	66%	44		57	74%	77	0.018	0.41
Dropout	8	38%	21		30	68%	44		41	54%	76	0.031	0.18
LP expansion	8	38%	21		43	96%	45		69	88%	78	<0.0001	0.33
LP neutrophils	12	57%	21		33	73%	45		68	87%	78	0.26	0.085
Cryptitis	9	43%	21		41	91%	45		75	96%	78	<0.0001	0.26
Crypt abscesses	8	38%	21		25	56%	45		60	77%	78	0.29	0.016
Ulceration	7	33%	21		38	84%	45		54	69%	78	0.0001	0.084
Paneth cells	0	0%	13		15	37%	41		33	45%	73	0.011	0.43
Phlebitis	6	27%	22		31	66%	47		46	59%	78	0.0041	0.46
Fibrin thrombi	4	18%	22		11	23%	47		11	14%	78	0.76	0.23
Apoptosis													
Cutoff ≥1/HPF	16	76%	21		34	76%	45		50	67%	75	1.0	0.41
Cutoff ≥2/HPF	15	71%	21		24	53%	45		32	43%	75	0.19	0.27
Cutoff ≥5/HPF	9	43%	21		6	13%	45		12	16%	75	0.012	0.8
Cutoff ≥10/HPF	2	10%	21		1	2%	45		1	1%	75	0.24	1.0

*Some biopsies had insufficient tissue to evaluate for all histologic features

CMV = cytomegalovirus, IBD = inflammatory bowel disease, LP = lamina propria, HPF = high power field

Figure 1 - 466

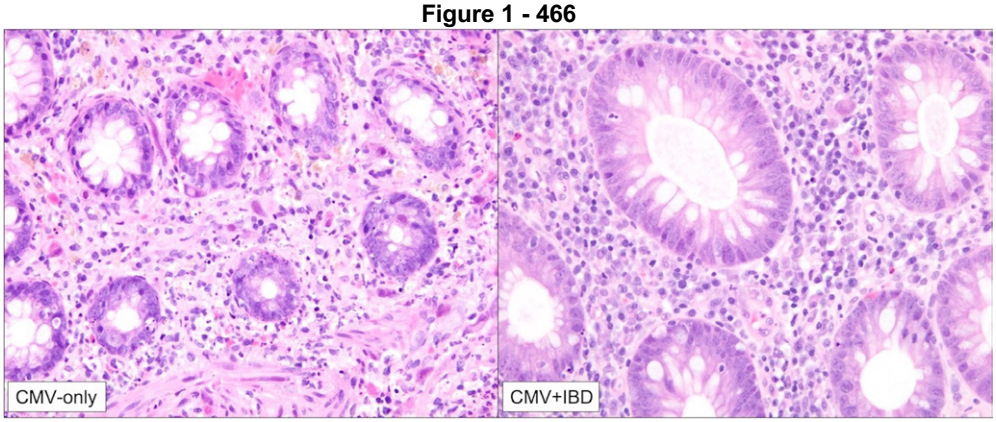

Figure 2 – 466

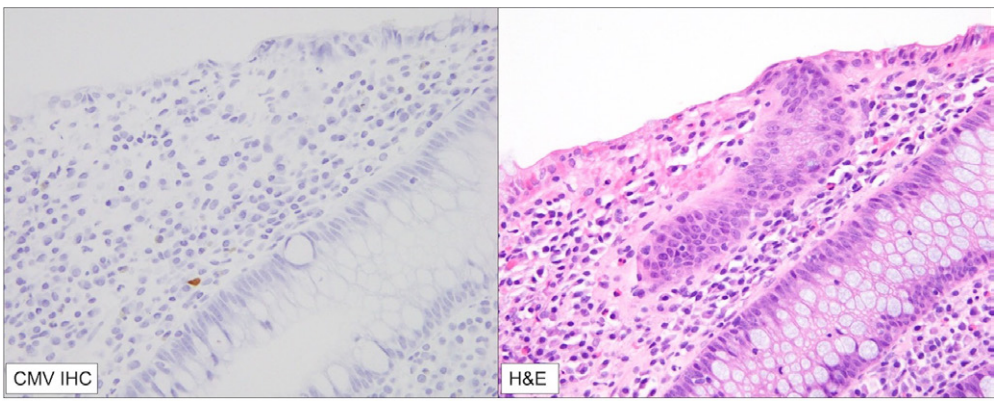

Conclusions: IBD patients with superimposed CMV infection are somewhat less likely to demonstrate crypt abscesses compared to their noninfected counterparts; apoptosis does not distinguish between the two groups. Equivocal IHC staining for CMV may indicate true infection in IBD patients.

467 Appendix Involvement is Uncommon in Gastrointestinal Cancer Predisposition Syndromes: A Pilot Study

Nandan Padmanabha[1], Raul Gonzalez[1], Monika Vyas[1]
[1]Beth Israel Deaconess Medical Center, Harvard Medical School, Boston, MA

Disclosures: Nandan Padmanabha: None; Raul Gonzalez: None; Monika Vyas: None

Background: Gastrointestinal cancer predisposition syndromes (GCPS) are generally characterized by involvement of the gastrointestinal tract by syndromic polyps. The number, histology, and malignant potential of the polyps vary among different syndromes. As appendiceal involvement is rarely reported, this study aimed to evaluate the involvement of the appendix in GCPS.

Design: We searched our archives for colonic resection specimens in patients who met clinical or genetic criteria for GCPS. Pathology reports were reviewed for documentation of an appendix in the specimen, and the presence of any appendiceal pathology. For each included case, we reviewed H&E-stained slides from the appendix, and documented patient age and sex, the type of specimen, and other specimen pathology. Electronic medical records were reviewed for clinical impression and genetic testing results.

Results: The cohort included 33 patients (18 males and 15 females, average age: 51.9 y, range 19-91y). Appendiceal and colonic pathology in these cases is summarized in Table 1. Familial adenomatous polyposis (FAP, classic and attenuated) formed the largest group in our cohort (n=14). Aside from a low-grade mucinous neoplasm (LAMN) in one case, the appendices were unremarkable or showed fibrous obliteration; no adenomas were found. This group was followed by mixed serrated/hyperplastic polyposis syndromes (n=5) and Lynch syndrome (n=5), both of which showed an appendiceal sessile serrated lesion in one case each. One case each of Peutz-Jeghers syndrome and juvenile polyposis showed hamartomatous polyps in the appendix, with low-grade dysplasia in the former (**Figure 1A-B).**

Table 1:

GCPS	Appendiceal pathology	Appendix unremarkable/fibrous obliteration	Colonic pathology
FAP (classic and attenuated) (n=14)	Mucinous neoplasm (n=1, 7.1%)	13 (93%)	1. Multiple tubular adenomas/tubulovillous adenomas (10-500) (n=14, 100%) 2. Adenocarcinoma (n=2, 14%)
Clinical polyposis syndrome (n=6)	0	6 (100%)	1. Multiple tubular adenomas (n=6, 100%) 2. Adenocarcinoma (n=1, 16.6%) 3. Sessile serrated adenoma, Hyperplastic polyps (n=1 , 16.6% each)
Lynch syndrome (n=5)	Sessile serrated adenoma (n=1, 20%)	4 (80%)	1. Adenocarcinoma (n=5, 100%) 2. Tubular adenoma (n=2, 40%) 3. Sessile serrated adenomas (n=1, 20%) 4. Hyperplastic polyps (n=1, 20%)
Mixed serrated/hyperplastic polyposis syndrome (n=5)	Sessile serrated adenoma (n=1, 20%), low grade appendiceal mucinous neoplasm (n=1, 20%)	3 (60%)	1. Sessile serrated adenomas (12-22) (n=4, 80%) 2. Hyperplastic polyps (3-50) (n=3, 60%) 3. Tubular adenomas (n=1, 20%) 4. Adenocarcinoma (n=1, 20%)
Peutz-Jeghers (n=1)	Hamartomatous polyp with low grade dysplasia (n=1, 100%)	0	Hamartomatous polyps with low grade dysplasia (>50) (n=1, 100%)
Juvenile polyposis syndrome (n=1)	Juvenile type inflammatory polyp (n=1, 100%)	0	Juvenile type inflammatory polyps (>200) (n=1, 100%)
MUTYH polyposis (n=1)	0	1 (100%)	Multiple tubular adenomas/ tubulovillous adenomas (~20), hyperplastic polyps (n=1, 100%)

Figure 1 - 467

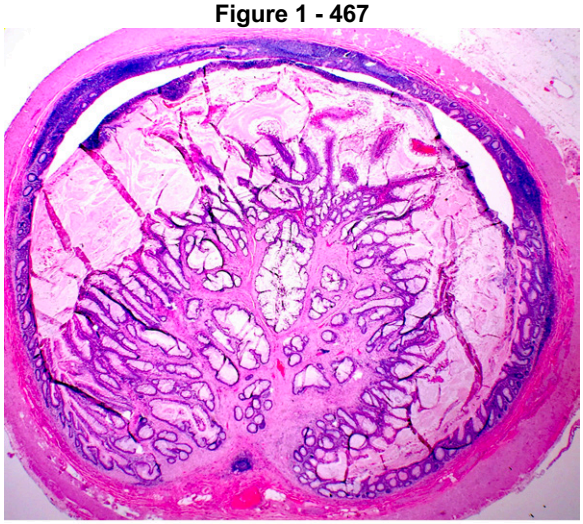

Fig A: A hamartomatous polyp involving the appendix, in a case of Peutz-Jegher's syndrome.

Figure 2 - 467

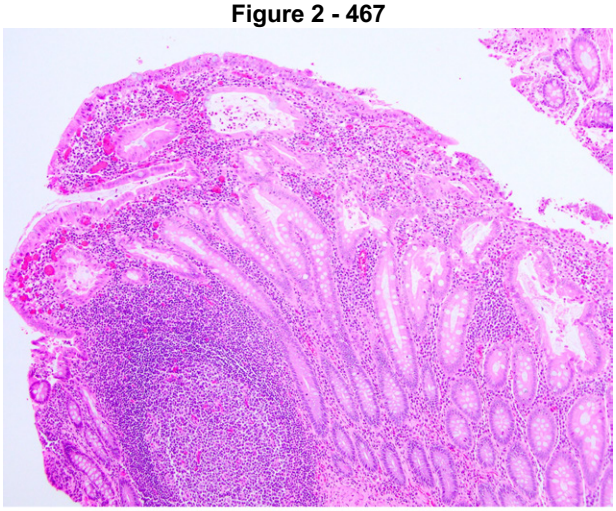

Fig B: A microscopic juvenile-type inflammatory polyp in the appendix, in a patient with Juvenile Polyposis.

Conclusions: Our data shows relative sparing of appendix in patients with FAP, while other GCPSs may show appendiceal involvement. This is important for surveillance, as prophylactic colectomy is not recommended for all GCPS, and the lumen of the appendix is not visualized on routine colonoscopy.

468 Gastrointestinal Glomus Tumors: A Proposal for Malignancy Criteria Based on a Clinicopathologic and Genetic Study of 27 Cases Demonstrating Chromosomal Instability in Malignant Tumors

David Papke[1], Lynette Sholl[2], Leona Doyle[1], Christopher Fletcher[1], Jason Hornick[3]
[1]Brigham and Women's Hospital, Boston, MA, [2]Harvard Medical School, Boston, MA, [3]Brigham and Women's Hospital, Harvard Medical School, Boston, MA

Disclosures: David Papke: None; Lynette Sholl: *Consultant*, Genentech; *Grant or Research Support*, Genentech; *Consultant*, Lilly; Leona Doyle: None; Christopher Fletcher: None; Jason Hornick: *Consultant*, Aadi Biosciences, TRACON Pharmaceuticals

Background: Glomus tumors of the GI tract harbor *CARMN-NOTCH2* fusions and have unpredictable behavior, with no established malignancy criteria.

Design: Clinicopathologic features were evaluated in 27 cases from consultation and institutional archives. Next-generation DNA sequencing (NGS) was performed on 15 tumors.

Results: Eighteen patients (67%) were male. Age ranged from 16-81 y (median 54.5 y). Primary sites were stomach (26 tumors: 9 body, 14 antrum, 3 unspecified) and distal esophagus (1). Tumor size ranged from 0.8–19.5 cm (median 4.2 cm).

Tumors were composed of lobules of epithelioid cells with sharp borders, pale eosinophilic to clear cytoplasm, and round nuclei. Thirteen tumors involved the serosa. Mitoses ranged from <1 – 34/10 HPF (median 4/10 HPF). Fifteen tumors, including all 14 with mitoses ≥ 2/10 HPF, showed atypia (3 mild, 9 moderate, 3 severe), defined as spindle cell morphology, nuclear irregularity, nuclear size variability, enlarged nuclei, or coarse chromatin. Necrosis was identified in 4 tumors; lymphovascular invasion in 5.

Follow-up was available for 13 patients so far (range 8 mo-10.5 y; median 4.1 y). Two had metastases at presentation, and five developed metastases on follow-up (4 liver; 1 each lung, peritoneum, cerebellum, and bones). Six were alive with metastases at last follow-up; one died of disease 10.4 y after presentation. Tumors with both atypia and mitoses ≥ 2/10 HPF were defined as malignant (15/27) because 7/10 tumors with both features metastasized, compared to 0/4 tumors lacking both features. Where assessable, serosal involvement was present in 0/4 benign and 6/6 malignant tumors.

By IHC, SMA and caldesmon were positive in all evaluated tumors and synaptophysin in 64%; KIT, DOG1 and chromogranin were negative. NGS showed *NOTCH2* alterations in 4/5 benign and 8/10 malignant tumors. Benign tumors lacked complex copy-number alterations (CNAs) (0/5), whereas 10/10 malignant tumors showed complex CNAs, including recurrent gain of 5q (7/10), loss of 9p21.3 (4/10, variably including *CDKN2A*/*B* and *MTAP*), and gain of 19p13.12 (4/10, including *NOTCH3*). Four malignant tumors had *ATRX* inactivating alterations.

Conclusions: Complex CNAs were identified in all tumors that were ≥ 5 cm, exhibited both cytologic atypia and ≥ 2 mitoses/10 HPF, involved the serosa, or metastasized. We propose that tumors ≥ 5 cm or with both atypia and mitoses ≥ 2/10 HPF should be considered malignant; CNA analysis might be helpful in borderline cases.

469 Investigating Potential Precursors of Appendiceal Goblet Cell Adenocarcinoma: A Paired Sequencing Study of Goblet Cell Adenocarcinoma and Co-incident Serrated Lesions

David Papke[1], Jonathan Nowak[1], Mark Redston[1]
[1]Brigham and Women's Hospital, Boston, MA

Disclosures: David Papke: None; Jonathan Nowak: None; Mark Redston: None

Background: Goblet cell adenocarcinoma (GCA) has no known precursor lesion. In our consultation practice, we observed a seemingly higher-than-chance rate of co-occurrence of GCA and serrated lesions, including low-grade appendiceal mucinous neoplasms (LAMN), sessile serrated polyps (SSP), and other unclassified serrated neoplasms (USN) lacking cytologic dysplasia.

Design: Reviewing clinical archives since 2015, we identified 10 cases of GCA co-occurring with LAMN (7 cases), USN (2 cases), or SSP (1 case), and 1 case of co-occurring GCA, LAMN and SSP. We also identified 3 cases of conventional adenocarcinoma with co-incident LAMN. Paired sequencing was performed on co-incident lesions in 6 cases using a next-generation DNA sequencing panel, including 3 LAMN/GCA, 2 USN/GCA, and 1 SSP/GCA.

Results: One LAMN/GCA, which exhibited a gradual spatial transition from areas diagnostic of LAMN to areas diagnostic of GCA, harbored shared somatic mutations in both components including *KRAS* G12V, *MED12* R961W, and *SMAD2*, *SOX9*, and *STK11* inactivation. One USN/GCA showed low-level gain of *CDK4* in both components, although they otherwise had distinct somatic alterations (USN: *KRAS* G13D and *ERCC1* S307I; GCA: *POLH* R383H variant of unknown significance [VUS]). In the other 4 cases, there were no detected shared somatic alterations between components.

Across all 6 cases, GCA exhibited *KRAS* G12V (1 case), *MED12* R961W (1), *ARID1A* loss of function (1), an *ERBB2* hotspot mutation (1), and *SMAD2*, *SOX9*, and *STK11* inactivation (all same case). The LAMNs harbored *KRAS* hotspot mutations (3 cases: G12D, G12V, Q61H), *ARID1B* loss of function (1), *ERBB4* R95C (1), *MED12* R961W (1), and inactivation of *SMAD2*, *SOX9* and *STK11* (all same case). The 2 USNs harbored: *KRAS* hotspot mutations (G12V and G12C both in 1 case; G13D in the other), *GNAS* R201H (1), and a *COL7A1* VUS (1). The SSP harbored *KRAS* Q61K and several VUS, including in *COL7A1* and *MED12*.

Conclusions: In 5/6 cases (2 LAMN/GCA, 2 USN/GCA, 1 SSP/GCA), serrated lesions were found to harbor different somatic alterations than the GCA in the same appendix. One LAMN/GCA exhibited shared somatic alterations between both components, suggesting that there might be a shared clonal origin for a subset of GCAs and LAMNs. Overall, the lack of clonal relationships in most cases suggests that there is another explanation for the frequent co-occurrence of serrated neoplasms and GCA, such as environmental or epigenetic factors.

470 Association Between Microsatellite Instability and Mismatch Repair Mutational Signature Status in 31,255 Clinically Advanced Colorectal Adenocarcinomas

Vamsi Parimi[1], Zoe Fleischmann[1], Douglas Lin[2], Natalie Danziger[2], Karthikeyan Murugesan[2], Lani Clinton[1], Douglas Mata[2], Brennan Decker[2], Matthew Hiemenz[2], Shakti Ramkissoon[3], Julia Elvin[2], Mia Levy[4], Jeffrey Ross[5], Richard Huang[6]
[1]Foundation Medicine, Inc., RTP, NC, [2]Foundation Medicine, Inc., Cambridge, MA, [3]Foundation Medicine, Inc., Morrisville, NC, [4]Foundation Medicine, Inc., Boston, MA, [5]SUNY Upstate Medical University, Syracuse, NY, [6]Foundation Medicine, Inc., Cary, NC

Disclosures: Vamsi Parimi: *Employee*, Foundation Medicine Inc.; Zoe Fleischmann: None; Douglas Lin: *Employee*, Foundation Medicine, Inc.; *Stock Ownership*, Roche; Natalie Danziger: *Employee*, Foundation Medicine Inc.; *Stock Ownership*, F. Hoffman La Roche Ltd.; Karthikeyan Murugesan: *Employee*, Foundation Medicine; *Stock Ownership*, Roche Holdings AG; Lani Clinton: None; Douglas Mata: *Employee*, Foundation Medicine, Inc.; *Speaker*, Astellas Pharma, Inc.; Brennan Decker: *Employee*, Foundation Medicine; *Stock Ownership*, Roche; Matthew Hiemenz: *Employee*, Foundation Medicine / Roche; Shakti Ramkissoon: None; Julia Elvin: *Employee*, Foundation Medicine; *Stock Ownership*, Hoffmann-La Roche; Mia Levy: None; Jeffrey Ross: *Employee*, Foundation Medicine; Richard Huang: *Employee*, Foundation Medicine; *Employee*, Roche

Background: Mismatch repair (MMR) deficiency imprints a specific mutational signature onto the cancer genome and underlies the pathogenesis of a subset of colorectal adenocarcinomas (CRCs). MMR deficiency is typically assessed by immunohistochemistry or by evaluating microsatellite instability (MSI) through PCR or next-generation sequencing (NGS). Functional MMR mutational signature (ms) analysis determined by NGS could potentially serve as a complementary orthogonal

method for evaluating MMR deficiency. We explored the relationship between MSI status and MMRms in a large cohort of clinically advanced CRC samples

Design: Thirty-one thousand two hundred fifty-five clinically advanced CRC samples were tested during routine clinical care using a tissue hybrid capture-based NGS comprehensive genomic profiling (CGP) assay. MSI status was determined by assessing 95 intronic homopolymer repeat loci, and MMRms was defined according to the COSMIC mutational signatures database (v2-March 2015).

Results: In all, 1,713 (5.5%) CRC cases were MSI-high (MSI-H), 28,585 (91.5%) were microsatellite -stable (MSS), and 957 (3%) were MSI-low or equivocal/unknown. The sensitivity, specificity, positive predictive value (PPV), negative predictive value (NPV), and accuracy of MMRms in predicting MSI-H status was 77.5% (95% CI: 75.5-79.5%), 95.6% (95% CI: 95.3-95.8%), 48% (95% CI: 46.5-49.5%), 98.8% (95% CI: 98.7-98.9%), and 94.7% (95% CI: 94.4-94.9%), respectively. While MSI and MMRms status were highly concordant (Point biserial correlation coefficient (r_{pb}) = +0.6, p=<0.0001), heterogeneity was overserved between MSI and MMRms status in a subset of cases: MSI-H/MMRms− (1.2%, 385/31,255) and MSS/MMRms+ (4.0%, 1263/31,255).

Conclusions: Our study signifies the prevalence of MSI and MMRms heterogeneity among CRC. Further analysis is needed to explore the clinicopathologic and genomic differences between patients with and without MSI and MMRms heterogeneity. Clinical studies should also assess whether the response to immunotherapy differs in these two subgroups.

471 Morphologic Spectrum of Gastric Pathology in Patients with Lynch Syndrome

Paige Parrack[1], Dan Feldman[2], Daniel Chung[2], Matthew Yurgelun[3], Vikram Deshpande[4], Deepa Patil[5]
[1]Brigham and Women's Hospital, Boston, MA, [2]Massachusetts General Hospital, Boston, MA, [3]Dana-Farber Cancer Institute, Boston, MA, [4]Massachusetts General Hospital, Harvard Medical School, Boston, MA, [5]Brigham and Women's Hospital, Harvard Medical School, Boston, MA

Disclosures: Paige Parrack: None; Dan Feldman: None; Daniel Chung: None; Matthew Yurgelun: *Advisory Board Member*, Janssen Pharmaceuticals; *Grant or Research Support*, Janssen Pharmaceuticals; Vikram Deshpande: None; Deepa Patil: None

Background: The stomach represents the second most common site of gastrointestinal tract cancer in Lynch syndrome (LS) patients. Surveillance esophagogastroduodenoscopy (EGD) interval is variable and depends on the presence of risk factors for gastric cancer and intestinalized gastritis. The morphologic spectrum of gastric polyps and their association with cancer and mutation status has not been well-characterized and forms the basis of our study.

Design: We performed clinicopathologic assessment of 284 biopsies (162 EGDs) and 7 gastrectomies from 54 patients identified from the LS registry and pathology database of two institutions. Polyp and adenocarcinoma (ADCA) subtype, dysplasia, genotype, and associated histological features were analyzed.

Results: The mean age of the cohort (M:12, F:39) was 54.6 years (range: 31-86 years). Multiple (>20) polyps were noted in 13 (24%) patients. Fundic gland polyps (FGP) and hyperplastic polyps (HP) occurred in 44/51 (86%) patients; 1/51 (2%) developed dysplasia while 9/51 (17%) developed ADCA with prior or concurrent dysplastic lesions. The biopsy level findings included normal mucosa (78; 28%), chronic gastritis with or without intestinal metaplasia (67; 24%), FGP without dysplasia (92; 32%), HP without dysplasia (8; 3%), HP with dysplasia (7; 2%), foveolar adenoma (3; 1%), intestinal adenoma (14; 4.9%), mixed polyps with dysplasia (4; 1%) and ADCA (11; 4%). All 28 dysplastic polyps were located in the fundus/body; 22 were low-grade and 6 were high-grade. The majority of the dysplastic lesions (20; 71%) were associated with autoimmune gastritis. Of the 9 ADCA (6- stage I, 3- Stage II), 6 were unifocal, fundic lesions (0.4 - 6 cm) and 3 were multifocal (2 fundic, 1 antral; 0.1 - 1 cm). All, except one ADCA arose in a background of prior/concurrent dysplastic lesions; background gastritis was seen in 6/9 ADCA cases (5- autoimmune, 1- lymphocytic gastritis). Patients with MSH-2 mutation had the highest proportion of biopsies with dysplasia/ADCA (25%) compared to MLH1 (3%), PMS2 (3%) and MSH6 (0%).

Conclusions: Nearly 84% of biopsies in LS patients showed normal mucosa, chronic gastritis, or FGPs. Dysplastic lesions and ADCA most commonly occur in the fundus/body in a background of chronic gastritis. As dysplastic HPs, mixed polyps, and adenomas have the greatest association with ADCA, patients with these lesions may benefit from a closer surveillance compared to those with non-dysplastic polyps.

472 Autoimmune Metaplastic Atrophic Gastritis: Regional Demographics and Prevalence

Julio Poveda[1], Oliver McDonald[1], Aatur Singhi[2], Jason Park[3], Monica Garcia-Buitrago[4], Elizabeth Montgomery[1]
[1]University of Miami Miller School of Medicine, Miami, FL, [2]University of Pittsburgh Medical Center, Pittsburgh, PA, [3]UT Southwestern Medical Center, Dallas, TX, [4]University of Miami Miller School of Medicine/Jackson Health System, Miami, FL

Disclosures: Julio Poveda: None; Oliver McDonald: None; Aatur Singhi: *Consultant*, Foundation Medicine; Jason Park: *Consultant*, HU Group (Miraca Holdings); Monica Garcia-Buitrago: None; Elizabeth Montgomery: None

Background: Autoimmune metaplastic atrophic gastritis (AMAG) is an uncommon corpus-predominant form of chronic gastritis characterized by immune-mediated damage to parietal cells resulting in gradual parietal cell loss and failure to absorb iron and vitamin B12. Traditionally, AMAG has been regarded as a disease of the elderly female patient of northern European descent. In this study, we assess the prevalence of AMAG in various population subsets in a large southeastern United States teaching hospital.

Design: We prospectively assessed gastric biopsies from sequential patients from our institution's clinics for cases of AMAG detected on gastric biopsies performed between 2020 and 2021. Clinical data including patient demographics, serologic studies as well as prior and current biopsy results were also documented for each case, when available

Results: Two of the authors analyzed 1,708 sequential "in-house" gastric biopsies from 1,692 patients for AMAG (and other types of gastritis) in the course of routine care between October 2020 to September 2021. We prospectively identified 75 patients (4.3%) with AMAG. These included 58 women (77%) and 17 men (23%) with median age of 60 years. Self reported demographics were as follows: 57 Hispanic, 9 Black, 8 White and 1 Asian. Several background pathologic changes were seen including hyperplastic polyps (n=4; 5%), neuroendocrine neoplasms (n=10; 19%) and pyloric gland adenomas (n=3; 4%). Interestingly, *Helicobacter pylori*-associated active chronic gastritis (HP-ACG) was observed in 231/1,692 patients (13%). Within the AMAG group, only 7 patients (9%) showed either concurrent HP-ACG or had previous biopsies showing HP infection.

Conclusions: Although AMAG has traditionally been considered a disease of elderly White females, the majority of affected patients in our population was Hispanic, the main population served by our Institution, and female. In contrast, we have previously observed AMAG in only 2% of patients in a population with few Hispanics. In addition, although our population is enriched for persons with HP infection, HP infection may not necessarily be a required antecedent factor.

473 Morphologic Spectrum of Immune Checkpoint Inhibitor (ICI) Associated Colitis: A Single Center Experience

Nina Rahimi[1], Trilokesh Kidambi[1], Yu Liang[2], Rifat Mannan[1]
[1]City of Hope Cancer Center, Duarte, CA, [2]City of Hope National Medical Center, Duarte, CA

Disclosures: Nina Rahimi: None; Trilokesh Kidambi: None; Yu Liang: None; Rifat Mannan: None

Background: ICIs have been exceptional novel treatment options in improving outcomes of various cancers. However, ICIs are known to elicit varied injury patterns in the gastrointestinal mucosa as well as other organs. In this study, we sought to evaluate the different histologic patterns of ICI-associated colitis and the association with specific agents.

Design: Institutional database was searched for patients who were diagnosed as ICI associated colitis in the last 4-years (2018-2021). Relevant clinical details and information about medications were gathered from the charts. Colonic biopsies were blindly reviewed, and histologic injury patterns were recorded.

Results: We identified 45 patients with ICI colitis (median age 45.3, range 36 - 88; F:M = 17:28), who received pembrolizumab (23/45, 51.1%), nivolumab (8/45, 17.7%), ipilimumab (1/45, 2.2%), ipilimumab+nivolumab (9/45, 20%), and few other agents (4/45, 8.8%) (atezolizumab and mogamulizumab). The different types of malignancies being treated were melanoma (10/45; 22.2%), renal cell carcinoma (5/45; 11.1%), colorectal adenocarcinoma (4/45; 8.9%), breast carcinoma (4/45; 8.9%), and other solid malignancies (22/45; 48.9%). Indications for colonoscopy included diarrhea (38/45, 86.3%), abdominal pain (7/45, 17.7%), fever (3/45, 7.8%), and nausea/vomiting (2/45, 3.9%). Histologic injury patterns were classified as: apoptotic colopathy (13/45, 28.9%), focal active colitis (3/45, 6.7%), diffuse active colitis (9/45, 20%), chronic active colitis (2/45, 4.4%), lymphocytic colitis (1/45, 2.2%), collagenous colitis (1/45, 2.2%), and mixed injury patterns (16/45, 35.6%) (Table 1).

Table 1 : Histologic injury patterns by immune checkpoint inhibitors

Colitis pattern	Total N=45 (%)	Pembrolizumab	Nivolumab	Ipilimumab	Ipilimumab +Nivolumab	Pembrolizumab +Nivolumab
Apoptotic colopathy	13 (28.9%)	7 (53.8%)	3 (23.1%)	0	3 (23.1%)	0
Focal active colitis	3 (6.7%)	2 (66.7%)	0	0	1 (33.3%)	0
Diffuse active colitis	9 (20%)	5 (55.6%)	1 (11.1%)	1 (11.1%)	2 (22.2%)	0
Chronic active colitis	2 (4.4%)	2 (100%)	0	0	0	0
Mixed injury pattern	16 (35.6%)	7 (43.8%)	5 (31.2%)	0	3 (18.7%)	1 (6.3%)
Lymphocytic colitis	1 (2.2%)	1 (100%)	0	0	0	0
Collagenous colitis	1 (2.2%)	0	1 (100%)	0	0	0

Figure 1 - 473

Histologic injury patterns of ICI colitis: A) **Apoptotic colopathy pattern**, depicting prominent crypt apoptosis; B) **Lymphocytic colitis pattern**, with increased intraepithelial lymphocytes; C) **Diffuse active colitis pattern**, having lamina propria lymphoplasmacytic inflammation with cryptitis, crypt abscess, and without evidence of chronicity; D) **Chronic active colitis pattern**, with architectural distortion, basal plasmacytosis, similar to inflammatory bowel disease

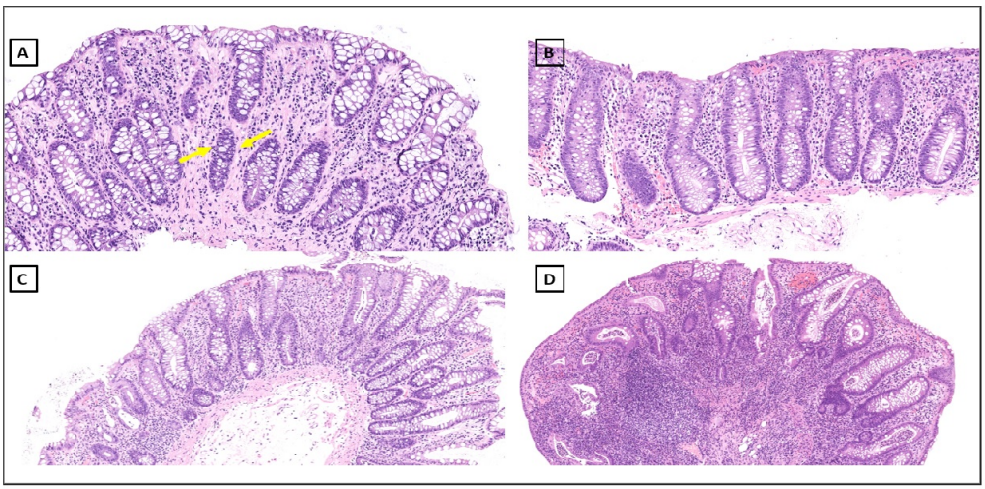

Conclusions: ICI colitis represents a varied spectrum of histologic injury patterns, of which apoptotic colopathy and mixed injury patterns were the most prevalent. None of the injury patterns could be attributed to a particular agent. ICI associated injury should be considered in the differential diagnosis of the common histologic colitis patterns. Correlation with the patient's clinical and medication history is vital in ascertaining the etiology and differentiating from the mimics.

474 Atrophy as a Novel Histologic Feature of Chronic Esophageal GVHD

Luisa Ricaurte[1], Amrit Kamboj[1], Vanessa Pazdernik[1], Sarah Jenkins[1], David Katzka[1], Christopher Hartley[1], Catherine Hagen[1]
[1]Mayo Clinic, Rochester, MN

Disclosures: Luisa Ricaurte: None; Amrit Kamboj: None; Vanessa Pazdernik: None; Sarah Jenkins: None; David Katzka: None; Christopher Hartley: None; Catherine Hagen: None

Background: Compared to other GI tract sites, esophageal GVHD is relatively rare and histologic characterization has been limited. The aim of this study was to correlate histologic features of esophageal GVHD with clinical and endoscopic characteristics to determine which histologic features may have clinical significance.

Design: The pathology database was searched from 2000-2021 for esophageal biopsies with histologic changes compatible with GVHD. Biopsies were assessed for selected histologic features. Corresponding GI tract biopsies (stomach, small bowel and colon) were assessed for presence of GVHD. Clinical and endoscopic data was collected through chart review.

Results: The study cohort consisted of 40 stem cell transplant patients (M:F 2.1:1; mean age 56.2 yrs). All patients were treated for GVHD with steroid therapy. 25 patients (62.5%) were clinically characterized as acute GVHD and 15 (37.5%) as chronic GVHD. 38 patients had corresponding biopsies from other GI sites with 25 (65.8%) showing evidence of GVHD in those biopsies. On esophageal biopsy, all patients had at least rare epithelial apoptosis. A minority of patients (20%) showed evidence of ulceration. Acanotholysis could not be assessed in most cases (70%) due to insufficient sampling of the stroma. In patients with sufficient sampling of stroma (n=12), acantholysis was noted in 2 patients (16.7%). 18 patients (45%) had neutrophils present on biopsy, and these patients were less likely to have evidence of GVHD in corresponding biopsies compared to patients without neutrophils (43.8% vs. 81.8%, p=0.02). No patients with neutrophils had histologic evidence of infection and only one patient with neutrophils was on mycophenolate therapy. 16 patients (40%) showed evidence of atrophy (Figure 1). Patients with atrophy were significantly less likely to have evidence of active GVHD in corresponding GI tract biopsies (40% vs. 82.6%, p=0.01) but more likely to have evidence of extraintestinal GVHD (100% vs. 70.8%, p=0.03). Patients with atrophy showed a trend towards being classified as chronic GVHD (56.3% vs. 25%, p=0.09) but this did not reach statistical significance. None of the remaining histologic features correlated with clinical evidence of GVHD (Table 1).

Histologic feature	Overall prevalence (n=40)	Correlation with clinical features (p value)			
		Corresponding biopsies with GVHD (n=38)	Clinical GVHD grade (n=40)	Endoscopic findings* (n=40)	Extraintestinal GVHD (n=40)
Apoptosis • Rare • Moderate • Abundant	14 (35%) 13 (32.5%) 13 (32.5%)	0.76	0.31	0.47	1.0
Basal vacuolization	37 (92.5%)	0.27	0.74	0.71	0.45
Basal lymphocytosis	30 (75%)	1.0	0.23	1.0	1.0
Basal atypia • No/mild • Moderate-marked	19 (47.5%) 21 (52.5%)	0.51	1.0	0.91	0.69
Eosinophils	12 (30%)	0.27	0.90	0.55	1.0
Neutrophils • Yes • No	18 (45%) 22 (55%)	7/16 (43.8%) 18/22 (81.8%) **0.02**	0.18	0.24	0.43
Atrophy • Yes • No	16 (40%) 24 (60%)	6/15 (40%) 19/23 (82.6%) **0.01**	0.49	0.15	16/16 (100%) 17/24 (70.8%) **0.03**
Spongiosis • Mild • Moderate • Marked	8 (20%) 12 (30%) 20 (50%)	0.27	0.22	0.44	0.86
Ulcer	8 (20%)	0.67	1.0	1.0	0.31

* Endoscopic findings classified as: 0=normal, 1=erythema, edema, 2=erosion, ulcer, stricture, furrow, desquamation

Figure 1 - 474

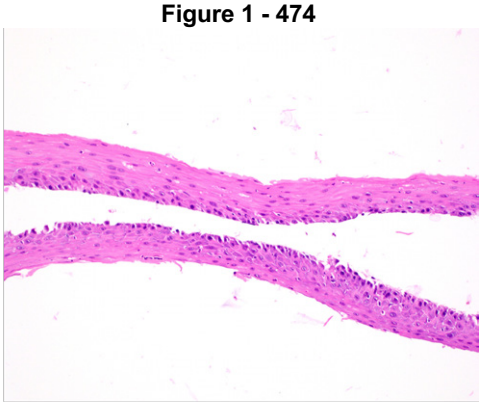

Figure 1: Example of esophageal atrophy showing marked attenuation and thinning of the squamous mucosa

Conclusions: The presence of neutrophils on esophageal biopsy was negatively associated with evidence of GVHD in corresponding biopsies and may indicate an alternative diagnosis other than GVHD. Esophageal atrophy may be a histologic correlate of chronic GVHD.

475 Development of an Artificial Intelligence Model for the Evaluation of Histopathologic Features of Eosinophilic Esophagitis

Luisa Ricaurte[1], Donnchadh O'Sullivan[1], Maria Cardenas F[1], Lindsey Smith[2], Hanna-Kaisa Sihvo[2], Thomas Westerling-Bui[2], Ravi Karthik[1], Crystal Lavey[1], Taofic Mounajjed[3], Christopher Hartley[1], Rish Pai[4], Rondell Graham[1], Puanani Hopson[1], Imad Absah[1], Roger Moreira[1]

[1]Mayo Clinic, Rochester, MN, [2]Aiforia, Inc, Cambridge, MA, [3]Hospital Pathology Associates, Minneapolis, MN, [4]Mayo Clinic, Scottsdale, AZ

Disclosures: Luisa Ricaurte: None; Donnchadh O'Sullivan: None; Maria Cardenas F: None; Lindsey Smith: None; Hanna-Kaisa Sihvo: *Employee*, Aiforia Technologies Plc; *Stock Ownership*, Solumo Pathologists Ltd; Thomas Westerling-Bui: *Employee*, Aiforia Inc.; Ravi Karthik: None; Crystal Lavey: None; Taofic Mounajjed: None; Christopher Hartley: None; Rish Pai: *Consultant*, Alimentiv Inc, Allergan, Verily, Eli Lilly, AbbVie, PathAI; Rondell Graham: None; Puanani Hopson: None; Imad Absah: None; Roger Moreira: None

Background: In an attempt to provide quantitative, highly reproducible, and standardized analyses in cases of eosinophilic esophagitis (EoE), we have developed an artificial intelligence (AI)-based digital pathology model for the evaluation of histologic features in the spectrum of EoE/esophageal eosinophilia. Here, we describe the development and validation of this novel AI tool.

Design: A total of 10,726 objects and 56.2 mm^2 of semantic segmentation areas were annotated on whole-slide images, utilizing a cloud-based, deep learning artificial intelligence platform (Aiforia Technologies, Helsinki, Finland). Our training set consisted of 40 carefully selected digitized esophageal biopsy slides which contained the full spectrum of changes typically seen in the setting of esophageal eosinophilia, ranging from normal mucosa to severe abnormalities with regards to each specific features included in our model. A subset of cases was reserved as independent 'test sets' in order to assess the validity of the AI model outside the training set. Five specialized experienced gastrointestinal pathologists scored each feature blindly and independently.

Results: The performance of the AI model for all cell type features was similar/non-inferior to that of our group of GI pathologists (F1-scores: 94.6 - 94.8 for AI vs human and 92.6 – 96.0 for human vs human). Result details are shown in Table 1. Segmentation area features were rated for accuracy using the following scale: 1. "perfect or nearly perfect" (95-100%, no significant errors), 2. "very good" (80-95%, only minor errors), 3. "good" (70-80%, significant errors but still captures the feature well), 4. "insufficient" (less than 70%, significant errors compromising feature recognition). Rating scores for tissue (1.01), spongiosis (1.15), basal layer (1.05), surface layer (1.04), lamina propria (1.15) and collagen (1.11) were in the "very good" to "perfect or nearly perfect" range, while degranulation (2.23) was rated between "good" and "very good".

FP, false positive; FN, false negative

	Eosinophils		Lymphocytes		Squamous nuclei	
	AI vs Human	Human vs Human	AI vs Human	Human vs Human	AI vs Human	Human vs Human
FP%	5.82	4.34	7.08	9.70	3.38	5.92
FN%	4.72	3.61	5.65	7.23	6.77	4.77
Error %	9.01	6.86	10.12	13.29	9.57	9.50
Precision%	95.26	96.38	94.51	92.74	96.87	94.90
Sensitivity %	95.27	96.38	94.35	92.74	93.23	95.23
F1-score %	**94.88**	**96.07**	**94.59**	**92.61**	**94.76**	**94.76**

Figure 1 - 475

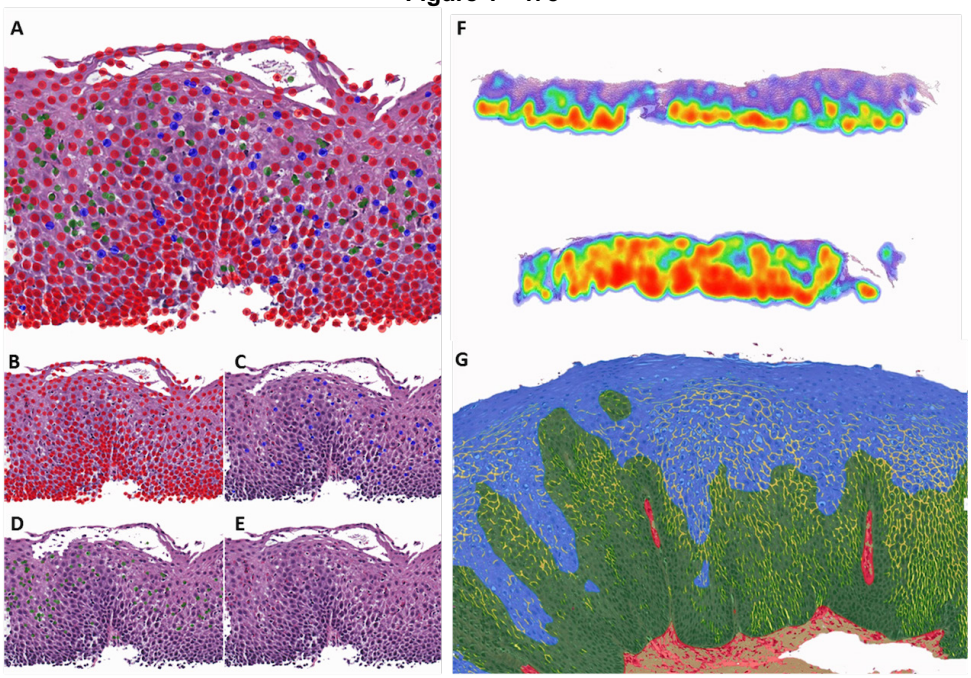

Figure 1 legend. Cell recognition feature of our model. H&E stain with all cell types (A); squamous cell nuclei in red (B); lymphocytes in blue (C); eosinophils in green (D), and original H&E (E). Heat map showing distribution of eosinophils in a biopsy sample (F). Semantic

Conclusions: Our newly developed AI-based tool showed an excellent performance (non-inferior to a group of experienced GI pathologists) for the recognition of various histologic features in the spectrum of EoE/esophageal mucosal eosinophilia. This tool represents an important step in creating an accurate and reproducible method for quantitative analysis to be used in the evaluation of eosinophilic diseases of the esophagus.

476 Patients With Sessile Serrated Lesions of the Appendix Have Increased Risk of Sessile Serrated Lesions of the Colorectum

Harry Rosenberg[1], Patrick Henn[2], Norman Carr[3], Brian Cox[4], Klaudia Nowak[5], Runjan Chetty[6], Stefano Serra[7], Raul Gonzalez[8]

[1]Beth Israel Deaconess Medical Center, Boston, MA, [2]University of Colorado Anschutz Medical Campus, Aurora, CO, [3]Basingstoke and North Hampshire Hospital, Basingstoke, United Kingdom, [4]Cedars-Sinai Medical Center, Los Angeles, CA, [5]Toronto General Hospital, University Health Network, Toronto, Canada, [6]Dublin, Ireland, [7]University Health Network, University of Toronto, Toronto, Canada, [8]Beth Israel Deaconess Medical Center, Harvard Medical School, Boston, MA

Disclosures: Harry Rosenberg: None; Patrick Henn: None; Norman Carr: None; Brian Cox: None; Klaudia Nowak: None; Runjan Chetty: None; Stefano Serra: None; Raul Gonzalez: None

Background: Sessile serrated lesions of the appendix (aSSLs) are often incidental findings in appendectomy specimens and have been shown to harbor premalignant potential. Their mutational profiles differ from colorectal SSLs (cSSLs), suggesting divergent biology. It is unclear whether identification of aSSLs warrants increased surveillance of the colorectum, as for cSSLs. This study aimed to address this question by evaluating the relationship between aSSLs and incidence of prior or subsequent cSSL diagnosis.

Design: We retrieved archival cases of aSSLs from our institutions. We excluded lesions found not to represent aSSLs, those identified during right hemicolectomy (which diminishes subsequent cSSL risk), those with prior history of colorectal carcinoma, those without prior or subsequent colonoscopy data, and those arising from cecum rather than appendix. We recorded patient history of prior or subsequent cSSLs, including conventional SSLs and traditional serrated adenomas (TSAs). A control group of appendectomy specimens lacking aSSLs, age- and sex-matched to the case group, was compiled for statistical comparison using chi-squared analysis, with significance set at $P<0.05$.

Results: After excluding 97 cases, a final cohort of 53 aSSL and 50 control appendectomies were included. In the aSSL cohort, mean patient age at diagnosis was 59 years old; 57% were female and 43% were male. Twenty-four (45%) patients in this group had colonoscopy screening at least one year after aSSL diagnosis, and 43 (81%) had colonoscopy prior to diagnosis. In the aSSL cohort, 19 (36%) patients had cSSLs (mostly SSL but one TSA). In the control group, mean patient age was 63 years old; 54% were female and 46% were male. Twenty-eight (56%) patients in this group underwent colonoscopy at least one year after appendectomy, and 43 (86%) had colonoscopy prior. Among the 50 control patients, 6 (12%) had cSSLs (also mostly SSL but one TSA). aSSL patients had significantly increased incidence of prior or subsequent cSSLs compared to control patients without aSSLs (36% vs. 12%, *P*=0.006) and had more cSSLs overall (*P*=0.024, Fig 1).

Figure 1 - 476

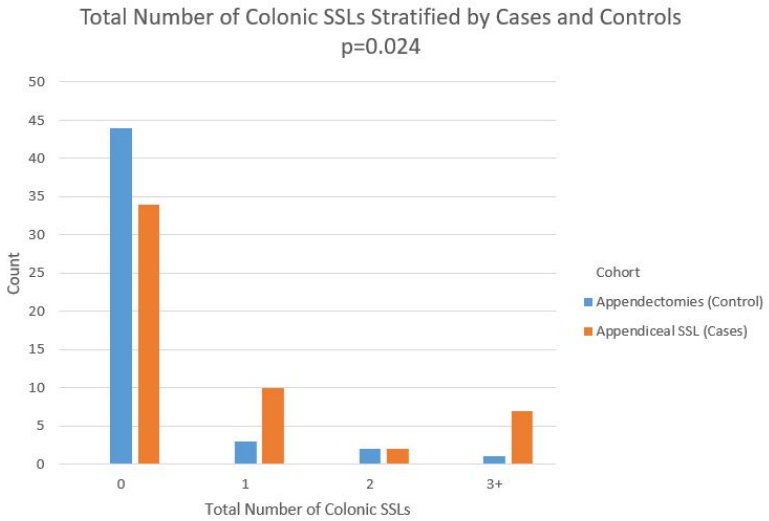

Conclusions: Our study found that aSSL patients are at significant risk of having a prior or subsequent diagnosis of cSSL. This suggests that aSSL belongs within the spectrum of colorectal SSL, meaning that diagnosis of aSSL at appendectomy should be considered when determining whether patients require shortened surveillance intervals to detect and remove premalignant serrated lesions of the colorectum.

477 Ordinary Colorectal Carcinoma Expressing Synaptophysin (OCCES): Clinicopathological Prognostic Factors and Molecular Analysis of a New Entity

Giovanna Sabella[1], Giovanni Centonze[1], Federica Grillo[2], Vincenzo Lagano[1], Giovanna Garzone[1], Martina Filugelli[1], Teresa Labella[1], Daniela Galbiati[1], Natalie Prinzi[3], Sara Pusceddu[4], Laura Cattaneo[5], Marcello Guaglio[1], Matteo Fassan[6], Stefano La Rosa[7], Fausto Sessa[7], Carlo Capella[8], Massimo Milione[1]
[1]Fondazione IRCCS Istituto Nazionale Tumori Milano, Milan, Italy, [2]University of Genova, Genova, Italy, [3]IRCCS Foundation, Istituto Nazionale dei Tumori, Milan, Italy, [4]Fondazione IRCCS Istituto Nazionale Tumori Milano, [5]IRCCS Foundation, Istituto Nazionale dei Tumori, Milano, Italy, [6]University of Padua, Padua, Italy, [7]University of Insubria, Varese, Italy, [8]Uni-Insubria, Varse, Italy

Disclosures: Giovanna Sabella: None; Giovanni Centonze: None; Federica Grillo: None; Vincenzo Lagano: None; Giovanna Garzone: None; Martina Filugelli: None; Teresa Labella: None; Daniela Galbiati: None; Natalie Prinzi: None; Sara Pusceddu: None; Laura Cattaneo: None; Marcello Guaglio: None; Matteo Fassan: None; Stefano La Rosa: None; Fausto Sessa: None; Carlo Capella: None; Massimo Milione: None

Background: Although colorectal carcinoma (CRC) is extremely common, 'mixed' tumors composed of non-neuroendocrine epithelial and neuroendocrine elements are rare, accounting for about 1-2% of all colorectal malignancies. These heterogeneous neoplasms include poorly known categories of amphicrine tumors, where non-neuroendocrine and neuroendocrine phenotype is synchronously expressed within the same cell. Although neuroendocrine differentiation in CRCs has been extensively assessed, no clear definition nor established criteria are currently available for OCCES.

Design: Synaptophysin immunohistochemical expression, by phenotypically malignant cells in a retrospective series of 663 ordinary CRCs with matched clinico-pathological and molecular features, was assessed. CRCs with synaptophysin positivity in > 30% of tumor glands were included in the study and compared to ordinary synaptophysin-negative CRCs. These data were correlated with Overall Survival (OS) and Disease-free Survival (DFS).

Results: Diagnosis of OCCES was confirmed in 27 (4.1%) patients and correlated with right colon site (p=0.003), Grade 2 (p=0.0007), marked intratumoral lymphocyte infiltrate (p=0.0006), and *BRAF* mutation (p=0.04). At univariate analysis variables associated with poor OS were 10-year increase in age (p= 0.001), stage IIII-IV (p= 0.001), OCCES status (p= 0.001), infiltrative growth at the invasive edge (p=0.04), and residual tumor R1-2 (p=0.03), while marked peritumoral lymphocyte infiltrate was associated with longer OS (p=0.04). At multivariable analysis only 10-year increase in age, stage-III-IV, and OCCES status (p<0.001) remained significantly associated with poor OS and marked peritumoral lymphocyte infiltrate with longer OS (p=0.02). Furthermore, comparable results were obtained with the same variables according to DFS; in addition, right colon site (p=0.04) was associated with longer DFS while *KRAS* mutation (p=0.04) was associated with poor DFS at univariate analysis. Therefore, in terms of both OS and DFS, synaptophysin immunohistochemical expression in >30% of gland forming tumor cells proved to be an independent negative prognostic factor.

Conclusions: Our study investigated the clinico-pathological and molecular features of the unexplored neoplastic OCCES providing the evidence that these tumors show worse OS and DFS compared to, morphologically indistinguishable, ordinary CRC.

478 Validation and Clinical Deployment of an AI-Based Algorithm for Detection of Gastric Adenocarcinoma and H. pylori in Gastric Biopsies

Judith Sandbank[1], Geraldine Sebag[2], Ayala Arad[2], Rachel Mikulinsky[2], Issar Yazbin[3], Inbal Gross[2], Ronen Heled[2], Manuela Vecsler[2], Chaim Linhart[2]
[1]Maccabi Health Services, Kiriat Ono, Israel, [2]Ibex Medical Analytics, Tel Aviv, Israel, [3]Ibex Medical Analytics, Israel

Disclosures: Judith Sandbank: *Primary Investigator*, Ibex Medical Analytics; Geraldine Sebag: *Employee*, Ibex Medical Analytics; Ayala Arad: *Employee*, Ibex Medical Analytics; Rachel Mikulinsky: None; Issar Yazbin: *Employee*, Ibex Medical Analytics; Inbal Gross: *Employee*, Ibex Medical Analytics; Ronen Heled: *Employee*, Ibex Medical Analytics; Manuela Vecsler: *Employee*, Ibex Medical Analytics; Chaim Linhart: *Employee*, Ibex Medical Analytics

Background: Computer-assisted diagnostic solutions to evaluate gastric biopsies hold promise to increase efficiency and accuracy in diagnosis. Despite several proof-of-concept studies, there remains a need for an AI-based solution that detects both cancer, as well as other pathologies with high accuracy that has been validated on large cohorts. A large healthcare provider with a centralized pathology laboratory handles > 140,000 histology accessions annually, of which ~ 18,000 are gastric biopsies. The growing shortage of pathologists, along with increased cancer incidence, has driven this lab, and others, to search for technologies to support pathologists in their diagnostic work.

OBJECTIVE: To clinically validate the performance of an AI-based algorithm in the detection of gastric adenocarcinoma (AdC), high-grade (HG) dysplasia, and H. pylori, and to implement it in routine clinical workflow.

Design: The algorithm, which is based on an ensemble of convolutional neural networks, was initially trained on > 750,000 image samples obtained from 1251 gastric biopsy slides (from multiple labs) that were manually annotated for relevant features by senior pathologists. The subsequent validation study was conducted on an AdC enriched set of 1,872 gastric biopsies (2,201 H&E slides) that were scanned at 40x magnification. These validation cases were distinct from the original training set. The algorithm was run in a blinded manner on the scanned slides and results were compared to the original pathology reports (ground truth).

Results: The algorithm demonstrated very high accuracy when compared with the ground truth in the detection of gastric AdC and high-grade dysplasia, with an area under the ROC curve (AUC) of 0.991 (Table 1). Additionally, the algorithm achieved an AUC of 0.913 for the detection of H. pylori. Following the validation study, the lab deployed the AI algorithm as a quality assurance system on all new gastric biopsies, where every biopsy result rendered by a pathologist is subsequently reviewed by the algorithm in real-time. The algorithm raises an alert whenever it encounters a potential discrepancy between the automated AI analysis and the original diagnosis, prompting a second human review.

Table 1 Algorithm performance

Analysis	Number of cases # positive/ negative cases	Performance			PPV	NPV
		AUC	Specificity	Sensitivity		
AdC / HG dysplasia	1,872 227 positive 1,615 negative	0.991	96.04%	96.04%	77.3%	99.4%
H. pylori	1,742 639 positive 1,103 negative	0.913	84.8%	85.4%	77.1%	90.7%

Conclusions: This study reports the successful large-scale validation and clinical implementation of an AI-based algorithm for detecting adenocarcinoma, high-grade dysplasia, and H. pylori in gastric biopsies, offering an important tool for computer-aided diagnosis in routine pathology practice.

479 Gastric Glandular Siderosis (GGS) but Not Lamina Propria Siderosis (LPS) is Associated with High Serum Ferritin Levels

Mrinal Sarwate[1], Neha Khaitan[2], Lindsay Alpert[3], Nika Tavberidze[4], Wei Zhang[5], Shaomin Hu[2]
[1]Cleveland Clinic Foundation, Cleveland, OH, [2]Cleveland Clinic, Cleveland, OH, [3]University of Chicago, Chicago, IL, [4]University of Wisconsin School of Medicine and Public Health, Madison, WI, [5]University of Wisconsin School of Medicine and Public Health/UW Health, Madison, WI

Disclosures: Mrinal Sarwate: None; Neha Khaitan: None; Lindsay Alpert: None; Nika Tavberidze: None; Wei Zhang: None; Shaomin Hu: None

Background: Three histologic patterns of gastric siderosis have been described. Pattern A (predominantly in the lamina propria stromal cells - LPS) and pattern B (mostly extracellular) have been associated with oral iron pill use and prior gastric mucosal injury. The clinical significance of pattern C (predominantly in deep glands - GGS) remains unknown.

Design: Two cohorts of cases were identified from 3 academic centers. Cohort #1 included 51 GGS cases with variable LPS and 5 cases with only LPS. Cohort #2 contained 27 gastric cases from patients with genetically confirmed hereditary hemochromatosis. Each case was evaluated for histopathologic features in the gastric (all cases) and liver (cohort #2 only) specimens. Clinical data were obtained by chart review.

Results: A total of 56 gastric siderosis cases (10 with GGS only, 10 with GGS and rare LPS, 31 with GGS and overt LPS, and 5 with LPS only) were identified (mean patient age 58, F:M ratio 1.3). Upon classifying the cases into 4 groups by percentage of glandular involvement (0%, n=5; <5%, n=10; 5 - <50%, n=30; ≥50%, n=11), regardless of LPS status, the degree of GGS was positively associated with serum ferritin levels ($p < 0.0001$) and blood transfusion ($p = 0.005$), negatively associated with oral iron pill use ($p = 0.01$), and not correlated with gastric mucosal injury (Table 1). The same cases were re-classified into 3 groups by degree of LPS (negative, n=10; rare, n=10; overt, n=36), regardless of GGS status, and the degree of LPS was positively correlated with oral iron pill use ($p = 0.005$), gastric mucosal injury ($p = 0.009$) and PPI use ($p = 0.04$), but not serum ferritin levels or blood transfusion. Minimal GGS (<5%) was mostly associated with overt LPS, although this was not statistically significant. Neither GGS nor LPS showed correlation with patient age, sex, alcohol abuse, NSAIDs use, degree of liver fibrosis or iron deposition, presence of esophageal varices or hereditary hemochromatosis. Gastric specimens from 27 patients with hereditary hemochromatosis (mean age 59, M:F ratio 2.9, 8 with cirrhosis, 11 with ≥3+ hepatic iron deposition) were also analyzed. GGS was identified in 1 patient who also had high serum ferritin level; none of the gastric biopsies showed LPS.

Table 1. Association of clinicopathologic features with degree of gastric glandular siderosis and lamina propria siderosis

			Degree of gastric glandular siderosis[#]					Degree of lamina propria siderosis[$]			
		All patients (n=56)	0% (n=5)	<5% (n=10)	5 - <50% (n=30)	≥50% (n=11)	p value	Negative (n=10)	Rare (n=10)	Overt (n=36)	p value
Age (years, mean ± SD)		58.3 ± 18.4	66.0 ± 23.2	69.3 ± 16.9	56.5 ± 18.1	49.6 ± 14	0.06	54 ± 15.2	52.8 ± 15.2	61 ± 19.8	0.52
Sex	**Male**	24	2	4	11	7	0.48	6	5	13	0.33
	Female	32	3	6	19	4		4	5	23	
Degree of lamina propria siderosis	**No**	10	0	0	8	2	0.11	N/A	N/A	N/A	N/A
	Rare	10	0	1	5	4		N/A	N/A	N/A	
	Overt	36	5	9	17	5		N/A	N/A	N/A	
Serum ferritin level (ng/ml, mean ± SD)		1328.9 ± 2518.7	116.7 ± 118.7	165.8 ± 253.2	655.7 ± 1373.6	4500.6 ± 3668.6	**<0.0001***	1087.9 ± 1689.2	2043.9 ± 3153.4	1207.0 ± 2554.5	0.65
Serum ferritin level	**Normal**	27	4	6	17	0	**0.001***	5	4	18	0.85
	High	26	1	2	12	11		4	5	17	
Gastric mucosal injury[&]	**No**	9	0	2	4	3	0.52	3	4	2	**0.009***
	Yes	47	5	8	26	8		7	6	34	
Oral iron pill use	**No**	22	0	2	12	8	**0.01***	8	5	9	**0.005***
	Yes	34	5	8	18	3		2	5	27	
Blood transfusion	**No**	35	4	6	23	2	**0.005***	7	4	24	0.26
	Yes	21	1	4	7	9		3	6	12	
Alcohol abuse	**No**	50	4	10	27	9	0.51	7	10	33	0.12
	Yes	6	1	0	3	2		3	0	3	
NSAIDs use	**No**	45	5	8	23	9	0.68	9	8	28	0.79
	Yes	11	0	2	7	2		1	2	8	
Proton pump inhibitor (PPI) use	**No**	20	2	5	10	3	0.71	7	3	10	**0.04***
	Yes	36	3	5	20	8		3	7	26	
Hereditary hemochromatosis	**No**	55	5	10	29	11	0.83	9	10	36	0.35
	Yes	1	0	0	1	0		1	0	0	
Esophageal varices	**No**	50	4	10	26	10	0.59	8	8	34	0.16
	Yes	6	1	0	4	1		2	2	2	

[#] The patients were divided into 4 groups based on the percentage of deep glandular involvement, regardless of lamina propria siderosis status
[$] The same patients were classified into 3 groups based on the degree of lamina propria siderosis, regardless of the glandular siderosis status
*** Indicate statistically significant**
[&] Gastric mucosal injury includes erosion, ulceration, reactive gastropathy and significant gastritis
N/A: Not applicable

Conclusions: GGS is associated with high serum ferritin levels and history of blood transfusion, whereas LPS is correlated with oral iron pill use, gastric mucosal injury and PPI use. There is no direct association between GGS and hereditary hemochromatosis or alcohol abuse.

480 Metastases to the Small Intestine: A Clinical and Pathologic Correlation Study

Radhika Sekhri[1], Kevin Kuan[1], Nicole Panarelli[2]
[1]Albert Einstein College of Medicine, Montefiore Medical Center, Bronx, NY, [2]Montefiore Medical Center - Moses Division, Bronx, NY

Disclosures: Radhika Sekhri: None; Kevin Kuan: None; Nicole Panarelli: None

Background: The small intestine is the most common recipient of metastatic malignancies in the tubal gastrointestinal tract; however, data on sites of origin are limited to clinical and autopsy case reports. The purpose of this study was to systematically evaluate patterns of metastatic spread to the small intestine and correlate site of origin with clinical presentation to provide guidance for histologic evaluation.

Design: We retrospectively searched clinical and pathology databases for small intestinal biopsy and resection specimens that contained metastatic malignancies between 1998 and 2021. Intra-abdominal tumors with direct extension to the small intestine were excluded. Demographic and clinical data were extracted from the electronic medical record.

Results: The study group included 62 patients (M:F = 0.7:1) with a mean age of 63 years. Cases included 7 biopsy and 55 resection specimens. Gynecologic and lower gastrointestinal tumors accounted for >50% of total cases and were also the most common malignancies to have their first recurrence in the small intestine along with those of urinary tract origin (Table 1). In 4 patients, small intestinal metastasis represented the first clinical presentation of their primary malignancy; these included 2 metastases from the lower gastrointestinal tract, one melanoma and one adenocarcinoma from the lung. Among sites of origin, the recurrence interval was longest for lower gastrointestinal cancers (mean: 50 months), whereas other tumor types tended to present with metastases within 2 years of original diagnosis.

Table 1. Metastases to the Small Intestine By Clinical Presentation

Site	Proportion of Total Metastases no. (%) (n=62)	Proportion of Small Intestine as First Recurrence no. (%) (n=42)	Proportion of Small Intestine as First Presentation of Malignancy no. (%) (n=4)	Time to Small Intestinal Recurrence for Known Primaries Mean (range), months
Lower gastrointestinal tract	19 (31)	16 (38)	2 (50)	50 (4-420)
Gynecologic tract	20 (32)	13 (31)	0	15 (2-48)
Genitourinary tract	11 (18)	7 (17)	0	23 (6-240)
Lung	4 (6)	3 (7)	1 (25)	7 (2-12)
Upper gastrointestinal tract	3 (5)	1 (2)	0	7 (1-12)
Melanoma	3 (5)	1 (2)	1 (25)	16 (15-18)
Breast	2 (3)	1 (2)	0	12

Conclusions: Most small intestinal metastases originate from lower gastrointestinal and gynecologic cancers in patients with known histories. Less common primary tumors, including melanoma and those from the lung, breast, and upper gastrointestinal tract tend to present with small intestinal metastasis shortly after initial diagnosis, and a recent history of these malignancies should raise suspicion for malignant etiology of a small intestinal stricture. Metastases from unsuspected malignancies originate from the same sites as known tumors; this pattern may help guide immunohistochemical workup of malignant strictures when no primary tumor is documented.

481 Practical Implications of Tumor Budding and Poorly Differentiated Clusters in pT1 Colonic Adenocarcinoma

Radhika Sekhri[1], Kevin Kuan[1], Nicole Panarelli[2]
[1]Albert Einstein College of Medicine, Montefiore Medical Center, Bronx, NY, [2]Montefiore Medical Center - Moses Division, Bronx, NY

Disclosures: Radhika Sekhri: None; Kevin Kuan: None; Nicole Panarelli: None

Background: Tumor budding (TB) and poorly differentiated clusters (PDC) are emerging risk factors for lymph node metastases in pT1 colonic adenocarcinomas that may prompt surgical resection for endoscopically-removed tumors. Reporting of these features as distinct from high-grade adenocarcinoma (HGC) may cause confusion among clinical colleagues who are unfamiliar with their implications. We performed this study to assess the prevalence of TB and PDC in unselected cases of pT1 colonic adenocarcinoma and their association with other features that pose a risk for lymph node metastases.

Design: We retrospectively identified consecutive cases of endoscopically (n=20) or surgically (n=22) resected pT1 colonic adenocarcinomas. Cases were reviewed by two pathologists for any HGC component, lymphovascular invasion (LVI), TB, and PDC. pT category, tumor grade, and TB grade were assigned according to College of American Pathologists' protocols. PDC were assessed as present or absent. Clinical follow-up information was derived from the electronic medical record.

Results: The study group includes 23 male and 19 female patients (average age: 67 years). Polyps were sessile (n=16) or pedunculated (n=26) and removed from the ascending (n=13), transverse (n=6), descending (n=4), or sigmoid (n=19) colon. Twenty-six study cases lacked any high-risk features. Of these 16 underwent primary surgical resection or subsequent resection due to close margin clearance, yielding 2 cases with 1 positive lymph node each. Sixteen study cases displayed 1 or more high-risk feature (Table). TB was present in 11 cases and was low-grade in 10 cases and intermediate-grade in 1 case. It occurred in isolation in 1 case (Figure 1A and B) or was associated with only PDC in 3 cases (Figure 1C and D), but with more established high-risk features, including LVI (n=7) and/or HGC (n=3) in most cases (64%). Data from resection specimens were available in 9 cases, and lymph node metastases were present in 2, 1 of which had TB and PDC, but no other high-risk features.

Table: Patterns of High-risk Features in Study Cases

Risk factors	Cases (n=16) No. (%)
Only LVI	3 (18.75)
TB + PDC	3 (18.75)
Only HGC	2 (12.5)
TB + LVI	2 (12.5)
TB + LVI + PDC	2 (12.5)
TB + LVI + PDC + HGC	2 (12.5)
Only TB	1 (6.25)
TB + LVI + HGC	1 (6.25)
Total	**16**

Figure 1 - 481

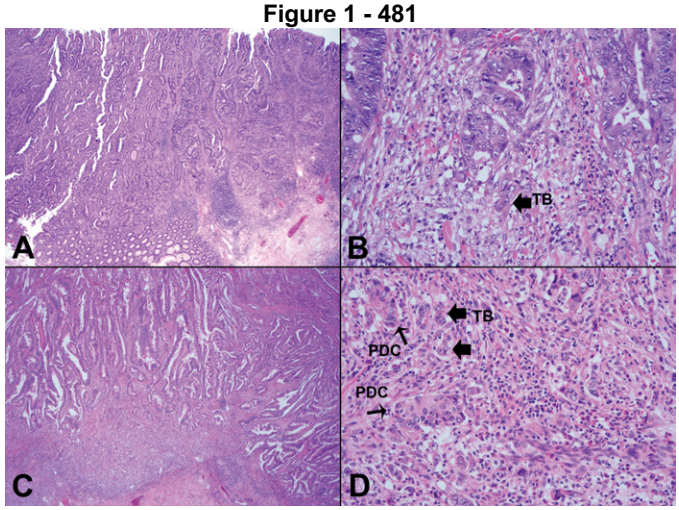

Conclusions: Most pT1 colonic adenocarcinomas with TB and/or PDC have other high-risk features that will drive surgical management. However, approximately 10% of total pT1 adenocarcinomas, in our series, had these features in isolation. The presence of lymph node metastases in 1 of 2 such cases with follow-up highlights the practical importance of discussing TB and PDC with clinical colleagues if these terms are used in reports.

482 Gastric Intestinal Metaplasia is a Risk Factor for Progression to Gastric Dysplasia and Carcinoma in Patients Who Undergo Gastric Biopsy: A Population-Based Study

Akram Shalaby[1], Melissa Kukowski[2], Cathy (Changqing) Ma[3], Jon Davison[4]
[1]University of Pittsburgh Medical Center Presbyterian Shadyside, PA, [2]University of Pittsburgh, Pittsburgh, PA, [3]Barnes-Jewish Hospital/Washington University, St. Louis, MO, [4]University of Pittsburgh School of Medicine, Pittsburgh, PA

Disclosures: Akram Shalaby: None; Melissa Kukowski: None; Cathy (Changqing) Ma: None; Jon Davison: None

Background: There is uncertainty over the cancer risk associated with gastric intestinal metaplasia (GIM) in the United States, a region with a relatively low incidence of gastric carcinoma (GC). We evaluated progression to gastric dysplasia or GC in large retrospective cohort of patients who underwent gastric biopsy.

Design: We searched for pathology reports from January 2005 to June 2021 for adults who underwent gastric biopsy for any clinical indication, in a multi-hospital healthcare system in Allegheny County, Pennsylvania. Natural language processing techniques were used to identify GIM (excluding IM at the GE junction and Barrett's esophagus), Helicobacter infection, dysplasia, and carcinoma with >99.5% verified accuracy. Progression was defined as: (1) any diagnosis of low grade dysplasia (LGD), high grade dysplasia (HGD), or carcinoma; (2) located in the stomach based on review of endoscopy reports and surgical resection specimens, and (3) diagnosed >6 months after the index non-dysplastic gastric biopsy.

Results: There were 18,647 patients included (Figure 1), with an average of 4.3 years of follow up, including 87 who subsequently progressed (48 LGD, 11 HGD, and 28 GC), an average of 3.5 years after initial endoscopy (Table 1). There were 2705 patients (14.5%) with non-dysplastic GIM, including 56.3% of progressors and 14.3% of non-progressors (Table 1), translating to a significantly higher rate of progression to dysplasia or GC in patients with GIM ($P<10^{-25}$, Figure 2). The incidence rate of GC was 1.2/1000 patient-years with non-dysplastic GIM, similar to that observed in other large population-based studies (1.0-2.5/1000 patient-years, PMID: 29228909), and similar to the incidence rate of adenocarcinoma in non-dysplastic Barrett's esophagus (1.0-3.0/1000 patient-years, PMID: 26021191). Adjusting for sex, age, race/ethnicity and Helicobacter gastritis, patients with non-dysplastic GIM were 5.6-fold (95% CI 3.6-8.6, $P<10^{-13}$) more likely to progress to dysplasia or GC compared to patients with no GIM.

	Non-progressors N=18,560	Progressors N=87	P value
Age, mean (range)	56.1 (18.0-96.6)	65.0 (21.3-94.5)	<0.000001
Sex, n (%) Male Female	6558 (35.3) 12002 (64.7)	32 (36.8) 55 (63.2)	0.778
Race/ethnicity, n (%) White Black Asian, Pacific Islander Other	15830 (85.3) 2171 (11.7) 263 (1.4) 296 (1.6)	68 (78.2) 18 (20.7) 0 (0) 1 (1.1)	0.073
Gastric intestinal metaplasia, n (%) Yes No	2656 (14.3) 15904 (85.7)	49 (56.3) 38 (43.7)	<0.000001
Helicobacter gastritis, n (%) Yes No	977 (5.3) 17583 (94.7)	11 (12.6) 76 (87.4)	0.006
End (highest) neoplasia grade, n (%) Negative for Dysplasia Low-grade Dysplasia High-grade Dysplasia Carcinoma	18560 (100) 0 (0) 0 (0) 0 (0)	0 (0) 48 (55.2) 11 (12.6) 28 (32.2)	N/A
Years to end of follow-up, mean (range)	4.3 (0.5-16.3)	3.5 (0.7-9.4)	0.014
Total number of endoscopies, mean (range)	2.5 (2.0-19.0)	3.9 (2.0-14.0)	<0.000001

Figure 1 - 482

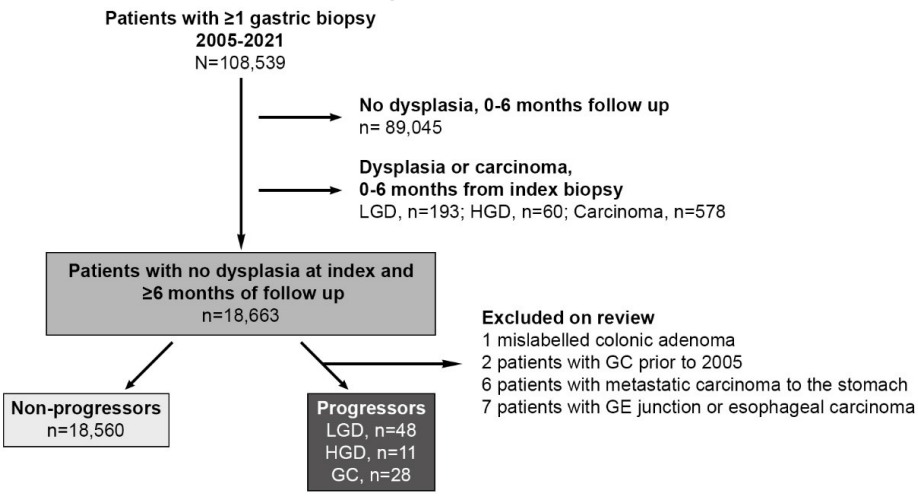

Figure 2 – 482

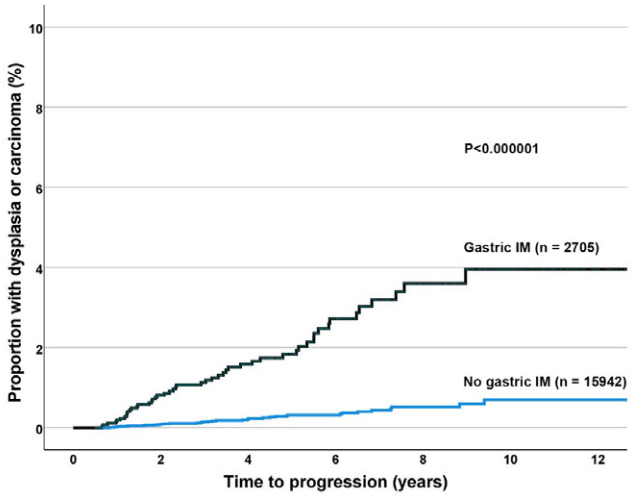

Conclusions: Patients with non-dysplastic GIM were more than 5 times as likely to progress to dysplasia or GC when compared to those without GIM, in one of the largest US population-based cohorts to date. Patients with GIM had a rate of progression to carcinoma similar to non-dysplastic Barrett's esophagus. However, given the low absolute rate of progression, stratification of patients with non-dysplastic GIM into low- and high-risk groups will better inform surveillance recommendations.

483 Additional Validation of a Deep Learning Algorithm to Quantify Histologic Features in Colorectal Carcinoma

Sameer Shivji[1], Reetesh Pai[2], Christophe Rosty[3], Daniel Buchanan[4], Mark Jenkins[4], Loic Le Marchand[5], Polly Newcomb[6], Steven Hart[7], Daniela Baum[8], Robert Grant[9], Noralane Lindor[8], Douglas Hartman[10], David Schaeffer[11], David Cyr[12], James Conner[13], Richard Kirsch[13], Rish Pai[8]

[1]Sinai Health System, Toronto, Canada, [2]UPMC Presbyterian Hospital, Pittsburgh, PA, [3]Envoi Specialist Pathologists, Brisbane, Australia, [4]University of Melbourne, Melbourne, Australia, [5]University of Hawaii, Honolulu, HI, [6]Fred Hutchinson Cancer Research Center, Seattle, WA, [7]Mayo Clinic, Rochester, MN, [8]Mayo Clinic, Scottsdale, AZ, [9]Princess Margaret Cancer Centre, University of Toronto, Toronto, Canada, [10]University of Pittsburgh Medical Center, Pittsburgh, PA, [11]Vancouver General Hospital, Vancouver, Canada, [12]University of Toronto, Toronto, Canada, [13]Mount Sinai Hospital, Toronto, Canada

Disclosures: Sameer Shivji: None; Reetesh Pai: *Consultant*, Alimentiv (formerly Robarts Clinical Trials); Christophe Rosty: None; Daniel Buchanan: None; Mark Jenkins: None; Loic Le Marchand: None; Polly Newcomb: None; Steven Hart: None; Daniela Baum: None; Robert Grant: None; Noralane Lindor: None; Douglas Hartman: *Speaker*, Philips; *Consultant*, Up To Date; *Consultant*, Iqvia; David Schaeffer: *Consultant*, Alimentiv Inc; *Advisory Board Member*, Satisfai Health Inc.; *Consultant*, Merck Canada, Pfizer, Diaceutics, Astellas; David Cyr: None; James Conner: None; Richard Kirsch: None; Rish Pai: *Consultant*, Alimentiv Inc, Allergan, Verily, Eli Lilly, AbbVie, PathAI

Background: We recently described the development and initial validation of a novel deep learning algorithm to evaluate and quantify histologic features in colorectal cancer (CRC), which demonstrated significant associations between algorithm-derived features and adverse prognostic factors derived from pathologist-based assessment (e.g. lymph node metastases, lymphovascular invasion, and stage) in a small cohort. In this study, we sought to apply this algorithm to a larger cohort of CRCs to further evaluate the association between algorithm-based assessment and expert pathologist assessment. Further, we also evaluated the relationship between algorithm derived features, molecular alterations, and CD8 immunohistochemistry.

Design: 4543 unique CRCs from 6 different cohorts were included in this study; pathologic data for each case was obtained from the final surgical pathology report, with a subset additionally having undergone expert pathologist review for the assessment of TB, PDC, and venous invasion. For each case, a single tumour slide deemed to be representative was digitized and evaluated by the algorithm. The algorithm segmented the tumor bed into: carcinoma (subclassified as low grade, high grade, signet ring), fat, mucin, necrosis, TB/PDC (as one feature), smooth muscle, and stroma (subclassified as immature, mature, inflammatory). Tumor

infiltrating lymphocytes (TILs) were captured as objects. The associations between algorithm outputs, expert pathologist assessment, molecular alterations, and CD8 T-cell density was evaluated.

Results: Pathologist-derived PDC and TB grade were strongly associated with algorithm measures of TB/PDC (Table 1 and Figure 1), tumor:stroma ratio, immature stroma, inflammatory stroma, and TILs. Lymphatic, venous, and perineural invasion also had significant associations with algorithm measures of TB/PDC, immature stroma, inflammatory stroma, high-grade morphology, tumor:stroma ratio, and TILs (Table 1). When stratified by mismatch repair (MMR) status, *BRAF* mut, *KRAS* mut, and CpG island methylation, significant differences in algorithm-derived features were identified (Table 1 and Figure 2). Finally, CD8 T-cell density was strongly associated with algorithm measures of TILs and inflammatory stroma.

Table 1. Associations between quantitative segmentation algorithm and clinicopathologic characteristics and molecular alterations.

Characteristic	Median Tumor: Stroma ratio (IQR)	Median %TB/PDC (IQR)	Median %Mucin (IQR)	Median %High-Grade (IQR)	Median %Immature Stroma (IQR)	Median %Inflammatory Stroma (IQR)	Median TILs per mm^2 of carcinoma (IQR)
Tumor budding							
Bd1 (N=492)	1.4 (1.0)	0.5 (0.8)	0.7 (17.0)	9.8 (17.2)	27.0 (15.5)	5.4 (7.0)	44.3 (66.4)
Bd2 (N=192)	1.1 (0.9)	1.1 (2.0)	0.3 (3.6)	12.8 (19.3)	33.0 (16.1)	4.1 (5.9)	35.1 (40.3)
Bd3 (N=239)	0.8 (0.7)	3.0 (3.7)	0.7 (4.4)	12.4 (18.0)	39.6 (20.4)	3.0 (4.0)	27.7 (30.1)
P-value	<0.0001	<0.0001	0.04	0.03	<0.0001	<0.0001	<0.0001
Lymphatic invasion							
No (N=1070)	1.3 (1.0)	0.7 (1.3)	1.5 (14.2)	9.3 (16.3)	33.0 (17.6)	3.8 (6.4)	39.5 (62.6)
Yes (N=762)	1.0 (0.9)	1.4 (2.9)	0.8 (6.0)	13.5 (23.2)	35.6 (19.1)	3.0 (5.1)	32.6 (39.9)
P-value	<0.0001	<0.0001	<0.0001	<0.0001	<0.0001	0.001	<0.0001
Perineural invasion							
No (N=1196)	1.3 (1.0)	0.8 (1.4)	0.9 (12.3)	9.9 (17.8)	32.0 (17.7)	4.0 (6.4)	37.8 (57.1)
Yes (N=330)	0.8 (0.7)	2.3 (3.9)	1.2 (6.5)	14.9 (22.4)	40.2 (20.7)	2.3 (3.9)	30.1 (33.7)
P-value	<0.0001	<0.0001	0.7	<0.0001	<0.0001	<0.0001	<0.0001
Venous invasion							
No (N=2832)	1.2 (1.0)	0.9 (1.7)	1.9 (14.4)	10.9 (19.4)	36.4 (18.6)	3.0 (5.2)	34.1 (51.3)
Yes (N=901)	0.9 (0.8)	1.9 (3.6)	1.3 (6.1)	15.2 (25.4)	41.6 (21.3)	2.3 (3.8)	27.8 (34.4)
P-value	<0.0001	<0.0001	<0.0001	<0.0001	<0.0001	<0.0001	<0.0001
Poorly differentiated clusters							
PDC G1 (N=397)	1.3 (1.0)	0.6 (1.0)	0.4 (7.5)	9.1 (12.8)	30.9 (15.8)	5.4 (8.0)	49.1 (53.5)
PDC G2 (N=133)	0.9 (0.8)	1.6 (2.5)	0.6 (5.7)	10.4 (18.1)	41.3 (21.8)	3.9 (5.0)	30.3 (40.5)
PDC G3 (N=98)	0.8 (0.7)	2.7 (3.9)	0.4 (2.2)	18.1 (22.4)	36.9 (21.3)	3.6 (4.1)	28.3 (21.8)
P-value	<0.0001	<0.0001	0.2	0.004	<0.0001	<0.0001	<0.0001
KRAS							
Wild-Type (N=1660)	1.1 (0.9)	1.1 (2.1)	2.7 (13.5)	12.6 (22.5)	37.1 (18.2)	2.6 (4.6)	32.6 (48.5)
Mutated (N=909)	1.1 (1.0)	1.2 (2.5)	1.6 (9.4)	10.4 (17.4)	39.0 (19.3)	2.1 (3.65)	28.8 (43.7)
P-value	1.0	0.2	<0.0001	<0.0001	0.001	<0.0001	0.001
BRAF							
Wild-type (N=2584)	0.9 (1.3)	1.2 (2.1)	1.7 (9.1)	11.2 (19.3)	38.9 (19.1)	2.3 (4.0)	29.1 (40.4)
Mutated (N=403)	1.3 (1.2)	1.3 (2.5)	9.3 (31.9)	22.1 (38.1)	34.0 (20.0)	3.4 (5.3)	53.2 (90.8)
P-value	<0.0001	0.3	<0.0001	<0.0001	<0.0001	<0.0001	<0.0001
MMR status							
MMRP (N=3146)	1.0 (0.9)	1.2 (2.4)	1.5 (6.7)	11.1 (18.0)	39.1 (19.5)	2.4 (4.1)	27.5 (35.2)
MMRD (N=875)	1.4 (1.1)	0.9 (1.7)	9.5 (33.6))	19.0 (38.8)	33.2 (18.6)	4.2 (6.7)	69.7 (104.4)
P-value	<0.0001	<0.0001	<0.0001	<0.0001	<0.0001	<0.0001	<0.0001
CpG Island Methylation (CIMP)							
Negative (N=1310)	1.1 (0.91)	1.2 (2.1)	1.9 (7.31)	11.2 (18.3)	39.6 (18.1)	2.2 (3.7)	29.3 (39.4)
Positive (N=203)	1.2 (1.0)	1.7 (3.5)	9.8 (28.9)	22.9 (45.5)	37.1 (17.9)	3.2 (5.4)	62.4 (99.3)
P-value	0.02	<0.0001	<0.0001	<0.0001	0.02	<0.0001	<0.0001
CD8 T-cell density							
Low (N=130)	1.2 (1.2)	1.3 (2.5)	0.6 (5.8)	12.0 (18.8)	30.1 (15.8)	2.1 (2.6)	31.6 (30.1)
Intermediate/High (N=295)	1.3 (1.0)	0.8 (1.5)	0.9 (14.1)	11.4 (21.9)	25.6 (13.1)	6.1 (7.6)	47.9 (73.4)
P-value	0.9	0.002	1.0	0.9	<0.0001	<0.0001	<0.0001

Figure 1 - 483

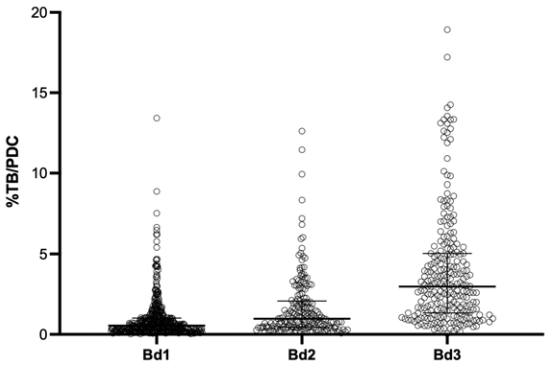

Figure 2 - 483

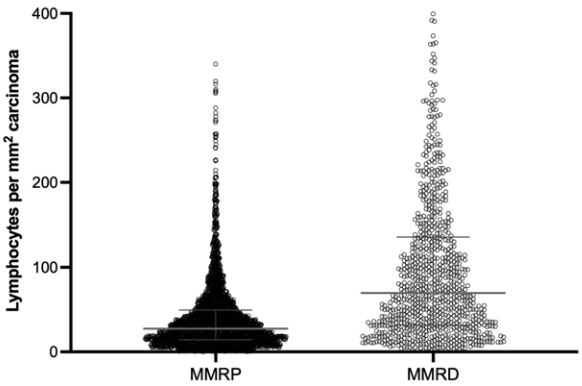

Conclusions: The findings further validate this quantitative segmentation algorithm, suggesting that this algorithm may prove a useful ancillary tool in the histologic and molecular assessment of CRC.

484 Quantitative Pathologic Analysis of Colorectal Carcinoma using Deep Learning Identifies Prognostic Histologic Signatures Independent of Stage and Mismatch Repair Status

Sameer Shivji[1], Reetesh Pai[2], Christophe Rosty[3], Daniel Buchanan[4], Mark Jenkins[4], Loic Le Marchand[5], Polly Newcomb[6], Steven Hart[7], Daniela Baum[8], Robert Grant[9], Noralane Lindor[8], Douglas Hartman[10], David Schaeffer[11], David Cyr[12], James Conner[13], Richard Kirsch[13], Rish Pai[8]

[1]Sinai Health System, Toronto, Canada, [2]UPMC Presbyterian Hospital, Pittsburgh, PA, [3]Envoi Specialist Pathologists, Brisbane, Australia, [4]University of Melbourne, Melbourne, Australia, [5]University of Hawaii, Honolulu, HI, [6]Fred Hutchinson Cancer Research Center, Seattle, WA, [7]Mayo Clinic, Rochester, MN, [8]Mayo Clinic, Scottsdale, AZ, [9]Princess Margaret Cancer Centre, University of Toronto, Toronto, Canada, [10]University of Pittsburgh Medical Center, Pittsburgh, PA, [11]Vancouver General Hospital, Vancouver, Canada, [12]University of Toronto, Toronto, Canada, [13]Mount Sinai Hospital, Toronto, Canada

Disclosures: Sameer Shivji: None; Reetesh Pai: None; Christophe Rosty: None; Daniel Buchanan: None; Mark Jenkins: None; Loic Le Marchand: None; Polly Newcomb: None; Steven Hart: None; Daniela Baum: None; Robert Grant: None; Noralane Lindor: None; Douglas Hartman: None; David Schaeffer: None; David Cyr: None; James Conner: None; Richard Kirsch: None; Rish Pai: None

Background: Novel histologic features, including tumour budding (TB), poorly differentiated clusters (PDC), and stroma type, have gained attention as adverse prognostic features in colorectal cancer (CRC). Challenges related to optimal means of assessment have limited their wide-spread adoption. We recently described the development and validation of a deep learning algorithm to quantify these histologic features in CRC. In this study, we applied this algorithm to a large cohort of CRCs to evaluate the association between these features and recurrence.

Design: 3618 stage 1-3 CRCs from 6 centers were collected of which 2951 had recurrence data. For each CRC, one representative slide was digitized and evaluated by the algorithm. The algorithm segmented the tumor bed into: carcinoma (subclassified as low grade, high grade, signet ring), fat, mucin, necrosis, TB/PDC (as one feature), smooth muscle, and stroma (subclassified as immature, mature, inflammatory). Tumor infiltrating lymphocytes (TILs) were captured as objects (Figure 1). K-means clustering was used to identify histologic signatures. Recurrence was evaluated using Kaplan-Meier. Hazard ratios were calculated from a Cox proportional hazard model using histologic signature, stage and MMR status.

Results: When assessed on the basis of quartiles, TB/PDC (*P*=1.7E-26), TILs (*P*=4.9E-18), tumor:stroma ratio (*P*=5.4E-11), immature stroma (*P*=3.4E-21), inflammatory stroma (*P*=1.9E-22), mature stroma (*P*=0.00004), and signet ring morphology (*P*=0.046) were significantly associated with recurrence free survival (RFS) (median follow up 62mo). K-means clustering identified 5 histologic signatures: Signature 1 (abundant TILs and inflammatory stroma), Signature 2 (high tumor:stroma ratio and low TB/PDC), Signature 3 (intermediate for all features), Signature 4 (high immature stroma, high TB/PDC, low tumor:stroma ratio), and Signature 5 (high immature stroma, very high TB/PDC, low tumor:stroma ratio). These histologic signatures were significantly associated with RFS (log rank *P*=1.9E-30), with signature 1 showing the most favorable clinical outcomes and signatures 4 and 5 the worst (Figure 1). This association was independent of stage and MMR status (Table 1).

Table 1. Cox proportional hazard regression analysis of recurrence free survival.

Variable	Univariate		Multivariate	
	HR (95% CI)	*P*-value	HR (95% CI)	*P*-value
Stage				
Stage 1 (N=506)	1 (Referent)	--	1 (Referent)	--
Stage 2 (N=1185)	1.85 (1.32-2.57)	0.0003	1.51 (1.08-2.12)	0.02
Stage 3 (N=1260)	4.36 (3.18-6.00)	5.4E-20	3.10 (2.24-4.27)	7.6E-12
Mismatch Repair Status				
MMRP (N=2191)	1 (Referent)	--	1 (Referent)	--
MMRD (N=553)	0.33 (0.24-0.44)	1.9E-13	0.46 (0.34-0.62)	4.6E-7
Histologic Signature				
Signature 1 (N=312)	1 (Referent)	--	1 (Referent)	--
Signature 2 (N=504)	2.50 (1.51-4.14)	0.0003	2.13 (1.23-3.68)	0.007
Signature 3 (N=1399)	3.53 (2.21-5.61)	1.1E-7	2.74 (1.64-4.56)	0.0001
Signature 4 (N=718)	6.77 (4.24-10.80)	1.1E-15	4.36 (2.60-7.30)	2.1E-8
Signature 5 (N=18)	9.95 (4.50-22.00)	1.4E-8	7.24 (3.20-16.44)	0.000002

Figure 1 - 484

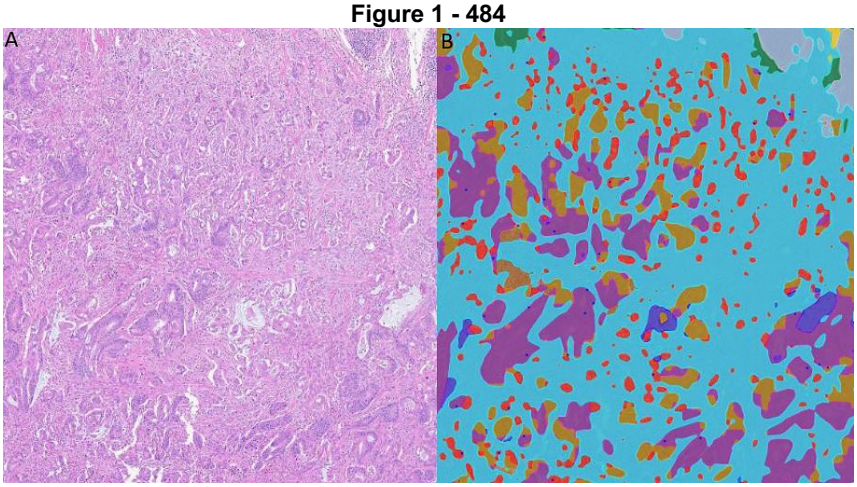

Figure 2 – 484

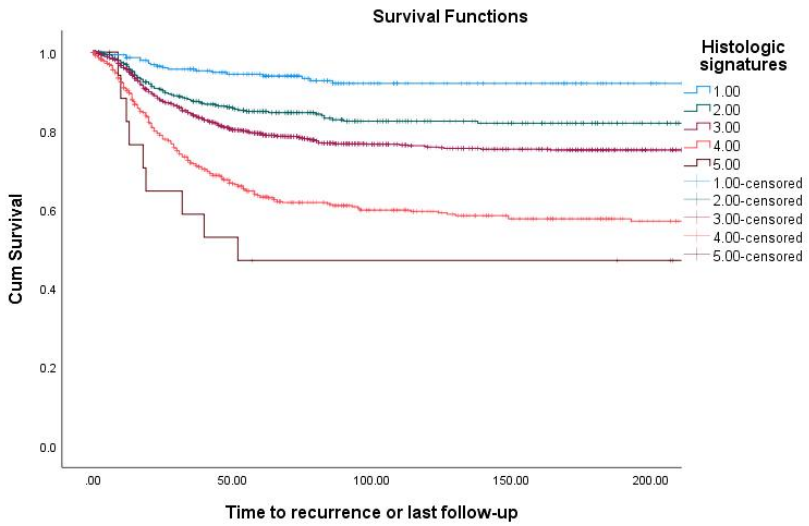

Conclusions: We identified 5 histologic signatures in CRC using deep learning that are associated with disease recurrence independent of stage and MMR status. Combined with routine pathologist-based assessment, these signatures may allow for more accurate risk stratification and personalized management.

485 HPV-related Adenocarcinoma of the Anorectum is a Rare Mimicker of Rectal Villous Adenomas: A Retrospective Single-center Series

Ayesha Siddique[1], Elizabeth Wu[2], Dongfang Yang[3], Sean Hacking[1], Evgeny Yakirevich[3]
[1]Alpert Medical School of Brown University, Providence, RI, [2]Rhode Island Hospital, Brown University, Providence, RI, [3]Rhode Island Hospital, Providence, RI

Disclosures: Ayesha Siddique: None; Elizabeth Wu: None; Dongfang Yang: None; Sean Hacking: None; Evgeny Yakirevich: None

Background: A recent series of HPV-related adenocarcinomas of the lower anogenital tract described rare tumors of the vagina, anorectum, and vulva that morphologically resembled endocervical adenocarcinomas.

The aims of this study were 1) to determine the frequency at which these tumors were mis-classified as rectal adenomas with a villous component, and 2) to determine the spectrum of p16 staining patterns in rectal adenomas that mimic this entity.

Design: A retrospective search of all anorectal and rectal adenomas with a villous component diagnosed between June 2015 and June 2020 was performed. The morphology of these adenomas was reviewed for the presence of a majority villous/villoglandular component, papillary architecture, abundant luminal serrations, and cytomorphologic features (i.e. foamy-gland features) resembling the previously described HPV-related anogenital adenocarcinomas. Cases meeting any of these criteria were stained for p16. Table 1 displays the inclusion criteria for our study. The spectrum of p16 positivity was scored from 0 to 3+ (Figure 1). HPV in situ hybridization was performed on tumors with diffuse, strong positivity (3+).

Results: Of 185 adenomas with a villous component, 22 had a villoglandular architecture and were selected for p16 IHC. Indications for colonoscopy included hematochezia (5; 22.7%), surveillance (6; 27.3%), abnormal imaging (9; 40.9%), rectal prolapse (1; 4.5%), being followed for FAP (1; 4.5%). Specimens included endoscopic mucosal resections (3; 13.6%), polypectomy (6; 27.3%), abdominoperineal resection (1; 4.5%), transanal excision (8; 36.4%), proctectomy (2; 9.1%), and low anterior resection (2; 9.1%).

Of these 22 cases, 2 were negative for p16 (9.1%); majority showed weak or focal immunoreactivity (13 cases; 59.1%), and some showed moderate, but heterogeneous staining (6 cases; 27.3%). One case demonstrated 3+ for p16. HPV in situ hybridization was done on this case and was positive for high-risk HPVs 16/18; HPV-ISH for 6, 11, 31, and 33 were negative, and were consistent with an HPV-related adenocarcinoma of the anorectum (Figure 2).

This patient was a 65 year old female who presented with hematochezia. The endoscopic findings displayed a 3.5cm anorectal polyp. The patient had adjacent anal intraepithelial neoplasia, Grade 3 but no known cervical dysplasia. The patient was alive and without disease at 6 months follow-up.

Table 1: Inclusion criteria
Step 1: All adenomas of the anorectum from June 2015 to June 2020 (n=1350)
Step 2: All adenomas with villous features (n=185)
Step 3: All adenomas with papillary or villiform/villoglandular architecture (n=22)
Step 4: p16 immunohistochemistry (n=22)
Step 5: HPV in situ hybridization for high risk HPV (n=1)

Figure 1 - 485

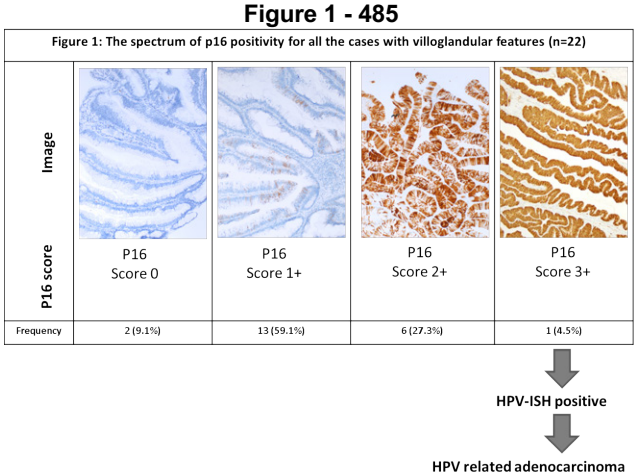

Figure 2 – 485

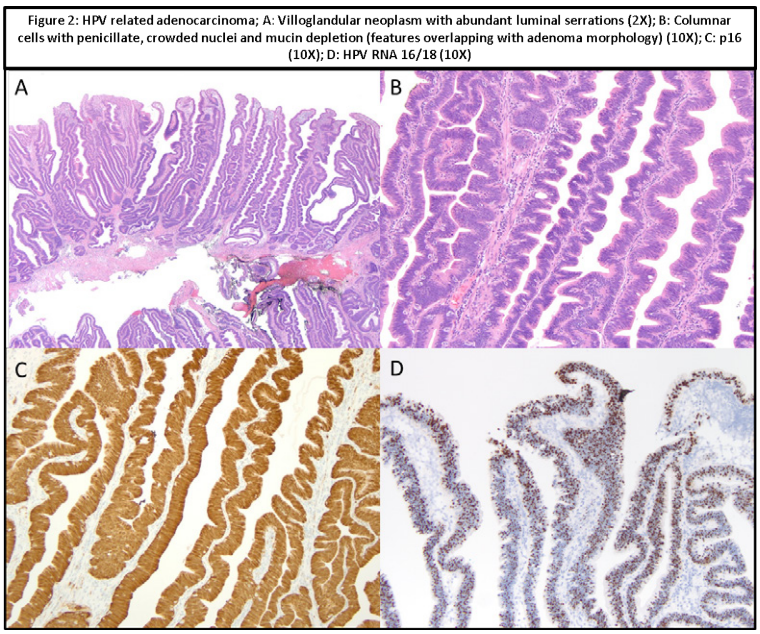

Conclusions: These findings suggest that p16 is a useful first line marker to distinguish adenomas from HPV adenocarcinomas

486 Digital Quantification Confirms Eosinophils are Increased in Mycophenolate Colitis Compared to Colonic Graft Versus Host Disease

Priyadharshini Sivasubramaniam[1], Benjamin VanTreeck[1], Lindsey Smith[2], Roger Moreira[1], Christopher Hartley[1], Catherine Hagen[1]
[1]Mayo Clinic, Rochester, MN, [2]Aiforia, Inc, Cambridge, MA

Disclosures: Priyadharshini Sivasubramaniam: None; Benjamin VanTreeck: None; Lindsey Smith: None; Roger Moreira: None; Christopher Hartley: None; Catherine Hagen: None

Background: Colonic graft versus host disease (GVHD) and mycophenolate (MMF) colitis have overlapping histologic features. A subset of stem cell transplant patients receive MMF as part of their prophylactic immunosuppressive regimen and are therefore at risk of developing both GVHD and MMF toxicity. Previous studies have suggested eosinophilic inflammation is a distinguishing feature of MMF toxicity. The aim of this study was to use digital image analysis to quantify eosinophils and compare cases of colonic GVHD and MMF colitis.

Design: Cases of colonic GVHD (n=30) and MMF colitis (n=15) were retrieved from the pathology archives. Normal colonic biopsies from transplant (n=10) and non-transplant (n=5) patients were selected for a control group. The degree of lamina propria eosinophilia was semiquantitavely graded via a low-power eyeball method: 0=rare/absent eosinophils, 1=normal number of eosinophils, 2=mildly increased eosinophils, or 3=markedly increased eosinophils. H&E stained whole-slide images were captured with Leica Aperio scanner at a resolution of 0.25um/pixel. The digitized images were then uploaded to Aiforia™ platform (Aiforia Inc., Cambridge, MA, USA) and convolutional neural networks (CNNs) were trained on annotations from 12 H&E-stained digitized slides. A model of two stacked CNNs was trained to identify (1) tissue, with epithelium versus lamina propria sublayers, and (2) eosinophils within the lamina propria sublayer only. This model was then applied to the remaining slides, with eosinophils normalized to mm2 of lamina propria.

Results: MMF colitis cases were more likely to have increased lamina propria eosinophils via semiquantitative analysis (2-3 vs. 0-1, 86.7% vs. 16.7%, p<0.0001) and via quantitative digital image analysis (mean 271.2 vs. 119.3 per stroma mm2, p=0.0019). The average quantitative eosinophil count for the control group was 181.5/stroma mm2. Quantitative eosinophil counts were not

significantly different for the GVHD (p=0.14) or MMF group (p=0.07) compared to the control group. The semiquantitative score correlated with increasing average quantitative eosinophil count (table 1) (p<0.0001)

Table 1: Comparison of quantitative eosinophil counts

Classification	Mean quantitative eosinophil count per stroma mm2 (range)	p-value (ANOVA or t-test)
Semiquantitative score	42.4 (2.6-107.1)	<0.0001
0	84.9 (9.8-259.7)	
1	239.3 (69.3-402.8)	
2	399.4 (198.9-641-2)	
3		
Clinical category	271.2 (31.7-569.5)	0.004
MMF	119.3 (2.7-641.2)	
GVHD	181.5 (7.9-402.9)	
Control		
Control group	181.3 (7.9-276.0)	0.99
Transplant	182.0 (47.6-402.9)	
Non-transplant		

Conclusions: Automated quantification of lamina propria eosinophils correlated with subjective semiquantitative evaluation of eosinophils. Digital analysis confirmed that lamina propria eosinophils are increased in cases of MMF colitis compared to colonic GVHD and may serve as an ancillary tool to distinguish these two entities.

487 Discrepant MMR Protein Status between Intestinal Adenoma and Carcinoma: Biological Significance and Practical Implication

Weihua Song[1], Chiyun Wang[1], Canan Firat[1], Binny Khandakar[1], Martin Weiser[1], Efsevia Vakiani[1], Zsofia Stadler[1], Jinru Shia[1]
[1]Memorial Sloan Kettering Cancer Center, New York, NY

Disclosures: Weihua Song: None; Chiyun Wang: None; Canan Firat: None; Binny Khandakar: None; Martin Weiser: None; Efsevia Vakiani: None; Zsofia Stadler: None; Jinru Shia: None

Background: The role of mismatch repair deficiency (MMRd) in Lynch syndrome (LS)-associated intestinal tumorigenesis, especially from a temporospatial perspective, has long been a topic of interest. Traditional view holds that MMRd serves to accelerate tumor progression after the tumor/adenoma has been initiated. More recently, there have been suggestions that subsets of LS tumors arise from preexisting MMRd-crypts either via the formation of an MMRd adenoma or through a “flat” pathway. In this study, we present a series of cases that provide further phenotypical insights on where in the LS- tumorigenesis pathway MMRd might occur and what it might imply biologically and clinically.

Design: Known LS cases with colorectal/small bowel tumors that exhibited discrepant intra-tumoral MMR IHC staining were evaluated pathologically, focusing on the topographic patterns of MMR staining along adenoma-carcinoma pathway. Sporadic MLH1-methylated tumors were included for comparison.

Results: Our study cases included 8 LS-associated and 3 MLH1 methylated intestinal tumors that had discrepant MMR IHC between adenoma and co-existing high-grade dysplasia (HGD, n=4) or carcinoma (n=7). While most tumors (including all MLH1-methylated) were discrepant in the form of “MMR-proficient (MMRp) in adenoma/MMRd in HGD or carcinoma”, 3 of 8 LS-associated tumors had a reversed pattern with MMRd in the adenoma and MMRp in HGD (n=1) or carcinoma (n=2) (Table 1, Fig. 1). In all tumors, the components that showed discrepant MMR IHC appeared distinctly clonal.

Table 1. Characteristics of the study cases.

Cases	Age/Sex	Tumor Site	LS/MLH1 methylated	MMR in Adenoma	MMR in HGD or Carcinoma
1	43/M	Rectum	MLH1 LS	MMRp	MMRd
2	36/M	Descending	PMS2 LS	MMRp	MMRp+d
3	42/M	Rectosigmoid	MSH2 LS	MMRp+d	MMRp
4	41/M	Rectum	PMS2 LS	MMRd	MMRp
5	79/M	Duodenal	Likely MLH1 LS	MMRp	MMRd
6	43/F	Sigmoid	MSH2 LS	MMRd	MMRp
7	60/F	Right colon	MLH1 LS	MMRp	MMRd
8	71/M	Rectum	MLH1 LS	MMRp	MMRd
9	75/F	Duodenum	MLH1 methylated	MMRp+d	MMRd
10	79/M	Cecum	MLH1 methylated	MMRp	MMRd
11	64/F	Transverse	MLH1 methylated	MMRp	MMRd

LS, lynch Syndrome; MMRp, MMR proficient; MMRd, MMR deficient; MMRp+d, part MMR proficient and part MMR deficient.

Figure 1 - 487

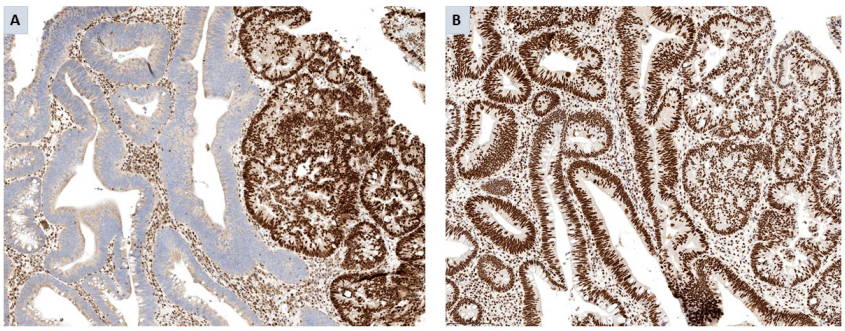

Fig. 1. Colonic carcinoma arising in a tubular adenoma in an MSH2-LS patient. The low grade component of the adenoma shows complete loss of MSH2 (A) and MSH6 (not shown) whereas the high grade dysplasia and carcinoma (intra-mucosal in this image) retains both MSH2 (A, right panel) and MSH6 (not shown). The entire tumor shows normal staining for PMS2 (B) and MLH1 (not shown).

Conclusions: In this study of intestinal tumors that followed the adenoma-carcinoma sequence and exhibited intra-tumoral MMR staining discrepancy, we observed that the dominant discrepant pattern was “MMRp in adenoma/MMRd in HGD or carcinoma”, in keeping with the notion that MMR-deficiency occurs after the adenoma has started to form. However, in 3 of 8 LS-associated tumors, we observed the emergence of MMRp HGD or carcinoma in MMRd adenomas. This deviates from the existing carcinogenesis models and warrants further investigation. Our observation that the components with discrepant MMR IHC appeared distinctly clonal suggests that distinct clonal loss of MMR should be regarded as abnormal. Whether and how such clonal loss of MMR in a carcinoma confers sensitivity to immunotherapy is an important ensuing question that also warrants further attention.

488 Diagnostic Yield of Colorectal Mass Biopsy: Is It All About Sampling?

Luz Sullivan[1], Rupinder Brar[1], Mustafa E Arslan[1], Michel Kmeid[1], Neharika Shrestha[1], Anne Chen[1], Hwajeong Lee[1]
[1]Albany Medical Center, Albany, NY

Disclosures: Luz Sullivan: None; Rupinder Brar: None; Mustafa E Arslan: None; Michel Kmeid: None; Neharika Shrestha: None; Anne Chen: None; Hwajeong Lee: None

Background: Desmoplasia, a crucial histologic feature for making a diagnosis of invasion (at least T1) in a colorectal cancer (CRC) biopsy, has recently emerged as a biomarker and prognosticator in CRC. We compared histopathologic features of diagnostic vs. non-diagnostic (diagnosis other than invasive adenocarcinoma, i.e., suspicious for invasion) colorectal biopsies and characterized corresponding resections.

Design: Colorectal biopsies (n=121) and subsequent resections (n=112) with CRC were retrieved. Biopsies were reviewed for sample size, levels examined, desmoplasia (%), intramucosal carcinoma (IMC: complex cytoarchitecture or single cell/small cell nests), benign tissue (%), low grade dysplasia (LGD) and inflammation. Additional parameters evaluated in resections included tumor grade, T stage, tumor/stroma ratio, tumor budding, mucosal involvement without desmoplasia and its grade, and surface

desmoplasia and inflammation. Electronic medical records were reviewed for intradepartmental consultation, tumor location, appearance and size, microsatellite instability (MSI) status and neoadjuvant therapy. Clinicopathological parameters between diagnostic vs. non-diagnostic biopsies were compared, with significant association defined as p<0.05.

Results: 82 (68%) biopsies were diagnosed as invasive adenocarcinoma. The presence of desmoplasia (Odds Ratio 12.9, 95% CI 5.07-32.60) was a strong predictor of making a diagnosis of invasion. Biopsies with IMC had more desmoplasia (30.2% vs. 0.67%, p<0.0001). Compared to non-diagnostic biopsies, diagnostic biopsies had more desmoplasia, IMC and marked inflammation, and less LGD. Diagnostic yield of biopsy was higher for tumors with high grade tumor budding, mucosal involvement by high grade dysplasia/IMC without LGD (suggestive of rapid growth or tumor colonization), and diffuse (>50% of tumor surface) surface desmoplasia. Sample size, amount of benign tissue, tumor location, appearance and T stage did not affect diagnostic yield. MSI-high tumors had less desmoplasia (p=0.049) in biopsies and higher tumor grades (p=0.011) than MS-stable tumors.

Table 1

	Diagnostic (n=82)	Non-diagnostic (n=39)	p-value
Levels examined, %	12.2	43.6	<0.001
Desmoplasia, mean, %	35.4	7.4	<0.0001
Complex cytoarchitecture (IMC), %	98.8	59.0	<0.0001
Single cell/small nests (IMC), %	45.1	5.1	<0.0001
Benign tissue, mean, %	22.9	33.8	NS
Low grade dysplasia (LGD), %	26.8	66.7	<0.001
Marked inflammation, %	53.7	25.6	<0.0001
Intradepartmental consultation, %	26.8	35.9	NS
Tumor size, mean, cm	5.25	5.29	NS
MSI-high, %	21.9	19.2	NS
*High tumor grade, %	11.7	0.0	NS
*Tumor/stroma ratio, stroma-high, %	41.7	39.1	NS
*Tumor budding, grade 2 to 3, %	33.3	8.3	0.0266
*Mucosal involvement without desmoplasia, %	78.3	100.0	0.0157
*Mucosal LGD, %	31.9	78.3	0.0003
*Mucosal high grade dysplasia/IMC without LGD	68.1	21.7	0.0003
*Tumor surface desmoplasia >50%, %	48.3	21.7	0.0447
*Tumor surface inflammation >50%, %	28.3	21.7	NS
*T stage 3/4, %	51.2	38.4	NS
Tumor location, left, %	64.6	71.7	NS

IMC-intramucosal carcinoma, *resections following neoadjuvant therapy excluded

Conclusions: CRCs with high-grade budding and diffuse surface desmoplasia unassociated with precursor (LGD) had higher diagnostic yield in biopsies. Desmoplasia appears to mirror the tumor microenvironment represented by activated epithelial-mesenchymal transition. As such, diagnostic yield of a biopsy is not solely dependent on sampling but also on the tumor's molecular subtype.

489 Common Acinar Differentiation and Occasional Acinar Cell Neoplasm Arising in Enterochromaffin-like Cell Proliferations-associated Gastric Type 1 Neuroendocrine Tumors

Orhun Taskin[1], Alessandro Vanoli[2], Francesca Capuano[3], Yersu Kapran[1], Olca Basturk[4], Stefano La Rosa[5], N. Volkan Adsay[6]

[1]Koç University, Istanbul, Turkey, [2]University of Pavia-IRCCS Policlinico San Matteo, Pavia, Italy, [3]University of Pavia, and San Matteo Hospital IRCCS Foundation, [4]Memorial Sloan Kettering Cancer Center, New York, NY, [5]University of Insubria, Varese, Italy, [6]Koç University Hospital, Istanbul, Turkey

Disclosures: Orhun Taskin: None; Alessandro Vanoli: None; Francesca Capuano: None; Yersu Kapran: None; Olca Basturk: None; Stefano La Rosa: None; N. Volkan Adsay: None

Background: Gastric type-1 neuroendocrine tumors (NETs) developing in the background of enterochromaffin-like (ECL) cell proliferations (secondary to atrophic gastritis and due to the trophic effect of compensatorily elevated gastrin) creates an interesting

model of tumorigenesis. Driving factors that lead for some cases to be more progression-prone have not yet been unraveled. Over the years, we have also encountered in this setting acinar differentiation raising questions about the versatility of this process.

Design: 42 cases of ECL-cell proliferations (32 with full-blown type 1 NETs) were analyzed with trypsin immunostain. Trypsin expression was evaluated semi-quantitatively as negative or positive (weak, moderate, strong) both in tumor cells and peritumoral ECL-cell proliferations. The positive and negative controls stained appropriately.

Results: ECL-cell proliferations as a whole expressed substantial amount of trypsin in 76% (n=32/42) of cases and among type 1 NETs 53% (n=17/32) exhibited trypsin expression (Figure 1A-B). In nine of ten cases (90%) with ECL-cell hyperplasia in the background of chronic atrophic gastritis without well-developed NET, trypsin was positive in ECL-cells (Figure 1C-D). The mean size of NETs with trypsin expression was 4.7 (±4.2) mm and those without was 5.2 (±5.3) mm (p=0.952). In 14/32 cases, both precursor and neoplastic components showed positivity; in 8/32 cases, the expression was noted in the ECL-cell precursors but not in the NET; in 2 cases, the expression was only noted in the NET component; in the remaining 8, no expression was seen in neither of the components. One case had both multiple independent frank NETs as well as a 3-cm acinar cell neoplasm (Figure 2) diffusely and strongly expressing trypsin with strong in-built controls, and showing all the morphologic characteristics of acinar differentiation. Only one case showed pancreatic acinar cell metaplasia in the mucosa.

Figure 1 - 489

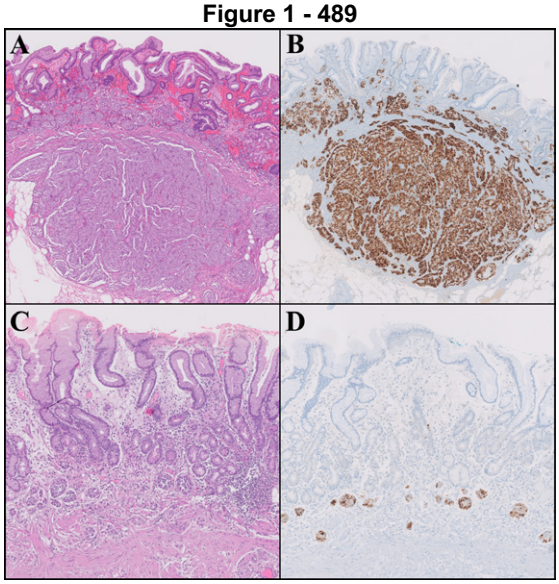

Figure 2 - 489

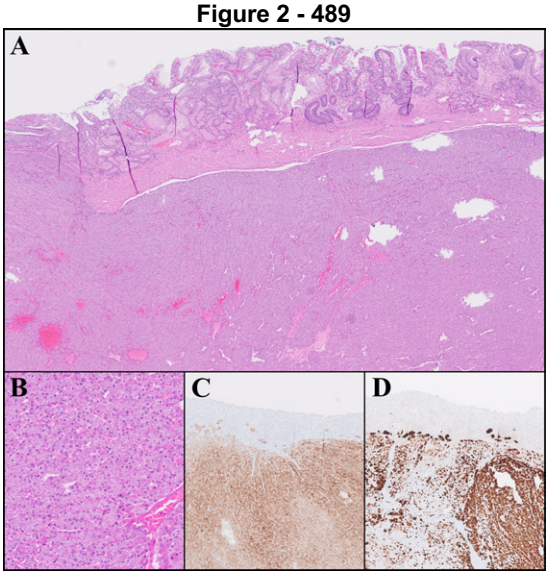

Conclusions: Both ECL-cell precursor proliferations and full-blown NETs arising in this setting show common expression of pancreatic acinar differentiation, and patients occasionally also develop acinar cell neoplasm. This brings new perspectives not only to the pathogenesis of this peculiar entity, but to the concept of cellular plasticity and selective cellular lineage development as well as to stem cells in the tumorigenesis.

490 Follow Up Biopsies in Gastrointestinal Immune Checkpoint Inhibitor Toxicity May Show Markedly Different Inflammatory Patterns Than Initial Injury

Nicole Tomm[1], Julianne Szczepanski[1], Jiayun Fang[2], Won-Tak Choi[3], Yue Xue[4], Namrata Setia[5], Dipti Karamchandani[6], Maria Westerhoff[1]

[1]University of Michigan, Ann Arbor, MI, [2]University of Michigan Hospitals, Ann Arbor, MI, [3]University of California, San Francisco, San Francisco, CA, [4]Northwestern University Feinberg School of Medicine, Chicago, IL, [5]University of Chicago, Chicago, IL, [6]UT Southwestern Medical Center, Dallas, TX

Disclosures: Nicole Tomm: None; Julianne Szczepanski: None; Jiayun Fang: None; Won-Tak Choi: None; Yue Xue: None; Namrata Setia: None; Dipti Karamchandani: None; Maria Westerhoff: None

Background: Gastrointestinal (GI) toxicity is a common manifestation of immune checkpoint inhibitor (ICI) injury, affecting up to 40% of patients. While histologic features of ICI GI toxicity have been described, we have encountered chronic colitis or

dramatically different inflammatory patterns in follow up biopsies of ICI colitis, with difficulty determining their clinical significance. The goal of this study was to determine the follow up biopsy manifestations of ICI toxicity with emphasis on clinical correlation.

Design: Our cohort included all patients with colonic ICI toxicity who had undergone more than one biopsy. Electronic medical record review was performed along with evaluation of histopathologic parameters for all biopsies (Figure 1). We determined if ICI toxicity biopsies exhibited features of inflammatory bowel disease (IBD), acute colitis, microscopic colitis, graft-versus-host disease (GVHD), or a combination of features. Follow up biopsies were also evaluated for resolution of colitis, and, if resolution was not achieved, whether the injury progressed to a different inflammatory pattern.

Results: Thirty-four ICI colitis patients had follow up biopsies (73 biopsies total). The predominant inflammatory pattern on initial biopsy was microscopic colitis (38%), followed by mixed patterns (24%), and IBD-like colitis (21%) (Figure 2). The follow up biopsies in 13 (38%) patients ultimately showed resolution of inflammation. Eleven (32%) patients had colitis that progressed to a different inflammatory pattern. Of these 11 cases, 36% had an IBD-like pattern and 27% had a mixed chronic colitis and GVHD-like pattern (Table 1). Those with a change in inflammatory pattern frequently had changed ICI drug types (45%). Overall, 23 patients were treated with IBD medications, 48% (n=11) of whom had an IBD-like pattern. Additionally, follow up biopsies correlated well with the status of the patient's symptoms.

Change in Inflammatory Patterns
Acute colitis à Microscopic colitis (n=1)
Acute colitis à Mixed chronic colitis + GVHD-like appearance (n=1)
Acute colitis à GVHD-like (n=1)
Acute colitis à IBD-like (n=1)
Mixed GVHD-like + microscopic colitis pattern à Acute colitis (n=1)
Mixed GVHD-like + chronic colitis pattern à IBD-like (n=1)
GVHD-like à Acute colitis (n=1)
Microscopic colitis à Mixed chronic colitis + GVHD pattern (n=2)
Microscopic colitis à IBD-like (n=2)

Figure 1 - 490

Clinical Data Collected	Histopathologic Findings Evaluated
ICI drug type Duration of ICI Indication for ICI Toxicity symptoms Microbiological results ICI toxicity treatment Symptom resolution Clinical outcome	Intraepithelial lymphocytosis (>20 lymphocytes/100 epithelial cells) Number of apoptoses in 10 high power fields Are apoptoses pominent on 10X magnification? Active inflammation severity (scored from 1-3) Combination of lymphocytosis, neutrophilia, and/or prominent apoptoses Crypt architectural distortion Crypt atrophy Lamina propria chronic inflammation Is the histologic pattern reminiscent of IBD, microscopic colitis, GVHD, or a mixture of features?

Figure 2 – 490

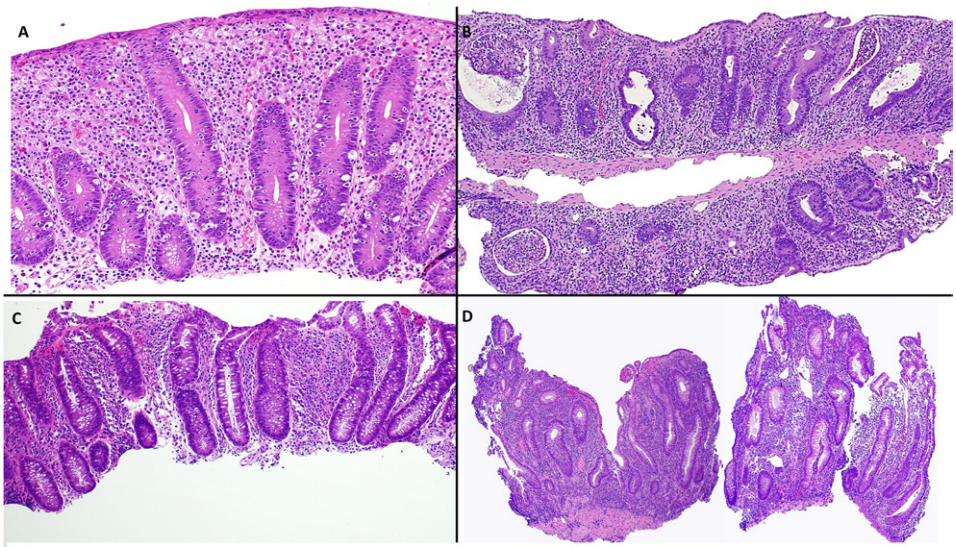

Figure 2. A) Mixed microscopic colitis/GVHD-like colitis pattern with follow-up biopsy (B) showing a chronic active colitis pattern with atrophic, distorted crypts and marked destruction. C) Microscopic colitis pattern with follow up biopsy (D) showing features identical to ulcerative colitis.

Conclusions: A third (32%) of our cases developed a different morphologic pattern of injury on follow-up, with the majority (36%) exhibiting a pattern identical to IBD. Pathologists need to be aware that an entirely different histology such as an IBD-appearance is possible on a follow up ICI toxicity biopsy and that this does not warrant a change in histologic diagnosis. Although it may be challenging to distinguish IBD and ICI toxicity on GI biopsy, pathologists may be assured to know that the same treatment is given to both.

491 Defining Amphicrine Carcinoma of the Gastrointestinal Tract: A Single Institutional Experience

Yi Tat Tong[1], Wai Chin Foo[1], Asif Rashid[1], Rebecca Waters[1], Susan Abraham[1], Deyali Chatterjee[1], Melissa Taggart[1]
[1]The University of Texas MD Anderson Cancer Center, Houston, TX

Disclosures: Yi Tat Tong: None; Wai Chin Foo: None; Asif Rashid: None; Rebecca Waters: *Advisory Board Member*, Astellas; *Advisory Board Member*, Astellas; Susan Abraham: None; Deyali Chatterjee: None; Melissa Taggart: None

Background: Tumors with dual differentiation are recognized and, recently, are classified as mixed endocrine-non-neuroendocrine neoplasms. Often dual differentiation is recognized as separate components; however, some neoplastic cells show both neuroendocrine and glandular differentiation (amphicrine cells). Tumors primarily composed of these cells have been termed ”amphicrine carcinoma” (AC). Few case series have documented this entity in the gastrointestinal tract; however, it has not been categorized in current tumor classification systems. Thus, the clinicopathologic characteristics and prognostic factors are not well established. The aims of this study are to describe the clinical and pathologic features of these tumors at a single institution to raise awareness of the entity, attempt to establish diagnostic criteria, and further characterize prognostic and predictive factors.

Design: Cases were chosen during prospective collection and retrospective review of pathology reports from gastrointestinal/hepatobiliary tumors from 2006 to 2021 with the term “amphicrine” in the diagnosis or comment section at a large tertiary cancer center. Treatment naïve tumors with any percentage of amphicrine cells and > 30% neuroendocrine differentiation. Immunohistochemical stains for synaptophysin and chromogranin and mucin stains were used to confirm components (Figure 1). Goblet cell adenocarcinoma and pancreatic primaries were excluded. Histologic, immunohistochemical, and molecular features and clinical parameters were noted.

Results: 18 cases were identified (10 colonic, 3 esophageal, 2 gastric, 2 hepatic, and 1 ampullary). More than 50% of the tumor was synaptophysin positive in 16 (89%) cases and >50% of tumor was positive for chromogranin in 12 (67%) cases. 12 tumors (67%) were almost all amphicrine. 4 (22%) tumors had extracellular mucin (ECM) comprising >50% of the amphicrine

component. The most common molecular abnormalities (7 tested) were *TP53* (4) and *BRAF* (4). Additional findings are displayed in Table 1.

Feature	Number (%)
Male	11 (61%)
Age (mean, range; years)	58.4, 43-84
Biopsy:Resection (initial diagnosis)	11 (61%):7 (39%)
Tumor size (mean, range; cm)	4.6, 1-11
Primary site evaluated	16 (of 16)
Morphology Nested Cribriform Dyshesive Tubular/Glandular Solid	11 4 7 4 6
Extracellular mucin in amphicrine component	12 (67%)
T category T2 T3 T4	1 (8%) 6 (50%) 5 (42%)
N category N0 N1 N2	2 (17%) 4 (33%) 6 (50%)
M category M0 M1	10 (83%) 2 (17%)
PNI and/or LVI	11 (61%)
Loss of MMR protein expression	1 (MSH2/MSH6) (7%)
Survival (mean, range; mo)	20, 0.6 - 61.9
Died of disease Alive with disease No evidence of disease Died of other cause Unknown	5 (28%) 7 (39%) 3 (17%) 1 (6%) 2 (12%)

Figure 1 - 491

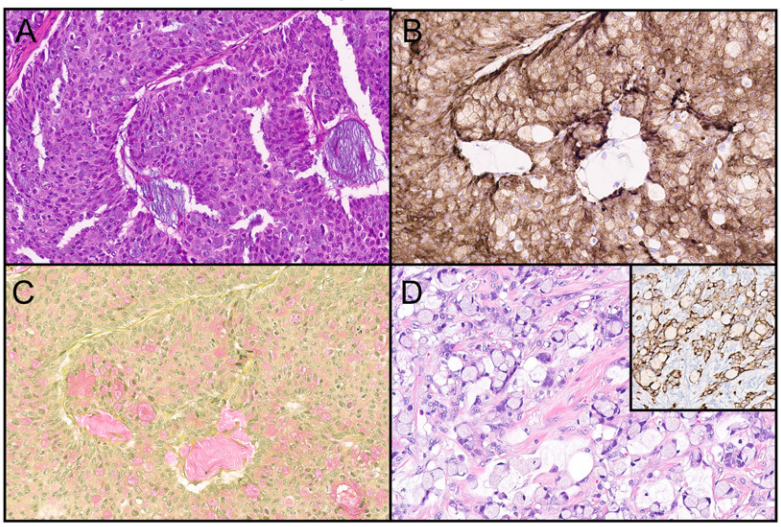

Figure 1. Amphicrine carcinoma with nested architecture. A. Cells with intracellular mucin are easily identified, H&E x200. **B.** The tumor cells, including those with intracellular mucin are diffusely and strongly positive for synaptophysin, x200. **C.** Mucicarmine highlights intra- and extracellular mucin, x200. **D. Amphicrine carcinoma composed of signet ring-like cells.** Nuclei are compressed to the periphery by intracellular mucin and cells are diffusely positive for synaptophysin (inset), x200.

Conclusions: ACs are suspected by their architecture (nested/cribriform/solid); although, some have ECM or signet ring-like cells. They are associated with poor prognostic features (lymphovascular/perineural invasion/nodal metastases). Most patients in

our series either died of, or are living with disease. Incorporation of these neoplasms into classification systems will help with recognition which may lead to additional insights and, perhaps, novel treatments for these patients.

492 Mixed Neuroendocrine Non-Neuroendocrine Neoplasms of the Digestive System: Clinicopathological Study of 70 Cases from a Single Oncology Centre

Sagar Tripathy[1], Rajiv Kumar[1], Mukta Ramadwar[1], Kedar Deodhar[1], Munita Bal[2]
[1]Tata Memorial Hospital, Mumbai, India, [2]Tata Memorial Centre, Mumbai, India

Disclosures: Sagar Tripathy: None; Rajiv Kumar: None; Mukta Ramadwar: None; Kedar Deodhar: None; Munita Bal: None

Background: Mixed neuroendocrine non-neuroendocrine neoplasms (MiNENs) are mixed tumors composed of morphologically recognizable neuroendocrine (NE) and non-NE components, each accounting for ≥ 30% of the neoplasm. Owing to their rarity, very little is known about their clinicopathologic spectrum.

Design: Clinicopathologic features of all MiNEN cases of the digestive system were reviewed after confirmation of the histologic diagnosis per the WHO 2019. The NE component in all cases was immunohistochemically confirmed. Neuroendocrine tumors with entrapped ducts and spatially discrete tumors were excluded.

Results: 70 MiNEN patients were included. The mean age was 55.1 years; the male-to-female ratio was 1.1. The sites of distribution were: the gallbladder (n=35), stomach (n=8), esophagus (n=7), ampulla (n=7), ascending colon (n=5), the gastroesophageal junction (n=2); rare sites included the duodenojejunal flexure, jejunum, sigmoid colon, rectum, pancreas, and liver with unknown primary (n=1 each, respectively). 45 (64.3%) patients underwent curative resection and 25 (35.7%) were palliative. The mean tumor size was 3.5cm. Microscopically, small cell neuroendocrine carcinoma (SCNEC) with adenocarcinoma combination was the commonest (n=34; 48.6%) histologic duet; the details of NE and non-NE pairs are provided in the table. The patterns of admixture were composite (n=56), collision (n=7), and amphicrine (n=7) type. The NE and non-NE counterparts formed >50% of the tumor in 48 (68.6%) and 13 (18.6%) cases, respectively; in 9 (12.8%), both counterparts were present equally. Lymphovascular emboli, perineural invasion, and necrosis were present in 33 (73.3%), 24 (53.3%) and 50 (75.8%) cases, respectively. Lymph-nodal metastasis was found in 22 (75.9%) cases with the majority (45.5%) revealing adenocarcinoma histology. Loco-regional recurrence was noted in 3 (4.3%) while 38 (54.3%) patients developed distant metastases with the liver being the commonest site (76.3%). On follow up (n=57; median 8.1 and range,1-43 months), 10 (17.5%) patients had no evidence of disease (NED), 38 (66.7%) were alive with disease (AWD) and 9 (15.8%) died of disease (DOD).

The Main Histologic Types in MiNEN

HISTOLOGICAL COMBINATIONS	n	%
1.Neuroendocrine Carcinoma Combinations	**50**	**71.4**
Neuroendocrine Carcinoma + Adenocarcinoma	43	61.4
Small cell NEC + Adenocarcinoma	34	48.6
Large cell NEC + Adenocarcinoma	9	12.9
Small cell NEC + Adenosquamous carcinoma	2	2.9
Small cell NEC + Anaplastic carcinoma	2	2.9
Neuroendocrine Carcinoma + Squamous cell carcinoma	2	2.9
Small cell NEC + Squamous cell carcinoma	1	1.4
Large cell NEC + Squamous cell carcinoma	1	1.4
Small cell NEC + Carcinosarcoma	1	1.4
2.Neuroendocrine Tumor Combinations	**20**	**28.6**
Neuroendocrine Tumor + Adenocarcinoma	19	27.1
NET, Grade 1 + Adenocarcinoma	14	20
NET, Grade 2 + Adenocarcinoma	2	2.9
NET, Grade 3 + Adenocarcinoma	3	4.3
NET, Grade 3 + Adenosquamous carcinoma	1	1.4
Note: NET grading was as per the WHO 2019 Abbreviations: NEC – Neuroendocrine carcinoma; NET – Neuroendocrine tumor		

Conclusions: MiNENs of the digestive system are rare tumors with aggressive clinicopathologic features and poor prognosis. The pathologic spectrum of MiNENs is wide-ranging and includes rare histologic combinations. Large multicentre studies with long-term follow-up are warranted.

493 Clinical and Immunological Correlates of Downregulation of HLA proteins and Beta-2-Microglobulin in Colonic Adenocarcinoma

Claire Trivin-Avillach[1], Amaya Pankaj[2], Azfar Neyaz[3], Sandra Cerda[4], Qing Zhao[5], Stuti Shroff[6], Rory Crotty[2], M Lisa Zhang[2], Deepa Patil[7], Omer Yilmaz[8], Vikram Deshpande[9], Osman Yilmaz[1]
[1]Boston Medical Center, Boston, MA, [2]Massachusetts General Hospital, Boston, MA, [3]University of Pittsburgh Medical Center, Pittsburgh, PA, [4]Boston University Medical Center, Boston, MA, [5]Boston University, Boston Medical Center, Boston, MA, [6]Massachusetts General Hospital, Watertown, MA, [7]Brigham and Women's Hospital, Harvard Medical School, Boston, MA, [8]Massachusetts Institute of Technology, Cambridge, MA, [9]Massachusetts General Hospital, Harvard Medical School, Boston, MA

Disclosures: Claire Trivin-Avillach: None; Amaya Pankaj: None; Azfar Neyaz: None; Sandra Cerda: None; Qing Zhao: None; Stuti Shroff: None; Rory Crotty: None; M Lisa Zhang: None; Deepa Patil: None; Omer Yilmaz: None; Vikram Deshpande: None; Osman Yilmaz: None

Background: Downregulation of human leukocyte antigen (HLA) class I is postulated to be a mechanism of adaptive immune escape in colon carcinoma and resistance of checkpoint inhibitors. We evaluate class I, class II and beta-2-microglobulin (B2MG) expression in a large cohort of resected colonic adenocarcinoma and correlate to the intratumoral immune infiltrate and key clinical, pathologic and genetic markers.

Design: We assessed 1206 colon carcinomas on representative tissue microarray sections, gathered clinicopathologic information, and immunostained for mismatch repair proteins (MMR). The percentage of the tumor cells with loss of HLA class I proteins, HLA class II, and B2MG was assessed. BRAF V600E immunohistochemistry was recorded. An automated platform was used to quantitate CD8, CD163, LAG3. PD-L1 on immune cells was quantitated manually.

Results: Downregulation of 3 HLA component proteins was associated with higher tumor stage, but, only correlation with B2MG was significant (p=0.0001). Decreased expression of HLA class I and class II was more common in MMR-deficient (dMMR) BRAF positive tumors; decreased B2MG was associated with MMR-proficient (pMMR) BRAF negative tumors. Low B2MG expression was associated with decreased disease-specific survival (p=0.006). This difference was only significant in pMMR tumors (p=0.005) and not in dMMR tumors (p=0.8). HLA class I (p=0.66) and II (p=0.79) did not correlate with disease decreased specific survival. Low B2MG was accompanied by decreased tumor expression of PD-L1 (p=0.0001), and CD8 (p=0.0001), CD163 cells (p=0.0001), LAG3 positive immune cells (p=0.001) almost exclusively in pMMR.

Conclusions: 1. Low B2MG was more common than HLA class I and class II proteins, and correlated with aggressive behavior and disease specific survival on univariate analysis. Decreased survival was most pronounced in pMMR. 2. Low B2MG was more common in pMMR tumors and BRAF positive tumors, while downregulation of HLA class I and class II proteins was more common in dMMR and BRAF negative tumors. 3. Low B2MG in pMMR was associated with low CD8, CD163 and LAG3 immune cells and low PD-L1 on tumor cells. 4. Low B2MG, low CD8 density may present an immune 'cold' phenotype in pMMR tumors and may aid in the understanding of resistance to immune therapy in this class of tumors. 5. Conversely, low HLA class I and class II proteins may account for resistance to checkpoint therapy in dMMR tumors.

494 Primary Anaplastic Large Cell Lymphoma of Gastrointestinal Tract: A Clinicopathologic Study of 25 Cases

Nasir Ud Din[1], Shabina Sikandar[1], Arsalan Ahmed[1], Zubair Ahmad[2], Zeeshan Ahmed[1]
[1]Aga Khan University Hospital, Karachi, Pakistan, [2]Aga Khan Hospital, Karachi, Pakistan

Disclosures: Nasir Ud Din: None; Shabina Sikandar: None; Arsalan Ahmed: None; Zubair Ahmad: None; Zeeshan Ahmed: None

Background: Anaplastic large cell lymphoma (ALCL) is an uncommon type of non-Hodgkin lymphoma composed of cohesive sheets of large atypical lymphoid cells which demonstrate strong positivity for CD30 (Ki 1). There are three ALCL types: primary cutaneous, systemic ALK positive ALCL and systemic ALK negative. ALK positive ALCL has a much better prognosis. Primary gastrointestinal tract (GIT) ALCL is very rare and may be difficult to diagnose. Its recognition is crucial as its clinical and prognostic ramifications are different from other malignant GIT Tumors.

The aim of this study is to describe the clinical, histological and immunohistochemical (IHC) features and behavior of primary GIT ALCL

Design: All cases of primary GIT ALCL diagnosed in our practice between May 2011 to April 2020, were included in the study. H&E slides of all cases were retrieved and reviewed, and diagnosis was confirmed independently by two pathologists. Additional and/or repeat immunohistochemical stains were performed in some cases. Results of molecular tests for ALK status are pending. Follow up was obtained.

Results: During the study period, 25 cases of primary GIT ALCL were reported. Ages ranged from 14 to 65 years. Mean and Median age was 41 and 45 years respectively. 21 patients were males and 4 females. Of the 25 cases, 18 involved the small intestine. Clinical features were non-specific and diverse. A number of patients presented with intestinal obstruction. Eleven cases were diagnosed on endoscopic biopsies and 10 on resection specimens. Mean tumor size in resection specimens was 4.2 cms. Histologically, all 25 cases showed a diffuse infiltrate composed of sheets of large anaplastic cells with pleomorphic horseshoe or kidney shaped nuclei and abundant pink cytoplasm. Strong membranous/cytoplasmic or golgi positivity for CD30 was seen in all 25 cases. Positivity for EMA was seen in 17 cases. Cytokeratins were negative in all cases. ALK was positive in 7 and negative in 18 cases. Follow up was available in 14 cases and ranged from as short as 2 days to as high as 60 months. Out of 14, 12 died within a few days to more than a year after diagnosis. However, 2 patients were surprisingly alive 35 and 60 months after diagnosis.

Conclusions: To our knowledge this is the largest series describing clinicopathological features of primary GIT ALCL. Most patients were male and tumor most commonly involved small intestine. Majority of cases were ALK negative. Prognosis was poor and most patients died within months of diagnosis.

495 Pathology Characteristics and Prognostic Determinants of Colorectal Adenocarcinoma at University Teaching Hospital of Kigali

Delphine Uwamariya[1], Belson Rugwizangoga[2], Deogratias Ruhangaza[3]
[1]CHUK, Kigali City, Rwanda, [2]University of Rwanda/CHUK, Kigali, Rwanda, [3]Butaro Hospital, Burera, Rwanda

Disclosures: Delphine Uwamariya: None; Belson Rugwizangoga: None; Deogratias Ruhangaza: None

Background: Colorectal cancer (CRC) is the second most diagnosed cancer in female and the third in men, arising from the epithelium of the Colo-rectum. It is known that colorectal cancer is common in developed countries than in developing countries which may be due to inaccurate data on the existence of the disease in that region combined with embracing western lifestyle expressed by the current trend of changes in cultural, social, and lifestyle practices playing a major part in the etiology of the CRC. The aim of this study was to document epidemiological, pathological characteristics and prognostics determinants of patients diagnosed with CRC in Rwanda.

Design: After obtaining the ethical approval from the Institutional review board (IRB) of the University of Rwanda (UR), College of Medicine and Health Sciences (CMHS) and permission from Kigali University Teaching Hospital (CHUK); Data from patients' files and reviewed glass slides for 101cases all from Kigali University Teaching Hospital (CHUK) were statistically analyzed and patient characteristics were described as mean and frequency accordingly. Comparisons were performed using Chi square tests, Fisher 'exact test and Odd ratio with 95% confidence interval (CI). Survival curves were plotted using the Kaplan–Meier method and log-rank test was used to assess the statistical differences in the observed survival curves by each categorical variable. A P value <0.05 was considered statistically significant. Statistical analyses were performed using Statistical Product and Service Solutions (SPSS), GraphPad Prism and MedCalc accordingly

Results: Mean age of participants was 54.26 years, main symptom was rectal bleeding (46.5%), rectum was the most common anatomical site representing 40.6%, conventional adenocarcinoma was 60.4%, most tumors were of Grade II (54.5%), most common stage was pT3N0 (20.8%), resection margins were free at 71.3%, lympho-vascular invasion was 49.5% of cases, a high immune response was in 71.3% of cases and of 101cases, 55.4% were still alive at the end of the data collection, with 29.3% have overall survival of 5 years.

Table 1. Distribution of age, sex, residence, main symptor and biopsy site for the study participants

Characteristics	n	Percent
Age (n=101)		
<50	42	41.6
51-75	54	53.5
>75	5	5
Sex (n=101)		
Male	48	47.5
Female	53	52.5
Residence (n=101)		
Eastern	17	16.8
Kigali City	33	32.7
Northern	13	12.9
Southern	25	24.8
Western	13	12.9
Main Symptom (n=101)		
Abdominal pain	25	24.8
Constipation	1	1
Obstruction	19	18.8
Perforation	9	8.9
Rectal bleeding	47	46.5
Duration of symptoms (n=101)		
< 6 months	52	51.5
> 24 months	4	4
13-24 months	7	6.9
7-12 months	38	37.6
Anatomic site (n=101)		
Ascending colon	28	27.7
Descending colon	27	26.7
Rectum	41	40.6
Transverse colon	5	5

N= Number

Table 2. Pathologic prognostic determinants of colorectal carci

Characteristics	Number	Percent
Tumor grade (n=101)		
Grade I	28	27.7
Grade II	55	54.5
Grade III	18	17.8
Tumor stage (n=101)		
Stage I	10	9.9
Stage II	21	20.8
Stage III	22	21.8
Stage IV	17	16.8
No stage	31	30.7
Margin status (n=101)		
Negative radial margin	72	71.3
Positive radial margin	29	28.7
Lympho-vascular invasion (n=101)		
Not present	52	51.5
Present	49	48.5
Perineural invasion (n=101)		
Not present	72	71.3
Present	29	28.7
Tumor border (n=101)		
Expansile	45	44.6
Irregular infiltrating	56	55.4
Immune response (n=101)		
High	72	71.3
Low	29	28.7

N=number

Table 3 Correlation between prognostic determinants and tumor grade & stage

Characteristics	*Tumor grade*		*OR (95% CI)*	*P**	*Tumor stage*		*OR (95% CI)*	*P*
	Low	*High*			*Low*	*High*		
Immune response	*(n=101)*				*(n=70)*			
High	42	30	2.6 (1.1 – 6.5)	0.03	27	27	2.2 (0.7 – 7.2)	0.19
Low	10	19			5	11		
Lymphovascular invasion	*(n=101)*				*(n=70)*			
Not present	38	14	6.7 (2.8 – 16.2)	<0.0001	19	21	1.18 (0.4 – 3.0)	0.7
Present	14	35			13	17		
Perineural invasion	*(n=101)*				*(n=70)*			
Not present	43	29	3.29 (1.3 – 8.24)	0.01	20	26	0.76 (0.3 – 2.0)	0.6
Present	9	20			12	12		
Tumor border	*(n=101)*				*(n=70)*			
Expansile	30	15	3.1 (1.4 – 7.0)	0.007	17	13	2.17 (0.8 – 5.7)	0.11
Irreg. infiltrating	22	34			15	25		
Margin status	*(n=101)*				*(n=70)*			
Neg radial marg.	46	26	6,7 (2.4 – 18.7)	0.0002	23	28	0.91 (0.3 – 2.6)	0.8
Pos radial marg.	6	23			9	10		
Histologic type	*(n=101)*				*(n=70)*			
Carcinoma, NOS	40	21	4.4 (1.8 – 10.4)	0.0007	22	23	1.43 (0.5 – 3.8)	0.47
Carcinoma, mucinous	12	28			10	15		

**P value by Fisher's exact test; NOS: not otherwise specified; OR: odds ratio; CI: confidence interval*

Figure 1 - 495

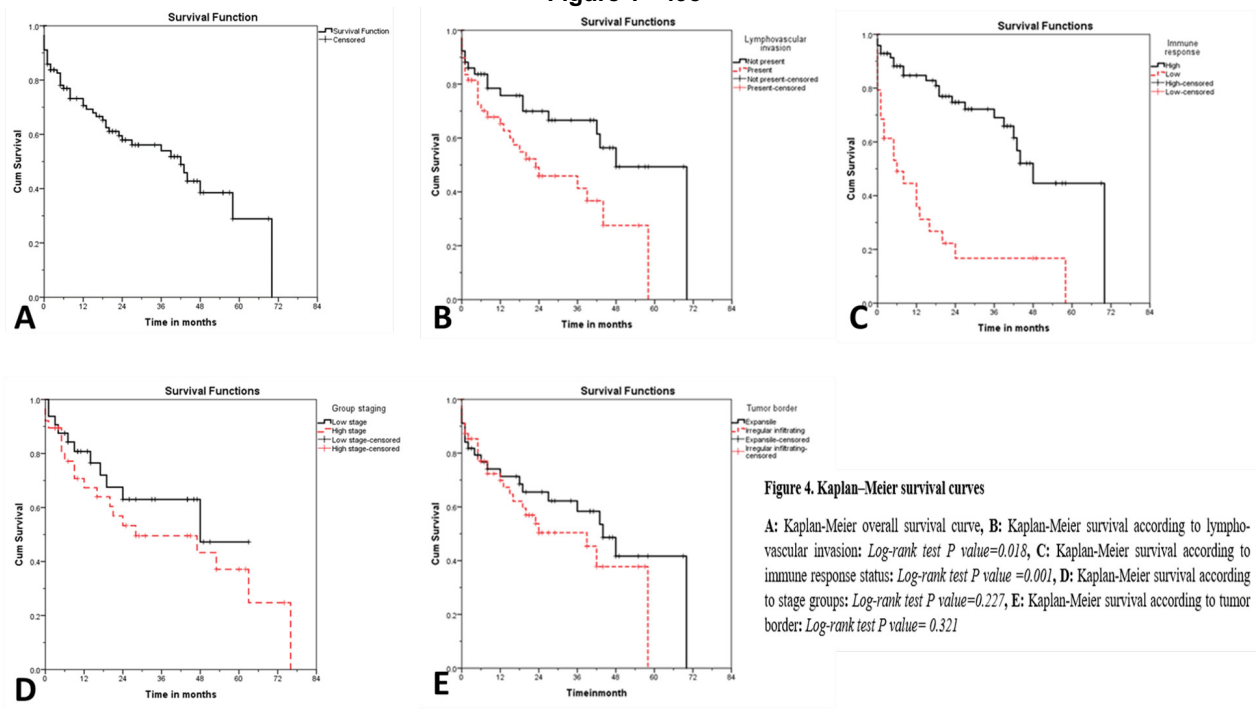

Figure 4. Kaplan–Meier survival curves

A: Kaplan-Meier overall survival curve, **B:** Kaplan-Meier survival according to lympho-vascular invasion: *Log-rank test P value=0.018*, **C:** Kaplan-Meier survival according to immune response status: *Log-rank test P value =0.001*, **D:** Kaplan-Meier survival according to stage groups: *Log-rank test P value=0.227*, **E:** Kaplan-Meier survival according to tumor border: *Log-rank test P value= 0.321*

Conclusions: The results of this study give a broad picture of colorectal adenocarcinoma patients in in Rwanda in terms of clinical pathologic characteristic and prognostic determinants and 55.4% of were still alive at the end of the data collection however only 29.3% have overall survival of 5 years.

496 Ki67 Proliferation Indices in Small Intestinal Well-Differentiated Neuroendocrine Tumors Are Most Prognostic When Evaluated on Mesenteric Tumors Deposits

Monika Vyas[1], Justin Cates[2], Raul Gonzalez[1]
[1]Beth Israel Deaconess Medical Center, Harvard Medical School, Boston, MA, [2]Vanderbilt University Medical Center, Nashville, TN

Disclosures: Monika Vyas: None; Justin Cates: *Advisory Board Member*, Eluciderm, Inc.; Raul Gonzalez: None

Background: Ki67 proliferation index is used for grading well-differentiated neuroendocrine tumors (NETs). Selection of best tissue for staining can be challenging, especially in small intestinal (SI) NETs, which can be multifocal and produce multiple lymph metastases (LN-mets) and mesenteric tumor deposits (MTD). This study aimed to determine parameters for selecting the most prognostically appropriate tissue for Ki67 staining in SI NETs.

Design: We searched our departmental archives for SI NETs with at least one LN-met and/or MTD. For each included case, we recorded patient age and sex; size of largest primary tumor, LN-met, and/or MTD; AJCC staging; and patient outcome (recurrence and disease-specific death). We stained the largest primary, LN-met, and MTD in each case for Ki67 (Biocare CRM325, 1:100). We photographed hotspot areas on each Ki67 slide and Ki67 index was calculated using QuPath digital image analysis software after training using a random forest supervised classifier (Fig 1A-1C). 20 cases underwent manual Ki67 counting to validate QuPath results. All variables were compared to patient outcomes using standard univariable Cox proportional hazard regression (α=0.05).

Results: Among 69 NETs from 42 female and 27 male patients (mean age 62 years; range 35-90 years), 63 had LN-mets and 42 had MTD. Mean sizes of the largest primary tumors, LN-mets, and MTDs were 1.9, 1.08, and 2.1 cm. Mean Ki67 was 1.64 (largest primaries), 2.02 (largest LN-mets), and 1.87 (largest MTDs). In 46 cases (67%), the Ki67 of a LN-met or MTD was higher than the primary tumor. Comparing grade of primary tumor and MTD, 30 were both grade 1, 3 were both grade 2, 6 had grade 1 primaries and grade 2 MTDs, and 3 had grade 2 primaries and grade 1 MTDs. Seventeen tumors (25%) recurred (median time to recurrence: 13 months). MTD Ki67 was associated with increased risk of recurrence (hazard ratio [HR] 1.46, 95% confidence interval [CI] 1.13-

1.89, *P*=0.0034), but primary and LN-met Ki67 did not, nor did Ki67 of the largest single focus for each case. Only distant metastases (HR 11.03, 95% CI 2.54-47.97, *P*=0.0014) and MTD Ki67 (HR 1.43, 95% CI 1.12-1.83, *P*=0.0044) were significant predictors of recurrent disease. Over a median follow-up of 41 months, only six patients (9%) died of disease, precluding survival analysis.

Figure 1 - 496

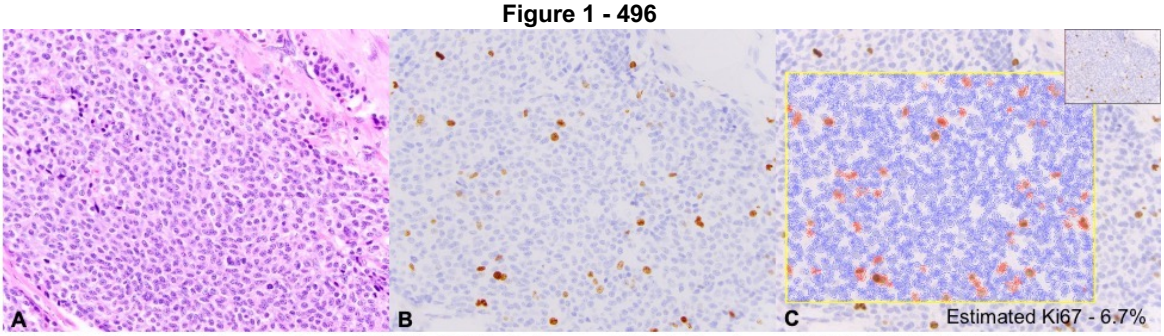

Fig 1: A: Mesenteric tumor deposit (H&E, 400X), B: Image of the hotspot area (Ki67, 400X), C: Digital image analysis for Ki67 quantification performed on image 1B

Conclusions: For meaningful Ki67 evaluation of SI NETs, the largest MTD should be stained, if available. Primary Ki67, LN Ki67, and "largest focus" Ki67 do not relate to patient recurrence, but MTD Ki67 does.

497 The Incorporation of Genomic Testing to the Evaluation of Appendiceal Mucinous Neoplasms Improves the Prognostic Classification of Patients with Disseminated Disease

Abigail Wald[1], Phoenix Bell[1], Patrick Henn[2], Brian Theisen[3], Susan Shyu[1], Marina Nikiforova[1], Aatur Singhi[1]
[1]University of Pittsburgh Medical Center, Pittsburgh, PA, [2]University of Colorado Anschutz Medical Campus, Aurora, CO, [3]Henry Ford Hospital, Detroit, MI

Disclosures: Abigail Wald: None; Phoenix Bell: None; Patrick Henn: None; Brian Theisen: None; Susan Shyu: None; Marina Nikiforova: None; Aatur Singhi: None

Background: Disseminated appendiceal mucinous neoplasms (AMNs) are a heterogeneous group of tumors with variable clinical behavior. Several studies have shown that the prognosis of disseminated AMNs is highly dependent on histologic grade as defined by the American Joint Cancer Conference (AJCC). Recently, comprehensive genomic profiling has elucidated the genomic landscape of AMNs; however, it's unclear if molecular testing can further stratify clinical outcome among patients with disseminated disease. Therefore, we evaluated the clinicopathologic and genomic features of 114 patients with disseminated AMN.

Design: Tumors from consecutive patients with disseminated disease from 2016 to 2020 were analyzed by targeted next-generation sequencing of 28 genes associated with gastrointestinal tract neoplasms. Genomic alterations were correlated with several clinicopathologic findings, such as AJCC grade, lymphovascular and perineural invasion, regional lymph node metastases, peritoneal cancer index (PCI), cytoreductive surgery (CRS), completeness of cytoreduction (CC) score, hyperthermic intraperitoneal chemotherapy (HIPEC) treatment, and overall survival (OS).

Results: Genomic alterations were identified in 110 of 114 (96%) disseminated AMNs. In descending order, the most prevalent genomic alterations were found in *KRAS* (82%), *GNAS* (61%), *TP53* (25%), *SMAD4* (21%), the mTOR genes (*PIK3CA* and *PTEN*, 8%), and *CDKN2A* (2%). No statistically significant clinicopathologic findings were associated with *KRAS* and/or *GNAS* mutations. However, collectively, alterations in *TP53*, *SMAD4*, *CDKN2A,* and the mTOR genes correlated with higher AJCC grade (G2/G3, 79% vs. 45%, p<0.001), lymphovascular invasion (30% vs. 11%, p=0.014), and perineural invasion (23% and 6%, p=0.011). In addition, the 3-year and 5-year OS rates for AMN patients with *TP53*, *SMAD4*, *CDKN2A*, and/or mTOR gene alterations were 71% and 48%, respectively, as compared with 88% and 83%, respectively, for patients that were wild-type for the aforementioned genes. By multivariate analysis, alterations in *TP53*, *SMAD4*, *CDKN2A*, and/or the mTOR genes in AMNs were a negative prognostic factor for OS and independent of AJCC grade, lymphovascular invasion, perineural invasion, PCI, CRS, CC score, and HIPEC treatment (p=0.029).

Conclusions: Genomic alterations in *TP53*, *SMAD4*, *CDKN2A,* and the mTOR genes in disseminated AMNs correlate with adverse clinicopathologic features and poor patient OS. Thus, molecular testing may aid in the prognostication of AMN patients with disseminated disease.

498 Digital Image Analysis in Risk Stratification of Midgut and Pancreatic Neuroendocrine Tumors

Xintong Wang[1], Michelle Kim[2], Dorian Mendoza[1], Jessica Whang[1], Robyn Jordan[1], Michael Donovan[2], Marcel Prastawa[3], Jack Zeineh[1], Abishek Sainath Madduri[1], Brandon Veremis[1], Max Signaevsky[1], Gerardo Fernandez[1], Stephen Ward[1]
[1]Icahn School of Medicine at Mount Sinai, New York, NY, [2]Mount Sinai Hospital Icahn School of Medicine, New York, NY, [3]Mount Sinai Hospital, New York, NY

Disclosures: Xintong Wang: None; Michelle Kim: *Consultant*, Novartis; *Speaker*, Medscape; Dorian Mendoza: None; Jessica Whang: None; Robyn Jordan: None; Michael Donovan: *Consultant*, PreciseDx; Marcel Prastawa: *Employee*, PreciseDx; Jack Zeineh: *Employee*, PreciseDx; Abishek Sainath Madduri: *Employee*, PreciseDX; Brandon Veremis: *Consultant*, PreciseDx; Max Signaevsky: None; Gerardo Fernandez: *Employee*, PreciseDx; Stephen Ward: None

Background: Neuroendocrine tumors (NETs) are an increasingly prevalent cancer in the US. While tumor stage and grade are used to predict outcomes, patients with similar stage and grade may have variability in clinical course. To better predict NET outcomes, we used PreciseDx image analysis algorithms to identify and quantify histologic features of NETs, and correlate them with clinical features and outcomes.

Design: We included patients with midgut NETs (MNETs) or pancreatic NETs (PNETs) diagnosed at Mount Sinai hospital from 1994-2017, who have at least one H&E slide to scan. We recorded demographics, tumor stage, grade, treatment, and outcome. We tested the PreciseDx Morphology Array ™ (PDxMA) previously trained on >300 breast and prostate slides, on a development set of NETs and compared against ground truth annotations performed by experienced GI pathologists. The PDxMA was updated with annotated ground truth and applied to an additional set of NETs with outcome data. Support vector regression for censored data (SVRc) was then used to build an NET progression-free survival (PFS) model.

Results: We identified 391 patients with MNETs (69%) or PNETs (31%), with mean age of 58 years, 51% female and 64% white. To test the accuracy of the PDxMA on NETs, we analyzed a development set of 20 cases (10 PNETs and 10 MNETs) which showed mitotic figure detector precision of 0.969, epithelium detector Dice overlap of 0.841, and nuclei detector Dice overlap of 0.841. Annotations derived during this evaluation were incorporated into the PDxMA and then applied to an additional 113 NETs. G1, G2, and G3 tumors were 62%, 33% and 5%. Stage I, II, III, IV were 17%, 17%, 21%, and 45%. Median PFS was 56 months. Feature selection and SVRc modeling identified factors such as tumor stage and grade, along with imaging features characterizing stromal nuclear distribution and shape variability, invasive glandular structure and epithelial nuclear distribution as well as mitotic figure distribution. NET PFS training model showed a concordance index (C-Index) of 0.81 (sensitivity 85%; specificity 82%) vs clinical only model with a C-index of 0.75 (sensitivity 71%; specificity 80%).

Conclusions: Epithelial and mitotic figure detector developed for other tumor types is applicable to pancreatic and small bowel NETs. Preliminary model with AI-based pathologic features add additional prognostic ability beyond clinical features, tumor stage, and tumor grade. This model will be further validated with the remaining cases in our cohort.

499 Lack of Increased Tumor Infiltrating Lymphocytes Occurs in 11% of Mismatch Repair-Deficient Colonic Carcinomas and is Associated with Mucinous Histology

Chiyun Wang[1], Canan Firat[1], Efsevia Vakiani[1], Martin Weiser[1], Jinru Shia[1]
[1]Memorial Sloan Kettering Cancer Center, New York, NY

Disclosures: Chiyun Wang: None; Canan Firat: None; Efsevia Vakiani: None; Martin Weiser: None; Jinru Shia: None

Background: Tumor infiltrating lymphocytes (TILs), defined as lymphocytes that infiltrate the tumor cell compartment exclusive of inflammatory cells associated with stromal tissue or luminal debris, are frequently increased in mismatch repair-deficient (dMMR) colorectal carcinomas. They reflect heightened tumor immunogenicity and are regarded as the basis for the relatively favorable prognosis and response to immunotherapy in these patients. However, there exist dMMR tumors that do not harbor increased TILs. Whether and how this low TIL subset behaves differently clinically remains to be determined. In this pilot study, we examine in a

cohort of colonic carcinomas (CCs) with known MMR status the frequency and pathologic and molecular characteristics of TIL-high versus TIL-low dMMR tumors.

Design: The case cohort consisted of 454 consecutive patients with stage I-III CCs who underwent curative resection at our institution in 2017-2018. 118 (26%) dMMR tumors were identified. TILs were scored as "TIL-high" if the mean number of TILs in 5 consecutive high-power-fields (HPFs) from an area of highest concentration was ≥4/HPF, and "TIL-low" if this number was <4/HPF. dMMR tumors thus stratified were comparatively analyzed for their pathologic features and genomic characteristics using sequencing data.

Results: Among 118 dMMR CCs, 13 (11%) were TIL-low. Strikingly, 10 of the 13 (77%) were either pure mucinous (n=5) or with mucinous features (<50% mucin, n=5), whereas only 48/105 (46%) dMMR/TIL-high tumors had a mucinous component (p=0.042). In 8/13 dMMR/TIL-low tumors (including all 3 with no overt mucin), the tumor glands appeared pancreatobiliary-like, exhibiting cuboidal cells with clear to eosinophilic cytoplasm and sharp apical borders. A significant higher proportion of dMMR/TIL-low tumors were stage IIB-III (with pT4 and/or nodal disease) when compared to the dMMR/TIL-high group (69% vs 30%, p=0.010). No significant difference was detected in mutational profile, MSIsensor score or tumor mutational burden between TIL-high and TIL-low groups.

Conclusions: A small but significant subset of dMMR CCs do not harbor increased TILs. These tumors have a propensity towards mucinous morphology and more frequently present with pT4 and/or nodal disease compared to dMMR/TIL-high tumors. Future trials aimed at evaluating the efficacy of immunotherapy should take this subset into consideration so as to better address whether and how the lack of increased TILs confers differential treatment response in dMMR tumors.

500 Somatic Mutations in FAT Cadherin Family Members Constitute an Underrecognized Subtype of Colorectal Adenocarcinoma with Favorable Clinicopathologic Features

Liangli Wang[1], Xiuli Liu[2], Feng Yin[1]
[1]*University of Missouri at Columbia, Columbia, MO,* [2]*Washington University School of Medicine, St. Louis, MO*

Disclosures: Liangli Wang: None; Xiuli Liu: *Consultant*, Arrowhead Pharmaceuticals; *Consultant*, PathAI; *Advisory Board Member*, AbbVie; Feng Yin: None

Background: Fat cadherin family members (Fat1, Fat2, Fat3 and Fat4) are conserved tumor suppressor that are recurrently mutated in several types of human cancers including colorectal adenocarcinoma (CRC). The aim of this study is to characterize the clinicopathologic features in CRC patients with somatic mutations in Fat cadherin family members.

Design: We analyzed 526 colorectal adenocarcinoma cases from The Cancer Genome Atlas PanCancer Atlas dataset. CRC samples were subclassified into 2 groups based on the presence or absence of somatic mutations in *Fat1*, *Fat2*, *Fat3* and *Fat4*. Individual clinicopathological data were collected after digital slides review. Statistical analysis was performed using T-test and chi-square test.

Results: This CRC study cohort had frequent mutations in *Fat1* (10.5%), *Fat2* (11.2%), *Fat3* (15.4%) and *Fat4* (23.4%) gene. Two hundred CRC patients (38.0%) harbored somatic mutations in one or more of the Fat family genes, and were grouped into the Fat-mutated subtype. Table 1 summarizes the clinicopathologic features of this CRC subtype. The Fat-mutated CRC subtype is more commonly located in the right side of the colon (51.0%), as compared with the rest of cohort (30.1%, P<0.001). It showed favorable clinicopathologic features, including lower rate of positive lymph nodes (pN1-2: 33.5% vs. 46.9%, P=0.002) and lower rate of metastasis to another site or organ (pM1: 7.5% vs. 16.3%, P=0.006). The Fat-mutated CRC subtype also showed a trend to be less advance for the tumor stage (pT3-4: 75.0% vs. 80.7%, P=0.093).

	Fat-mutated	Fat-wild type	*P* value
Mean age (SD)	66.5 (12.9)	65.3 (13.0)	0.912
Sex Female Male	98 (49.0%) 102 (51.0%)	154 (47.2%) 170 (52.1%)	0.689
Location Left side Right side	65 (32.5%) 102 (51.0%)	181 (55.5%) 98 (30.1%)	<0.001 *
pT Stage pT1-2 pT3-4	50 (25.0%) 150 (75.0%)	61 (18.7%) 263 (80.7%)	0.093

pN Stage pN0 pN1-2	133 (66.5%) 67 (33.5%)	172 (52.8%) 153 (46.9%)	0.002 *
pM Stage pM0 pM1	153 (76.5%) 15 (7.5%)	235 (72.1%) 53 (16.3%)	0.006 *
Differentiation Grade G1-2 G3	145 (72.5%) 47 (23.5%)	255 (78.2%) 67 (20.6%)	0.332
Lymphovascular Invasion Positive Negative	61 (30.5%) 90 (45.0%)	117 (35.9%) 140 (42.9%)	0.313
Mucinous adenocarcinoma	30 (15.0%)	38 (11.7%)	0.267
Total	200 (38.0%)	326 (62.0%)	

Conclusions: Fat cadherin family genes are frequently mutated in CRC, and their mutation profile defines a subtype of CRC with favorable clinicopathologic characteristics.

501 Common Pathologic Staging Errors in Treatment Naïve Colonic Adenocarcinoma Resection Specimens Upon Subspecialist Review and Effects on Post-Operative Management and Outcomes

Erika Wheeler[1], Sarah Helman[2], Andrea Bafford[2], Kristen Stashek[2]
[1]University of Maryland Medical Center, Baltimore, MD, [2]University of Maryland School of Medicine, Baltimore, MD

Disclosures: Erika Wheeler: None; Sarah Helman: None; Andrea Bafford: None; Kristen Stashek: None

Background: Postoperative management in patients with colorectal adenocarcinoma (CRC) and the decision to pursue chemotherapy and/or radiation is dependent on T stage and node status. In this study, surgical resection specimens for CRC were reviewed to assess accuracy of staging and what effect staging errors had on management and outcomes.

Design: A CERNER database search was performed with 504 CRC resection specimens identified between 2013 and 2021. Cases that received neoadjuvant chemotherapy and/or radiation were excluded from analysis. All H&E stained slides, pathology reports and clinical histories were reviewed by a subspecialist gastrointestinal pathologist to assess for errors in pathologic staging.

Results: After exclusion of neoadjuvant cases, 327 resections were reviewed. 29 staging errors were discovered upon subspecialist review (29/327, 9%). The most common staging error was understaging of the T level (24/29, 83%). In 2 of these cases, pT3N0 tumors that were initially considered to have positive radial margins were corrected to pT4N0 tumors with negative margins. In 1 case, a T4a tumor was downstaged to T3 and in another a pT3N1c was initially thought to be pT3N0. Finally, in 3 (10%) cases, anal canal primaries were mistakenly staged as rectal cancers. None of these errors would have definitively changed post-operative management, but 4 (1.2%) may have influenced the decision to pursue postoperative chemotherapy. Please see the table below for further details regarding staging errors.

Description of error	# of cases	Initial path stage	Change in path stage	Initial CS	New CS	Potential pitfalls, post-operative management and outcomes
Colorectal (CR)checklist used instead of anal canal (AC)	2	pT2N0 (CR)	pT1N0 (AC)	I	I	Pitfall: Anal canal primaries are often mislabeled on requisition as rectal. No change in CS or post-operative management.
	1	pT1N0 (CR)	pT1N0 (AC)	I	I	
Change in pT stage (CR)	1	pT1N0	pT2N0	I	I	Pitfall: Tangential sectioning (ileocecal valve primary) made depth of invasion assessment challenging No change in CS or post-operative management.
	5	pT2N0	pT3N0	I	IIA	Pitfall: Desmoplastic stromal response at invasive edge was mistaken for muscle. 5/10 upstaged clinically, but no change in post-operative management
	5	pT2N+	pT3N+	IIIB	IIIB	
	4	pT3N0	pT4aN0	IIA	IIB	Pitfall: Tumor with perforation and/or inflammation continuous with serosal surface (4/11 cases).
	7	pT3N+	pT4aN+	IIIB/IIIC	IIIB/IIIC	

						Pitfall: Single or focal tumor cells at serosal surface (7/11 cases) 4 node negative cases had a change in clinical stage from IIA to IIB: • None of the four received post-operative chemotherapy, despite presence of other high-risk features (LVI, EMVI). • 1/4 developed metastatic disease • 1/4 died from other causes • 2/4 free of disease No change in post-operative management for N+ cases
	1	pT4aN+	pT3N+	IIIB	IIIB	Pitfall: Desmoplasia continuous with serosal surface, but no tumor cells or continuous inflammation present No change in CS or post-operative management
	2	pT3N0 + radial margin	pT4N0, neg radial margin	IIA	IIB	Pitfall: Mistook serosal surface as a radial margin in sigmoid colectomy specimen (2/2 cases) ½ received postoperative chemotherapy and developed metastatic disease ½ did not receive postoperative chemotherapy and is free of disease
	1	pT3N0	pT3N1c	IIA	IIIB	Pitfall: Failed to mention tumor deposit in N staging Patient received postoperative chemotherapy anyway due to presence of multiple high risk features (LVI, EMVI)

Conclusions: Confusion in staging colorectal adenocarcinoma continues to exist. Understanding common pitfalls is necessary to ensure patients are appropriately staged and receive correct postoperative management. The most commonly encountered error in staging is seen with assessing depth of invasion and involvement of serosal surface. When in doubt, deeper levels and review by a subspecialist is recommended to ensure appropriate management.

502 Correlation of Clinical, Pathologic, Genetic Parameters, and Intratumoral Immune Milieu in Serrated Adenocarcinoma of the Colon

Osman Yilmaz[1], Andrew Crabbe[2], Amaya Pankaj[2], Azfar Neyaz[3], Sandra Cerda[4], Qing Zhao[5], Stuti Shroff[6], Rory Crotty[2], M Lisa Zhang[2], Omer Yilmaz[7], Deepa Patil[8], Vikram Deshpande[9]

[1]Boston Medical Center, Boston, MA, [2]Massachusetts General Hospital, Boston, MA, [3]University of Pittsburgh Medical Center, Pittsburgh, PA, [4]Boston University Medical Center, Boston, MA, [5]Boston University, Boston Medical Center, Boston, MA, [6]Massachusetts General Hospital, Watertown, MA, [7]Massachusetts Institute of Technology, Cambridge, MA, [8]Brigham and Women's Hospital, Harvard Medical School, Boston, MA, [9]Massachusetts General Hospital, Harvard Medical School, Boston, MA

Disclosures: Osman Yilmaz: None; Andrew Crabbe: None; Amaya Pankaj: None; Azfar Neyaz: None; Sandra Cerda: None; Qing Zhao: None; Stuti Shroff: None; Rory Crotty: None; M Lisa Zhang: None; Omer Yilmaz: None; Deepa Patil: None; Vikram Deshpande: None

Background: Serrated adenocarcinoma (SAC), a recognized WHO variant of colonic adenocarcinoma, is purported to be an end-product of serrated neoplasia pathway. Yet, a diagnosis of SAC is infrequently rendered, and little is known about its prognostic implications, its immune microenvironment, and association with mismatch repair and molecular alterations.

Design: We assessed 846 consecutive colon cancers on representative tissue microarray sections, and recognized tumors with >5% serrated pattern as SAC (n=37). We performed immunohistochemistry for mismatch repair proteins (MMR), human leukocyte antigen (HLA) class I and class II proteins, beta-2-microglobulin (B2MG), CD8, CD163, LAG3, PD-L1, FoxP3 and *BRAF* V600E; We noted *KRAS* mutational status, when available. We then performed automated quantification; manual quantification was used for PD-L1 tumor cells and immune cells. We also evaluated 34 SAC on whole slides to assess the incidence of other histologic features including presence of precursor lesions.

Results: We identified a rate of SAC of 4.5% and precursor lesions in 27% of cases (7/34), and these were mostly tubular adenomas (6/7; 86%). SAC exhibited higher numbers of CD8 lymphocytes (p=0.004) but did not reveal a difference in the expression of HLA class I or II, B2M, PD-L1 on tumor cells or a difference of expression of PD-L1, LAG3, FOXP3 and CD163 on immune cells. There was no association with deficient mismatch repair (dMMR), BRAFV600E, or KRAS mutational status relative to conventional adenocarcinoma. Lastly, there was no difference in disease specific survival between SAC and conventional colonic carcinoma (p=0.26).

Conclusions: While SAC has distinctive morphologic features, it lacks a significant association with regard to a serrated precursor polyp, MMR status, BRAFV600E status, and disease specific survival relative to conventional adenocarcinoma. Nevertheless, the increased numbers of intratumoral CD8 cells in SAC, raises awareness of a possible role of a unique immunologic background.

503 PD-L1 Expression in the Immune Compartment of Colon Carcinoma

Osman Yilmaz[1], Amaya Pankaj[2], Azfar Neyaz[3], Stuti Shroff[4], Rory Crotty[2], M Lisa Zhang[2], Sandra Cerda[5], Qing Zhao[6], Deepa Patil[7], Omer Yilmaz[8], Vikram Deshpande[9]

[1]Boston Medical Center, Boston, MA, [2]Massachusetts General Hospital, Boston, MA, [3]University of Pittsburgh Medical Center, Pittsburgh, PA, [4]Massachusetts General Hospital, Watertown, MA, [5]Boston University Medical Center, Boston, MA, [6]Boston University, Boston Medical Center, Boston, MA, [7]Brigham and Women's Hospital, Harvard Medical School, Boston, MA, [8]Massachusetts Institute of Technology, Cambridge, MA, [9]Massachusetts General Hospital, Harvard Medical School, Boston, MA

Disclosures: Osman Yilmaz: None; Amaya Pankaj: None; Azfar Neyaz: None; Stuti Shroff: None; Rory Crotty: None; M Lisa Zhang: None; Sandra Cerda: None; Qing Zhao: None; Deepa Patil: None; Omer Yilmaz: None; Vikram Deshpande: None

Background: Programmed cell death ligand 1 (PD-L1) on tumor cells is a significant prognostic biomarker for a number of malignancies, although less is known about the significance of PD-L1 positive immune cells in colon carcinoma. The purpose of this study is to evaluate the role of PD-L1 in a large cohort of colon carcinomas to identify patterns of PD-L1 expression in the tumor microenvironment and its correlation with other key immune subsets to better understand the prognostic impact of these immune cells.

Design: We assessed 1206 colon carcinomas on representative tissue microarray sections, gathered relevant clinicopathologic information, and performed immunohistochemical staining for mismatch repair proteins, CD8, CD163, LAG3, PD-L1, Fox3 and BRAF V600E. We then performed automated quantification; manual quantification was used for PD-L1 tumor cells and immune cells. Dual PD-L1/ PU.1 immunostains were also performed.

Results: The majority of PD-L1 positive cells expressed PU.1 thus representing tumor associated macrophages. Based on the median number of PD-L1 positive immune cells (7.6 per mm^2), we classified tumors into two classes: 1) PD-L1 immune cell low and 2) PD-L1 immune cell high. PD-L1 immune cell high colon carcinomas showed favorable prognostic pathologic features including less frequent extramural venous invasion (p=0.0001), and lower AJCC (p=0.0001); they were also more commonly associated with deficient mismatch repair (dMMR) (p=0.0001) and BRAF V600E. PD-LI immune cell high tumors were associated with high CD8, CD163 and LAG3 positive cells (p=0.0001, respectively). PD-L1 immune cell high and LAG3 high colon carcinomas were associated with improved disease specific survival (p=0.0001 and 0.001, respectively), whereas FOXP3 showed no significance (p=0.95). PD-L1 expression on tumor cells was not associated with disease specific survival. On multivariate analysis of chemotherapy naïve stage 2 colon carcinomas only extramural venous invasion (p=0.002) and -PD-L1 immune cell expression (p=0.032) correlated with disease specific survival.

Conclusions: Resected colonic carcinoma s with high expression of PD-L1 and LAG3 proteins on immune cells were associated with improved prognosis in colon carcinoma. The mechanism underlying the improved prognosis of colon carcinomas bearing high numbers of immunoregulatory cells needs further investigation.

504 Clinicopathological Features of Intestinal and Foveolar Gastric Adenomas

Sherehan Zada[1], Whayoung Lee[1], Cary Johnson[2], Xiaodong Li[1], Vishal Chandan[3]
[1]UCI Medical Center, Orange, CA, [2]University of California, Irvine, Irvine, CA, [3]University of California, Irvine, Orange, CA

Disclosures: Sherehan Zada: None; Whayoung Lee: None; Cary Johnson: None; Xiaodong Li: None; Vishal Chandan: None

Background: Gastric adenoma (GA) is a polypoid proliferation of dysplastic epithelium. The two most common morphologic subtypes are intestinal (IGA) and foveolar (FGA) types. Very few prior studies with contested results have looked into the details of the background gastric pathology and behavior of these two types of GAs. In this study we evaluate the background gastric mucosa and risk of adenocarcinoma, specifically in relation to these two histologic types of GAs.

Design: We studied 65 GAs from 50 patients (M: F;1:1) between 2004-2018. They were classified as IGA (pseudostratified columnar epithelium with elongated pencil shaped overlapping nuclei), FGA (columnar or cuboidal foveolar epithelium with apical mucin cap), or hybrid (HGA) (showing features of both types, of at least 10%), based on histologic evaluation. Additional features of GAs (size, location, multiplicity, architecture, degree of dysplasia, presence of adenocarcinoma within the polyp) and the surrounding gastric mucosa (type of gastritis and intestinal metaplasia) were also recorded. Follow up data was available for 42 patients (mean 49 months).

Results: GAs were most frequently solitary (85%), mean patient age was 71 years (range 16-90; 2 pts with FAP) and distributed throughout the stomach (body/fundus 42%, antrum/pylorus 52%, cardia 2%, unknown 4%). Most of the adenomas were small (25(38%) were <1cm, and 42(65%) were <2cm) and majority were tubular (80%) in architecture. 8 (12%) polyps showed adenocarcinoma. 43(66%) were IGA, 14(22%) FGA and 8(12%) HGA. FGA and HGA were significantly more likely than IGA to be larger (≥ 2cm in size) (p=0.03) and show high grade dysplasia (p=0.002). IGA was significantly more likely than FGA and HGA to be multiple (p=0.036), recur after resection (p=0.015), arise in a background of autoimmune atrophic gastritis (AMAG) (p<0.001) and show flat dysplasia in the surrounding stomach (p=0.002). The differences in polyp location, presence of adenocarcinoma within the polyp, background environmental type of atrophic gastritis (EMAG) and H. pylori infection were not statistically significant (p>0.05).

	Subtypes		
	Intestinal (n=43)	Hybrid (n=8)	Foveolar (n=14)
Size			
≥ 2 cm[1]	8 (18.6%)	3 (37.5%)	4 (28.6%)
Location			
Antral/pylorus	22 (51.2%)	6 (75%)	6 (42.9%)
Body/fundus	17 (39.5%)	2 (25%)	8 (57.1%)
Multiple[2]	8 (18.6%)	1 (12.5%)	1 (7.1%)
High-grade dysplasia[3]	9 (20.9%)	4 (50%)	6 (42.9%)
Adenocarcinoma			
Intramucosal	4 (9.3%)	2 (25%)	0
Submucosal invasion	1 (2.3%)	0	1 (7.1%)
Recurrence[4]	6 (14.0%)	1 (12.5%)	0
Association with			
H. pylori	1 (2.3%)	0	1 (7.1%)
Intestinal metaplasia	30 (69.8%)	7 (87.5%)	6 (42.9%)
AMAG[5]	12 (27.9%)	0	0
EMAG	3 (7.0%)	1 (12.5%)	0
Flat dysplasia[6]	4 (9.3%)	0	0

[1] Intestinal vs. Hybrid+Foveolar, p=0.03 [2] Intestinal vs. Hybrid+Foveolar, p=0.036
[3] Intestinal vs. Hybrid+Foveolar, p=0.002. [4] Intestinal vs. Hybrid+Foveolar, p=0.015
[5] Intestinal vs. Hybrid+Foveolar, p<0.001 [6] Intestinal vs. Hybrid+Foveolar, p=0.002

Conclusions: The results of our study show certain distinct clinicopathologic differences between IGA and FGA. FGA is more likely to be larger (≥ 2cm) and show high grade dysplasia. IGA is more likely to be multiple, recur after resection, arise in a background of AMAG and show flat dysplasia in the surrounding stomach.

505 Evaluation of the Gray-Zone in Staging Between T3 and T4a Colonic Adenocarcinomas

Bassel Zein-Sabatto[1], Michael Behring[1], Smitha Mruthyunjayappa[1], Venkata Dayana[1], Goo Lee[1], Deepti Dhall[1], Upender Manne[1], Sameer Al Diffalha[1], Chirag Patel[1]
[1]The University of Alabama at Birmingham, Birmingham, AL

Disclosures: Bassel Zein-Sabatto: None; Michael Behring: None; Smitha Mruthyunjayappa: None; Venkata Dayana: None; Goo Lee: None; Deepti Dhall: None; Upender Manne: None; Sameer Al Diffalha: None; Chirag Patel: None

Background: AJCC guidelines for assessment of peritoneal involvement in colorectal cancer (CRC) are unclear and subject to misinterpretation by pathologists, specifically for tumors ≤1 mm from serosa with associated reaction. Since the significance of such tumors is unclear with controversial findings in literature, we investigated tumors close to the serosal surface with bridging fibrotic and/or inflammatory reaction (BFIR) and their association with overall survival.

Design: Two pathologists reviewed 232 CRC resections staged as pT3 or pT4 during an 11-year period (2003-2013). Tumors considered pT4b and/or involved non-peritonealized surfaces (n=32) were excluded. The tumor-serosa relation was assessed based on two parameters: 1) distance (≤1 mm or >1 mm), and 2) presence of BFIR. The tumors were classified into distinct categories as shown in Table 1. Consensus from 3 other GI pathologists was obtained on equivocal cases. Patients with C3 tumors (n=8) and follow-up time ≤3 months (n=25) were excluded. Univariate analysis for overall survival was tested with a Kaplan-Meier Log Rank test.

Results: Cases originally staged pT3 or pT4a (n=200) were categorized as C1 (n=44, 22%), C2 (n=61, 30.5%), C3 (n=8, 4%), C4 (n=31, 15.5%), or C5 (n=56, 28%). The majority of the C2 cases (≤1 mm with BFIR; Figure 1) were originally reported as pT3 (n=52, 85%); 9 (15%) were reported as pT4a.

For survival analysis, a total of 175 cases were included. In univariate analysis, while not reaching statistical significance, relative to C5 (unequivocal T3), the categories with the highest hazards of overall death were C1 (HR 1.53, 0.66-3.56) and C2 (HR 1.4, 0.68-2.88), Figure 2. C4 had a consistent (but not significant) protective effect in relation to both C1 (HR 0.32, 0.1-1.02) and C5 (0.49, 0.16-1.52).

Table 1. Tumor categorized based on tumor-serosa distance and presence of BFIR, with their corresponding AJCC stage.

Category	*Equivalent AJCC pT stage*	*Distance from serosa*	*Bridging fibrotic and/or inflammatory reaction (BFIR)*	*n=200 N (%)*
C1	**pT4a** (Unequivocal)	**0**	**N/A**	44 (22%)
C2	**pT3/pT4a** (Controversial)	**≤1 mm**	**Present**	61 (30.5%)
C3	**pT3** (Unclear significance)	**≤1 mm**	**Absent**	8 (4%)
C4	**pT3** (Unclear significance)	**>1 mm**	**Present**	31 (15.5%)
C5	**pT3** (Unequivocal)	**>1 mm**	**Absent**	56 (28%)

Figure 1 - 505

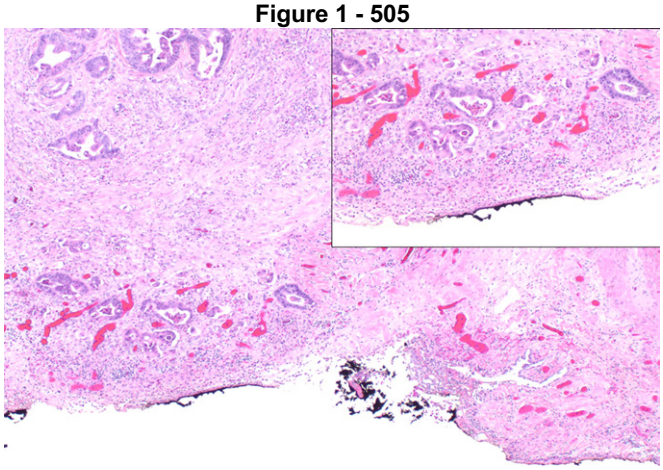

Figure 2 – 505

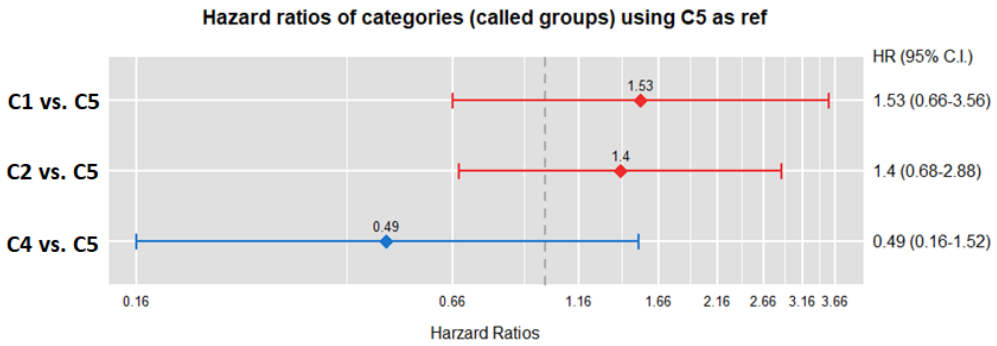

Conclusions: CRCs which are ≤1 mm from serosa with BFIR (C2) are frequently encountered in practice (32% of cases in our cohort), but remain inconsistently staged among pathologists. In terms of overall survival, our study suggests that CRCs with tumor-serosa distance ≤1 mm with BFIR (C2) will behave similar to tumors unequivocally involving serosa (pT4a). Also, C4 tumors (>1 mm from serosa with BFIR) appear to behave similar to C5 (unequivocal T3) tumors. Further investigation on a larger cohort with correlation to disease-specific survival is needed to support including the controversial C2 tumors in AJCC pT4a stage in future iterations and can lead to more reproducibility of CRC stage reporting amongst pathologists.

506 Expression of Transcriptional Regulators ASCL1, NEUROD1, POU2F3, and YAP1 in High-Grade Neuroendocrine Carcinomas of the Tubular Gastrointestinal Tract: Correlation with Histopathologic Subtypes and Molecular Profiles

M Lisa Zhang[1], Lauren Ritterhouse[2], Jaimie Barth[1], Yin (Rex) Hung[1], Mari Mino-Kenudson[2]
[1]Massachusetts General Hospital, Boston, MA, [2]Massachusetts General Hospital, Harvard Medical School, Boston, MA

Disclosures: M Lisa Zhang: None; Lauren Ritterhouse: *Advisory Board Member*, Loxo Oncology; *Consultant*, Amgen; *Speaker*, Merck; *Advisory Board Member*, AstraZeneca; Jaimie Barth: None; Yin (Rex) Hung: *Consultant*, Elsevier; Mari Mino-Kenudson: *Consultant*, AstraZeneca, H3 Biomedicine; *Primary Investigator*, Novartis; *Advisory Board Member*, BMS, Sanofi

Background: High-grade neuroendocrine carcinomas (HGNEC) of the tubular gastrointestinal (GI-HGNEC) tract are uncommon and continue to pose uncertainty in subtyping and biological behavior. Immunohistochemistry for transcriptional regulators ASCL1, NEUROD1, POU2F3 and YAP1 was recently introduced to subtype small cell carcinoma (SCC) of the lung. We sought to evaluate the role of transcriptional regulator expression in the histologic subtyping of GI-HGNEC.

Design: 28 cases (21 HGNEC, 7 mixed HGNEC-adenocarcinoma) were reviewed. The HGNEC component was subtyped into SCC, large cell neuroendocrine carcinoma (LCNEC), or “intermediate” NEC with some features of SCC and LCNEC (HGNEC-NOS) in each case based on evaluation of the H&E, immunostains for neuroendocrine markers (synaptophysin, chromogranin, INSM1) and Ki67. Immunohistochemistry for ASCL1, NEUROD1, POU2F3 and YAP1 were evaluated for dominant marker expression and correlated with the histologic subtypes. In cases with sufficient tissue, next-generation sequencing (NGS) was performed and analyzed.

Results: 21 (75%) patients were men; mean age was 61 years. The primary sites were esophagus (n=3), stomach (n=6), small intestine (n=4) and large intestine (n=15). Biopsies and resections each comprised 13 and 15 cases, respectively. 20 specimens represented primary tumors, while 8 were from metastases. Histologically, the HGNEC component was classified as SCC in 8, LCNEC in 9, and HGNEC-NOS in 11 cases. One LCNEC appeared to transition from areas of well-differentiated neuroendocrine tumor (WDNET). The expression profiles of ASCL1, NEUROD1, POU2F3 and YAP1 were as follows: 3 ASCL1-dominant (2 HGNEC-NOS with prominent SCC features and 1 SCC); 12 NEUROD1-dominant (7 SCC, 4 LCNEC, 1 HGNEC-NOS); 3 POU2F3-dominant (2 LCNEC, 1 HGNEC-NOS); and 10 null pattern (all non-SCC). Notably, all NEUROD1-dominant LCNEC were mixed with adenocarcinoma or WDNET. NGS performed in 9 cases showed recurrent mutations in *TP53* (n=6); *KRAS* (n=3); *APC, PIK3CA*, *NRAS*, *BRCA2*, *KDR* and *CDKN2A* (n=2 each). Molecular profiling of the remaining cases is underway.

Conclusions: All SCC had ASCL1- or NEUROD1-dominant expression profiles, though NEUROD1-dominant tumors also included LCNEC with uncommon morphologies. In contrast, POU2F3-dominant and null pattern profiles were exclusively seen in non-SCC, suggesting a role for transcriptional regulator expression profiles in subtyping GI-HGNEC, particularly those with "intermediate" morphologic features.

507 Increased Risk of Non-Conventional Dysplasia in Patients with Primary Sclerosing Cholangitis Associated with Inflammatory Bowel Disease

Ruth Zhang[1], Gregory Lauwers[2], Won-Tak Choi[1]
[1]University of California, San Francisco, San Francisco, CA, [2]H. Lee Moffitt Cancer Center & Research Institute, University of South Florida, Tampa, FL

Disclosures: Ruth Zhang: None; Gregory Lauwers: None; Won-Tak Choi: None

Background: Patients with primary sclerosing cholangitis and inflammatory bowel disease (PSC-IBD) have a higher risk of developing colorectal neoplasia than those with IBD alone. The mechanism by which concomitant PSC increases the risk of colorectal neoplasia is unknown. Seven distinct non-conventional dysplastic subtypes have been described in IBD. Despite the lack of high-grade morphologic features, crypt cell (CCD), hypermucinous (HMD), and goblet cell deficient (GCD) dysplasias often show molecular features characteristic of advanced neoplasia (aneuploidy) and are associated with advanced neoplasia on follow-up. We aimed to characterize features of dysplasia in PSC-IBD patients.

Design: A cohort of 173 PSC-IBD patients were analyzed. All dysplastic lesions (n = 153) from 54 patients were subtyped as either conventional or non-conventional dysplasia (including CCD, HMD, GCD, dysplasia with increased Paneth cell differentiation [DPD], traditional serrated adenoma [TSA]-like, sessile serrated lesion [SSL]-like, and serrated dysplasia, not otherwise specified [SD NOS]).

Results: The cohort included 109 (63%) men and 64 (37%) women with a mean age of 26 years and a long history of IBD (mean: 14 years). The majority of patients (80%) had ulcerative colitis. A total of 153 dysplastic lesions were detected in 54 (31%) patients, 35 (64%) of whom had multifocal dysplasia. Patients with dysplasia were more likely to have pancolitis (96%, p = 0.026) and a longer IBD duration (mean: 17 years, p = 0.021) than those without dysplasia (85% and 12 years, respectively). Dysplasia was often non-conventional (n = 93; 61%), endoscopically/grossly flat or invisible (n = 101; 66%), and detected throughout the colon (including 63 [41%] left, 61 [40%] right, and 29 [19%] transverse). All seven subtypes were identified, including 46 (30%) CCD, 23 (15%) HMD, 12 (8%) GCD, 7 (5%) DPD, 3 (2%) TSA-like, 1 (1%) SSL-like, and 1 (1%) SD NOS. Follow-up information was available for 86 lesions, of which 32 (37%) were associated with advanced neoplasia within a mean follow-up time of 55 months.

Conclusions: Non-conventional dysplasia develops at a high rate (61%) in PSC-IBD patients and is often endoscopically/grossly flat or invisible (66%). The vast majority of these lesions (n = 81; 87%) represented high-risk subtypes (CCD, HMD, and GCD). These findings underscore the importance of recognizing these non-conventional subtypes and having a low threshold to advise colectomy once dysplasia is detected in PSC-IBD patients.